Titre: Title:	Free-Radical Polymerization of Polystyrene Using Microreaction Technology
Auteur: Author:	Lionel Sergio Méndez Portillo
Date:	2011
Type:	Mémoire ou thèse / Dissertation or Thesis
Référence: Citation:	Méndez Portillo, L. S. (2011). Free-Radical Polymerization of Polystyrene Using Microreaction Technology [Thèse de doctorat, École Polytechnique de Montréal]. PolyPublie. https://publications.polymtl.ca/551/

URL de PolyPublie: PolyPublie URL:	https://publications.polymtl.ca/551/
Directeurs de recherche: Advisors:	Philippe A. Tanguy, & Charles Dubois
Programme: Program:	Génie chimique

UNIVERSITÉ DE MONTRÉAL

FREE-RADICAL POLYMERIZATION OF POLYSTYRENE USING MICROREACTION TECHNOLOGY

LIONEL SERGIO MÉNDEZ-PORTILLO
DÉPARTEMENT DE GÉNIE CHIMIQUE
ÉCOLE POLYTECHNIQUE DE MONTRÉAL

THÈSE PRÉSENTÉE EN VUE DE L'OBTENTION
DU DIPLÔME DE PHILOSOPHIAE DOCTOR (Ph. D.)
(GÉNIE CHIMIQUE)
AVRIL 2011

UNIVERSITÉ DE MONTRÉAL

ÉCOLE POLYTECHNIQUE DE MONTRÉAL

Cette thèse intitulée:

FREE-RADICAL POLYMERIZATION OF POLYSTYRENE USING MICROREACTION TECHNOLOGY

présentée par: MÉNDEZ-PORTILLO Lionel Sergio
en vue de l'obtention du diplôme de: Philosophiae Doctor
a été dûment acceptée par le jury d'examen constitué de:

Mme. HEUZEY Marie-Claude, Ph. D., Présidente
M. TANGUY Philippe, Ph. D., Membre et directeur de recherche
M. DUBOIS Charles, Ph. D., Membre et codirecteur de recherche
M. GRMELA Miroslav, Ph. D., Membre
M. DUBÉ Marc, Ph. D., Membre

To my wife Iris…

…and to my children:

Mélanie Alejandra, Lionel Sergio and José Emmanuel

ACKNOWLEDGEMENTS

Many people inspire us during different periods of our lives leaving part of them with us whether in the form of an idea, a feeling or a memory. Thus, I wish to explicitly thank the many people who in one way or another during my time in Montreal contributed not only to the achievement of this project but more significantly, to shape the character of the person I am today:

My research advisor Prof. Philippe A. Tanguy, to whom I wish to express my sincere gratitude for his guidance and unconditional support during all these years not only professionally but on a personal level; for his understanding during some of the most difficult times in my life and for trusting me with the opportunity to pursue my project with such invaluable freedom and conviction.

My research co-advisor Prof. Charles Dubois, to whom I am indebted not only for his technical guidance and advice but also for his friendship, trust, confidence and encouragement to keep growing and moving forward even in the hardest times.

Dr. Mourad Heniche for his friendship and support; for his always patient technical advice which helped me to expand my knowledge, and for his overall positive contribution to my research.

Prof. Louis Fradette whose office doors were always opened for me; for his willing disposition, insights and suggestions to help me and to improve the quality of my work.

The faculty members of the Department of Chemical Engineering and URPEI whom I crossed paths with during my graduate studies: Prof. François Bertrand, Prof. Jamal Chaouki, Prof. Marie-Claude Heuzy, Dr. Andrea Costa. The secretaries of the Department of Chemical Engineering and those at the URPEI throughout the years: Mme. Chantal Bénard, Mme. Marlene Bois, Mme. Michelle Rozon, Mme. Josiane Archambault and especially Mme. Diane Raymond-Pimparé for their always affable disposition and great contribution during all my related paperwork. The technicians and analysts of the Department of Chemical Engineering especially to Jean Huard, Robert Delisle, Daniel Dumas, Martine Lamarche, Carol Pinchaud and Gino

Robin for their prompt and efficient disposition towards my experimental requirements, and whose expertise and patience greatly helped to materialize my project.

The Mexican Council of Science and Technology (CONACYT) for their financial support during my graduate studies.

My colleagues and friends at the URPEI and Polytechnique throughout the years, especially Rouzbeh Jafari and particularly Babak Esmaeili Pour Farsangi, a good friend and great chemical engineer for his reliable and practical advice and his always kind disposition to help. My friends at the other end of the hallway around the 5th floor of the Aisenstadt Building: Mariya Marinova and Zoé Périn-Levasseur. My mexican friends at the red side of the hill: Julio Morales and Rodrigo Mendoza. And of course a special mention to the *"mexi-can connection"* my dear friends: Magdalena Brito Bazán, Enrique Mateos Espejel, Christian A. Rivera Aparicio and Hilda Garza Villareal (*viva Monterrey!*) who were always there in the trenches with me and with whom I shared a lot of difficult and stressful moments, but with whom I also shared laughter, great get-togethers and very fond memories. Their support and friendship during these years have made the journey more enjoyable and unforgettable.

Prof. Gabriel Ascanio Gasca and Prof. Tomás Lozano Ramírez for their friendship, support and advice; for their favor and positive involvement in my career throughout all these years since my early days in Montréal many blizzards ago.

Prof. Carlos A. Guerrero Salazar and Prof. Juan Antonio Aguilar Garib from the Department of Materials Science and Engineering of the UANL for their support, example and friendship.

Herr Prof. Francisco Eugenio López Guerrero for his friendship, example and professional mentorship ever since my first endeavours in the research field at the School of Mechanical and Electrical Engineering of my cherished *Alma Mater* the Autonomous University of Nuevo León (UANL).

My friends and brothers back in my hometown of Monterrey, NL who have patiently held the line in the southern front until my return.

My parents-in-law José Cruz and Gloria, and their daughters and sons Gloria, Hiram, Melissa and José who have always supported us in all sorts of ways; for their unforgettable and pleasant visits throughout our stay in Montréal.

My Senpais Ricardo Sosa and Juan Heberto Vega García for shaping in me character and teaching me to improvise, adapt and overcome any obstacle with patience, prudence and endurance.

The departed during my time in Montréal: Osvaldo Leonel Martínez Casillas who made me feel at my home whenever I was around his; Daniel Salvador González Villareal known as *papá* to those of us who are like brothers to his son, for sharing his wisdom when showing us that all hardship *"es parte del crecimiento"*; my uncle José Luis Portillo Tijerina, too late I found that we could have been closer friends than blood can relate; my long estranged grandfather José Méndez García who I finally met for the first time after 28 years during only one day; and my beloved son José Emmanuel Méndez Mendoza with whom I could share only a few moments which however are worth a lifetime, from heaven he has been my ever-present accomplice and surely it was him who pushed me through during the most difficult moments, what a ride we had that day my son… *Vaya con Dios*.

My siblings (and *compadres*) José Alejandro and Gabriela del Carmen, and my parents Lionel Sergio and María del Carmen; for all their prayers, sacrifice, encouragement and unconditional support since way back in 1979. For the priceless long-distance medical consulting and expertise of my siblings, who are also my role models whose deep knowledge, utmost ethics and passion for the science and art of Medicine is to this day my standard of professionalism. And of course for the exemplary lead and guidance of the true heroes of my life: my parents, who raised me with the courage to pursue my dreams and to never abandon my convictions.

My children who are the other driving force in my life. Being their father is the greatest honour I will ever have. My little girl Mélanie Alejandra who with her purest innocence encouraged me to "finish the book I was writing", my little boy Lionel Sergio who urged me to finish since "I was taking too long and he wished I could be already there", and my little angel José Emmanuel who found his own way to be here accompanying me always.

Finally, words cannot remotely express my love, gratitude and admiration to my beautiful wife Iris. She is the main driving force in my life and the one who has made all of this possible, she who stands unconditionally by my side and who keeps her faith in me always. She is the only person in my family that I was given the chance to choose… and God knows that you are, and will always be, the greatest decision of my life. *Te Amo preciosa*.

"No sólo no hubiera sido nada sin ustedes, sino con toda la gente que ha estado a mi alrededor desde el comienzo; algunos…siguen hasta hoy. ¡Gracias…

…totales!"

(Gustavo Cerati)

L…

RÉSUMÉ

La technologie de microréaction chimique est un sous domaine de l'ingénierie des procédés qui se concentre sur l'étude des réactions chimiques réalisées à l'intérieur de systèmes miniaturisés communément appelé *microréacteurs*.

Les microréacteurs sont essentiellement des mélangeurs statiques miniaturisés fonctionnant en mode continu pour écoulements entraînés par la pression. Ils peuvent être constitués d'un ou plusieurs microcanaux parallèles de longueurs différentes de l'ordre des micromètres. Les microréacteurs se différencient fortement des réacteurs de synthèse traditionnels par plusieurs caractéristiques clés reliés à l'intensification des procédés telles que des plus élevés gradients de concentration et température, et une réduction du temps de mélange, une capacité de transfert de chaleur plus élevé, une augmentation de la surface d'échange surface/volume, etc. Les microréacteurs attirent de ce fait de plus en plus l'attention de la communauté scientifique qui y voit l'opportunité d'accéder à des voies de synthèse jusqu'alors inaccessibles dans les réacteurs classiques.

Il existe actuellement de nombreux microréacteurs disponibles commercialement conçus pour atteindre des conditions de haute pression et température. Ces microréacteurs peuvent être produits en masse par des techniques de fabrication de pointe. Par conséquent, de nouvelles applications sont envisagées afin de les utiliser comme outils de production alternatifs dans différents domaines de l'ingénierie. Un exemple serait l'utilisation de cette technologie pour la production de polymères. Les avantages présentés par les microréacteurs en termes de contrôle de température et conditions de mélange sont non négligeables lorsque l'on considère les réactions de polymérisation, généralement fortement exothermiques et extrêmement sensibles en termes de mélange des réactifs. Malgré cela, la technologie de microréaction n'a été que très peu utilisée dans les processus de polymérisation en continu.

Pour faire l'évaluation du vrai potentiel de ce type de technologie la caractérisation hydrodynamique du microréacteur est une étape essentielle. Dans ce contexte, la distribution du temps de séjour (DTS) est un outil majeur pour caractériser l'hydrodynamique d'un réacteur

chimique quelque soit l'échelle. La DTS renseigne sur le comportement d'un écoulement, sur les processus de mélange et leur interaction avec la cinétique des réactions survenant à l'intérieur d'un réacteur. Le temps passé par une molécule sous les conditions de réaction dans un système aura une incidence sur la probabilité de cette dernière de réagir. De ce fait, la mesure, l'interprétation et la modélisation de la DTS sont des aspects importants pour la prédiction de la composition finale d'un système impliquant une réaction chimique.

On note toutefois, que dans la plupart des cas sur la technologie de microréaction, l'étape de caractérisation a été menée sur des équipements de laboratoire destinés à des fins de visualisation et non conçus pour l'opération dans des conditions de haute pression et température. Seuls quelques rapports expérimentaux existent sur la caractérisation des unités commerciales de microréaction et les informations sur leur utilisation en tant que réacteur de polymérisation sont rares. On comprend de ce fait pourquoi des études de faisabilité sont nécessaires afin de déterminer dans quelle mesure la technologie de microréaction peut être appliquée pour les réactions polymérisation. Pour de telles applications, la distribution du débit total dans chacun des microcanaux peut affecter le transfert de chaleur et l'efficacité du mélange modifiant les conditions de réactions pendant la polymérisation, jouant ainsi rôle sur les propriétés finales du produit.

L'objectif général de ce projet est d'évaluer la faisabilité d'utiliser la technologie de microréaction pour la production en mode continu de polymère tout en développant une meilleure compréhension de l'écoulement et des caractéristiques de mélange pour la conception de microréacteur le plus performant. La réaction de polymérisation du monomère styrène en utilisant des initiateurs de peroxyde sera utilisée comme système de réaction. La méthodologie de ce projet est planifiée pour s'adresser à l'hydrodynamique et à la performance du mélange, à la capacité de transfert de chaleur et au niveau de conversion de polymères obtenus dans deux microréacteurs ayant des mécanismes de micromélange différents et des échangeurs de chaleur intégrés. Les mécanismes de mélange considérés sont le mécanisme de division-et-recombinaison d'écoulements (SAR par ses sigles an anglais: *split-and-recombination*), et la subdivision d'écoulement par des structures interdigitaux; et ce qui sont les deux principes de mélange les plus fréquemment utilisés pour les microréacteurs commerciaux.

ABSTRACT

Microreaction technology is presently a well established subfield of the chemical microprocess engineering that focuses on the study of chemical reactions conducted inside of the structured channels of miniaturized flow vessels commonly referred as *microreactors*.

Microreactors are essentially miniaturized static mixers that operate in continuous mode under pressure driven flow. They can be composed of single or multiple parallel microchannels of different lengths with typical cross sections in the micrometer range. The gradients of the physical properties of a material are increased when its linear dimensions are reduced and some of theses gradients, *e.g.* temperature and concentration, are particularly important for the control of chemical engineering processes. Consequently, microreaction technology has drawn great attention from the process engineering community during the last decades due to their theoretical benefits in terms of transport phenomena and due to their new envelope of reaction conditions otherwise inaccessible in macroscopic equipment.

Presently, there is a large repertoire of commercially available microreactors designed and built for mechanical robust operation which can be mass produced by state-of-the-art manufacturing techniques. Therefore, new applications are being sought for existing microreaction equipment trying to incorporate them as alternative production tools into different fields of engineering. In this context polymer reaction engineering applications could fully exploit the benefits of microreaction conditions in terms of temperature control and fast mixing since polymerization reactions are usually highly exothermic and extremely sensitive to the level of mixing of the reactants. Nevertheless microreaction technology has not been extensively applied in continuous polymerization processes.

Residence time distribution (RTD) theory is a major tool for reactor characterization at any scale level that provides substantial insight of flow behavior and mixing processes and their interaction with the kinetics of reactions occurring inside a flow vessel. The time a molecule spends under reaction conditions in a reactive system will affect its probability of reacting; therefore the

measurement, interpretation and modeling of RTD are important aspects for the prediction of the final composition of the system.

However, for the most part such type of characterization has been conducted on laboratory equipment intended for visualization purposes and not for more demanding operating conditions. Only few experimental reports exist on the characterization of commercial microreaction units and information about their capabilities as polymerization reactors is not available at all. In this context feasibility studies are necessary in order to determine the extent of applicability of microtechnology in the polymer reaction engineering field. For such applications, the flow distribution in microchannel networks can affect the heat transfer and mixing efficiency at the microscale modifying the working conditions accessible during polymerization which will consequently affect the final properties of the product.

The general objective of this project is to test the feasibility of individual microreaction units to be used for continuous polymer production and to develop a better understanding of the flow and mixing characteristics of specific microreactor commercial designs. The peroxide initiated polymerization of styrene monomer will be used as reaction system. The methodology of this project is structured as to address the hydrodynamic and mixing performance, the heat transfer capabilities and the level of conversion of polymer achieved on two microreactors featuring different micromixing mechanisms with integrated heat exchangers. The mixing mechanisms considered are the split-and-recombination (SAR) mechanism and the multilamination of flow by means of interdigital structures which are two mixing principles most frequently featured by commercial microreactors.

The following specific objectives are defined:

1. To conduct the experimental mixing and flow characterization of two different microreactors provided with an integrated heat-exchanger featuring respectively the split-and-recombination and the multilamination micromixing mechanism.

2. To determine the effect of the manifold flow distribution on the mixing performance and distribution of residence times of the proposed microreactors.

3. To characterize the heat transfer capabilities of the proposed microreactors and to determine the influence of the flow conditions on the free-radical polymerization of styrene monomer conducted inside the microreactors aimed at achieving 30% of conversion.

Experimental Hydrodynamic and Mixing Characterization

The objective of this part is to conduct the experimental characterization of two microreactors designed for high temperature and pressure conditions. The microreactors feature the split-and-recombination and the multilamination mechanism respectively, and are provided with distribution manifolds to produce flow parallelization. Although the classical theory of RTD and the well known Villermaux/Dushman method are applied for the description of the hydrodynamics and mixing performance, to the best of our knowledge this is the first time that these specific microreactor models will be characterized. The contribution of this investigation is to provide better insight of the flow performance and mixing capabilities of the classical SAR and multilamination mechanisms in the exact flow configuration in which they will operate as implemented within these microreaction units. A more specific interest is to verify the suitability of applying the classical RTD analysis techniques to metallic microreactors tackling their inherent experimental difficulties such as restricted visualization of flow structures, constrained measurements at precise inlet and outlet planes, and influence of peripherals fluid lines in the stimulus signal.

The hydrodynamic and mixing characteristics of a split-and-recombination and a multilamination microreactor operating in laminar flow regime were investigated by means of RTD analysis and the Villermaux/Dushman method. The one-shot tracer input approach successfully allowed the RTD characterization of non-transparent metallic microreactors with unavoidable large peripheral volumes. Thus, this simple approach can be applied for the characterization of any microreaction unit. The *E(t)* signal recovery procedure by deconvolution in the Fourier domain proved to be a

reliable method for signal treatment during RTD analysis which simplifies the computational time as compared to other methods. The flow behavior in microfluidic structures was found to be adequately represented by the axial dispersion model which strength lies in that the relationship between the model parameters and the geometry of the reactor is well established from a theoretical basis. A decrease of the quadratic dependence of axial dispersion on fluid velocity was observed for both microreactors.

The hydrodynamic performance of the SAR microreactor is greatly affected by the flow distribution stage in the embedded manifolds. Inhomogeneous flow distribution was found to be caused by hydrodynamic imbalances (*i.e.* different ratios of flow rates) and by geometrical imbalances in the design. Since flow visualization is restricted in both microreaction units further investigation by means of CFD is recommended to clarify the extent of role of the manifold design on the flow distribution in the microchannel network.

From RTD analysis it is found that the SAR and LLMR operate more efficiently at low velocity conditions, *i.e.* long mean residence times. On the other hand, it was found from the iodide-iodate system that depending on the acid concentration the SAR and LLMR operates more efficiently at low *Da* whereas at higher values of $Da > 10$ the segregation indexes are comparable to those produced by a T-junction. Therefore, a compromise exists between the temporal and spatial mixing capabilities in both microreactors. A slightly better mixing performance can be achieved by the LLMR when compared to the SAR especially at low velocity conditions albeit at the expense of higher energy expenditure. The SAR mechanism advantage thus relies in achieving comparable mixing at considerably lower pressure drops.

Numerical Investigation

Microreactors achieve fast mixing by diffusion between very thin fluid layers that are produced by a variety of geometrical constraints (*i.e.* micromixing mechanisms). These constraints divide the main flow of reactant into several substreams. Thus, the mixing performance of microreaction systems also depends on the capability of the embedded manifolds to attain homogeneous

distribution of the fluids among the microchannel network. In order to obtain a faithful representation of the flow distribution mechanism and a true insight of the RTD of the microdevices, the complete manifold structures have been considered in this investigation. An analysis based on the complete microreactor volume can be of great assistance in the explanation of experimental results.

Due to the high aspect ratio of the microchannels, one challenge to overcome during the CFD analysis of microstructures is the number of elements needed to mesh the complete flow path. A suitable small element size must be chosen in order to have a minimum number of elements covering the shortest dimension of the microchannel. Due to high aspect ratios found in microfluidic devices, *i.e.* length over width, the use of such small element sizes can produce several hundreds of elements in the axial direction of one micromixing channel considerably increasing the computational effort. Also, a high aspect ratio may cause element skew that can negatively impact the solution of the simulation. The need for small element sizes can produce convergence issues when the element volumes reach the dimensional tolerance and precision limits ($\sim 10^{-15}$) of the programming code.

The methodology applied in this work is based on the aforementioned *decoupled CFD-mixing analysis*. The pressure drop is considered to describe the flow pattern while the intensity of segregation and the residence time are used to characterize the mixing. Pressure drop values computed from the velocity field for different flow conditions are used to validate the simulations with experimental data. The technique of injection and tracking of inert tracer particles described by **Heniche & Tanguy (2006)** is applied to allow for the quantification of concentration in the micromixing channels and for the estimation of CFD-based residence time distributions.

Heat Transfer Characterization and Continuous Flow Free-Radical Polymerization

The objective of this investigation was to characterize the heat transfer capabilities of two microreactors and to demonstrate their potential as chemical reactors for conducting the continuous free-radical polymerization of styrene monomer. The microreactors operate

respectively with the split-and-recombination (SAR) and multilamination mixing mechanism; and both units feature an integrated forced-convection heat exchanger. For the highest flow conditions investigated, the SAR and multilamination heat exchangers achieved maximum overall heat transfer coefficients of 3.02 and 2.8 kW/m^2-K respectively reaching efficiencies of ~0.95. Monofunctional, bifunctional, and tetrafunctional peroxide initiators were used for the polymerization runs at two reaction temperatures, *e.g.* 100 and 130 degrees C. The monofunctional initiator was able to produce conversions higher than 20% only at 100 degrees C, the bifunctional initiator achieved the same level of conversion at 130 degrees C only, and the tetrafunctional initiator produced higher levels of conversion at both temperatures. Low values of polydispersity indexes (*PDI* <1.7) were obtained for all the reaction conditions investigated with the samples obtained in the multilamination microreactor exhibiting an overall lower value than those produced in the SAR configuration.

CONDENSÉ EN FRANÇAIS

La technologie de microréaction est de nos jours une branche bien établie de l'ingénierie du micro procédé qui se concentre sur l'étude des réactions chimiques menées au sein des canaux d'écoulement miniaturisées communément appelés microréacteurs. De nos jours, il existe un vaste éventail de microréacteurs commerciaux, pensés et créés pour des opérations fiables et robustes. Ils peuvent être produits en grande quantité grâce à des techniques de conception de pointe. Par conséquent, la caractérisation de l'équipement de microréaction existant est nécessaire afin de trouver de nouvelles applications à cette technologie. Dans ce contexte, l'ingénierie des réactions de polymérisation pourrait bénéficier de l'expertise acquise à la microéchelle en termes de contrôle de la température et de haute vitesse de mélange étant donné que les réactions de polymérisation sont généralement hautement exothermiques et extrêmement sensibles au niveau de mélange des réactifs. Néanmoins, l'application de la technologie de microréaction aux procédés de polymérisation en mode continu est encore très limitée. L'objectif général de ce travail est de caractériser deux types de microréacteurs pour une meilleure compréhension de leur caractéristiques hydrodynamiques et de transfert de chaleur afin d'évaluer leur potentiel pour la production de polymères en mode continu.

Les deux microréacteurs investigués respectivement sont conçus à partir du principe de division-et-recombinaison de l'écoulement (SAR de l'acronyme anglais: *split-and-recombination*) et de multilaminage de l'écoulement aux moyens de structures interdigitales. Il s'agit des deux approches de conception les plus fréquemment rencontrées dans les microréacteurs industriels. Le microréacteur SAR est un prototype conçu en vue de supporter des conditions de haut débit et de haute pression. Le microréacteur par multilaminage *(LLMR-MIX-SI)* est commercialisé par IMM (Mainz, Germany) et se distingue par une haute capacité de transfert de chaleur. Ces deux modèles de microréacteurs sont munis d'un système de refroidissement à convection forcée. À notre connaissance, il y a peu d'information disponible décrivant leur performance.

Dans le but d'atteindre l'objectif principal de cette thèse la méthodologie de recherche de ce projet est divisée en trois objectifs spécifiques: i) la caractérisation expérimentale de l'hydrodynamique des microréacteurs, ii) l'investigation numérique de leur efficacité

hydrodynamique par mesure de la distribution des débits, et iii) la caractérisation du transfert de chaleur et les caractéristiques du procédé de polymérisation opéré en mode continu.

Deux aspects majeurs de la caractérisation expérimentale ont été abordés: l'analyse de la distribution des temps de séjour (DTS) et l'évaluation du mélange grâce à la méthode de Villermaux/Dushman. Les expériences de baisse de pression visaient à estimer le diamètre équivalent d'un tube droit qui produirait la même baisse de pression que les microréacteurs dans les mêmes conditions identiques de longueur et de débit afin de comparer leur performance et d'obtenir un paramètre géométrique pour l'évaluation de la consommation d'énergie dans des autres conditions d'opération.

Les diamètres équivalents trouvés sont de 0.602 mm pour le microréacteur SAR et de 0.411 mm pour le microréacteur de multilamination; ce dernier présente des baisses de pression 5 fois supérieures à celles observées dans la géométrie SAR. Ces valeurs peuvent être utilisées pour une plus ample estimation des baisses de pression à différentes conditions d'opération.

L'analyse de la DTS a été réalisée aux moyens de la technique d'injection d'un traceur par impulsion. Reconnue comme étant très fiable, cette approche permet d'obtenir avec une bonne précision la DTS de n'importe quel microréacteur. Elle est très utile pour étudier des systèmes opaques possédant un grand volume périphérique par rapport aux volumes actifs des microréacteurs. Dans ces conditions, la réponse DTS obtenue à la sortie du microréacteur est considérablement affectée par les caractéristiques du signal d'entrée. Par conséquence, le vrai signal du microréacteur doit être récupéré au moyen d'une opération de déconvolution. La déconvolution dans le domaine de Fourier s'est avérée être une méthode précise pour le traitement du signal qui réduit notablement l'effort de calcul comparativement à la méthode de la convolution directe couplée avec une méthode itérative d'optimisation des paramètres. Cette étude démontre également que cette approche simple peut être appliquée en tant qu'alternative pour la caractérisation de n'importe quelle unité de microréaction.

Grâce à des prédictions plus proches des données expérimentales, un modèle empirique d'écoulement est souvent préféré au modèle de dispersion axiale pour la détermination de la DTS

dans des microréacteurs. Par contre, dans ce travail le modèle classique de dispersion axiale s'est avéré être un meilleur choix pour prédire adéquatement le comportement de l'écoulement dans les structures microfluidiques. La meilleure performance du modèle de dispersion axiale par rapport au modèle empirique est en grande partie due au fait que les paramètres du modèle empirique sont purement heuristiques alors que ceux du modèle de dispersion axiale sont théoriquement liés à la géométrie du microréacteur et aux effets du phénomène de dispersion.

Les microréacteurs ont été comparés à des tubes équivalents produisant les mêmes baisses de pression. Les réacteurs tubulaires continus opérant en régime laminaire démontrent une dépendance quadratique de leur coefficient de dispersion axiale en fonction de la vitesse du fluide. Par contre, les deux mécanismes de micro mélange investigués dans ce travail ont montré une réduction significative de leur dépendance quadratique en fonction de la vitesse, ce qui est attribuée à l'homogénéisation efficace dans la direction radiale du traceur injecte.

L'analyse de la DTS révèle que les deux microréacteurs opèrent plus efficacement lors de longs temps de résidence, *i.e.* avec un nombre de Damköhler $Da > 10$. D'autre part, la caractérisation du mélange par la méthode de Villermaux/Dushman montre qu'en fonction de la concentration d'acide les microréacteurs opèrent plus efficacement pour un *Da* faible. Cela renforce la thèse de l'efficacité de courts chemins de diffusion dans les microréacteurs favorisant un mélange rapide par mécanisme moléculaire même lors d'un court temps de séjour. Cela suggère également que les débits produisant des valeurs de $Da < 10$ sont les conditions optimales d'opération pour tirer parti des capacités de mélange rapide de ces types de microréacteurs. Une performance de mélange légèrement supérieure peut être réalisée par la structure de type multilamination par rapport à la SAR en particulier dans des conditions de faible vitesse, mais cependant au détriment d'une surconsommation d'énergie.

L'avantage du microréacteur SAR est qu'il permet des performances de mélange comparables à des baisses de pression beaucoup plus faibles. Par ailleurs, on constate que la performance hydrodynamique du microréacteur SAR est grandement affectée par la distribution d'écoulement dans les collecteurs intégrés au microréacteur. Il a été montré qu'une distribution des débits non

homogène est attribuable aux déséquilibres hydrodynamiques, c'est-à-dire les différents rapports de débits dans chaque entrée, liés à la conception géométrique.

La visualisation directe de l'écoulement dans les microréacteurs est limitée en vertu des matériaux de construction en acier inoxydable. Ainsi, la modélisation de l'écoulement par dynamique des fluides numérique (CFD pour *Computational Fluid Dynamics*) a été appliquée pour caractériser la DTS et la capacité de mélange des microréacteurs retenus. L'objectif spécifique de cette partie est de clarifier le rôle du collecteur sur la distribution de l'écoulement dans le réseau des micros canaux.

Une étude CFD d'un microréacteur présente des difficultés. En raison du factor de forme élevé des micros canaux, le nombre d'éléments finis nécessaires pour le maillage complet du domaine d'écoulement est un des défis à surmonter lors de l'analyse CFD de microstructures. Une taille d'élément appropriée, suffisamment petite, doit être choisie afin d'avoir un nombre minimum d'éléments pour discrétiser la plus petite dimension des micros canaux. L'utilisation de d'éléments finis de petites tailles engendre des maillages très denses. Cela augmente considérablement la taille du système matriciel résultant de la discrétisation des équations différentielles gouvernant les phénomènes d'échange et par conséquent l'effort de calcul. Autre aspect et non des moindres, un factor de forme élevé est aussi susceptible de provoquer une forte distorsion des éléments du maillage ce qui peut nuire à la convergence de la solution. De plus, lorsque les éléments du maillage sont trop petits des effets d'échelle apparaissent qui poussent les codes CFD à leur limite de précision ne permettant pas de garantir la validité des prédictions.

Ce problème a été abordé en faisant un changement d'échelle des propriétés du fluide et sur les conditions de frontière avec le but d'augmenter la précision des calcules. Aussi pour diminuer le temps pour la résolution des systèmes d'équations on a suivi le partitionnement en sous-sections des structures 3D microfluidiques. L'utilisation de l'élément fini MINI mis en œuvre dans le logiciel par éléments finis POLY3D (Rheosoft, Inc.) a permis de réduire fortement la taille du système matriciel. Ce type d'élément est peu coûteux par rapport au nombre de degrés de liberté par élément généré qui influe directement sur la taille du système linéaire final à résoudre. Les valeurs expérimentales de baisses de pression sont utilisées pour valider les résultats des

simulations à différentes conditions d'écoulement. Les résultats numériques de baisses de pression sur les deux microréacteurs sont en excellent accord avec la théorie de l'écoulement laminaire et avec les résultats expérimentaux.

La phase de post-traitement a permis d'évaluer la distribution des débits dans les collecteurs du microréacteur SAR. La méthode de suivi de particules quant à elle a servi à l'analyse de la DTS. Les particules sont injectées à partir des deux entrées et suivies jusqu'à la sortie.

Il a été montré que dans le principe d'opération du microréacteur SAR, la conception géométrique des collecteurs de distribution produit un déséquilibre de l'écoulement dans le réseau de micros canaux. Par conséquent, chacun des cinq micros canaux de mélange se comportent comme des réacteurs indépendants avec différentes concentrations et différentes conditions d'écoulement. Cela est confirmé lors de l'analyse numérique d'injection de traceurs dans le réseau de micros canaux par les deux entrées. La quantité de traceurs détectés dans des micros canaux adjacents varie d'environ 12.5%. Pour le cas où un rapport d'alimentation égale est utilisé uniquement le microcanal central reçoit 50% de particules de chaque entrée. Pour les conditions dans lesquels le rapport d'alimentation est différent de un, un effet de recirculation à travers un ou deux micros canaux est détecté. Cela confirme les résultats obtenus au cours de la caractérisation expérimentale des deux microréacteurs.

Les changements dans les débits d'alimentation peuvent fournir un degré de contrôle dynamique des concentrations et des temps de séjour des réactifs dans le but de modifier la vitesse de réaction et de conversion lors d'une réaction chimique. Toutefois, on constate que pour le microréacteur SAR le comportement de l'écoulement détériore davantage tout déséquilibre déjà présent en lien avec la géométrie du microréacteur. De toute évidence, des améliorations dans la conception du SAR sont nécessaires afin de le rendre mieux adapté à un usage industriel.

En raison du mécanisme de multilamination du microréacteur LLMR, l'étape de mélange de ce microréacteur est confinée à la structure interdigitale. Ainsi, le mélange sur le LLMR n'est pas affecté par l'efficacité d'un collecteur. Cependant, la conception du LLMR comprend un distributeur après l'étape de mélange afin de séparer l'écoulement dans le but d'améliorer le

transfert de chaleur. Il se trouve que la symétrie du distributeur est capable de répartir uniformément le débit dans toutes les conditions analysées. Ce constat peut servir de ligne directrice pour l'amélioration de la conception de microréacteurs conçus selon le même principe.

Les DTS obtenues au moyen de la CFD montrent que le comportement de l'écoulement dans les microréacteurs peut être décrit avec précision par le modèle de convection pure. Les sections de réaction et de mélange des deux microréacteurs présentent un comportement similaire à celui des réacteurs tubulaires en régime d'écoulement laminaire. Toutefois, les réponses de décroissance exponentielle détectées sont caractéristiques des réacteurs à écoulement mixte et de plusieurs réacteurs à écoulement piston en parallèle. Les sections du microréacteur SAR sont ainsi mieux décrites comme un ensemble de réacteurs à écoulements parallèles avec un bon mélange radial.

Les résultats obtenus à partir de la simulation numérique ont permis de déterminer en régime d'écoulement laminaire les conditions d'opération optimales à partir desquelles les microréacteurs permettent d'atteindre le degré le plus élevé de mélange, la répartition la plus équilibré des débits et la plus étroite distribution des temps de séjour (DTS). Ces conditions de fonctionnement ont été exploitées pour étudier la polymérisation du styrène dans les microréacteurs continus. Nous avons considéré la réaction à radical-libre du styrène en présence d'initiateurs peroxyde a deux températures de réaction: 100 et 130 degrés Celsius. Trois types d'initiateurs chimiques on été employés: Luperox-A75 mono-fonctionnel, Luperox-331M80 bi-fonctionnel et Luperox-JWEB50 tetra-fonctionnel. En utilisant l'eau comme fluide modèle et différentes valeurs de capacité thermique de l'écoulement, la caractérisation du transfert de chaleur dans les microréacteurs a été faite durant la phase préliminaire de ce travail de recherche.

Pour les deux microréacteurs SAR et LLMR, le transfert thermique pendant la polymérisation continue du styrène à radicale-libre a été étudié en fonction du taux de conversion, du poids moléculaire et du type d'initiateur. Au débit de 420 ml/min, des coefficients de transfert de chaleur globaux de 3.04 et 2.8 kW/m2-K ont été obtenus respectivement pour le SAR et le LLMR. L'échangeur de chaleur SAR s'avère plus efficace lorsque son second dispositif plat de réaction en bas fonctionne en mode contre-courant. Au sujet du LLMR, la différence entre le rapport de surface-sur-volume des plaques de transfert de chaleur du fond et du haut est d'environ

24. Cependant, pour les conditions d'écoulement étudiées les deux plaques présentent des propriétés de transfert de chaleur comparables dépassant largement les objectifs fixés. Par conséquent, ce microréacteur convient bien pour les procédés où le transfert thermique est essentiel.

Nous avons montré dans cette recherche qu'une combinaison appropriée de la température de réaction, du débit, du type d'initiateur et de la concentration les microréacteurs permet d'atteindre un taux de conversion d'au moins 30%. Bien que de faibles poids moléculaires moyens soient obtenus, de faibles indices de polydispersité sont également obtenus. Cette caractéristique est d'une grande importance pour la production de matériaux tels que les peintures, les enduits et les films.

En outre, la polymérisation dans les microréacteurs peut être exploitée comme protocole d'initiation dans des procédés nécessitant une étape de pré polymérisation. Pour les taux de conversion atteints, les deux microréacteurs produisent des indices de polydispersité proches de la valeur limite théorique de 1.5. De façon générale, le microréacteur LLMR produit des valeurs de PDI plus basses comparativement au SAR. Ceci est conforme à nos résultats précédents qui dans des conditions d'écoulement identiques montrent que le LLMR a un rendement en mélange légèrement supérieur.

De manière générale, les résultats obtenus dans ce projet démontrent que la technologie de micro réaction est un bon choix pour effectuer des réactions de polymérisation en mode continu. Il apparaît qu'il est en pratique possible d'obtenir un taux de conversion d'au moins 25% en opérant le microréacteur dans des conditions, hydrodynamique et de mélange, optimales; des taux de conversion plus élevés exigeraient des temps de séjour plus longs c'est à dire des débits plus faibles. Les taux de conversion obtenus sont suffisamment élevés et font en sorte que l'étape de pré polymérisation apparaît utile dans le cadre d'un procédé de polymérisation visant la production de matériaux polymères à poids moléculaire élevé, de copolymères ou encore de structures composites.

Il a été constaté que la distribution de l'écoulement du fluide a un impact important sur la réduction de la consommation d'énergie des microréacteurs, tout en maintenant le même degré d'efficacité du mélange, en augmentent le temps de séjour et en multipliant les surface d'échange. Cependant, le choix de la géométrie du microréacteur afin d'assurer une distribution du débit homogène, est essentielle a la performance du mélange et de la DTS.

Des nouveaux arrangements microfluidiques et des concepts géométriques optimisés sont nécessaires pour distribuer efficacement l'écoulement principal dans plusieurs canaux afin d'exploiter pleinement les possibilités de mélange et de transfert de chaleur opérés dans les différents microcanaux. Une bonne stratégie pour supporter ce type de développement consiste à employer les simulations CFD afin d'étudier le potentiel des nouvelles géométries.

TABLE OF CONTENTS

LIST OF TABLES

LIST OF FIGURES

NOTATION

Symbol	Description	Units
a	Concentration of species a in terms of volume fraction	dimensionless
A	Area under the concentration curve	mol-s/m^3
A_{in}	Total area of inlet plane	m^2
A_T	Heat transfer area	m^2
b	Concentration of species b in terms of volume fraction	dimensionless
Bo	Bodenstein number	dimensionless
C	Concentration	mol/m^3
C_c	Cold fluid heat capacity	W/K
C_{cr}	Characteristic concentration	M^{n-1}
C_f	Cost function	dimensionless
C_h	Hot fluid heat capacity	W/K
C_{in}	Tracer input concentration signal	mol/m^3
C_{out}	Tracer output concentration signal	mol/m^3
COV	Coefficient of variance	dimensionless
C_p	Specific heat	J/kg-K
C_r	Heat capacity ratio	dimensionless
d_{eq}	Equivalent diameter	m
D	Axial dispersion coefficient	m^2/s
Da	Damköhler number	dimensionless
D_{diff}	Molecular diffusion coefficient	m^2/s
E	Exit-age distribution function	dimensionless
f	Friction factor	dimensionless
I_s	Intensity of segregation	dimensionless
J	Content of particles in a line-sample	particles-mm
k_{cr}	Characteristic reaction constant	M^{1-n}/s
k_i	Number of counts per bin	dimensionless
Symbol	**Description**	**Units**

l	Length	m
m	Mass flow rate	kg/s
M_w	Weight average molecular weight	g/mol
n	Reaction order	dimensionless
N_b	Total number of bins	dimensionless
N_t	Total number of tracer particles	dimensionless
P	Pressure	Pa
Pe_r	Reaction Peclet number	dimensionless
Q	Volumetric flow rate	m^3/s
r	Radial position of tracer particles	m
r_Q	Ratio of flow rates	dimensionless
R	Radius of the inlet tube	m
Re	Reynolds number	dimensionless
s	Frequency	Hz
Sc	Schmidt number	dimensionless
S_s	Scale of segregation	mm
t	Time	s
t_{cr}	Characteristic reaction time	s
t_{diff}	Diffusion time	s
t_m	Mean residence time	s
T	Temperature	K
T_c	Temperature of the cold fluid	K
T_h	Temperature of the hot fluid	K
T_i	Inlet temperature	K
T_o	Outlet temperature	K
U_o	Overall heat transfer coefficient	W/m^2-K
v	Fluid mean velocity	m/s
$\mathbf{v}$	Velocity vector	m/s
V	Active volume,	m^3
X	Line-sample	mm
Symbol	**Description**	**Units**

X_s	Segregation index	dimensionless
Y	Yield of the Dushman reaction	dimensionless
Y_{st}	yield of the Dushman reaction in total segregation	dimensionless
ΔT_{ln}	Logarithmic mean temperature difference	dimensionless
ε	Heat transfer efficiency	dimensionless
μ	Newtonian viscosity	Pa-s
μ_k	Mean value of counts per bin	dimensionless
ρ	Mass density	kg/m^3
$\boldsymbol{\tau}$	Stress tensor	Pa

CHAPTER 1

INTRODUCTION

1.1 MICROREACTION TECHNOLOGY

Microreaction technology is presently a well established subfield of the chemical microprocess engineering that focuses on the study of chemical reactions conducted inside of the microstructured flow channels of miniaturized chemical reactors commonly referred as *microreactors*.

A microreactor can be formally defined as "*a casing for performing chemical reactions that is designed or selected to induce and exploit deliberately microflow phenomena*" (**Ehrfeld et al., 2001**).

Microreactors are essentially miniaturized static mixers that operate in continuous mode under pressure driven flow. They can be composed of single or multiple parallel microchannels of different lengths, shapes, cross sections and aspect ratios. The characteristic dimensions of the microchannels cross sections, usually in the micrometer range, are too large in order to interact with the reactants on a molecular level. Hence, the kinetic mechanisms of chemical reactions conducted in microreaction equipment are expected to remain unchanged. On the other hand, the gradients of the physical properties of a material are increased when its linear dimensions are reduced. The temperature and concentration gradients are particularly important for the control of chemical engineering processes. Consequently, microreaction technology has drawn great attention from the process engineering community during the last decades due to the benefits that can be expected from equipment miniaturization. Moreover, the small cross sections of the microchannels generate typical fluid layers that can be manipulated to stretch to a few tenths of micrometers. Thus, fast mixing by diffusion in the range of milliseconds is possible inside microreactors (**Hessel *et al*., 1997; Knight *et al*., 1998; Ehrfeld *et al*., 1999; Löb *et al*., 2004**). These benefits have been the main driver for extensive research and characterization of

microdevices that presently can be mass produced by state-of-the-art manufacturing techniques such as micromachining with laser radiation (LIGA process) (**Ehrfeld & Lehr, 1995; Arnold *et al.*, 1995**), micromolding, advanced mechanical milling based on precision engineering (**Kussul *et al.*, 1996**), micro-electrodischarge machining (μ-EDM) (**Ehrfeld *et al.*, 1996; Richter *et al.*, 1997**), laser ablation (**Zissi *et al.*, 1996**) and bulk micromachining (**James *et al.*, 1993**) among others. Some of these techniques have allowed for the construction and commercialization of tightly assembled metallic microreactors with high pressure and temperature ratings. These mechanically robust microdevices along with their fast mixing and efficient heat transfer (**Brandner *et al.*, 2000; Schubert *et al.*, 2001**) have opened a new envelope of reaction conditions otherwise inaccessible in macroscopic equipment.

Other advantages such as increased safety of operation and system versatility place microreaction technology as an attractive alternative over conventional large-scale reactors for specific applications. For instance, the active volume of microreaction equipment is significantly small typically amounting to a few microlitres and the material hold-up can be further decreased when a batch process is replaced by a continuous microreaction system. This smaller hold-up increases safety of operation and due to shorter residence times the selectivity of the process can be improved. If higher production volumes are desired, an increase in throughput can be achieved by a *numbering-up* approach instead of a conventional scale-up strategy. A larger number of microreactors results in higher flexibility in adapting production rates to varying demand since a certain number of units can be disconnected or added to a microreaction production plant. A plant design based on a large number of small microreaction units can offer the versatility to perform a wide variety of reactions by changing the piping network (**Ehrfeld *et al.*, 2001**). This flexibility may be further supported by a considerably broader range of operating conditions attainable in microreactors as compared to a macroscopic system. Finally, the numbering-up approach guarantees that the desired features of a single microreaction unit are maintained when increasing the total size of the production plant. Thus, the hydrodynamic and reaction performance of individual microreaction units becomes of critical importance when envisioning the numbering-up production approach. Specific fields (*e.g.* pharmaceutical industry, fine chemicals) have been identified where either microreactors exhibit a better performance than conventional large-scale reactors or their lower specific production capacity is counterbalanced by cost savings due to

other factors such as replacement of batch processes by a continuous system, process intensification, increased safety, better control of product properties, and on-site/on-demand production (**Ehrfeld *et al*., 2001; Hessel *et al*., 2004**).

Despite the aforementioned advantages of microreaction technology, there is still skepticism about its potential application for industrial production. These reservations are mainly in regard to limited yields (**Ehrfeld *et al*., 2001**) and to high energy consumption in processes involving highly viscous and/or non-Newtonian fluids (*e.g.* polymerization reactions). Concerns have arisen among the chemical engineering community about possible fouling problems in microreactors and about if acceptable levels of reliability can be reached for automated industrial processing. Large chemical manufacturers assume that acceptable production has to occur in hundreds or even thousands of parallel streams. They refer to problems of uniformly splitting one main stream into a multitude of substreams as a major concern. Cleaning procedures after shutdown of the system, common for laboratory equipment, are said to be inconceivable for industrial production plants composed of thousands of microchannels (**Hessel *et al.*, 2004**).

Therefore, in order to be industrially successful microreaction technology must be able to meet certain general criteria when compared to conventional production techniques. These criteria can be related to attaining the necessary operating conditions to: 1) improve the quality of the final product or 2) improve the characteristics of the process itself (*e.g.* increased safety, elimination of separation processes, improved selectivity and yield, energy savings). Moreover, microreactors must be capable to sustain a reliable continuous operation by the numbering-up approach in order to achieve targeted production levels.

1.2 MICROREACTION TECHNOLOGY IN POLYMER REACTION ENGINEERING

Polymerization reactions are usually highly exothermic and are extremely sensitive to the level of mixing of the reactants (**Nauman & Buffham, 1983**). Polymer reaction engineering applications could fully exploit the benefits of microreaction conditions in terms of temperature control and

fast mixing. Nevertheless microreaction technology has not been extensively applied in continuous polymerization processes. One probable cause is that the highly viscous fluids particularly encountered in polymer reaction engineering applications might limit or even restrict the equal flow distribution of reactants among several parallel microchannels. This inhomogeneous distribution of reactants can affect the selectivity and degrade the overall yield of the process counterbalancing the improvements achieved in one single microchannel. Also, the viscosity evolution of a polymerizing mixture as well as the non-Newtonian behaviour of polymer solutions might pose major challenges not only in terms of the flow distribution but also on the energy consumption derived from the pressure drops produced by such highly viscous materials flowing through the small microchannels cross sections.

In order to assist the potential polymer production in microreaction systems, a decrease of the process viscosity can be achieved by the use of high temperature reaction conditions. Since the polymerization rate increases with the reaction temperature, in order to prevent a reaction runaway this alternative demands for a strict control over the heat of reaction which in principle can be attained using microreaction equipment. On the other hand, the polymer final properties such as the average molecular weight and polydispersity index are known to be affected as the temperature of polymerization is increased thus presenting a compromise if a high reaction temperature condition is chosen. In order to avoid this effect, another common practice to control the viscosity of a polymerizing mixture is the addition of an organic solvent, *i.e.* solution polymerization. In this scenario and depending on the conversion level desired, the solvent content could influence the kinetics of the reaction restricting the yield of the product and/or affecting the evolution of rheologically based polymer morphologies. Furthermore, the interaction between active radicals and common organic solvents during the polymerization can decrease the polymer final molecular weight due to the transfer-to-solvent effect. Also, other factors must be taken into account when conducting a polymerization in the presence of an organic solvent such as the solubility of the polymer in solvent, the separation of the final product from the solvent, the purity of the products and the toxic effect of residuals.

Such advantages, challenges and potential limitations of polymerization in microreactors have not been properly addressed in the available scientific literature and experimental evidence of the

polymerization capabilities of microreactors is limited. Characterization of polymerization processes conducted in microreactors is required in order to assess the benefits and possible drawbacks of this type of technologies as compared to conventional large-scale polymerization techniques.

1.3 MIXING CHARACTERIZATION OF MICROREACTORS

The mixing state of reactants is of critical importance for polymerization reactions and a homogeneous mixing at the early states of the reaction can modify the reaction conditions and the course of polymerization. Fast mixing by diffusion between thin fluid layers is indeed one of the main features of microreaction technology. An understanding of the fluid mixing mechanisms in microreactors is critical in order to fully exploit the characteristics of microflow phenomena for process engineering applications. The mixing operation can be characterized by experimental techniques and numerical simulations. These latter are especially useful in the microscale where microreactors operate in the laminar flow regime. Besides reduction of fluid layers by geometrical constraints microreaction equipment has also relied in specific designs such as grooved walls or bending and turning concepts in order to promote streaming phenomena (*i.e.* secondary flows) to improve the radial mixing in single microchannels. The mixing improvement effects of these secondary flows have been detected experimentally by test reactions and corroborated by flow visualization in transparent microfluidic devices (**Ehrfeld *et al.*, 1999; Engler *et al.*, 2004; Schönfeld & Hardt, 2004; Kockmann *et al.*, 2006**). The causes of such mixing effects have been better understood by the use of computer simulations (**Mengeaud *et al.*, 2002; Stroock *et al.*, 2002a; Stroock *et al.*, 2002b; Aubin *et al.*, 2003; Hardt & Schönfeld, 2003**). Local flow information is of critical importance in the conception of micromixing mechanisms and optimization of microreactor designs. However, flow parameters such as velocity, pressure and temperature are hardly accessible by common experimental techniques due to the relative size between microchannels and existing measuring probes. Thus, *computational fluid dynamics* (CFD) appears as a valuable tool in order to describe 3D microflow mechanisms and to characterize the hydrodynamic performance of microreaction units with intricate internal

flow structures. Numerical simulations can be especially of great assistance for the flow characterization of microreactors manufactured in non-transparent materials.

Reactor analysis of a flow system at any scale level is oriented towards the understanding of the relationship of the characteristics affecting its performance, *i.e.* kinetics, flow patterns, mixing, mass transfer and heat transfer (**Nauman, 2008**). *Residence time distribution* (RTD) theory is a major tool for analysis that provides substantial insight of flow behavior and mixing processes and their interaction with the kinetics of reactions occurring inside a flow vessel. The time a molecule spends under reaction conditions in a reactive system will affect its probability of reacting. Therefore the measurement, interpretation and modeling of RTD are important aspects for the prediction of the final composition of the system. Since its first stages of development and consolidation (**Danckwerts, 1953**) the RTD remains one of the most relevant parameters for reactor characterization.

In order to quantify the mixing capabilities of microreactors competitive-parallel reactions have been applied. Specifically, the iodide-iodate reaction system has been adapted for the characterization of continuous flow in microdevices in what is also known as the *Villermaux/Dushman method*. While the analysis of RTD provides information about the state of macromixing, conclusions drawn from the yield and selectivity of the Villermaux/Dushman method can be related to the state of micromixing of the components in the reactive mixture.

The preceding methodologies of RTD analysis and the Villermaux/Dushman method, which will be discussed in subsequent chapters, have been applied experimentally for the characterization of prototype and commercial microfluidic devices. However, some difficulties inherent to the size and volumes of microreactors have to be considered during the adaptation of these techniques. For instance, during the RTD analysis the contribution of the volumes of the peripheral fluid lines to the final residence time has to be considered since these volumes are around the same order of magnitude than the actual microreactor active volume.

Regarding numerical simulations, the use of validated CFD codes have facilitated the application of different criteria for the characterization of flow and mixing characteristics such as the

concepts of *scale and intensity of segregation*. These concepts as defined by **Danckwerts (1952)** are related respectively to the dispersive and distributive characteristics of the flow system and both quantities are defined and determined by statistical methods at specific measuring points. This fact highlights the suitability of CFD techniques to measure these quantities at very accurately defined planes and flow locations, an otherwise troublesome task during experimental procedures in microdevices. Other criteria not easily derived from experimental characterization techniques but readily accessible by numerical simulations, *e.g.* stretching and elongation efficiency, deformation rate and the Lyapunov exponent, have been used to characterize the flow and mixing capabilities of macroscopic static mixers (**Rauline *et al.*, 1998, Heniche & Tanguy, 2005**) and applied to microscale flow devices as well (**Aubin *et al.*, 2003**).

1.4 SCOPE OF THE PROJECT

Although extensive effort by the scientific community has been directed towards the experimental and numerical characterization of microdevices based on new micromixing mechanisms, most of such investigations have been conducted on laboratory equipment intended for visualization purposes and not for more demanding operating conditions. Presently, there is a large repertoire of commercially available microreactors designed and built for mechanical robust operation. These microreaction units are usually constructed with several parallel microchannels in order to increase the throughput while retaining the process performance of individual flow structures, and are often designed with different flow sections within the same unit (*i.e.* mixing, heat transfer, reaction). While single microchannel geometries have been extensively characterized, the flow performance of microchannel networks employed in high throughput commercial microreactors have not been investigated. Only few experimental reports exist on the characterization of such units and information about their capabilities as polymerization reactors is not available at all. In this context feasibility studies are necessary in order to determine the extent of applicability of microtechnology in the polymer reaction engineering field. For such applications, the flow distribution in microchannel networks can affect the heat transfer and mixing efficiency at the microscale modifying the working conditions accessible during polymerization which will consequently affect the final properties of the product.

1.5 GENERAL OBJECTIVE

The general objective of this project is to develop a better understanding of the hydrodynamic and mixing characteristics of the split-and-recombination and the multilamination microreactor commercial designs in order to test the feasibility of microreaction technology to be used for continuous polymer production.

The peroxide initiated polymerization of styrene monomer will be used as reaction system. A conversion level of 30% is set as the primary objective since this level of conversion is known to be critical in the development of another styrene polymerization process, *i.e.* the High-impact Polystyrene (HIPS) system. The characteristic morphology of the polybutadiene and polystyrene phases in the HIPS system is achieved during a phase inversion process between the polybutadiene matrix and the polystyrene droplets. This phase inversion occurs in the range of 20-30% of conversion. There are different critical variables that affect this phase inversion process such as thermodynamic equilibrium, system viscosity, state of micromixing, and shear rate achieved in order to reduce and sustain droplet size, among others. Some of these variables, *e.g.* viscosity, micromixing and shear rate, could be greatly affected by microreaction conditions. However, microreactor characterization must be conducted beforehand in order to determine the hydrodynamic performance of the system, and consequently select the optimal operating conditions. Therefore, as a preliminary stage of the HIPS process, this work will focus on a polystyrene-only system aimed at proving that at least 30% of conversion can be achieved in microreactors.

The methodology of this project is structured as to address the hydrodynamic and mixing performance, the heat transfer capabilities and the level of conversion of polymer achieved on two microreactors featuring different micromixing mechanisms with integrated heat exchangers. The mixing mechanisms considered are the split-and-recombination (SAR) mechanism and the multilamination of flow by means of interdigital structures which are two mixing principles most frequently featured by commercial microreactors.

CHAPTER 2

LITERATURE REVIEW

2.1 INTRODUCTION

The present chapter is devoted to the review of the scientific literature necessary for the development of this project. The effort is oriented towards the identification of suitable microreactors with industrial potential, especially those commercially available, and to provide information on the appropriate techniques for their characterization. The body of this literature review is organized around four main concepts. The first serves as a historical background briefly outlining the evolution in industrial processing from agitated tanks to the implementation of the static mixer for the improvement of continuous flow processes. The second and third concepts refer to the publications that have focused on the experimental and numerical characterization methods adapted to microfluidic devices. The last concept deals with publications that have reported the application of microreaction technology for polymerization processes. Finally, this chapter closes with a summary section including a series of tables condensing the surveyed literature on selected topics as well as a brief discussion leading to the formulation of the specific objectives of the project that are stated in the next chapter.

2.2 BACKGROUND ON PROCESSING IN CONTINUOUS OPERATION

2.2.1 Polymerization in Tubular Reactors

Mixing is an essential unit operation in the process industry that includes the mixing of miscible fluids in single phase flow, dispersion of gas into a continuous liquid phase, dispersion of immiscible phases for the formation of emulsions, three-phase contacting, mixing of solids and heat transfer enhancement among others. These mixing processes have been traditionally

performed by means of mechanically agitated tanks. In order to meet the increasing demand of plastic materials, polymerization reaction systems for continuous and semi-continuous operation were developed based on these agitated tanks commonly referred to as *continuous stirred tank reactors* (CSTR). The scale-up of such processes has been a necessary engineering endeavour that has brought a compromise between increased production, material quality and energy savings. When the volume of a CSTR is increased, the surface-to-volume ratio is reduced which added to the viscous nature of polymerization reactions can restrict the heat and momentum transfer capabilities of the system. Large temperature variations influence the distribution of molecular weights of polymer materials thus affecting the properties of the final product. Also, this effect compromises process safety since large temperature gradients in a polymerization tank coupled to the viscous nature of the reactive mixture can originate a reaction runaway.

Tubular reactors for polymerization in continuous operation (**Citron-Cordero et *al.*, 1968; Wallis *et al.*, 1975a; Baillagou & Soong, 1985; Hamer & Ray, 1986**) have been used as an alternative to the CSTR in order to overcome the problems related to heat transfer and temperature control. Besides high heat transfer capabilities tubular reactors also offer simple geometry, low cost of operation/maintenance and depending on the flow regime reached they can achieve flat velocity profiles providing narrow residence time distributions. In addition, due to their small hold-up time tubular reactors exhibit increased process safety as compared to a process conducted in a CSTR. One of the most comprehensive investigations of continuous polymerization in tubular reactors was reported by **Wallis *et al.* (1975a, 1975b)**. In that work a tubular reactor of 2.362 cm of diameter and 6 m of length was used for the bulk polymerization of polystyrene up to 32.1% of conversion and weight average molecular weights in the range of 80,000 to 140,000 gr/mol.

Despite the aforementioned advantages, elongated velocity profiles caused by changes in viscosity can affect the performance of a polymerization tubular reactor (**Lynn & Huff, 1971**). One of the operational difficulties of tubular reactors used for continuous polymerization is the relationship between the hydrodynamics of the reactive media and the kinetics of the polymerization reaction. The factors governing the kinetics of a polymerization reaction, *i.e.* reactant concentration and temperature, largely depend on the hydrodynamic performance of the

reactor. This hydrodynamic performance is influenced by the viscosity of the reactive media which in turn depends on the reaction temperature, polymer conversion and its average molecular weight. Furthermore, the elongated velocity profiles produced by changes of the viscosity of polymer solutions may cause the polymer to sediment in the tube walls promoting fouling or plugging of the reactor. Fouling will further change the heat transfer performance of a tubular reactor affecting the polymer characteristics. Distorted velocity profiles can be minimized if a recirculation stream is introduced into the main flow line (**Lynn & Huff, 1971; Nguyen *et al.*, 1990; Cabral *et al.*, 2003**) and depending on the flow conditions the ratio of recirculation can be modified in order to achieve nearly flat velocity profiles. Recycle reactors, *i.e.* reactors featuring a recirculation stream have been frequently used in combination with tubular reactors fitted with in-line static mixers placed at the exit of the recirculation loop in order to improve the radial homogenization of the main flow. Static mixers achieve homogenization without the use of moving parts and the energy required for mixing is supplied by the pumps. Static mixers are used in continuous processes for units operations such as mixing, heat and mass transfer, dispersing and chemical reaction engineering applications.

2.2.2 Static Mixers

Static mixers are composed of motionless inserts called *elements* which are installed in empty pipes or columns. The objective of these elements is to distribute the fluid in the transverse direction to the main flow. Each static mixer element divides the incoming flow and recombines it in a geometric sequence so that intensive radial mixing produces nearly plug flow behavior. They can provide homogenization of feed streams with minimum residence times and thus, a better control of the rate of production; they require less maintenance and usually exhibit lower energy consumption than a CSTR. Presently, there are a wide variety of static mixers designs available and their performance is well characterized. According to **Thakur *et al.* (2003)** there are approximately 2000 US patents and more than 8000 literature articles that describe static mixers and their applications as well as more than 30 commercial models currently available for specific industrial tasks.

The most investigated application of static mixers in tubular polymerization reactors combines a recycle tubular reactor in a prepolymerization stage followed by a tubular reactor fitted with in-line static mixers (**Tien *et al.*, 1985; Meyer *et al.*, 1988; Meyer & Renken, 1990; Nguyen *et al.*, 1990; Chen, 1994**). Based on a pilot-plant investigation by **Tien *et al.* (1985)** a two stage polymerization process for crystal polystyrene called *SDS process* (**Tauscher *et al.*, 1996**) began commercial operation in 1988 using a recirculation loop reactor for prepolymerization up to 60% of conversion and a completely tubular reactor vessel to further increase the conversion. Both reactors were fitted with *Sulzer SMX* static mixers. Another two stage process for continuous bulk polymerization of crystal polystyrene was reported by **Chen (1994)** in which a tubular reactor fitted with *Kenics* static mixers was used as a second polymerization reactor to advance conversion form 70% to 95%. In the above mentioned investigations it was shown that the flat velocity profiles obtained by means of the static mixers produced low temperature gradients along the tubular reactor that allowed for a better control of polydispersity. In these investigations the choice of a recirculation loop with in-line static mixers was used as a prepolymerization stage reactor in order to ensure a good mixing state and to increase conversion to acceptable levels (> 20%) before entering the tubular reactor.

2.2.3 Microreaction Technology in an Industrial Process

Indeed the improvement of a prepolymerization stage was one of the first cases reported in which microreaction technology was used for polymer reaction engineering applications. Microreactors can be regarded as miniaturized static mixers and in principle their performance should exceed or at least be comparable to that of conventional static mixers. In this context, some potential benefits of microreactors such as enhanced process reliability and increased reactor efficiency were assessed experimentally in one of the first investigations of a continuous polymerization system involving microreactors. The case study was conducted at *Axiva* (Frankfurt) and consisted in the application of microreactors in the prepolymerization stage of the production of acrylates (**Bayer *et al.*, 2000a**) where the interdigital mixing mechanism employed for the premixing of reactants was able to narrow the distribution of molecular weights of the polymer produced. The aforementioned work of **Bayer *et al.* (2000a)** on polymerization and that of **Wörz *et al.* (2001a-b)** regarding improvements in yield and selectivity of industrial reactions were the first

experimental investigations that showed the promising results and potential benefits of microreaction systems for industrial production.

2.3 MIXING MECHANISMS OF MICROREACTORS

Due to their small channel dimensions microreactors usually operate in the laminar flow regime and many flow arrangements based on different mixing mechanisms have been used for microreactor development (Figure 2.1). The majority of this type of mixing mechanisms is based on diffusional mixing between fluid layers without any assistance of turbulence.

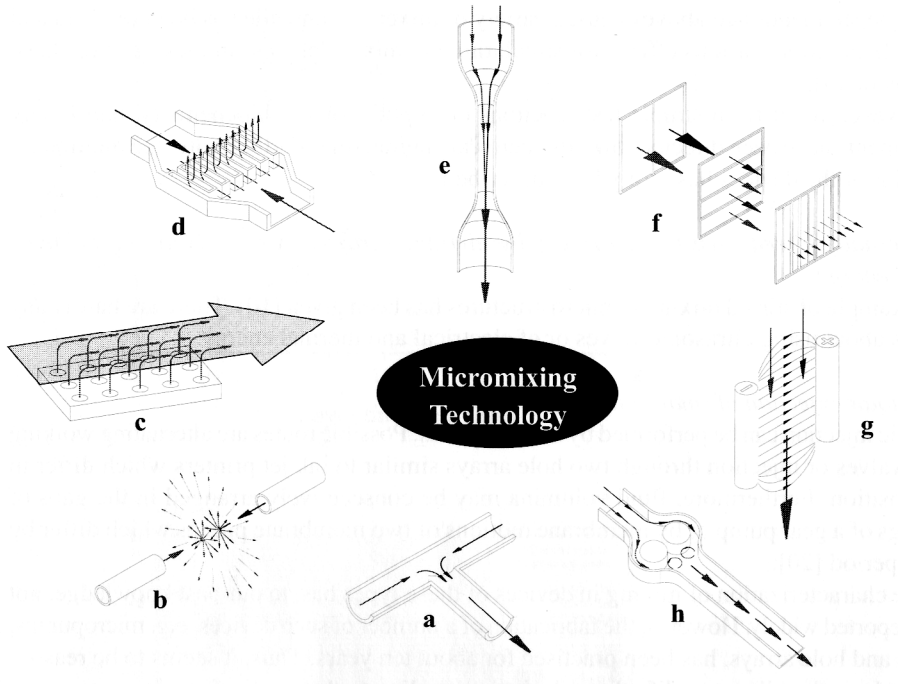

Figure 2.1 Flow arrangements based on different mixing mechanisms (**Löwe *et al.*, 2000**) most commonly used in microfluidic devices: a) contacting of two substreams, b) collision of two substreams of high energy, c) injection of many small substreams of one component into a main stream of another component, d) injection of many substreams of two components, e) decrease of diffusion path perpendicular to the flow direction by increase of the flow velocity, f) manifold splitting and recombination of a stream consisting of two fluid lamellae of two components, g) externally forced mass transport, h) periodic injection of small fluid segments.

The formation of thin fluid layers is achieved simply by division of the main stream into several substreams or, in the case of a single microchannel, by the reduction of the channel width along the flow axis. Thus, large contacting surfaces and small diffusional paths are generated.

Although diffusion is the dominant mechanism on the microscale, a number of microdevices improve their mixing efficiency by means of assisting streaming phenomena such as secondary transverse flow produced by grooved channels (**Stroock *et al.*, 2002b**) or by flow bending and turning concepts (**Mengeaud *et al.*, 2002; Hardt & Schönfeld, 2003; Engler *et al.*, 2004; Schönfeld & Hardt, 2004**).

From the mixing mechanisms shown in Figure 2.1, the injection of many substreams (d) and the split-and-recombination of streams (f) are two mechanisms that have been extensively investigated and which are the base of design of several commercially available microreactors.

2.3.1 Multilamination Mechanism

A micromixing device featuring the injection of streams of two components was developed by the *Institut für Mikrotechnik Mainz* (*IMM)* in Germany. In this type of microdevice two different fluids are split into many substreams by means of a multilamination inlay (Figure 2.2a) yielding a typical layer thickness of a few tens of micrometers (**Ehrfeld *et al.*, 1997; Ehrfeld *et al.*, 1999; Haverkamp *et al.*, 1999**). By means of the interdigital arrangement of the microchannels, an alternated configuration of layers of the fluids to be mixed is generated and fast mixing by diffusion takes place when the laminated flow leaves the multilamination inlay perpendicularly to the direction of the feed flow (Figure 2.2b).

Besides from homogeneous mixing processes, interdigital microdevices have been applied in multiphase processes, *e.g.* liquid-liquid dispersion. The droplet size and droplet size distribution as a function of the varying flow conditions have been the subject of different investigations for the generation of emulsions and semi-solid creams with interdigital microreactors (**Haverkamp *et al.*, 1999; Bayer *et al.*, 2000; Pennemann *et al.*, 2005; Löb *et al.*, 2006**). Other applications such as gas-liquid contacting have been explored although to a lesser extent (**Löb *et al.*, 2004**).

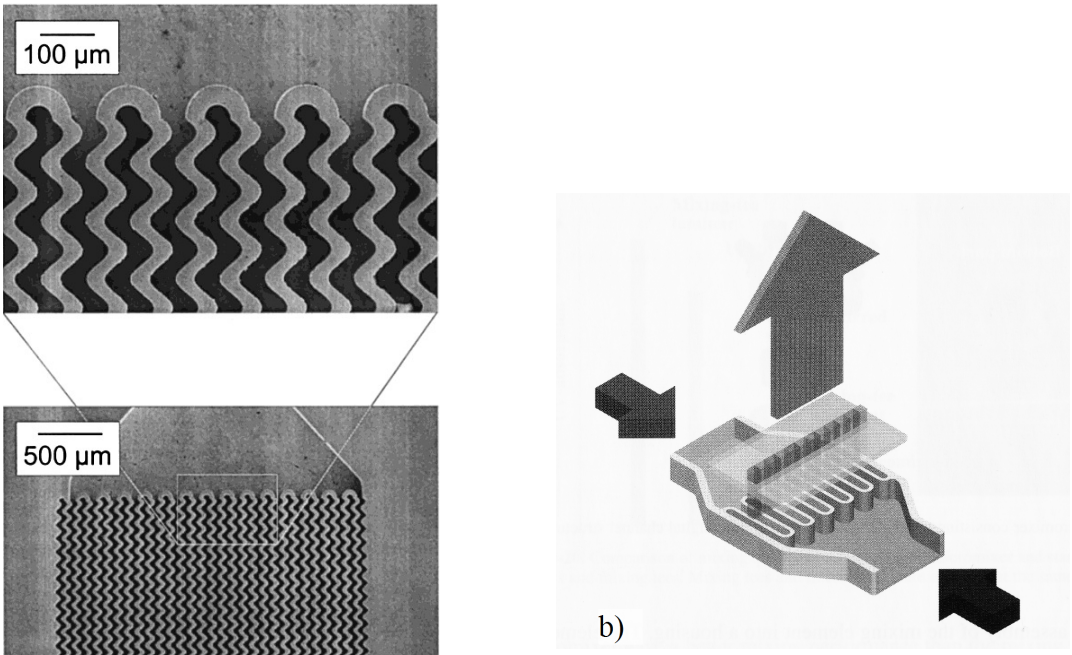

a)

Figure 2.2 Interdigital microdevice by *IMM*: a) scanning electron micrographs of the multilamination inlay (from **Ehrfeld *et al.*, 1999**), b) schematic of the flow direction (from **Ehrfeld *et al.*, 2001**).

Another interdigital microreactor with high heat transfer capabilities has been developed by the *IMM* specifically for liquid-liquid contacting applications. This liquid-liquid interdigital microreactor was developed in conjunction with BASF (**Wörz *et al.*, 2001a-b**) in order to improve the selectivity and yield during the thermally sensitive synthesis of a vitamin precursor. The design features an interdigital mixing structure and includes an integrated heat exchanger targeting to conduct the reaction in isothermal conditions. With the purpose of extending its operational range this microreactor was constructed with a modular design (**Richter *et al.*, 2000**) consisting of four parallel micromixing plates based on the single plate version of the *LLMR-MIX-SI* microreactor (**www.imm.de**). Although the BASF reaction is not extremely sensitive to mixing, by-product reductions of 50% and an increase of 20% of the overall yield at nearly

isothermal conditions were reported by **Wörz *et al.* (2001a-b)**. According to **Ehrfeld *et al.* (2001)** another liquid-liquid reaction more sensitive to the degree of mixing has been performed in this type of modular microreactor. Even though no further details of this latter investigation are disclosed, it is noted that good results were obtained indicating that the interfacial areas achieved with this interdigital microreactor might be higher than for a simple bilayer system (*e.g.* mixing tee). However, no information has been documented either on the hydrodynamics, heat transfer capabilities or mixing performance of the *LLMR-MIX-SI* microreactor or its modular version.

2.3.2 Split-and-recombination (SAR) Mechanism

This well known principle of stream split-and-recombination (SAR) has been applied in many macroscopic static mixers. The two configurations that have been most applied to achieve the split-and-recombination mixing sequence in microdevices are the ramp-like (Figure 2.3) microchannels and fork-like elements (Figure 2.4) (**Schwesinger *et al.*, 1996**).

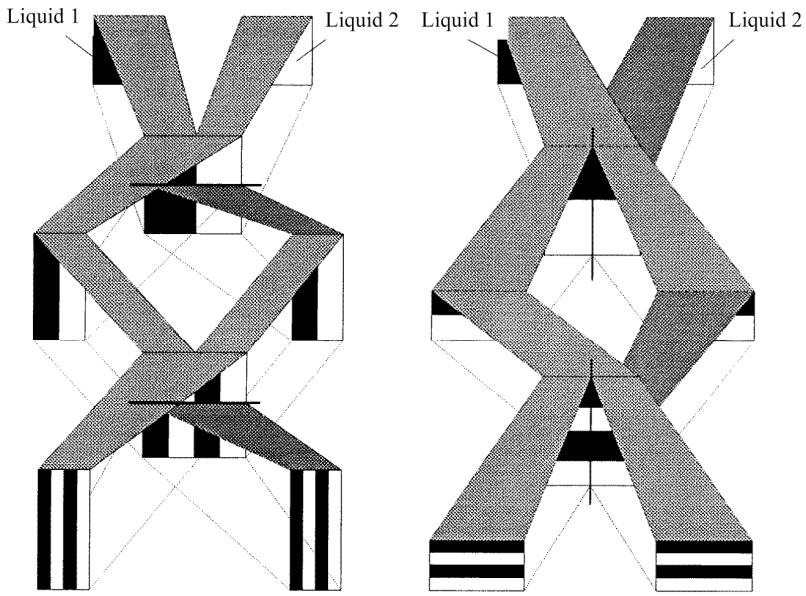

Figure 2.3 Split-and-recombination principle using ramp-like structures: a) vertical split and horizontal recombination; b) horizontal split and vertical recombination (from Schwesinger et al., 1996).

The distinctive feature of the split-and-recombination mechanism in comparison to the multilamination mechanism is that fluid lamination can be achieved without mechanically dividing the flow by walls thus eliminating the need for replication of single microchannel constraints. Hence, larger throughputs at a given pressure drop can be obtained.

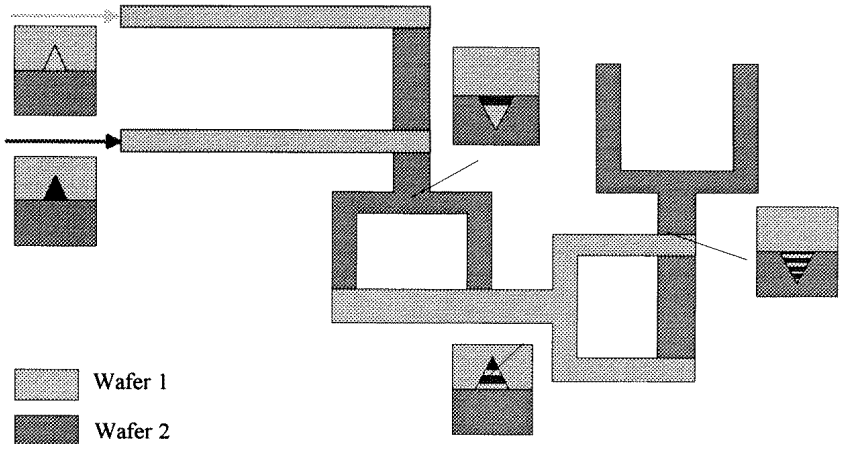

Figure 2.4 Schematic representation of the split-and-recombination fork-like elements (from **Schwesinger *et al.*, 1996**).

Kirner *et al.* (2004) conducted a mixing characterization by means of optical analysis on a silicon chip with a single SAR microchannel denominated *Statmix 6* featuring 8 fork-like elements in series. **Günther, M. *et al.* (2004)** and **Bošković & Loebbecke (2008)** used the same *Statmix 6* microdevice for applying their methodology on the characterization of the distribution of residence times.

Bošković & Loebbecke (2008) also investigated another SAR microreactor made of silicon and glass and composed of 11 parallel microchannels featuring 8 G-shaped elements in series in which the inlets of the typical fork-like element are modified as to form a G-shaped structure in order to arrange the splitting elements longitudinally along the flow direction (Figure 2.5).

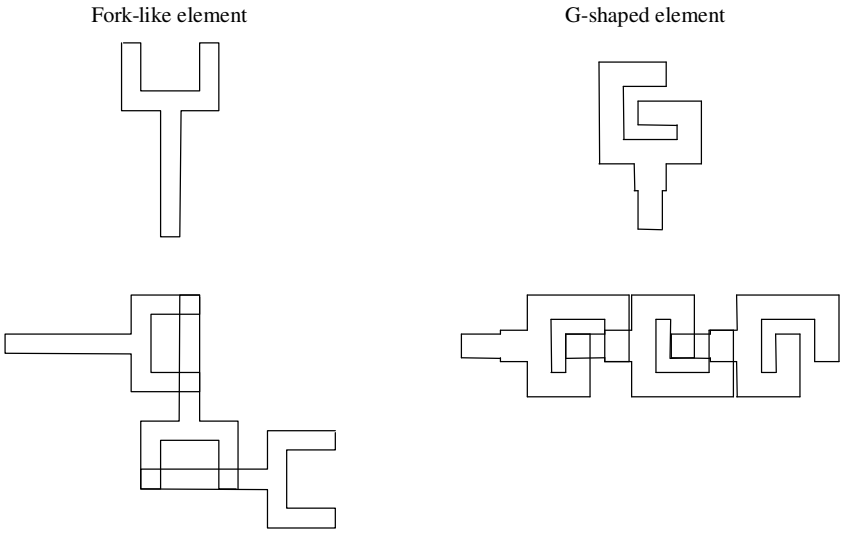

Figure 2.5 Schematic representation of the spatial arrangement of the typical fork-like element and the G-shaped element in the SAR structures.

This microreactor was first used in an automated microreaction system for optimization of chemical processes in liquid phase (**Ferstl *et al.*, 2004**) and is an improved version of the *accoMix* micromixer (Figure 2.6) which was also used in the same work and manufactured by *Accoris GmbH* (Germany) in silicon and featuring a network of 9 parallel microchannels with 6 G-shaped elements per channel (**Antes *et al.*, 2003; Hessel *et al.*, 2004; Panić *et al.*, 2004**).

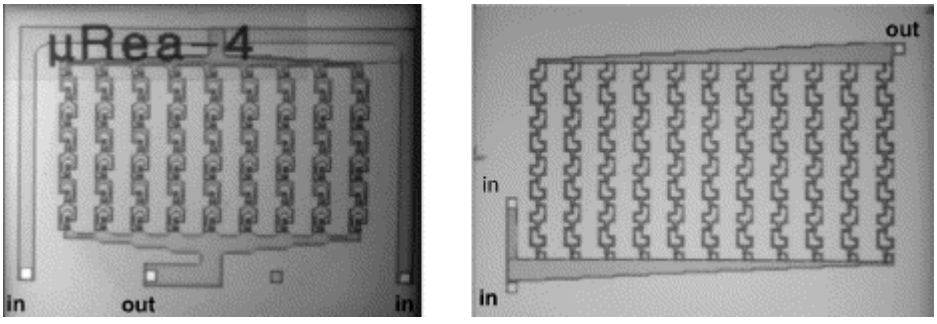

Figure 2.6 Infrared images of the first 9-microchannel version of the *accoMix* micromixer (left) and the improved 11-microchannel design (right) used in **Ferstl *et al.* (2004)**.

2.4 CHARACTERIZATION OF MICROREACTORS

2.4.1 Residence Time Distribution

The performance of a chemical reactor at any scale level is related to the extent of reaction achieved and to the amount of feed that can be processed per unit time for a determined reactor volume. The extent of reaction is associated with the fraction of reactants converted into products, *i.e.* selectivity, while the amount of feed can be associated to the total production rate of the desired product, *i.e.* overall yield. The yield is directly related to the time spent by the key reactants inside the reaction vessel. On the other hand selectivity is related to the hydrodynamics of the reaction vessel. Selectivity can be defined as the ratio of the rate of formation of a desired product r_D to the rate of formation of an undesired product r_U. If the rate laws of formation are defined as:

$$r_D = k_D C_A^{\alpha_D} \tag{2.1}$$

$$r_U = k_U C_A^{\alpha_U} \tag{2.2}$$

where k is the equilibrium constant, C_A is the concentration of the key reactant A and α is the rate of the reaction, then the following expression for the selectivity S_{DU} is obtained:

$$S_{DU} = \frac{r_D}{r_U} = \frac{k_D}{k_U} C_A^{\alpha_D - \alpha_U} \tag{2.3}$$

Thus, the term α_D-α_U will determine the characteristic flow pattern necessary in order to maximize the selectivity of the reaction. If $\alpha_D > \alpha_U$ then C_A should be made as large as possible to maximize selectivity and a reaction vessel where the concentration of A starts at a high value and decreases progressively should be used, *e.g.* batch or plug flow reactors. On the other hand, in order to maximize the selectivity when $\alpha_U > \alpha_D$ a reactor in which the value of C_A is kept to a minimum should be used, *e.g.* CSTR or mixed flow reactor. The batch, plug flow and CSTR are concepts of idealized reactors each possessing distinctive flow patterns and consequently

different degrees of mixing. Thus, the selectivity of a chemical reaction is related to the mixing characteristics of the flow vessel. Real reactors usually deviate from the idealized behaviors of plug and mixed flow and in order to predict their performance this deviation must be quantified. The analysis of the residence time distribution is a methodology that allows for this quantification.

The concept of *residence time distribution* (RTD) applies to temporal mixing and measures features of ideal or non-ideal flows associated with the bulk flow patterns or *macromixing* in a flow vessel. The term *micromixing* applies to spatial mixing at the molecular scale that is bounded but not determined uniquely by the residence time distribution. The bounds are extreme conditions known as complete segregation and maximum mixedness. They represent, respectively, the least and most molecular-level mixing that is possible for a given RTD (**Paul *et al.*, 2004**).

Although a specific RTD is not unique to a type of reactor, any given flow vessel exhibits a corresponding RTD that reveals distinctive information about its particular type of mixing (Figure 2.7). The RTD is one of the most informative characterizations of a chemical reactor.

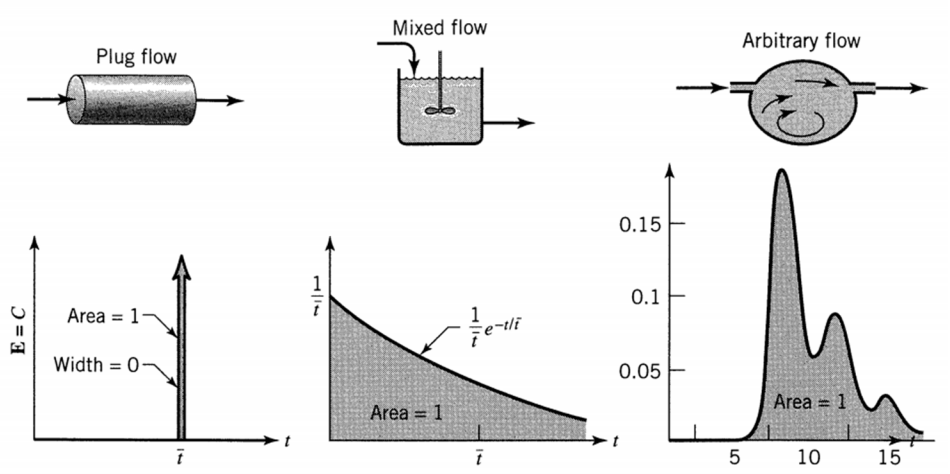

Figure 2.7 Schematic representations of the concentration-time responses expected for plug, mixed and arbitrary flow reactors (from **Levenspiel, 1999**).

The RTD of a chemical reactor allows for the prediction of conversion for first order reactions and to delimitate the lower and upper bounds for higher order reaction kinetics. Knowledge of the state of micromixing (*i.e.* degree of segregation) under specific operating conditions is necessary in order to interpret experimental results obtained from test reactions such as series-parallel reactions.

Therefore, the analysis of RTD has been adapted to the microscale for the hydrodynamic characterization of microfluidic devices. However, due to the size of microfluidic structures some technical problems have to be overcome in order to successfully apply the principles of RTD analysis to microreactors. One of the most obvious concerns is the volume of the peripheral fluid lines connecting to the microreactor. In macroscopic equipment, such volumes are relatively small in proportion to the working volume of the flow vessel and they are usually regarded as negligible during the analysis. For microfluidic devices the volumes of the peripheral tubing for the fluids are of the same order of magnitude or even greater than the microreactor working volume. Thus the influence of such volumes has to be taken into account during the treatment of the response signals obtained from RTD analysis. Also, as the mean residence time of the flow vessel is reduced when increasing the total flow rate, the duration and shape of the stimulus signal become more critical.

The residence time distribution of a reactor is obtained experimentally by introducing a suitable tracer stimulus (*e.g.* pulse, step, random input) (**Nauman & Buffham, 1983; Levenspiel, 1999**) into the fluid entering the reactor and measuring the transient response of the concentration *C(t)* of the tracer at the exit of the reactor.

The exit-age distribution function *E(t)* of a reactor is then calculated by dividing the response curve *C(t)* of an idealized pulse by the area under its curve:

$$E(t) = \frac{C(t)}{\int_0^\infty C(t)dt} \tag{2.4}$$

The observed mean residence time t_m is then obtained by the following equation:

$$t_m = \int_0^\infty t \cdot E(t)dt \tag{2.5}$$

However, idealized tracer pulses require instantaneous introduction of tracer homogeneously distributed across the flow path without disturbing the velocity flow field. This condition is difficult to achieve experimentally owing to the fact that it takes a finite time to inject the tracer. Also, in laminar flow reactors the shape of the input is distorted by the parabolic velocity profile (**Nauman & Buffham, 1983**) and consequently the response curve is affected by the way in which the tracer is introduced and detected (**Levenspiel, 1999**). When the injection of the tracer does not approach a perfect pulse stimulus, treatment of the so-called *sloppy* (**Fogler, 1999**) or *one-shot* (**Levenspiel, 1999**) tracer inputs offers an alternative to obtain RTD information provided that stimulus signal can be recorded at the inlet and outlet of the microreactor.

The signal obtained from *one-shot* pulse experiments must not be used directly to evaluate the *E(t)* function of the vessel under treatment. The recorded output signal is the result of the convolution of the input and reactor response signal *E(t)* and can be calculated as the convolution integral in the time domain as:

$$C_{out}(t') = \int_0^t C_{in}(t'-t) \cdot E(t) \tag{2.6}$$

Therefore, in order to obtain the true RTD curve of the reactor, the signal *E(t)* has to be retrieved from the convoluted output curve $C_{out}(t')$. However, deconvolution in the time domain is not a trivial operation and usually is avoided by instead performing a direct convolution followed by a *nonlinear least squares fitting* (NLSF) procedure to the output signal (**Westerterp, Swaaij & Beenackers, 1984; Günther, M. *et al.*, 2004; Bošković & Loebbecke, 2007**). This methodology requires the postulation of a flow model assumed to predict the signal *E(t)* with sufficient accuracy. Then, the convolution integral of $C_{in}(t')$ and *E(t)* is performed. The theoretical response curve thus obtained is fitted to the experimental curve $C_{out}(t')$ by varying the parameters of the model assumed for *E(t)*. Even if this strategy circumvents deconvolution in the time domain, it results in a time consuming procedure requiring significant computational efforts. The

approximation of the fitting is based on the flow model chosen. Flow models (*e.g.* axial dispersion, tanks-in-series, pure convection) are a useful tool to interpret reactor performance since they provide a physical meaning to the statistical parameters obtained from concentration-time curves.

The *axial dispersion model* is a one parameter flow model that is used to describe mass transport by convection and diffusion in non-ideal tubular reactors. This model assumes moderate axial dispersion superimposed on plug flow and its solution is subjected to the type of boundary conditions assumed, which in turn depend on the flow characteristics of the system. A situation that is often encountered in real experimental systems is the *open-open* boundary conditions (**Levenspiel, 1999**). For this type of systems the solution of the axial dispersion model for the concentration of a solute is given as:

$$C(t) = \frac{A}{2\sqrt{\pi(D/v \cdot l) \cdot t \cdot t_m}} \exp^{\left[\frac{-(t-t_m)^2}{4(D/v \cdot l) \cdot t \cdot t_m}\right]} \tag{2.7}$$

where A is the area under the concentration-time curve, D is the axial dispersion coefficient, v is the mean flow velocity and l represents the length of the pipe or tube.

The axial dispersion coefficient D (m^2/s) characterizes the degree of backmixing during flow and the dimensionless group $D/v \cdot l$, called the *vessel dispersion number*, represents the spreading process of the tracer in the axial direction. The axial dispersion coefficient combines the spreading effect of the parabolic velocity profile as well as the narrowing effect produced by radial molecular diffusion. The reciprocal of the *vessel dispersion number* is called the *reaction* Peclet number Pe_r which is used in reaction systems with the length of the reactor l as the characteristic length:

$$\frac{1}{Pe_r} = \frac{D}{v \cdot l} = \left(\frac{D}{v \cdot d_{eq}}\right)\left(\frac{d_{eq}}{l}\right) \tag{2.8}$$

where d_{eq} is the diameter of the tube. According to Eq. 2.8 the vessel dispersion number is the product of an intensity of dispersion in the radial direction and a geometric factor. For l/d_{eq} ratios greater than 30 an experimental flow correlation exists (**Nauman & Buffham, 1983**) for the term $D/v \cdot d_{eq}$ as a function of the Reynolds and Schmidt numbers:

$$\frac{D}{v \cdot d} = \frac{1}{Re \cdot Sc} + \frac{Re \cdot Sc}{192} \tag{2.9}$$

The axial dispersion coefficient can be determined experimentally from a pulse tracer experiment where the distribution of the concentration can be fitted to a suitable model in order to obtain the values of $D/v \cdot l$.

Levenspiel (1999) presents a chart (Figure 2.8) adapted from a previous work (**Ananthakrishnan *et al.*, 1965**) that suggest the optimal model to be used for fitting RTD when analyzing a system in laminar flow conditions. In this chart the term $Re \cdot Sc$ is defined as the *Bodenstein number* for mass diffusion, *i.e.* using the molecular diffusion $\mathscr{D}$ and not the axial dispersion coefficient D.

Günther, A. *et al.* (2004) and **Trachsel *et al.* (2005)** utilized a piezoelectrically activated flow injection technique for determining RTD of a pulse of tracer in segmented gas-liquid microfluidic systems. The geometries investigated were single rectangular microchannels made of polydimethylsiloxane (PDMS) with cross sections of 400 µm by 150 µm. Their injection technique assumed the introduction of a perfect pulse and the signals measured at different axial positions were considered to be the true RTD signals of the reactors. They found that for Pe_r ~2500 the behavior of a microchannel with a length of 1063 mm fell under the description of Taylor regime (*i.e.* narrow distribution) while for a length of 150 mm the region fell under the pure convection regime (*i.e.* spreading effect by parabolic velocity profiles).

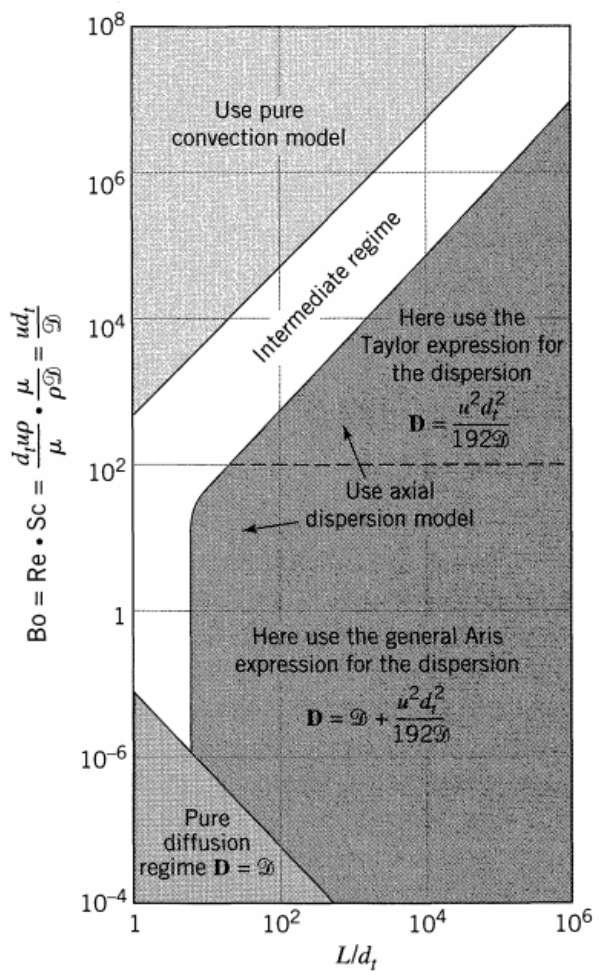

Figure 2.8 Map showing the optimal flow models to be used for laminar flow conditions (from **Levenspiel, 1999**).

Günther, M. *et al.* (2004) highlighted the importance of the effect of peripheral lines in the analysis of RTD in microreactors. They used a self-developed set-up to perform the RTD analysis of a tracer pulse in a split-and-recombination microreactor (*Statmix 6*) consisting of a single channel with eight split-and-recombination stages with an internal volume of 8.5 µL while their measuring set-up had an internal volume of 18 µL. They took into account this effect by recording independently the input and output signals and then performing the convolution in the time domain by assuming a mathematical model and fitting the theoretical response signal to that recorded experimentally. While they found that the *axial dispersion* model provided a better fit than the *tanks-in-series* model, they stated that visual inspection of the fit showed that the axial dispersion model was not optimal for describing the flow behavior of the microreactor; even

though the optimal fitting criteria (*i.e.* R^2, sum of least squares of deviation) were not disclosed. However, the obtained exit-age distribution curves where discussed on a qualitative basis and the values of the model parameters where neither disclosed nor compared quantitatively. Some experimental issues were detected such as stagnancy and dead volumes arising from using just one inlet of the microreactor during the analysis.

Bošković & Loebbecke (2008) investigated the RTD in three different microreactor geometries all featuring the split-and-recombination mixing principle. Two microdevices consisted of a single microchannel conduit. In one of them, denominated as *ST-Mixer*, the flow is rotated 90 degrees along the flow direction at each of 32 mixing stages. The other single channel SAR microreactor is the *Statmix 6* also used by **Günther, M. *et al.* (2004)** as discussed in the preceding paragraphs. The last microreactor analyzed was the G-shaped microreactor used by **Ferstl *et al.* (2004)**. All microreactors were capped at one inlet and filled with water in order to avoid dead volumes. **Bošković & Loebbecke (2008)** further developed the procedure of **Günther, M. *et al.* (2004)** using the direct convolution and NLSF procedure assuming a flow model. They used a fast sampling HPLC pump in order to generate tracer impulses as the stimulus signal. They performed deconvolution in the frequency domain as comparison of their direct convolution results and found good agreement between both methodologies. Additionally to the axial dispersion model the concentration-time curves were fitted to an *empirical* model proposed by **Ham & Platzer (2004)**:

$$E(t) = \frac{M \cdot N \cdot {t_k}^N}{t^{N+1}} \cdot \left(1 - \frac{t}{t_{\max}}\right)^{N-1} \cdot \left[1 - \frac{{t_k}^N}{t^N} \cdot \left(1 - \frac{t}{t_{\max}}\right)^N\right]^{M-1} \tag{2.10}$$

where

$$t_k = \frac{t_{\max} \cdot t_{\min}}{t_{\max} - t_{\min}} \tag{2.11}$$

and M and N are model parameters related to the vessel dispersion number.

In that work the empirical model was retained on the basis of the smallest sum of squares of deviation (~0.00724) during the fitting and the microreactors were described qualitatively by the first three moments of the distribution (*e.g.* mean, variance, skewness). All the microreactors showed similar values of variance although the ST-mixer and the G-shaped mixer exhibited more symmetrical responses with lower values of skewness. While these statistical moments by themselves can convey quantitatively a sense of the shape and spread of a given curve, they are not as convenient for describing flow behavior when they are not associated to any geometrical characteristic of the reactor. The parameters of the empirical model were not disclosed; however, the relationship between the model parameters of the empirical model with the physical characteristics of the process is not straightforward as discussed by **Ham & Platzer (2004)**. Hence, while providing a better fit than other models, the lack of physical meaning of its parameters render this model somewhat impractical for the description of flow behavior.

Lohse *et al.* (2008) developed a non-intrusive technique for the RTD analysis of fluorescent tracer pulses in single and parallel microchannel geometries. Since stimuli close to perfect impulses were reproduced the response curves obtained were assumed to be the exit-age distribution functions of the microdevices and were fitted directly to the axial dispersion model. Although details of the statistical parameters of the fit were not reported, visual inspection of the fitted curves showed that the axial dispersion model was able to closely reproduce the behavior of flow parallelization in the microfluidic structures.

Adeosun & Lawal (2009) followed a numerical and experimental approach for the investigation of RTD characteristics in a T-junction single microchannel. The injection was made at the inlet flow line as close as possible from the microdevice inlet and detection of the tracer pulse was recorded at the inlet and outlet of the microchannel in order to perform the subsequent NLSF procedure. Flow rates from 0.2 – 0.5 mL/min allowed for mean times between 23 and 9 s. They expanded on the work of **Günther, A. *et al.* (2004)** and **Bošković & Loebbecke (2008)** and concluded that the while the empirical model had a better fit to the experimental curves than the axial dispersion model (*i.e.* lower sum of squares of deviation), they both predicted reasonably well (within 10% error) the theoretical mean residence times.

Köhler *et al.* (2010) also analyzed the RTD of dye pulses in the Statmix6 micromixer as well as in an interdigital micromixer manufactured by *mikroglas chemtech GmbH* (Mainz) at different flow rates and viscosities. The internal volume of the interdigital micromixer is 15 µL and is twice the volume of the Statmix6. Flow rates from 0.05 to 3 mL/min allowed for mean residence times between 0.75–50 s. They concluded that the connecting lines before the micromixing structures have a strong influence on the total mixer residence time and that complex RTD behavior (*e.g.* bimodal, asymmetric curves) are not originally caused by the complex structures of the micromixing channels. In their work asymmetric input responses with sharp first-appearance times and a distinctive shoulder producing a bimodal distribution were detected for fluids with increased viscosities (2.2 – 5.9 mPa-s). Also they found a non-monotonic shift of the spread of the RTD at low viscosities and intermediate flow rates ($Re < 30$) for the interdigital structure and for a PTFE tube investigated for comparison. They concluded that for higher flow conditions ($Re > 30$) the RTD curves were nearly independent of the flow conditions. This behavior was attributed to more orderly laminar flow at low *Re* and to hydrodynamic complex flow (*e.g.* engulfment flows) for the case of higher *Re*.

2.4.2 Mixing characterization by the Villermaux/Dushman Reaction

The iodide-iodate system, also called the *Villermaux/Dushman method*, is a chemical competitive-parallel test reaction that has been widely applied as a standard test for the characterization of the mixing performance of microreaction systems. This method was originally developed by **Fournier *et al.* (1996a, 1996b)** for the investigation of macroscopic mixing in stirred tanks. The principles of such method allow for great flexibility and the experimental conditions can be adapted to obtain the best sensitivity according to the mixing capabilities of the mixer whether in batch or continuous operation. **Ehrfeld *et al.* (1999)** reported the first application of this reaction system for microdevices while **Guichardon & Falk (2000)** proposed general guidelines for adapting the method to continuous flow processes. **Panić *et al.* (2004)** addressed the influence of the reactant concentrations on the sensitivity of the results for the comparison of different types of micromixers.

The determination of mixing efficiency is based on the analysis of two competitive-parallel reactions. The acid-catalyzed reaction of potassium iodide (KI^-) with potassium iodate (KIO_3^-) to elemental iodine (I_2) (Eq. 2.12) competes with the faster neutralization of the acid (Eq. 2.13) by a borate buffer-system (**Fournier *et al.*, 1996a**):

$$5I^- + IO_3^- + 6H^+ \longleftrightarrow 3I_2 + 3H_2O \tag{2.12}$$

$$H_2BO_3^- + H^+ \longleftrightarrow H_3BO_3 \tag{2.13}$$

$$I^- + I_2 \longleftrightarrow I_3^- \tag{2.14}$$

A buffer solution of $KI/KIO_3^-/H_2BO_3^-$ in the basic range is mixed with diluted sulphuric acid (H_2SO_4). In the case of perfect mixing the acid is only consumed by the fast neutralization and no iodine is formed since there is no local excess of acid. If imperfect mixing is present, the local excess of acid significantly enhances the velocity of the otherwise slow formation of iodine. In turn, iodine can be detected by a UV-Vis spectrophotometer as a triiodide compound (Eq. 2.14) with characteristic absorption bands centered at 351 nm, 286 nm and 253 nm.

Iodine formation can be attributed to local deviation of the average concentration of acid due to imperfect mixing and the triiodide compound can be quantified to characterize the mixing performance. However, even in the absence of acid aggregates, the formation of iodine is thermodynamically possible if the buffer equilibrium (dependent of *pH*) is modified. The final *pH* of the solution has to be in the basic range to ensure that the measured concentration of iodine is a result of imperfect mixing due to momentary local excess of acid and not an effect of thermodynamic formation of iodine in acidic medium. In the work of **Panić *et al.* (2004)** excessively high concentrations of iodine were detected in the entire flow range analyzed when a final *pH* value of 7.6 was obtained. A better sensitivity was obtained at higher *pH* values (from 8.3 to 9.4) where a clear influence of the flow conditions on the mixing performance was observed. On the other hand, if a strong basic *pH* is used the iodine formed is thermodynamically unstable and disassociation can be present. To prevent this effect **Guichardon & Falk (2000)**

have recommended using a $7 < pH < 9.7$. **Panić *et al.* (2004)** employed an in-line measurement of the reaction product so the time delay for analysis was minimized concluding that the distance between the outlet of micromixer and spectrophotometric readings had no effect on the amount of product obtained indicating complete consumption of the reactants.

The kinetics of the Dushman reaction has been described in details by **Guichardon *et al.* (2000)**. The rate law is expressed as:

$$r_1 = k_1(H^+)^2(I^-)^2(IO_3^-) \tag{2.15}$$

where the kinetic constant k_1 is a function of the ionic strength μ_i. It was established in the same work that for small ionic strengths (10^{-1} M) experimental data is in agreement with the Debye-Hückel's theory:

$$\log_{10}\left(\frac{k_1}{k_0}\right) = -a\sqrt{\mu_i} \tag{2.16}$$

where $a = 3.664$ and $k_0 = 10^{9.281}\text{M}^{-4}\text{s}^{-1}$.

For greater ionic strengths, the rate constant k_1 is expressed as:

$$\log_{10} k_1 = 8.383 - 1.511\sqrt{\mu_i} + 0.237\mu_i \tag{2.17}$$

The concentration of boric acid ($H_2BO_3^-$) in the borate buffer solution (Eq. 2.18) is calculated from the equilibrium equation (Eq. 2.19) and the kinetic constant (Eq. 2.20) in dynamic equilibrium for borate ions with *pH* of approximately 10 (**Weast, 1986; Fournier *et al.*, 1996**).

$$H_3BO_3 + OH^- \longleftrightarrow H_2BO_3^- + H_2O \tag{2.18}$$

$$H_2BO_3^- = k_2(H_3BO_3)(OH^-) \tag{2.19}$$

$$k_2 = 73529.4 \ \frac{L}{mol} \tag{2.20}$$

Usually in the literature applying the Villermaux/Dushman method the mixing quality is defined in terms of a segregation index (**Trippa & Jachuck, 2004; Kockmann *et al.*, 2006; Men *et al.*, 2007; Fan *et al.*, 2010**). However, the segregation index is a relative parameter that depends on the concentration of the chemicals used (**Fournier *et al.*, 1996**) and for comparison purposes the mixing analysis has also been conducted utilizing the pure spectrophotometric signal (**Ehrfeld *et al.*, 1999; Panić *et al.* 2004; Kölbl *et al.*, 2008; Kölbl *et al.*, 2010**). **Kölbl *et al.* (2010)** have made the first attempt to describe the relationship between the optical density measured and the hydrodynamic conditions in *"V-type"* micromixers by means of an empirical correlation which includes specific geometrical characteristics of the micromixer.

For the application of this method to continuous flow, the concentration of reactants in the fluid reservoirs must be adjusted according to the ratio of flow rates. The effect of the flow conditions on the formation of triiodide in the Villermaux/Dushman method can only be determined and compared if the feeding ratio is kept constant during the analysis. The modification of this ratio will change the final concentration of reactants in the reaction section thus overshadowing the effect of the geometry on the mixing performance.

When low concentrations of reactants are present, the reaction rate in competition with the mixing process is relatively slow and the mixing quality may appear to be optimal. On the other hand, the reaction rate will increase when using high concentrations of reactants and the mixing quality will deteriorate for the same hydrodynamic conditions. In the literature applying the Villermaux/Dushman method for the characterization of microreactors, the results of the test reaction are usually presented in the form of the triiodide concentration as a function of the volumetric flow rate where a low triiodide value indicates better mixing. The iodide-iodate results in the literature exhibit the same qualitative trend: as the volumetric flow rate increases the segregation index or absorbance value decreases with an exponential decay behavior indicating better mixing. However, the initial concentration of reactants modifies the time scale for reaction

and the reduced mean residence times resulting from higher flow conditions might have an impact on the level of conversion of the Villermaux/Dushman reaction.

2.4.3 Computational Fluid Dynamics

Microreactors having parallel microchannel networks and intricate flowing structures such as the multilamination or split-and-recombination mechanisms are examples of complex microfluidic geometries that cannot be approximated by the behavior of a straight individual microchannel with a comparable active volume. Knowledge of the flow characteristics at specific downstream locations is undoubtedly the most ideal approach for a complete understanding of the hydrodynamic and mixing performance of microfluidic devices. However, such information is difficult to obtain by experimental means and CFD simulations have become a fundamental strategy for the characterization of such complicated microfluidic structures.

CFD tools have been applied to the simulation of flow in microchannels for single and multi-phase systems allowing to gain a better insight of the flow patterns and secondary flows of new micromixing mechanisms (**Mengeaud *et al*., 2002; Stroock *et al*., 2002a; Stroock *et al*., 2002b; Hardt & Schönfeld, 2003; Wong *et al.*, 2004; Park & Kwon, 2008**); on the characterization and optimization of microchannel shapes and distribution manifolds (**Kim *et al*., 2000; Gobby *et al*., 2001; Chen & Chen, 2002; Commenge *et al*., 2002; Tonomura *et al.*, 2004**) and on the characterization of mixing efficiency of microdevices (**Aubin *et al*., 2003; Engler *et al*., 2004; Wong *et al*., 2004; Aubin *et al.*, 2005; Serra *et al*., 2005; Kockmann *et al*., 2006; Gamrat *et al*., 2008; Lee & Lee, 2008; Yu *et al*., 2008**). Recently, CFD simulations have been used for the estimation of RTD in microfluidic devices (**Adeosun & Lawal, 2005; Adeosun & Lawal, 2009; Aubin *et al.*, 2009; Cantu-Perez *et al.*, 2010a-b**).

Usually, in the context of CFD the mixing performance is compared on the basis of intensity of segregation defined by Danckwerts in 1952. The influential paper about the characteristics of mixtures by **Danckwerts (1952)** states that when mutually soluble liquids are brought together two things happen: 1) the liquids are broken into *"clumps"* which are intermingled, and 2) molecular interdiffusion occurs across the boundaries of said clumps. It continues by saying that

unless molecular diffusion takes place the composition at any point will be that of one of the pure components and it will vary discontinuously from one region to another. It elaborates that the breaking-up of clumps and the interdiffusion mechanism are largely independent processes which produce distinguishable results and that "the former reduces the size of the clumps, while the latter tends to obliterate differences of concentration between neighbouring regions of the mixture [*sic*]". Danckwerts defines two quantities to describe these different processes, namely the *scale of segregation* and the *intensity of segregation*. The scale of segregation is a measure of the size of the clumps after the break-up process while the intensity of segregation measures how well intermixed the two fluids are. Therefore, the scale of segregation is a measure of the dispersive attributes of the flow system while the intensity of segregation is a measure of the distributive characteristics.

The intensity of segregation is a statistical parameter that was defined by **Danckwerts (1952)** as:

$$I_s = \frac{\sigma_a^2}{\overline{a \cdot b}} \equiv \frac{\sigma_b^2}{\overline{a \cdot b}} \tag{2.21}$$

where a and b represent the concentrations of two different miscible species in terms of their volume fractions. The parameter I_s represents the extent to which the concentration in a given region departs from the mean value in a given cross section. As defined in Eq. 2.21, the intensity of segregation has a value 0 when the concentration is uniform, *i.e.* when there is no difference between the concentration of either species with the mean value of the whole system in any given cluster; and a value 1 in a complete segregated state, *i.e.* when the concentration values in any cluster are either only a or b. Danckwerts states that during the mixing of two miscible liquids the value of I_s is progressively reduced by the effect of molecular diffusion and not directly affected by the mechanical process of mixing; in the absence of diffusion the mixture would remain "grainy".

The intensity of segregation is obtained by statistical estimations performed over specific cross sections of the flow conduit. Thus, the advantages of CFD techniques for such calculations in complicated structures become quite evident.

One approach for the estimation of the intensity of segregation by means of CFD is to solve the continuity and unsteady-state convection-diffusion equations. Once their solution is obtained, the concentration in a given plane in the system can be known as a function of time. Another approach consists on the particle tracking method which is based on a Lagrangian frame of reference that follows the paths of massless particles. Such paths are obtained from the solution of the continuity and momentum transfer equations. Both approaches posses advantages and drawbacks and the selection of either must be evaluated according to the purpose of the analysis and the characteristics of the flow system.

At first glance the results obtained by solving the convection-diffusion equation should be the preferred choice since the momentum and mass transfer mechanism are coupled in such strategy. Nevertheless, the unsteady-state solution of the resulting equations may pose a great computational effort depending on the characteristics of the geometries analyzed. The particle tracking method is based on the solution of the equations of motion only and does not take into account the molecular diffusion mechanism. This approach is sometimes preferred since it avoids the introduction of numerical diffusion that results when a scalar is tracked.

Recalling the definition of the intensity of segregation proposed by Danckwerts and discussed in the preceding paragraphs, the use of the particle tracking method for the quantification of the intensity of segregation presents a seemingly contradiction since the solution of the equations in which it is based do not account for the effect of molecular diffusion of mass. Relying on the statistical nature of the definition of scale and intensity of segregation the particle tracking method has been exploited nonetheless for mixing characterization purposes. Since there is no diffusion assisting the mixing process, any distribution of concentration will be discontinuous at any scale level in the cross section over which the analysis is performed. Acknowledging this fact, the particle tracking method translates to an estimation of concentration of tracer *positions* in spatially regular regions of predetermined size usually defined by a grid. Thus, the choice of the grid size at the control plane is of critical importance to compute the concentration values required to define the degree of segregation. Even though the level of segregation thus obtained

will be affected only by the mechanical aspects of the flow, the size of the grid will dictate the level of resolution of the segregation scale.

Another statistical parameter called the *coefficient of variation CV* has been used to quantify the degree of mixing (**Rauline *et al.*, 1996; Rauline *et al.*, 2000; Aubin *et al.*, 2003; Heniche *et al.*, 2005**). Statistically the *CV* is defined as the ratio of the standard deviation of a variate divided by the mean value of its distribution:

$$CV_a = \frac{s_a}{\bar{a}} \tag{2.22}$$

where s_a is the standard deviation of the concentration of species a. It is usually stated that the *CV* varies from 0 to 1 with zero indicating a complete mixed stated while 1 represents complete segregation. The *CV* is a measure of relative variability about the mean and is recommended that this coefficient be used in ratio form and not as a percentage since it can readily exceed unity (**Rosander, 1957**). Values of *CV* higher than 1 are statistically possible and might result even in fractional form when some regions or clusters exhibit a concentration that is far greater than the mean. Thus, the use of a range between 0 and 1 to characterize the degree of segregation from Eq. 2.22 should be taken with care. On the other hand, the values of I_s in fractional form vary between 0 and 1.

The same two approaches can be followed for the numerical calculation of residence time distributions (RTD) in continuous flow microreactors where distribution functions at a given cross section can be reproduced from the concentration of species obtained by solving the convection-diffusion equation; or from tracking the position of massless particles along the flow vessel.

Aubin *et al.* (2003) investigated by means of CFD the mixing quality in two different micromixer geometries called the diagonal- and the staggered-herringbone mixers (**Stroock *et al.*, 2002b**). Several quantification techniques were used which had been previously applied for the numerical characterization of macroscale static mixers, *e.g.* stretching efficiency, Lyapunov

exponent, deformation rate. A qualitative characterization was conducted by the Lagrangian approach of particle tracking. This procedure allows for a visual evaluation of the state of mixing by means of Poincaré sections. Poincaré sections are generated by tracking massless particles through the flow and recording their positions at different downstream coordinates. These positions are superimposed to construct a 2D plot in which the dispositions of the points reveal the chaotic nature of the flow. In order to quantify the homogeneity of the mixture the concept of *intensity of segregation* was applied as well as the calculation of the stretching and Lyapunov exponent to represent the mixing efficiency. The simulations were performed using CFX5^{TM} which is a commercial software based on the finite volume method. The tracer particle and the stretching technique were found to be suitable for microfluidic characterization whereas the quantification method based on the deformation rate did not appear to be well adapted to compare such micromixer geometries producing secondary flows.

Adeosun & Lawal (2005) utilized CFD simulations to characterize the hydrodynamics characteristics of a T-junction microchannel as well as other proposed optimized geometries. The *species mass fraction distribution* (SMFD) was used to describe qualitatively the state of mixing of two liquid species while the RTD was used to quantitatively measure the degree of macromixing. The methodology was based on the solution of the momentum and mass transport equations by the commercial software FLUENT^{TM}. It was concluded that multilamination mechanism with aspect ratios of 10 yielded the best performance results with coefficients of variation of 27% compared to almost 50% obtained for a conventional T-junction mixing mechanism.

Aubin *et al.* (2005) continued their investigations in the staggered-herringbone mixers (SHM) by performing a numerical study of the effect of its geometrical parameters on the mixing performance. In their numerical methodology they applied a restitution coefficient of unity to the microchannel walls in order to avoid particle trajectories from being trapped near the walls where the local velocity is close to zero. With this strategy they found that less than 2% of the particles were stopped between injection and detection planes. In their work they addressed the importance of the statistical grid used for the quantification of tracer positions when the tracer particle tracking technique is used to evaluate flow performance. They conducted the statistical analysis

of tracer particle positions by adapting a *point-event distance* methodology. Instead of delimiting a square grid for the evaluation of tracer positions, equidistant points are distributed in the plane and used as the frame of reference to calculate tracer positions. This allows the reference points to better fit the cross section. They also used the striation thickness as a parameter for comparative assessment.

Adeosun & Lawal (2009) conducted a numerical and experimental characterization of RTD in T-junction and L-junction microchannels. Following their previous work the numerical RTD results are based on the solution of the convection-diffusion equation. The difference between the values of the mean residence time t_m and coefficient of variation (CV) obtained from the numerical mixing-cup and through-the-wall measurements are less than 12%. The values of t_m and CV for the through-the-wall measurement are respectively lower and higher than those obtained for the mixing-cup measurement. An important contribution of this work consisted on the comparison between the axial dispersion model and the empirical model during the RTD description. The empirical model has been recently preferred for the modeling of RTD in microstructures due to the better fitting provided. The results of **Adeosun & Lawal (2009)** show that while qualitatively the empirical model offers a better fit both models provide similar values of the mean residence times and variance which for instance showed a maximum difference of less than 8%.

Aubin *et al.* (2009) applied their methodology of particle tracking for the numerical investigation of RTD in rectangular microchannels as a function of the aspect ratio. They found that in order to obtain narrow residence times, *i.e.* high fluid Pe, the microchannels should be designed with aspect ratios approximately ≤ 0.3.

Cantu-Perez *et al.* (2010a-b) conducted the experimental and numerical investigation of residence time distributions in straight and zigzag microstructured plate reactors and in microchannels with herringbone structures. The numerical residence time distributions were based on the particle tracking method modified to include a term representing a random walk. Random walks are stochastic models used in the domain of RTD in order to account for the molecular diffusion otherwise absent in the Lagrangian approach of particle tracking of massless

particles which is based on the solution of the equations of motion. It was shown that such random walk model was able to well represent the analytical solution of the pure convection and axial dispersion models at *Pe=30*. It was concluded that secondary flows narrow the RTD at high *Pe* ~10^4. For smaller *Pe* ~10^2 where mass transfer by diffusion plays a more important role it was found that microchannels with structures that induce secondary flows produce about the same RTD than straight microchannels. The numerical solution of the continuity and Navier-Stokes equations was obtained in the COMSOL Multiphysics 3.3 platform while the particle tracking algorithm was conducted in the MATLAB programming platform.

Cortes-Quiroz *et al.* (2010) utilized the ANSYS CFX-11 commercial modeling software for the numerical simulation and optimization of the staggered-herringbone micromixer. In this case, the convection-diffusion equation was solved and the criteria for the analysis were the intensity of segregation and the pressure drop. The results of this investigation are very specific to the design parameters of the staggered-herringbone micromixer such as groove pitch and depth; however it is a good example where the intensity of segregation is used for the characterization of microfluidic devices. Intensities of segregation from 0.25 to 0.8 were reported for a corresponding pressure drop from 2.5 x 10^{-4} to 80 x 10^{-4} bars.

Worner (2010) presented an approximation to the pure convective RTD of fully developed laminar flows based on an analytical procedure. He proposed a *simplified engineering RTD model* for the description of laminar flows in rectangular microchannels of varying aspect ratios. While this model fulfills the criterion of infinite values of the second and higher moments of the distribution in the absence of molecular diffusion as demonstrated by **Nauman (1977)**, it is valid only for laminar flows in the absence of molecular diffusion.

The practical application of convective models such as that discussed by **Worner (2010)** resides on the assumption of fully developed flow and a negligible influence of molecular diffusion. The range of validity (Fig. 2.8) of a given flow model, *e.g.* pure convection, pure diffusion, axial dispersion regime, will depend on the geometrical characteristics of the system and the fluid properties. **Nauman (2008a)** propose the criterion established by **Merrill & Hamrin (1970)** for neglecting molecular diffusion in the radial direction which was derived for a first-order reaction:

$$\frac{\mathscr{D}_a \cdot t_m}{R^2} < 0.003 \tag{2.23}$$

where $\mathscr{D}_a$ is the molecular diffusion coefficient of species *A* and *R* is the radius of the tube. Eq. 2.23 is very similar to the criterion proposed by **Bosworth (1948)** who defines the limit of the right hand side of Eq. 2.23 as 0.00308. According to this latter criterion, a geometrical relationship for neglecting molecular diffusion in the radial direction can be defined as:

$$\frac{l}{d_h} < \frac{Pe_f}{649.3} \tag{2.24}$$

where l and d_h are the length and hydraulic diameter of the flow conduit, and Pe_f is the fluid Peclet number, *i.e.* the version of *P*e that uses the characteristic length that determines the mechanical behavior of the fluid.

2.5 POLYMERIZATION IN MICROREACTORS

Efficient heat transfer is one of the important features of microreaction technology that can be beneficial for temperature sensitive processes such as free-radical polymerizations. Free-radical polymerization is an important method for the industrial synthesis of polymers as free-radicals are compatible with a wide variety of functional groups which are not compatible with ionic and metal-catalyzed polymerizations (**Yoshida *et al.*, 2005**). Since free-radical polymerization reactions are highly exothermic, the molecular weight and molecular weight distribution largely depend on the heat transfer and temperature control during the reaction. Generally, the heat of reaction in polymerizations increases in proportion to the reactor volume while the heat removal capacity decreases due to the reduction of the surface-to-volume ratio. In the microscale, the heat transfer rate increases due to the large surface-to-volume ratios encountered in microreactors (**Schubert *et al.*, 2001**) and the temperature control becomes more efficient leading to a better control of molecular weight distribution (**Bayer *et al.*, 2000a**). Due to the enhanced mass

transport at such small scales and to high heat transfer capabilities microreactors can be a suitable alternative for the study of highly exothermic, fast and diffusion-limited chemical reactions.

The first investigation to report the advantages of microreaction technology in polymer reaction engineering applications was made by **Bayer *et al.* (2000a)**. While the operating conditions and technical data were not disclosed, they reported a reduction of the distribution of molecular weights during the solution polymerization of acrylates such as polymethyl methacrylate (PMMA) and polyacrylic acid (PAA) thus preventing fouling of the tubular reactor in which the high molecular weight species (~10^5 – 10^6 g/mol) were assumed to cause precipitation inside a static mixer originally used as a premixing stage of the continuous process.

Nisisako *et al.* (2004) successfully manufactured functional poly(1,6-hexanediol diacrylate) polymer beads suspended in polyvinyl alcohol using a two-stage process involving the use of a circular T-shaped micromixer. Two immiscible fluids were introduced into separate microchannels and then one liquid was forced into the main flow at a T-junction to form micro droplets which were polymerized in batch at a subsequent stage by means of UV-light radiation.

Chang *et al.* (2004a, 2004b) obtained polymer beads using a self-developed microfluidic device made of glass. Polymethyl acrylate (PMA) and polyvinyl acetate (PVA) polymer particles were prepared in a similar procedure to that of **Nisisako *et al.* (2004)** using gamma-ray initiated dispersion polymerization in a device consisting of 120 straight microchannels with cross-sections of 50 µm x 50 µm and 120 mm in length. The particle size was controlled by the pulse rate of the gamma rays and the minimum size obtained was 1.3 µm. However, the polymerization was conducted in the downstream channel after droplet formation and was essentially a batch process with a polymerization time of 360 minutes.

Serra *et al.* (2005, 2007) have studied by means of CFD the free-radical polymerization of styrene in two multilaminated (*HPIMM* and *SFIMM* models both from IMM) and in a conventional T-junction microreactors. They obtained almost isothermal conditions in their simulations and found that a low *polydispersity index* (PDI) (*i.e.* <2.5) can be maintained for a

larger range of diffusion coefficients ($1 \times 10^{-11} - 1 \times 10^{-8}$) when the microreactor radius is lower than ~0.25 mm.

Iwasaki & Yoshida (2005) reported the solution free-radical polymerization of acrylates in a tube reactor of 500 µm of internal diameter using AIBN (azobisisobutyronitrile) as the chemical initiator. The monomers butyl acrylate (BA), methyl methacrylate (MMA), styrene (St), benzyl methacrylate (BMA) and vinyl benzoate (VBz) were polymerized at two different temperature conditions of 80 and 100 degrees C. It was concluded that the use of small reactor dimensions did not lead to significantly different results when comparing the polydispersity index obtained in standard laboratory-scale reactors for low exothermic monomers like St or VBz. However, for highly exothermic monomers like BA, the molecular weight distribution was found to be considerably narrower (PDI ~3.14) than for the batch system (PDI ~10.3). They claimed that this effect is caused directly from the high surface-to-volume ratio of the tube reactor which allows a better removal of the heat released by the polymerization. Even though the PDI of polystyrene was not significantly improved (*i.e.* ~1.74 for all mean residence times), the conversion achieved in the microscale reactor at 100 degrees C was considerably higher (34.3% max.) for all the flow conditions investigated. The increase in conversion was more pronounced for mean residence times lower than 10 minutes reaching 31.1% of conversion at that point compared to 18% achieved in a batch reactor. No fouling was assumed after 360 minutes of continuous operation during PS polymerization since no significant increase of pressure drop was detected. Nonetheless, this was a four stages process in which a union-tee (i.d. 800 µm) was used to bring the reactants into contact and three coiled tube sections were used: complete mixing of reactants (i.d. 250 µm x 2 m at 25C), reaction (i.d. 500 µm x 9 m at 100C) and termination (i.d. 500 µm x 1 m at 0C).

Okubo *et al.* (2009) used two different reaction systems for the free-radical polymerization of styrene monomer: i) suspension polymerization using emulsion droplets, and ii) slug polymerization using segmented flow. In the first system an emulsion is formed by the *K-M micromixer* (**Nagasawa *et al.*, 2005**) using lauroyl peroxide and polyvinyl alcohol as chemical initiator and stabilizer respectively. The K-M micromixer operates under the principle of multilamination of flow although in this specific mixer the thin fluid layers are produced by two

concentric annuli and then channelled towards the center before being forced into a central channel that collects all the layers and directs them towards the outlet. A feeding ratio of St to polyvinyl alcohol of 1:8 was used for total flow rates ranging from 4.5 to 45 mL/min. The microfluidic device was used only for the emulsification stage while the polymerization reaction was conducted in a coiled tube of internal diameter of 2.15 mm and ~10 m of length for a mean residence time of 8 minutes at the lowest flow condition. For the second system the segmented flow was produced by a union-tee while the polymerization was conducted again in a coiled tube with an internal diameter of 1 mm and ~55 m of length for mean residence times between 8 and 10 minutes. It was reported that the PDI was reduced from a value of 2 in a batch process to a value of 1.53 in the slug polymerization case. Molecular weights of ~28,000 g/mol were obtained at 75 degrees C with polymer conversions lower than 10% for the slug system. At 95 degrees C polymer particles with a reduced molecular weight of 12,000 g/mol were obtained in the slug polymerization system for a total conversion of 23%.

2.6 TEST SYSTEM: FREE-RADICAL POLYMERIZATION OF POLYSTYRENE

Styrene monomer is one of the petrochemical intermediates for which demand is increasingly rapid. It is primarily used in the manufacture of plastics and synthetic rubber. Major styrene plastics are crystal polystyrene, rubber-modified polystyrene (HIPS), styrene acrylonitrile copolymer (SAN) and rubber-modified styrene acrylonitrile copolymer (ABS). Free-radical polymerization is an important method for polystyrene synthesis since free-radicals are compatible with a wide variety of functional groups which are not compatible with ionic and metal-catalyzed polymerization (**Yoshida *et al.*, 2005**). Free-radical polymerizations are highly exothermic and the molecular weight and molecular weight distribution is sensitive to the reaction temperature. High-impact polystyrene is a well characterized material and its kinetic mechanism has been investigated for many decades. Still, the parameters affecting the particular HIPS morphology have not been completely clarified. The heterogeneous nature of HIPS is known to be affected by the mixing conditions and the process viscosity especially during the early stages of the polymerization (up to 30% conversion).

2.6.1 Types of Initiator

Considering a temperature of 120°C using dicumyl peroxide as initiator with an efficiency of 0.6, the polymerization time is 360 seconds in order to reach 30% conversion. However, if the reaction temperature is increased by 20°C the time for reaching 30% conversion is reduced to 45 seconds. The limit of conversion is decreased as the reaction temperature increases. The use of more effective initiators at those temperatures could increase the level of conversion. **Estenoz *et al.* (1996)** experimentally investigated the bulk polymerization of styrene monomer in the presence of dissolved polybutadiene using different types of mono- and bi-functional initiators. They determined that the L-256 bi-functional initiator [2,5-dimethyl-2,5 bis(2-ethylhexanoyl peroxy)] used at temperatures above 120°C can promote phase inversion and rubber grafting at low conversions around 15% and also reduce the prepolymerization times by 38% as compared with the values obtained for conventional mono-functional initiator terbutylperoctoate (TBPO). The prepolymerization time to achieve 30% of conversion was 363 minutes for L-256 and 443 minutes for TBPO in a 2.5L batch reaction volume. The boiling point of styrene monomer is 145.2°C at 1 atmosphere and its heat of vaporization is 36,930 J/mol. The heat of formation of polystyrene from styrene monomer at 25°C is 72,502 J/mol (**Carter *et al.*, 1975**), thus approximately one mol of styrene monomer is evaporated per each two mol of styrene monomer polymerized. Hence, an effective heat transfer capacity at least equal to the heat of formation at the temperature of polymerization must be provided in order to maintain a liquid phase flow. The heat of reaction is a function of the heat capacity which in turn depends on the temperature.

2.7 SUMMARY

In this section a series of tables is included condensing the previously cited investigations into five main topics: the experimental characterization of mixing efficiency, experimental characterization of residence time distribution, numerical characterization of microreactors, the continuous flow polymerization in microreactors and investigations performed on the two geometries selected for this investigation. The content in each table is arranged in chronological order and relevant features of the investigations in turn are highlighted.

Table 2.1 Mixing characterization of microreactors by the Villermaux/Dushman method

Authors	Microdevice	Active volume	Flow conditions	Observations
Ehrfeld *et al.* (1999)	a) Interdigital *SSIMM* (from IMM) b) Arrangement of 10 parallel *SSIMM*	40 µL (single unit)	a) 1.3 bars @ 50 mL/min (max) b) 1.7 bars @ 16.6 mL/min (max)	Acid concentration: 0.1374 M Sharp exponential decrease of triiodide absorption (improved mixing) up to 3.5 mL/min. Mixer array showed same trend levelling off at around 8.3 mL/min. Parallelization allowed same mixing quality at higher flow rates.
Panić *et al.* (2004)	a) SAR mixer b) Interdigital *SSIMM* micromixer (by IMM) c) Triangular interdigital mixer (by Mikroglas) d) SAR caterpillar *CPMM-V1.2-R1200* micromixer (by IMM) e) T-junction	a) ~70 µL b) 40 µL c) 15 µL d) 78 µL e) ~25 µL	@ 15 mL/min a) 0.3 bar b) 7.8 bar c) 2 bar d) 0.3 bar e) 0.3 bar	Using double acid concentration (0.030 M) a better sensitivity was detected. Absorbance values used. The *SSIMM* interdigital mixer showed the best mixing performance levelling off (max. efficiency) at 2-5 mL/min. T-junction exhibited the same performance as the other mixers at much less pressure drop although at twice the flow rate. At 2 mL/min the SAR mixer showed a decrease in mixing performance.
Trippa *et al.* (2004)	Y-junction squared microchannels with different diagonal length: a) 1 mm b) 2 mm	a) 204 µL b) 408 µL	9-60 mL/min	Acid concentration: 0.1 M. Segregation indexes below 0.08. Lower hydraulic diameter achieved segregation indexes nearly 5 times lower at 40 mL/min. Acrylic transparent unit.

Table 2.1 Continued

Authors	Micromixer	Active volume	Flow conditions	Observations
Nagasawa *et al.* (2005)	*KM* mixer: collision of two substreams in a star-shaped geometry	not disclosed	1-10 mL/min	Acid concentration: 0.138 M. Absorbance values nearly equivalent to those of *SSIMM* interdigital mixer but with larger microchannel diameter. The mixing principle relies on the kinetic energy of the flow collision. T-junction mixer exhibited absorbance values higher than 1.2 at low flow rates <2 mL/min. Metallic unit.
Kockmann *et al.* (2006)	T-junctions and different self-developed micromixers based on bending and turning concepts	not disclosed	Pressure drop <1 bar @ 250 mL/min (max)	Acid concentration: 0.028 M. T-junctions exhibited segregation indexes from 0.02 to 0.003. The proposed new geometries achieved indexes below 0.001 starting at flow rates of 115 mL/min with values as low as 0.0002. Meandering channels responsible for improved mixing by secondary flows. Silicon and glass.
Men *et al.* (2007)	*StarLam300* (by IMM): injection of two streams into one flow-through mixing chamber	5 mL	Pressure drop <1 bar @ 5.3 L/min (max)	Acid concentration: 0.03 M. Segregation indexes below 0.02 at 0.83 L/min and as low as 0.002 at 5.3 L/min. Segregation index exhibited a quadratic reduction as a function of energy dissipation. Designed for high flow rates. Metallic unit.

Table 2.1 Continued

Authors	Micromixer	Active volume	Flow conditions	Observations
Kölbl *et al.* (2008)	*V-type* mixers: multilamination principle	~17 µL	50-333 mL/min	Acid concentration: 0.015, 0.03 and 0.045 M. Absorbance values used for comparison. Highest acid concentration allowed more contrast between mixers. Relationship between concentration and absorbance is quadratic. Designed for high flow rates. Metallic unit.
Lee & Kwon (2009)	Self-developed multilamination mixer with recirculation zones	not disclosed	0.1-9.75 mL/min	Acid concentration: 0.549M. Absorption values of ~1 at 6.6 mL/min. Mixing efficiency from 60-98% at 0.1-9 mL/min. *SSIMM* interdigital mixer was found to decrease its efficiency from 85 to 75% in the same range. Transparent design with recirculation zones in the downstream channel.

Table 2.2 Experimental residence time distribution (RTD) analysis applied to microreaction technology

Authors	Microdevice	Active volume and flow rate	*E*(t) calculation	Observations
Günter, M. *et al.* (2004)	*Statmix6* (silicon): single fork-like shaped SAR microchannel	8.5 µL; 40-200 µL/min	Convolution with model and NLSF	Dead volumes caused by the capped inlet. Insufficient description of flow by the axial dispersion model. Distortion of peripheral lines in the output signals. Self-developed set-up.
Günter, A. *et al.* (2004)	Single meandering microchannel (PDMS)	72 µL; gas/liquid: 30/10 µL/min 70/10 µL/min	Direct optical method	Only one inlet used. Piezoelectrically activated pulse injection. Synthesis of sol-gel colloidal particles. Segmented flows reduced the RTD. Detection of fluorescence intensity: restricted to transparent devices.
Trachsel *et al.* (2005)	Single meandering microchannel (PDMS)	72 µL; gas/liquid: 30/10 µL/min 70/10 µL/min	Direct optical method	Only one inlet used. Piezoelectrically activated pulse injection. Decrease of channel cross section increased the RTD due to increased menisci area. Detection of fluorescence intensity: restricted to transparent devices.
Bošković & Loebbecke (2008)	a) SAR single microchannel (silicon) b) 11 parallel G-shaped SAR microchannels (silicon) c) *Statmix6* (silicon)	a) ~200 µL b) 85 µL c) 8.5 µL 0.5-2 mL/min	Convolution with model and NLSF (deconvolution in Laplace domain)	Account for the distortion of peripheral lines. Only one inlet used. Dispersion model fitted only satisfactorily at higher flow rates. Empirical model provided a better fit for all flow conditions. Restricted to transparent devices.
Lohse *et al.* (2008)	Single straight microchannel (PDMS)	0.12 µL; 0.4-1.2 µL/min	Direct optical method (deconvolution in Fourier domain)	Precise tracer injection. Unsuccessful deconvolution in frequency domain due to weak signal-to-noise ratio. Self-developed set-up. Restricted to transparent devices.

Table 2.2 Continued

Authors	Microdevice	Active volume and flow rate	*E*(t) calculation	Observations
Adeosun & Lawal (2009)	T-junction single microchannel	6.4 µL; 0.2-0.5 mL/min	Convolution with model and NLSF	One and two inlets were used. Axial dispersion model and empirical model both provided good prediction of theoretical mean times when one inlet was used.
Cantu-Perez *et al.* (2010a)	Laminated microstructured plate with straight and zigzag microchannels	(volumes not disclosed); 0.2-2 mL/min	Deconvolution in Fourier domain	Single inlet microdevices. At high fluid velocities secondary flows are thought responsible for narrowing the RTD in zigzag channels. Restricted to transparent microdevices.
Cantu-Perez *et al.* (2010b)	*Staggered-herringbone Micromixer* (SHM)	2.5 µL; 0.5-1 mL/min	Deconvolution in Fourier domain	Single inlet microchannel. Fitted to axial dispersion model with mass exchange with a stagnant zone. Secondary flows reduced the RTD in SHM at high flow velocities. Restricted to transparent microdevices.
Köhler *et al.* (2010)	a) *Statmix6* (silicon) b) Interdigital triangular micromixer (by Mikroglas)	a) 8.5 µL b) 15 µL 0.050-3 mL/min	Convolution with model and NLSF	Tracer shoulders and bimodal distributions observed for viscosities higher than water (2.2 mPa-s). Non-monotonic shift of RTD for different flow rates at moderate viscosities observed in interdigital structure and conventional tubing. Empirical model.

Table 2.3 Numerical mixing analysis applied to microreaction technology

Authors	**Microdevice**	**Characterization**	**Numerical approach**	**Observations**
Aubin. *et al.* (2003)	Diagonal (DM) and *Staggered-herringbone Micromixer* (SHM)	Intensity of segregation (variance), stretching, deformation rate	Particle tracking	CFX5 (FVM) commercial package. *Re* ~2. Deformation rate was found not to be well adapted for mixing characterization of such mixers.
Engler *et al.* (2004)	T-junction single microchannel	Mixing quality index	Solution of convection-diffusion equation	CFD-ACE+ (FVM) commercial package. *Re* = 7-200. Mixing quality of 1-30% at 0.15-4.6 mL/min.
Adeosun & Lawal (2005)	T-junction single microchannel and different multilaminated mixers	RTD	Solution of convection-diffusion equation	FLUENT (FEM) commercial package. Meshes sizes of 0.5 to 1.8 million nodes. Flow rates from 0.3 to 1.5 mL/min. *CV* used for comparison purposes (varying from 0.27 to 0.45).
Aubin. *et al.* (2005)	*Staggered-herringbone Micromixer* (SHM)	RTD, striation thickness, variance	Particle tracking	CFX5 (FVM) commercial package. *Re* ~2. Point-event distances method for estimation of variance. Restitution coefficient applied at the walls to avoid the loss of particles.
Kockmann *et al.* (2006)	90 degree bend squared microchannel	Mixing quality index	Solution of convection-diffusion equation	CFD-ACE+ (FVM) commercial package. *Re* = 0.1-200. Mixing quality exhibited a parabolic behavior as a function of *Re*: decrease from 40 to 5% for $0.1 < Re < 7$; and a quadratic increase up to 40% again for $7 < Re < 200$.

Table 2.3 Continued

Authors	Microdevice	Characterization	Numerical approach	Observations
Adeosun & Lawal (2009)	T-junction single microchannel (by Mikroglas)	RTD	Solution of convection-diffusion equation	FLUENT (FEM) commercial package. *Re* = 10-25. Flow rates = 0.2-0.5 mL/min. Good fit with the axial dispersion model and semi-empirical model. *CV* used to compare RTD with values ranging from 0.37 to 0.42.
Aubin *et al.* (2009)	Rectangular straight microchannels with varying aspect ratio	RTD	Particle tracking	CFX11 (FVM) commercial package. *Re* ~0.014-1.68. Weighted by volumetric flow rate. Aspect ratios < 0.3 are proposed as the optimal values for narrow RTD.
Cantu-Perez *et al.* (2010a)	Laminated microstructured plate with straight and zigzag microchannels	RTD	Particle tracking with random walks	COMSOL Multiphysics 3.5. Numerical RTD at 0.2 mL/min was in good agreement with experimental data.
Cantu-Perez *et al.* (2010b)	*Staggered-herringbone Micromixer* (SHM)	RTD	Particle tracking with random walks	COMSOL Multiphysics 3.5. *Re* = 0.013. At high *Pe* ~10^4 the RTD for the SHM remains unaffected.
Cortes-Quiroz *et al.* (2010)	*Staggered-herringbone Micromixer* (SHM)	Mixing index	Solution of convection-diffusion equation	CFX11 (FVM) commercial package. *Re* = 1. Mixing index used as originally defined by Danckwerts. Mixing indexes from 0.40 to 0.80.

Table 2.4 Microreaction technology applied for polymerization reactions

Authors	Microdevice	Product	Flow conditions	Observations
Bayer *et al.* (2000)	10 *SSIMM* interdigital microreactors	a) PMMA b) PAA	Mass flow rate: 6.6 kg/hr 150˚C	Continuous solution polymerization. Better mixing reduced local segregation of reactants leading to reduction of high molecular weight polymer fractions. Used as premixing stage for the elimination of fouling material in a macroscopic static mixer.
Chang *et al.* (2004)	Parallel straight microchannels (glass) (50 x 50 µm)	PVA	Residence time: 360 min 20˚C	Batch gamma-ray initiated dispersion polymerization. Narrower size distribution than conventional large-scale reactor. Particle size in the µm range.
Nisisako *et al.* (2004)	T-shaped microchannel (glass) (220 x 30 µm)	PVA	Volumetric flow rate: 0.1-27 mL/hr	Batch gamma-ray initiated dispersion polymerization. Formation of monodisperse polymer beads. Controlled sizes of 30-120 µm diameters.
Iwasaki & Yoshida (2005)	a) *KM* micromixer b) SS union-tee (i.d. of 800 µm) + 9 m of coiled SS tubing as a reactor (i.d. of 500 µm)	a) PBA b) PBM c) PMMA d) PVB e) PS	Residence time (min); yield (%): a) 1.5-5.0; 72-90 b) 3.0-12; 42-83 c) 0.5-10; 8-75 d) 5.0-15; 35-69 e) 5.0-15; 14-34 100˚C	Continuous solution polymerization. No fouling after 6 hours of continuous operation. Reduction of PDI for exothermic polymerizations only (*i.e.* PMMA, PBA).

Table 2.4 Continued

Authors	Microdevice	Product	Flow conditions	Observations
Okubo *et al.* (2010)	a) *KM* micromixer + 10 m of coiled SS tubing (i.d. 2.15 mm) b) T-junction + 55 m of coiled SS tubing (i.d. 1 mm)	a) PS b) PS, PMMA	a) 4.5-45 mL/min @ 85˚C, reaction time: 10 min. b) 1 mL/min @ 75, 85 and 95˚C, reaction time: 8 min.	Suspension polymerization (a) and polymerization in segmented flow (b). Conversions lower than 10% for the slug system. Slug polymerization improved polydispersity index by 10%. PS particles of around 10 µm successfully polymerized by suspension polymerization.

Table 2.5 Investigations on the liquid/liquid microreactor *LLMR-MIX-SI* manufactured by IMM

Authors	Objective	Reaction	Flow conditions	Observations
Wolf *et al.* (1997)	Description of the fabrication technique by μ-EDM	N/A	N/A	
Richter *et al.* (1998)	Description of the fabrication technique by μ-EDM and flow principle	N/A	N/A	
Richter *et al.* (2000)	Description of the fabrication and assembly of the four stacked plates model	N/A	N/A	
Wörz *et al.* (2001a-b)	Demonstration of microreactor process intensification	Cyclization reaction of a vitamin precursor as a intermediate stage of a BASF process	Residence times: 0.2-120 s	Single and four stacked plates version. Improvement of yield from 70% in industrial production to 95%. Reduction of by-products in as much as 50%. Improved yield due to efficient mixing and isothermal operation.
Caravieilhes *et al.* (2001)	Estimation of liquid/liquid mass transfer coefficients of catalyzed reactions	H-transfer reduction of dimethylitaconate catalyzed with water soluble rhodium phosphine	Residence time: 20-2 s @ 1-7 mL/min respectively	Four stacked plate version. Conversion of 40% lower than in batch. Performance is attributed to the design characteristics of the microreactor which does not allow for the most efficient capabilities at low flow rates. When compared to the *SSIMM* this latter achieved conversion up to 80%.

Table 2.6 Investigations on split-and-recombination microreactors featuring parallel microchannels

Authors	Objective	Geometry	Flow conditions	Observations
Antes *et al.* (2003)	Study of the nitration of toluene using nitric acid	Silicon micromixer *accoMix* (by Accoris, Germany): 9 parallel microchannels with G-shaped structures. Fluid inlet placed in central position of distribution manifold.	0.01-0.1 mL/min and 15 mL/min	Improved mixing allowed omission of an acid catalyst. Yields above 85% compared to 10% obtained in macroscopic batch process. Fluctuation in concentration among microchannels and along individual channels. Fluctuations were found to occur randomly and not caused by the fluidic structure.
Ferstl *et al.* (2004)	Test of an automated microreaction and monitoring system by a nitration reaction of benzoic acid	a) *accoMix* b) Improved silicon version of the *accoMix*: 11 G-shaped microchannels and trapezoidal manifolds fed from the side.	0.1-40 mL/min	Increase of 10% conversion in the improved version. Although the results were not disclosed it was stated that the improved flow distribution and mixing performance of the new design could be confirmed by thermographic measurements and by the Villermaux/Dushman reaction respectively.
Panić *et al.* (2004)	Mixing performance by the Villermaux/Dushman method	*accoMix*	0.1-20 mL/min	Mixing performance exhibited a quadratic decrease as a function of flow rate. However, form 1 to 3 mL/min the mixing efficiency decreased to improve again after this limit.
Bošković & Loebbecke (2008)	Experimental characterization of RTD	11 channel version of the *accoMix*	0.5-2 mL/min	Analysis based on the variance and skewness of the distributions. Comparison with 2 other single channel micromixers. Higher skewness was attributed to less developed secondary flows in SAR structure. Tailing effect caused by inhomogeneous parallelization of flow.

2.8 ANALYSIS OF THE LITERATURE REVIEW

The current knowledge about the advantages of microchemical process engineering technology is abundant and a great amount of scientific effort has been oriented towards the better understanding of novel mixing mechanisms implemented at the microscale. One of the most investigated geometries has been the T-junction (*i.e.* mixing by the contacting of two streams) along other single-channel microstructures usually made of glass or transparent polymers. State-of-the-art manufacturing techniques have allowed for the mass production of more complex and mechanically robust microreaction units which for the purpose of increased throughput often rely on parallelization of flow. In most instances these microreactors consist of consecutive flow sections with different active volumes including distribution manifolds that produce particular microfluidic structures quite different from those encountered in laboratory test microdevices. The characterization of emerging microreaction units remains a necessary stage in order to evaluate the true potential for the transition of microreaction technology to the industrial scene. Under the scope of the information presented in this chapter it is possible to assess the current state of knowledge and characterization procedures of the performance of microfluidic devices and particularly about the multilamination and split-and-recombination mechanisms.

2.8.1 Microreaction Units

Only certain investigations have focused on the characterization of metallic microreactors such as the *KM* mixer, *V-type* mixer, *SSIMM* interdigital structure, split-and-recombination *Caterpillar* and the *StarLam300*; these latter three manufactured for commercialization by the IMM (Mainz).

In this context the multilamination model *SSIMM* manufactured by IMM has been extensively investigated in its original single-module version. From the available studies that compare the mixing performance of different microfluidic devices this multilamination mixing structure is among the ones exhibiting the best performance over a flow rate range of 0.1-100 mL/min. An alternative model designed for high heat transfer capabilities and also featuring the

multilamination mechanism has been developed by IMM under the model designation *LLMR-MIX-SI*. This alternative version exhibits a promising potential for a better control of exothermic reactions. The available literature on this latter microreactor model mainly consists of descriptive studies about its conceptualization and manufacturing techniques. Only two publications have reported on the improvements of the yield and conversion of chemical reactions achieved in this microreactor model. One of those investigations was related to a proprietary industrial process developed by BASF and although no specific information was disclosed the heat transfer capabilities of the four-plate version of the *LLMR-MIX-SI* microreactor were concluded to be the main reason for the observed improvement. Presently no other information is available about neither the single nor the modular four-plate version of this microreactor model.

Microfluidic devices featuring the split-and-recombination mechanism have exhibited a similar mixing performance as compared to multilamination structures although producing lower pressure drops at the same flow conditions. This potential for improved mixing at much lower pressure drops is one of the attractive features of this type of microreactor design. For the purpose of increased throughput a few parallel-microchannel versions of this mixing mechanism have been manufactured implementing trapezoidal manifolds which are claimed to be the optimized geometries for achieving homogeneous flow distribution. Only two publications have investigated the mixing performance and the RTD characteristics of the parallel-channel version of split-and-recombination microdevices.

The multilamination and split-and-recombination mechanisms represent two attractive mixing alternatives that can be exploited for industrial applications. Despite being featured by certain microreaction units designed for high pressure and temperature conditions there is still a lack of experimental information regarding these type of microreactors which is required to evaluate and compare their process performance. In this project we have selected two microreaction units each featuring one of the aforementioned mixing principles. The multilamination unit is a commercial model manufactured by IMM (Mainz) while the split-and-recombination unit is a prototype design manufactured by Atotech (Berlin).

2.8.2 Experimental Characterization

The mean residence time and residence time distribution (RTD) are essential process parameters for the performance evaluation of continuous flow reactors at any scale level. However, information about active volumes of microfluidic structures has not been explicitly disclosed in the available literature in a consistent manner. Until recently the experimental RTD characterization of microfluidic devices was not systematically applied. With the exception of two investigations dealing with more complex geometries, RTD analysis has been performed on single microchannel structures. A great effort has been placed on obtaining nearly perfect tracer impulses and on the precise tracer detection at the inlet and outlet planes of straight microchannels. The resulting detection systems are limited to transparent devices and sometimes to the specific microreactor set-up around which they were built. Metallic microreactors along with their connecting ports and fluid lines prevent such precise tracer injection and detection. Investigations about the application of RTD analysis techniques to this type of microreaction units are still needed not only for performance evaluation purposes but also for describing how to tackle their particular experimental restrictions. Another important subject regarding the RTD analysis is that frequently microfluidic structures are not adequately described by classical RTD flow models, *e.g.* the axial dispersion model. Thus, an empirical model has been applied since it is capable to provide a better fit to the experimental concentration-time signals. The parameters of this empirical model are purely fitting parameters which are not directly related to any geometrical characteristic describing the flow system. In order to better describe the RTD behavior of microfluidic devices a suitable model not relying on empirical parameters should be developed. Alternatively, a suitable correlation between the empirical and theoretical parameters should be explored. The discrepancies between the classical axial dispersion model and the experimental RTD functions require appropriate attention since there is experimental evidence of a shift in direction and of a non-monotonic behavior of the axial dispersion effects in continuous flow microfluidic devices. Thus far, such behaviors are known to be independent of changes in viscosity and hydrodynamic conditions.

2.8.3 Numerical Simulation

Numerical simulations have been applied for the mixing characterization and RTD analysis of microfluidic devices. These studies have focused for the most part on T-junctions and on the staggered-herringbone mixer (SHM). Information about numerical RTD of other type of microreactor geometries is not presently available.

Residence time distributions can be obtained numerically using two approaches: the solution of the unsteady-state convection-diffusion equation, and the particle tracking method. When applying the particle tracking method for the estimation of RTD **Nauman (2008b)** recently highlighted the shortcomings of CFD codes to account for the low fluid velocities near the walls of the system, *i.e.* the non-slip velocity condition. A strategy of particle restitution (**Aubin *et al.*, 2009**) has been proposed in order to conserve the massless tracer particles that are lost in the boundary layer region. This strategy has been questioned (**Wörner, 2010**) due to its failure to meet the theoretical criteria of infinite variance in the absence of molecular diffusion (**Nauman, 1977**). However, **Nauman (1991)** concluded that even in the absence of molecular diffusion a finite variance is obtained when the RTD analysis is performed weighting the tracer particles by the volumetric flow rate and not by the cross-sectional area. This type of weighting is only necessary when the RTD is obtained by means of the particle tracking method and the amount of tracer particles is constant throughout the injection plane, *i.e.* the number of injected particles is not proportional to the fluid velocity. Weighting by flow rate gives the proper result according to the conceptual definition of RTD. Still this strategy requires to be validated in the microscale since it is known that even in macroscopic continuous flow systems experimentally obtained distributions exhibit discrepancies when compared to numerical RTD weighted by flow rate.

The particle tracking method can be useful for the reduction of computational time during the calculation of RTD in complicated 3D microfluidic structures. Reasonable estimates of mean times and RTD can be obtained in order to provide a valuable insight of the mixing capabilities of the system from a purely mechanistic point of view, *i.e.* neglecting the contribution of molecular diffusion. The difference between residence time distributions obtained by the particle tracking method and those obtained by the solution of the convection-diffusion equation offer an alternative to quantify the relative importance of the diffusion mechanism over the mixing

performance in particular microreactor geometry. The effect of the mechanics of mixing is relevant in microreactors that reduce the fluid layer thickness in a geometrical sequence, *e.g.* split-and-recombination. The difference between these two CFD approaches in the microscale has not been previously addressed.

2.8.4 Polymerization in Microreactors

Regarding the application of microreaction technology to polymer reaction engineering, the available experimental studies conducted on polymerization in microscale geometries are limited. A conclusion can be drawn that microtubes and micromixers can significantly improve the control of polymerization reactions; the former by allowing a rapid removal of the heat released by the polymerization and the latter by promoting an efficient mixing of the reactants. A microfluidic device combining both advantages would be desirable for the control of a wider range of polymerization reactions. Single channel T-junction microreactors have been used to some extent for such type of reactions although only in two occasions in continuous operation as highlighted in Table 2.4. Moreover, the microreactors have been used as premixing stages while the actual polymerization is conducted in coiled tubing reactors. The *SSIMM* interdigital microreactor from IMM exhibited promising potential for the control of reaction temperature and molecular weight. Nevertheless, experimental investigations on the performance of interdigital or split-and-recombination microreactors for conducting free-radical polymerizations have not been reported until now.

CHAPTER 3

SPECIFIC OBJECTIVES

Based on the information provided in the previous chapter regarding the review of the pertinent literature, we state the following hypothesis for this project:

The hydrodynamic and heat transfer characteristics of two microreactors provided with integrated heat exchangers and featuring respectively the split-and-recombination and the multilamination micromixing mechanisms, can be used to conduct the free-radical polymerization of styrene reaching a conversion level of at least 30% which is critical in other polymerization systems.

In order to reach the general objective of the project and to prove the previous hypothesis, the following specific objectives are defined:

1. To conduct the experimental mixing and flow characterization of two different microreactors provided with an integrated heat-exchanger featuring respectively the split-and-recombination and the multilamination micromixing mechanism.

2. To determine the effect of the manifold flow distribution on the mixing performance and distribution of residence times of the proposed microreactors.

3. To characterize the heat transfer capabilities of the proposed microreactors and to determine the influence of the flow conditions on the free-radical polymerization of styrene monomer conducted inside the microreactors aimed at achieving 30% of conversion.

CHAPTER 4

OVERALL METHODOLOGICAL APPROACH

AND

ORGANIZATION OF THE ARTICLES

4.1 CONTENT OF THE ARTICLES

This chapter is aimed at providing a brief overview of the research methodology followed for the achievement of the specific objectives of the project as well as describing the organizational structure of the remainder of this work. Chapters 5 through 7 compose the body of this thesis and each will be devoted to the development of one specific objective; consequently the pertinent methodology and characterization techniques will be described in detail in the corresponding chapter. Each of these three chapters is conceived to be the subject of a scientific publication, thus their structure and development is organized accordingly. Chapter 8 covers a general discussion of the results and the overall conclusions. Finally, Chapter 9 briefly elaborates on some opportunities for future research on the subject of microreaction technology.

Chapter 5 is entitled "*Characterization of the hydrodynamics and mixing performance of a split-and-recombination (SAR) prototype microreactor and a multilamination commercial microreactor*".

In this chapter we report on the experimental characterization of two mechanically robust microreactors designed for high temperature and pressure operating conditions thus having promising industrial potential. One of the microreactors selected is a prototype design while the other is a commercialized model. To the best of our knowledge no prior evidence of their hydrodynamic performance was available in the open literature. Although the two mixing

principles analyzed are well known there is still a significant amount of insight to be gained about the performance of these microfluidic structures in the exact flow configuration in which they are implemented, which would be typical of an industrial setup. Also, we address the suitability of applying classical Residence Time Distribution characterization techniques to these types of metallic microreactors tackling their inherent experimental difficulties such as restricted flow visualization, constrained measurement at precise inlet and outlet planes, and influence of the volumes of peripheral fluid lines. The methodology consists of:

1. Pressure drop experiments with a Newtonian fluid in laminar flow regime
2. Residence Time Distribution analysis using the pulse tracer input technique
3. Mixing performance evaluation by the Villermaux/Dushman method for continuous flow

Chapter 6 is entitled "*Numerical investigation of the hydrodynamics of a split-and-recombination and multilamination microreactors*".

In this chapter we report on the numerical characterization of the hydrodynamics and Residence Time Distribution (RTD) of two mechanically robust microreactors designed for high temperature and pressure conditions. This work can be regarded as a standalone study aimed at providing a better insight of the performance of the split-and-recombination and multilamination microfluidic structures in the exact flow configuration in which they would be implemented in an industrial scenario. To the best of our knowledge no prior evidence of the hydrodynamic performance of these specific microreaction units was available in the open literature. The 3D modeling of the flow field requires the simultaneous numerical solution of the steady-state incompressible Navier-Stokes momentum and continuity equations solved by means of the finite element method. Due to the complexity of the geometries and the high aspect ratios of the microchannels, the meshes of the computer-aided design models required a large number of elements. In order to overcome this computationally expensive problem, the MINI finite element implemented in the commercial 3D finite element software POLY3D (Rheosoft, Inc.) is applied. The particle tracking technique is used for the estimation of numerically based RTD. The mixing performance is evaluated by the scale and intensity of segregation concepts. Control planes for

the detection of tracer particles are defined at the inlet of each micromixing channel as well as at the outlet port of both microreactors in order to determine the effectiveness of the flow distribution achieved by the manifolds. The methodology consists of:

1. Validation of numerical simulations by pressure drop experimental results
2. Determination of the flow distribution in the microchannel network
3. Mixing performance evaluation using the scale and intensity of segregation concepts calculated by means of the particle tracking method
4. Residence Time Distribution analysis by means of the particle tracking method

Chapter 7 is entitled "*Free-radical polymerization of styrene using a split-and-recombination and multilamination microreactors*".

In this chapter the heat transfer capabilities of the microreactors are first characterized as a function of the thermal capacities of the fluids. The microreactors are then used to conduct the free-radical polymerization of styrene monomer at two different reaction temperatures, *e.g.* 100 and 130 degrees C; and using different types of chemical initiators. Conversions are estimated gravimetrically and molecular weights and molecular weights distributions are obtained by gel permeation chromatography. The methodology consists of:

1. Heat transfer characterization of the integrated heat exchangers of the microreactors using water as the test fluid at different fluid thermal capacities and flow configurations, *e.g.* parallel and counterflow mode.
2. Free-radical polymerization of styrene monomer in continuous flow aiming at 30% of conversion using mono-, bi-, and tetrafunctional organic peroxide initiators.

4.2 STATEMENT OF CONTRIBUTIONS

The Ph.D. student, in the role of the principal author of this thesis, and the student supervisor and co-supervisor certify that all co-authors listed below take public responsibility for their part of the publication; they meet the criteria for authorship in that they have participated in the conception, execution, or interpretation, of at least that part of the publication in their field of expertise; they have accepted the student contribution as indicated below; and they have consented to their work being included and published as a part of this thesis.

In the case of Chapter 5 entitled "*Characterization of the hydrodynamics and mixing performance of a split-and-recombination (SAR) prototype microreactor and a multilamination commercial microreactor*":

Contributor	**Statement of Contribution**
Lionel Sergio Méndez Portillo	Writing of the manuscript, experimental design, conducted experiments, and data analysis
Louis Fradette	Aided in analysis and interpretation of the Residence Time Distribution experiments
Charles Dubois	Co-supervision, providing of the multilamination microreactor, expertise in hydrodynamics and reaction engineering
Philippe A. Tanguy	Supervision, providing of the split-and-recombination microreactor, expertise in hydrodynamics and mixing process

In the case of Chapter 6 entitled "*Numerical investigation of the hydrodynamics of a split-and-recombination and multilamination microreactors*":

Contributor	Statement of Contribution
Lionel Sergio Méndez Portillo	Writing of the manuscript, creation of 3D solid models and meshing, run of CFD simulations, data analysis and post-processing, programming of extra post-processing code
Mourad Heniche	Aided in analysis and interpretation of the CFD simulations and numerical RTD results
Charles Dubois	Co-supervision, providing of the multilamination microreactor, expertise in hydrodynamics and reaction engineering
Philippe A. Tanguy	Supervision, providing of the split-and-recombination microreactor, expertise in hydrodynamics and mixing process

In the case of Chapter 7 entitled "*Free-radical polymerization of styrene using a split-and-recombination and multilamination microreactors*":

Contributor	Statement of Contribution
Lionel Sergio Méndez Portillo	Writing of the manuscript, experimental design, conducted experiments, and data analysis
Charles Dubois	Co-supervision, providing of the multilamination microreactor, expertise in polymerization reaction engineering
Philippe A. Tanguy	Supervision, providing of the split-and-recombination microreactor, expertise in hydrodynamics and mixing process

CHAPTER 5

CHARACTERIZATION OF THE HYDRODYNAMICS AND MIXING PERFORMANCE OF A SPLIT-AND-RECOMBINATION (SAR) PROTOTYPE MICROREACTOR AND A MULTILAMINATION COMMERCIAL MICROREACTOR

Lionel S. Méndez-Portillo, Louis Fradette, Charles Dubois, Philippe A. Tanguy

Department of Chemical Engineering, École Polytechnique de Montréal
P.O. Box 6079, Station Centre-Ville, Montreal, QC.
Canada H3C 3A7

ABSTRACT

The aim of this work was to quantify the performance of two well known mixing techniques used in microreactors: the split-and-recombination (SAR) and the multilamination by means of an interdigital structure mixing mechanisms. The residence time distribution (RTD) and the mixing performance in laminar flow regime were experimentally characterized by the tracer pulse-input technique and the iodide-iodate Villermaux/Dushman method. RTD analysis indicates by-passing caused by uneven flow distribution in the manifolds of both microreactors. A decrease of the quadratic dependence of axial dispersion on fluid velocity is produced by the improved tracer homogenization achieved in the microfluidic structures. The iodide-iodate method shows that below a critical Damköhler number the microreactors exhibit a superior mixing performance than a conventional T-junction. The interdigital microreactor displayed the best mixing capabilities for all the flow conditions investigated. However, the estimation of energy dissipation confirms that the improved mixing performance of the interdigital microreactor is obtained at the expense of greater energy expenditure when compared with the split-and-recombination microreactor.

5.1 INTRODUCTION

Microreaction technology is the subfield of the chemical micro process engineering that focuses on conducting chemical reactions inside microfluidic devices. Microreactors can achieve fast mixing by diffusion between thin fluid layers (**Ehrfeld *et al.*, 1997; Ehrfeld *et al.*, 1999a; Haverkamp *et al.*, 1999**) and their small active volumes provide high surface-to-volume ratios resulting in efficient heat transfer capabilities (**Ehrfeld *et al.*, 1999b; Schubert *et al.*, 2001**). The manufacturing of microdevices has evolved from polymeric or ceramic transparent materials intended for visualization to more robust microreaction units made of stainless steel, which are designed for demanding industrial applications and allow attaining high pressure and temperature operating conditions. Aiming at higher throughputs, these units are manufactured with parallel microchannels of different aspect ratios and shapes based on a variety of mixing principles (**Löwe *et al.*, 2000; Stroock *et al.*, 2002; Hardt & Schönfeld, 2003; Schönfeld & Hardt, 2004**).

While the benefit of process intensification in single microchannels is multiplied by parallelization to achieve high production volumes, a problem of uniform reactants distribution in the microchannel network may arise. The hydrodynamic and mixing characterization of these commercially available microfluidic devices is therefore a requirement in order to gain a better insight of their process engineering performance and identify suitable applications. Classical experimental techniques such as residence time distribution (RTD) analysis and parallel/consecutive reaction methods adapted to the microscale have provided the basis to quantitatively evaluate the performance of different types of microfluidic devices.

The characterization of metallic microreactors can pose experimental difficulties not encountered in transparent geometries. For instance the volumes of the connecting tubing and fittings are usually equal or greater in magnitude than the active volume of the microreactors and the influence of these peripheral lines cannot be avoided in practice. Previous works have investigated the mixing characteristics (**Ehrfeld *et al*., 1999; Trippa *et al*., 2004; Kockmann *et al*., 2006; Men *et al*., 2007; Kölbl *et al*., 2008**) and the residence time distribution functions (**Günther *et al*., 2004; Trachsel *et al*., 2004; Bošković & Loebbecke, 2008; Lohse *et al*., 2008; Adeosun & Lawal, 2009; Köhler *et al.*, 2010**) of single and multiple channel microfluidic structures. Some of these works applied specialized injection and detection systems developed for specific transparent microdevices that allow for precise measurement at the planes of interest. Therefore, in this context very few studies (**Günther *et al*., 2004; Bošković & Loebbecke, 2008**) had to deal with the effect of peripheral lines during the experimental RTD analysis of microdevices.

In the present study, the metallic microreactors selected are based on the split-and-recombination and the multilamination mechanism respectively, and are provided with distribution manifolds to produce flow parallelization. The split-and-recombination microreactor model is a prototype design and no data was available about its hydrodynamic characteristics. The multilamination microreactor is an already commercialized model that, according to the manufacturer's specifications, is able to operate with fluid viscosities up to 1 Pa-s, between flow rates of 0.01-0.55 mL/min and residence times in the 0.3-18 s range. No other information about the characterization of this latter model is available in the open literature.

The contribution of this work is to get a better insight about the hydrodynamic characteristics of the classical split-and-recombination and multilamination mechanisms in the exact flow configuration in which they are implemented, which would be typical of an industrial setup. A necessary stage for this purpose is to address the suitability of applying the classical RTD analysis techniques to metallic microreactors tackling their inherent experimental difficulties such as restricted visualization of flow structures, constrained measurements at precise inlet and outlet planes, and the influence of peripherals fluid lines in the stimulus signal.

5.2 CHARACTERIZATION METHODS

5.2.1 Pressure Drop

The pressure drop is a classical parameter that can be used to compare the performance of microreactors. Recently, it has been shown that when the surface roughness is accounted for the pressure drop results fall within the laminar flow theory prediction (**Gamrat *et al.*, 2008**). The general consensus in the literature is that the governing fluid dynamics proposed by classical continuum theory are also valid at the microscale (**Judy *et al.*, 2002; Bavière *et al.*, 2004; Bucci *et al.*, 2004; Gamrat *et al.*, 2008**). Conclusions about the flow regime in which a microreactor is operating can be obtained when pressure drop measurements are compared to the laminar flow theory and experimental correlations. Also, in passive mixing devices such as microreactors, the pressure drop ΔP is related to the energy dissipation ε of the mixing process (Eq. 5.1) as:

$$\varepsilon = \frac{\Delta P \cdot v}{\rho \cdot l} \tag{5.1}$$

where v is the flow mean velocity, ρ is the mass density and l is the microreactor or tube length between the pressure detection points.

In this work the pressure drop data obtained from the microreactors is entered into the Hagen-Poiseuille equation (Eq. 5.2) in order to calculate an equivalent diameter d_{eq} of a straight tube that would produce the same pressure drop along the same length l as that of the microreactors.

$$\Delta P = \frac{128 \cdot Q \cdot \mu \cdot l}{\pi \cdot d_{eq}^{\ 4}} \tag{5.2}$$

In Eq. 5.2 Q is the volumetric flowrate and μ is the fluid dynamic viscosity. Once d_{eq} is obtained the pressure drop data is transformed into a non-dimensional friction factor f used for the systematic representation of flow data in pipes and ducts. From the definition of the friction factor and a force balance on the fluid in the direction of flow (**Bird *et al.*, 2002**) the friction factor is related to the pressure drop by Eq. 5.3.

$$\Delta P = f \cdot \left(\frac{1}{2} \rho v^2 \right) \cdot 4 \left(\frac{l}{d_{eq}} \right) \tag{5.3}$$

If the equivalent diameter properly represents the geometrical constraints of the microreactors then the f values should follow the prediction of laminar flow when plotted as a function of the Reynolds number Re calculated as:

$$Re = \frac{\rho \cdot d_{eq} \cdot v}{\mu} \tag{5.4}$$

5.2.2 Residence Time Distribution

The residence time distribution (RTD) is one of the most informative characterization techniques for chemical reactors at any scale level. The RTD of the microreactors is obtained experimentally in this work by introducing a pulse-input stimulus (**Nauman & Buffham, 1983; Levenspiel, 1999**) into the fluid entering the reactor and measuring the transient response of the concentration

of the tracer at the exit plane. The exit-age distribution function $E(t)$ is then calculated by dividing the response curve $C(t)$ of this pulse by the area under the curve:

$$E(t) = \frac{C(t)}{\int C(t)dt} \tag{5.5}$$

The mean residence time t_m is obtained by:

$$t_m = \int_0^\infty t \cdot E(t)dt \tag{5.6}$$

Due to the requirement of connection ports, tracer pulses are difficult to achieve experimentally precisely at the inlet plane of the reaction section of commercial microreactors. In order to apply the RTD analysis in this type of units, the so-called *sloppy* (**Fogler, 1999**) or *one-shot* (**Levenspiel, 1999**) tracer input is used. With this approach, information about the RTD can be obtained irrespective of the shape of the stimulus signal, provided that such signal can be recorded at the inlet and outlet of the flow vessel. The input signals are recorded independently by using a piece of tubing of the same length and diameter as the input lines leading to each microreactor. The internal diameter of the tubes leading to the SAR and LLMR was 1/8 in. and 1/16 in. respectively. It will be assumed for the rest of this analysis that the *one-shot* tracer input signals recorded using this approach are of the same shape of those entering the microreactor.

The output signal $C_{out}(t')$ obtained at the exit of the microreactor from a *one-shot* tracer input is the result of the convolution in the time domain of the input signal $C_{in}(t')$ and the reactor response signal $E(t)$:

$$C_{out}(t') = \int_0^t C_{in}(t'-t) \cdot E(t) \tag{5.7}$$

The $E(t)$ function of the reactor is then retrieved from the convoluted output curve. Deconvolution in the time domain is not a trivial operation and usually is avoided by instead performing a direct convolution of the input signal with a given flow model. The resulting curve

is fitted to the response $C_{out}(t')$ obtained from experiments and the model parameters are optimized by a *nonlinear least squares fitting* (NLSF) procedure (**Westerterp, Swaaij and Beenackers, 1984; Günther, M., *et al.*, 2004; Bošković & Loebbecke, 2008; Adeosun & Lawal, 2009; Köhler *et al.*, 2010**). Even if this strategy circumvents deconvolution in the time domain, it results in a time consuming procedure requiring significant computational efforts.

The alternative presently followed to obtain the exit-age distribution function $E(t)$ of the microreactors consists in performing the analysis in the frequency domain where the Laplace or Fourier transform of the convolution integral (Eq. 5.7) is equivalent to the product of the transforms of the input signal and system response $E(t)$. Therefore, the deconvolution in the frequency domain is defined simply as:

$$E(s) = \frac{C_{out}(s)}{C_{in}(s)} \tag{5.8}$$

where $C_{out}(s)$, $C_{in}(s)$ and $E(s)$ are the output, input and system signals transformed to the frequency domain. Once the deconvolution is performed, the data is inversed to the time domain. Deconvolution in the frequency domain can be performed by the Laplace or Fourier transforms. The Laplace frequency domain is frequently preferred over the Fourier transform due to the latter having real and imaginary components and an oscillatory behavior. We have conducted the analysis in the Fourier domain since its advantage resides in the application of the computationally efficient *Fast Fourier Transform* (FFT) algorithm. In rectangular form the division of the signals in the Fourier domain is expressed as:

$$E(s) = \mathrm{Re}\,E(s) + \mathrm{Im}\,E(s) \tag{5.9}$$

$$\mathrm{Re}\,E(s) = \frac{\mathrm{Re}\,C_{out}(s)\cdot \mathrm{Re}\,C_{in}(s) + \mathrm{Im}\,C_{out}(s)\cdot \mathrm{Im}\,C_{in}(s)}{\mathrm{Re}\,C_{in}(s)^2 + \mathrm{Im}\,C_{in}(s)^2} \tag{5.10}$$

$$\mathrm{Im}\,E(s) = \frac{\mathrm{Im}\,C_{out}(s)\cdot \mathrm{Re}\,C_{in}(s) - \mathrm{Re}\,C_{out}(s)\cdot \mathrm{Im}\,C_{in}(s)}{\mathrm{Re}\,C_{in}(s)^2 + \mathrm{Im}\,C_{in}(s)^2} \tag{5.11}$$

The tracer inputs and output signals are filtered and then transformed to the Fourier domain by using a deconvolution routine developed specifically for our application using the programming platform of the Origin 6.0 software (OriginLab, Co.). The filtering step is critical in order to obtain reliable results during deconvolution operation and the degree of filtering depends on the characteristics of the signal recorded and the level of noise and acquisition rate of the data (**Smith, 1997**).

The $E(t)$ functions obtained are then fitted with the *axial dispersion model* which is a one parameter flow model used to describe non-ideal tubular reactors in laminar flow conditions. An *empirical model* proposed by **Ham & Platzer (2004)** has been found (**Bošković & Loebbecke, 2008; Adeosun & Lawal, 2009; Köhler *et al.*, 2010**) to provide a better fit than the axial dispersion model when applied to microfluidic devices. However, the relationship between the empirical model parameters and the geometrical characteristics of the flow system has not been well established so far. Our choice of the axial dispersion model over the empirical model lies in that the parameters of the axial dispersion model are theoretically derived from the flow properties and geometrical characteristics of an empty tube allowing for a direct comparison of flow performance. The solution of the axial dispersion model for open-open boundary conditions (**Levenspiel, 1999**) is given in non-dimensional form as:

$$E_\theta = \frac{1}{2\sqrt{\pi\theta(D/v\cdot l)}}\exp\left[-\frac{(1-\theta)^2}{4\theta(D/v\cdot l)}\right] \tag{5.12}$$

From the fitting curves the dimensionless group $D/v\cdot l$ is obtained. This term is called the *vessel dispersion number* and represents the spreading process of the tracer in the axial direction. The reciprocal of the vessel dispersion number is also known as the *reaction* Peclet number Pe_r used in reaction systems with the length of the reactor l as the characteristic length:

$$\frac{1}{Pe_r} = \frac{D}{v\cdot l} = \left(\frac{D}{v\cdot d_{eq}}\right)\left(\frac{d_{eq}}{l}\right) \tag{5.13}$$

The vessel dispersion number is the product of an intensity of dispersion in the radial direction and the geometric factor l/d_{eq}. Introducing the value of d_{eq} obtained from pressure drop experiments into Eq. 5.13 the vessel dispersion number of the microreactors can be compared to an equivalent empty tube producing the same pressure drop. The vessel dispersion number of an empty tube is calculated by a classical flow correlation (**Levenspiel, 1999**) as a function of *Re* and the Schmidt number *Sc* for $l/d_{eq} > 30$ as:

$$\frac{D}{v \cdot d_{eq}} = \frac{1}{\mathrm{Re} \cdot Sc} + \frac{\mathrm{Re} \cdot Sc}{192} \tag{5.14}$$

To assess the contribution of molecular diffusion in the spread of the tracer concentration in the microreactors investigated, the criterion for neglecting radial diffusion in continuous laminar flow reactors proposed by **Nauman (2008)** is used:

$$\frac{D_{diff} \cdot t_m}{R^2} < 0.003 \tag{5.15}$$

where R is the radius of an empty tube and D_{diff} is the coefficient of molecular diffusion of the tracer in the fluid medium. The values of the diffusion coefficient of the triiodide compound that were introduced in Eq. 5.15 range between 0.86 – 1.13 x 10^{-9} m^2/s (**Newson & Riddiford, 1961; Ruff *et al.*, 1972; Cantrel *et al.*, 1997**).

5.2.3 Mixing Characterization by the Villermaux/Dushman Method

The Villermaux/Dushman method, also called the iodide-iodate system, is used in this work for the mixing characterization of the microreactors in continuous flow operation (**Fournier *et al.*, 1996a-b**). Details of the kinetic mechanism, constants of the Dushman reaction and its adaptation to continuous flow can be found in the studies of **Weast (1986), Guichardon *et al.* (2000)** and **Panić *et al.* (2004)**. Iodine formation is attributed to local deviation of the average concentration of acid due to imperfect mixing and the triiodide compound is quantified by spectrophotometry to characterize the mixing performance. Optical detection of iodine in the form of triiodide

compound is conducted at an absorption band of 351 nm where the risk of signal saturation is reduced.

The formation of iodine is thermodynamically possible if the buffer equilibrium (dependent of *pH*) falls too far in the acidic range. On the other hand, if a strong basic *pH* is reached the iodine formed is thermodynamically unstable and disassociation can occur. From results reported in previous investigations (**Guichardon & Falk**, **2000; Panić *et al.*, 2004**) it is presently concluded that a *pH* value between 8.3 and 9.7 provides a suitable range of operating conditions to avoid the aforementioned effects.

Knowledge of the time scale of reaction is necessary in order to evaluate the real contribution of the hydrodynamic performance of the microreactors to the yield of the Dushman reaction. This time scale is given by the characteristic reaction time t_{cr} (**Mann, 2009**) as:

$$t_{cr} = \frac{1}{k_{cr} \cdot C_{cr}^{\,n-1}} \tag{5.16}$$

where k_{cr} and C_{cr} are respectively the constant of the rate of disappearance and the initial concentration of the reference reactant, and n is the reaction order. In this case the sulphuric acid (*i.e.* limiting reactant) is considered as the reference reactant.

Although for comparison purposes the mixing performance is often reported using only the pure spectrophotometric signals (**Ehrfeld *et al.*, 1999; Panić *et al.* 2004; Kölbl *et al.*, 2008; Kölbl *et al.*, 2010**) we report the amount of triiodide detected in terms of a segregation index X_s:

$$X_s = \frac{Y}{Y_{ST}} = \frac{4\left[\left[I_3^-\right] + \left[I_2\right]\right]}{\left[H^+\right]_0} \cdot \frac{6\left[IO_3^-\right]_0 + \left[H_2BO_3^-\right]_0}{3\left[IO_3^-\right]_0} \tag{5.17}$$

where Y is the detected selectivity of the experiment and Y_{ST} is the selectivity at the total segregation state (**Fournier *et al.*, 1996a; Trippa & Jachuck, 2004; Kockmann *et al.*, 2006; Men *et al.*, 2007; Fan *et al.*, 2010**). The segregation index is a relative parameter that depends

not only on the mixing capabilities of the system but also on the concentration of the reactants. Nevertheless, knowledge of the reactant concentrations if reported along with the flow conditions and active volumes of investigated microreactors can provide a sufficient basis for comparison between different studies.

The segregation index is then evaluated as a function of the Damköhler number *Da* defined as:

$$Da = k_{cr} \cdot C_{cr}^{n-1} \cdot t_m = \frac{t_m}{t_{cr}} \tag{5.18}$$

The Damköhler number physically represents the ratio of the rate of consumption of a reactant by the rate of convective transport in the reactor. Commercial microreactors may operate with parallelization of flow, varying microchannel dimensions and consecutive flow sections; consequently different *Re* can be calculated within the same microfluidic structure. Moreover, depending on their active volumes, microreactors operating at the same flow rate may possess quite different mean residence times. Comparison of mixing performance as a function of *Da* can provide a better insight about the capabilities of the microfluidic structures as chemical reactors.

5.3 EXPERIMENTAL SECTION

5.3.1 Description of the Microreactors

Two microreactors have been considered in this work (Figure 5.9). A prototype microreactor featuring a split-and-recombination mechanism (further referenced as SAR) was provided by *Atotech GmbH* (Berlin, Germany). Another liquid/liquid microreactor (further referenced as LLMR) was acquired from *IMM GmbH* (Mainz, Germany) under the model designation *LLMR-MIX-SI* and is based on the multilamination of flow by means of an interdigital structure. Both microreactors are equipped with an integrated forced-convection heat exchanger. The maximal pressure rating provided by the manufacturers is 100 bar for the SAR and 50 bar for the LLMR.

A union tee of 1/8 in. internal diameter was also used for the purpose of comparing the mixing performance.

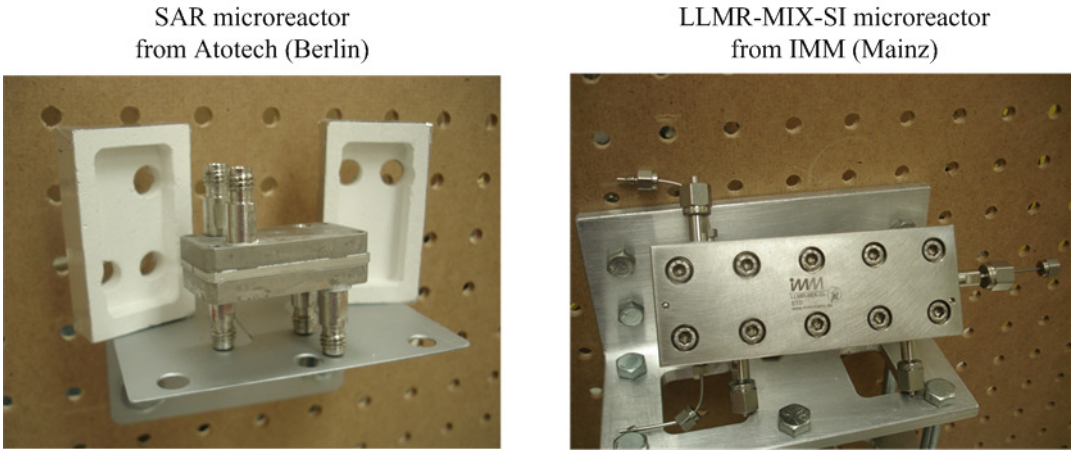

Figure 5.1 Split-and-recombination (SAR) prototype (left) and multilamination commercial microreactor (right) used in this investigation both assembled by means of stacked plates.

5.3.1.1 Split-and-recombination Microreactor

The SAR microreactor consists of a stacked arrangement of 8 plates assembled in the order depicted in Figure 5.10a. In the concept of stacked arrangement of plates, the flow passages are machined into the plate surfaces forming carved or tunnel-like structures (Figure 5.10b).

Each cover plate has a distribution manifold machined in the bottom surface that allows the fluids to be divided into five mixing microchannels that use the classical split-and-recombination principle. The mixing section is created by two plates featuring a G-shaped structure (**Antes *et al.*, 2003; Ferstl *et al.*, 2004; Bošković *et al.*, 2007**), which is employed to arrange the splitting elements longitudinally along the flow direction (Figure 5.2b).

The Mixing Plate 1 (Figure 5.2a) has five columns with five rows of G-shaped structures machined *in the bottom* of its surface while the Mixing Plate 2 has five columns with five rows of *inversed* G-shaped structures machined *in the top* of its surface but shifted longitudinally a certain distance in relation to those machined in the Mixing Plate 1. When the two mixing plates

are assembled one above the other, each of the outlets of the G-shaped structures in the Mixing Plate 1 coincides exactly with the shifted inlet of the microstructures of the Mixing Plate 2 thus creating a total of five long mixing microchannels composed of 10 G-shaped structures. In this way the fluid inside is switching from the upper to the lower plate as the mixing proceeds.

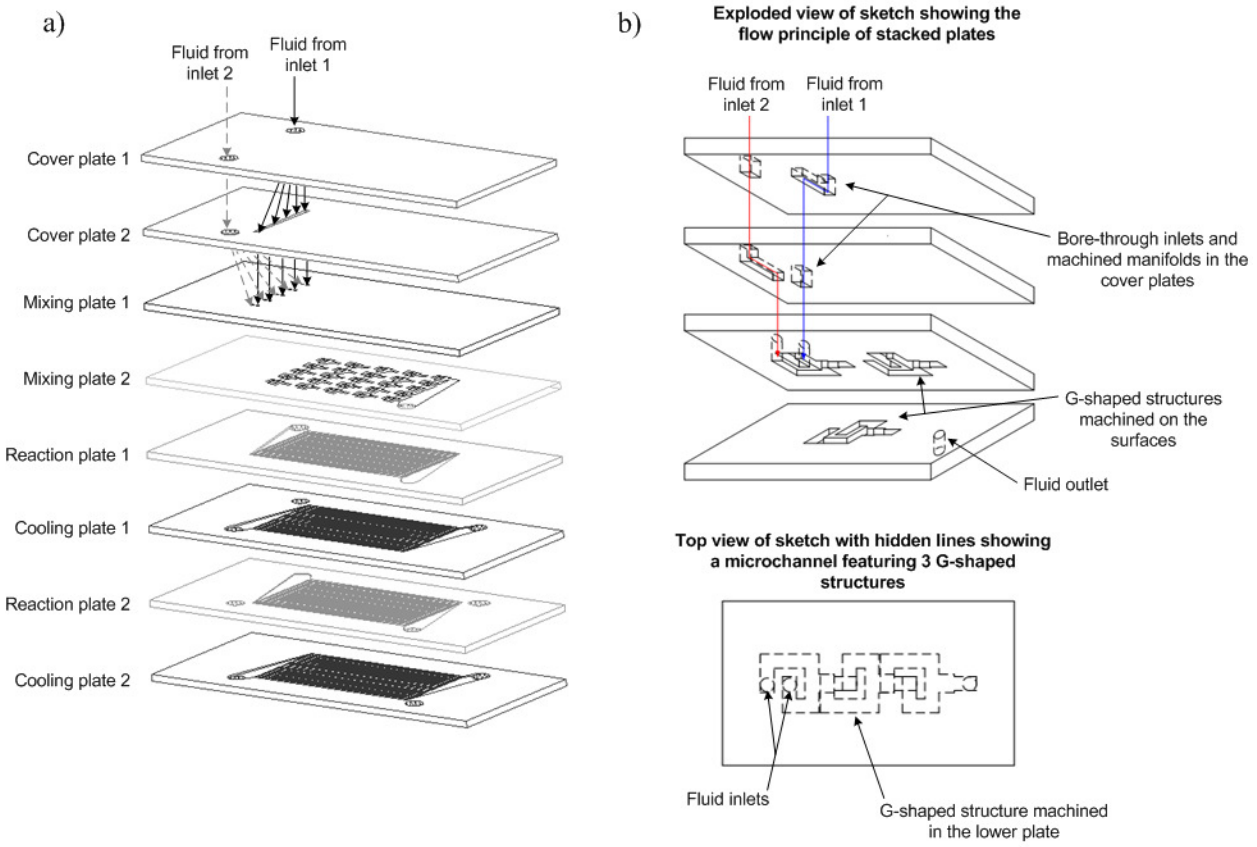

Figure 5.2 Schematics of the SAR microreactor: a) stacked arrangement of plates and b) sketch of the flowing principle of the G-shaped mixing structures.

The outlets of the mixing cavities converge to a structure that recombines the flow of the five microchannels. After passing the micromixing section the now mixed fluids flow along two stacked plates that are connected in series. These plates consist of two trapezoidal manifolds at the inlet and outlet of 31 straight parallel microchannels machined on the plate surface. The reaction plates increase the residence time of the microreactor. Views of the resulting internal flow path of the SAR are presented in Figure 5.11. The forced-convection heat exchanger system

consists of two parallel plates (not shown in Figure 5.11) identical in design to the reaction plates that are placed below both reaction plates.

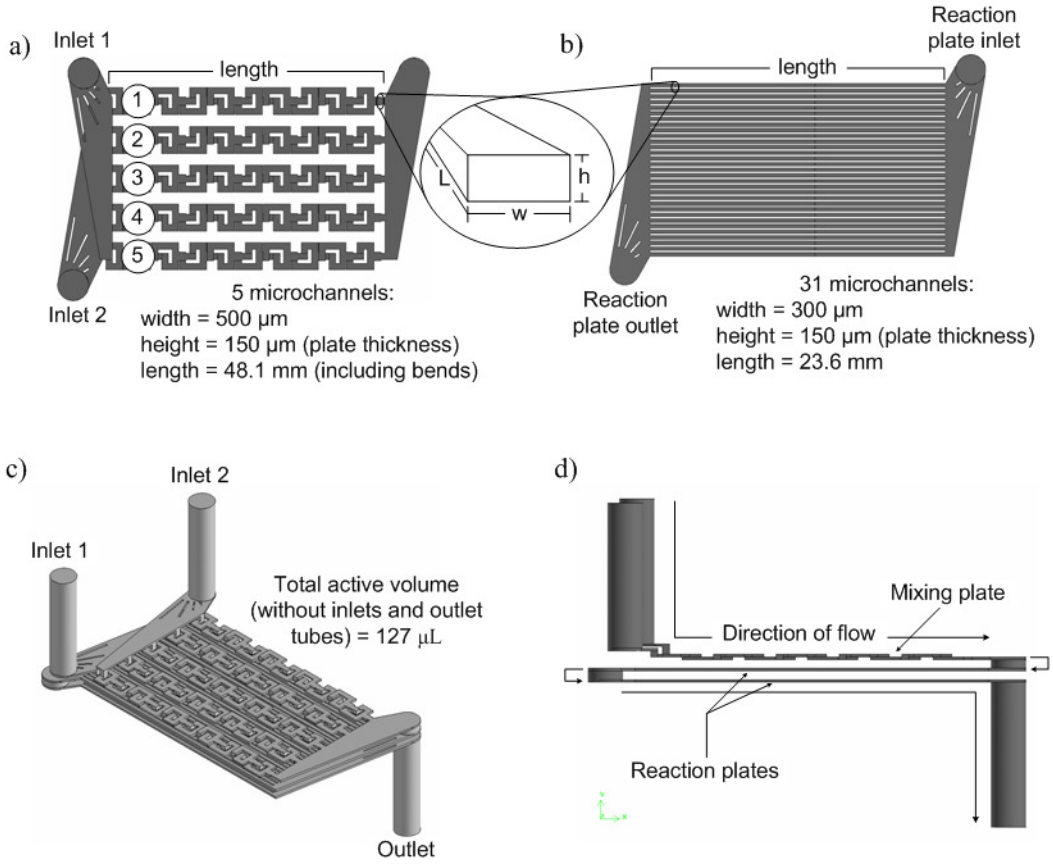

Figure 5.3 Internal flow path of the SAR: a) top view of the mixing section, b) top view of the reaction section, c) isometric view of the complete active volume and d) lateral view of the complete flow path generated.

5.3.1.2 LLMR-MIX-SI Multilamination Microreactor

The LLMR microreactor (**Wörz *et al.*, 2001; Hessel *et al.*, 2004**) consists of a stack of four machined plates. The first plate is composed of two inlets that feed the reactants into a mixer inlay in which the fluids are contacted through an interdigital structure where the multilamination mechanism takes place. After this stage the fluid advances to a second plate where a distribution manifold separates the flow into eight microchannels with a depth of 900 µm and an aspect ratio of 15 (Figure 5.12).

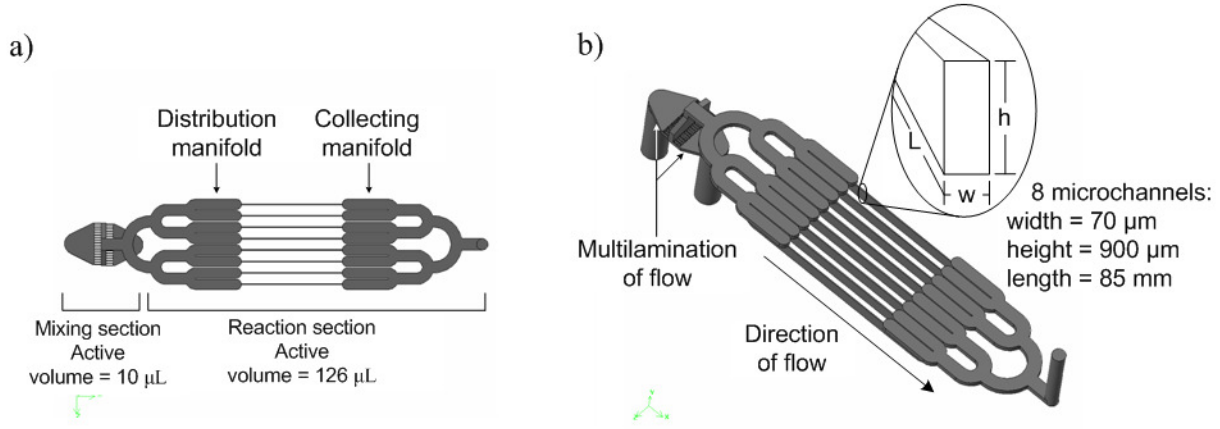

Figure 5.4 Views of the resulting flow path produced by the cavities of the plates of the LLMR: a) top view and b) isometric view.

Table 5.7 presents the geometrical values of the microchannels of the microreactors. The active volumes were estimated gravimetrically by comparing the weights of the empty microreactors with those measured when filled with water. As a check, the microreactors were filled with a syringe graduated in microlitres and the volume required to fill the microdevices was compared to that obtained by gravimetric measurement. Considering the density of water as 998.7 kg/m^3 at 21°C the difference is 2%. The volume estimated for the 1/8 in. union tee used for comparison purposes was 450 microlitres including the volume of the fluid line leading to the point of spectrophotometric measurement.

Table 5.1 Geometrical values of the microchannels featured by the SAR and LLMR microreactors

Microreactor	Section	Number of channels	Microchannels dimensions (mm)			Active volume (µL)	Total flow length (mm)
			width	height	length		
SAR	Mixing Reaction	5 31	0.5 0.3	0.15 0.15	48.1 23.6	20 107	150.5
LLMR	Mixing slit Reaction	18[(a)] 8	0.045 0.07	0.25 0.9	2 85	10 126	149.1
1/8 union tee	Mixing	1	-	-	-	450	50

(a) number of interdigital divisions

The lengths considered for the pressure drop calculations include the total length of the microreactor sections listed in Table 5.1 plus the length of their respective inlets and outlet ports. The total flow system can be regarded as composed by three volume sections: the inlet line, the microreactor structure, and the outlet line. The geometrical characteristics of these sections are listed in Table 5.2 in which the empty spaces correspond to the equivalent diameters to be calculated from pressure drop experiments.

Table 5.2 Geometrical parameters of the different sections of the total flow system composed by the inlet and outlet lines and the microreactor volume

Geometrical factors	SAR				LLMR			
	Inlet	Reactor	Outlet	Total	Inlet	Reactor	Outlet	Total
V (µL)	300	127	200	627	41	136	41	218
l (mm)	96	150.5	63	309.5	64	149.1	64	227
d_i (mm)	2	-	2	-	0.9	-	0.9	-

5.3.2 Experimental Set-up

The schematic of the experimental set-up is depicted in Figure 5.13. Two high permeation liquid chromatography (HPLC) pumps with maximum pumping capacity of 10 mL/min and 0.1 mL/min increments were used to supply the fluids to the microreactors. All experimental runs of pressure drop, RTD analysis and Villermaux/Dushman method were conducted at ambient temperature.

For the pressure drops measurements a calibrated differential pressure transducer (Omega PX81-100DV) was connected to one inlet and the outlet of the microreactors. The uncertainty of the measurement for this type of transducer is 0.25% f.s. (~0.0172 bars).

An in-line measurement system was implemented using a *Varian Cary 5000* UV-Vis spectrophotometer adapted with a fiber optic coupler from *Harrick Co*. The flow cell consisted of a bore-through stainless steel union cross that allows for the colinear alignment of the spectrophotometer fiber optic cables. A quartz sleeve with an internal diameter of 2 mm was used as a flow-through cuvette. For the readings during the RTD analysis, the pressure transducer and

fittings were removed in order to prevent their additional volumes from interfering with the measured signals.

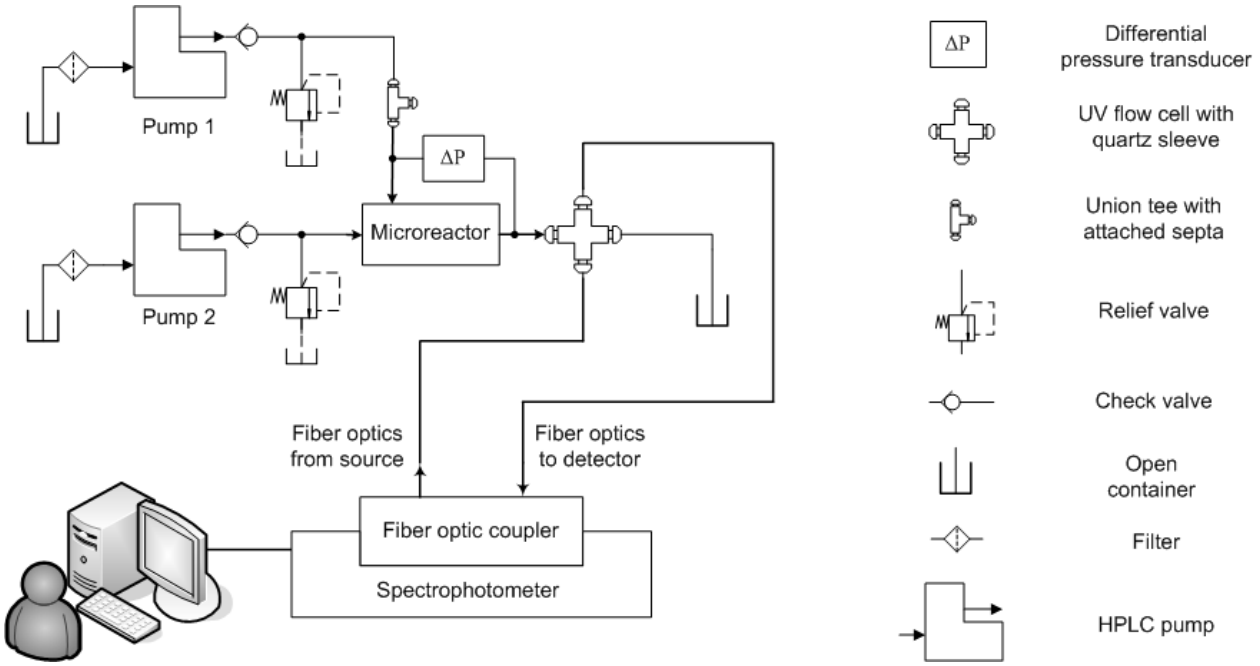

Figure 5.5 Schematic of the experimental set-up.

5.3.3 Spectrophotometer Calibration

The spectrophotometer was calibrated using triiodide standards obtained by the stoichiometric reaction of 0.1 mg/mL elemental iodine (I_2) dissolved in a fresh aqueous solution of potassium iodide (0.05 mol/mL). From these concentrations the amount of triiodide formed in dynamic equilibrium can be calculated from the equilibrium equation and the equilibrium constant for the triiodide compound provided by **Palmer *et al.* (1984)**. The extinction coefficient was obtained from the slope of an absorbance-concentration plot of different triiodide samples with known concentrations (*i.e.* triiodide standards). The value of the extinction coefficient for the triiodide compound obtained in this work is 2676 m^2/mol, which is in agreement with those reported in previous studies (**Custer & Natelson, 1949; Awtrey & Connick, 1951; Herbo & Sigallia, 1957; Palmer *et al.*, 1984; Guichardon & Falk, 2000**). It was found that the Beer-Lambert law was valid up to an absorbance value of approximately 1.6 corresponding to a concentration in

dynamic equilibrium of 5.910 x 10^{-5}M of I_2 (initial concentration of 0.015 mg/mL) and 5.883 x 10^{-5}M of I_3.

5.3.4 Flow Conditions

Due to the maximal pressure rating provided by the manufacturers, during the pressure drop characterization the SAR microreactor was tested up to 70 mL/min using external water supply in addition to the HPLC pumps while the LLMR was tested up to 20 mL/min. For the RTD analysis distilled water was used to simultaneously feed both inlet ports of the microreactors as opposed to using only one inlet (**Bošković & Loebbecke, 2008**) since it resembles more accurately the real mixing process and the risk of a potential dead zone for the tracer as encountered by **Günther, M. *et al*., 2004** is avoided. The RTD analysis and the Villermaux/Dushman method were investigated at four flow rate values per inlet maintaining a feeding ratio of one: 0.1, 0.5, 1.0, and 10.0 mL/min. In order to investigate the influence of the distribution manifolds, the SAR microreactor was analyzed by varying the ratio of flow rates at five flow conditions per inlet (*e.g.* 0.1, 0.5, 1.0, 5.0 and 10 mL/min) resulting in 25 different flow rate combinations.

5.3.5 Residence Time Distribution

For the RTD analysis tracer pulse experiments were performed consisting of the injection of an aqueous iodine (I_2) solution in the form of the triiodide (I_3) compound through Inlet 1 of the microreactors. The pulse consisted of 1% of the active volume of the microreactor and was injected manually through a septa secured to a union tee. Syringes graduated in microlitres and adapted with plunger locks were used in order to ensure the same injection volume in each run. In all the experiments, the injection time was lower than 0.5 s. As a check, the experiments were conducted using bromocresol purple as tracer producing equivalent results. The absorption peaks of bromocresol purple (pH ~6.8) were found at 589, 376.5 and 296 nm. The wavelength of 589 nm was selected due to the higher absorbance values detected; hence less amount of tracer was required. Both tracers are inert and assumed to not significantly affect the fluid properties of the

water used as the working fluid during the experiments. The experimental runs for the RTD analysis consisted of at least 5 random replicates per flow condition.

5.3.6 Villermaux/Dushman Method

For this method only flow ratios equal to one were analyzed. Technical grade materials were used as received. For a given concentration of sulphuric acid (H_2SO_4) the concentrations of the other reactants were determined by stoichiometry. In order to completely neutralize the acid the quantity of $H_2BO_3^-$ added to the buffer solution was four times that required by stoichiometry; the sulfuric acid was then the limiting reactant. Table 5.3 summarizes the concentrations of reactants used in the present work for a ratio of flow rates equal to one.

Table 5.3 Concentrations of reactants in the fluid reservoirs for the Villermaux/Dushman method applied to continuous flow for equal ratios of feeding rate

Reactants		Set of concentrations				
		Preliminary	1	2	3	4
H_2SO_4	(mol/L)	0.360	0.0360	0.0180	0.0180	0.0090
KI	(gr/L)	7.968	7.968	7.968	1.992	0.996
KIO_3	(gr/L)	1.284	1.284	1.284	0.321	0.160
H_3BO_3	(mg/mL)	5.62	5.62	5.62	1.405	0.702
NaOH	(gr/L)	3.635	3.635	3.635	0.908	0.4543
$H_2BO_3^{-(b)}$	(mol/L)	0.0897	0.0897	0.0897	0.0221	0.0112
pH_{buffer}		10.41	10.41	10.41	10.03	10.22
pH_{final}		8.39	9.17	9.56	8.16	8.44
Reaction time t_{cr}	(s)	7.5×10^{-6}	0.017	0.24	0.17	2.17

(b) calculated in dynamic equilibrium

Sodium hydroxide ($NaOH$) and boric acid ($H_2BO_3^-$) were first dissolved in water to prepare a fresh buffer solution in the basic range. Potassium iodide (KI^-) and potassium iodate (KIO_3^-) were then added to the buffer solution. Using this sequence the thermodynamic formation of iodine can be prevented. Potassium iodide was added in excess in order to further produce the triiodide compound. The final pH of the buffer solutions prepared in this work were lower than 10.41.

In a preliminary test an acid concentration of 0.18M (**Guichardon & Falk, 2000**) resulted in signal saturation. The acid concentration was then lowered to 0.018M and those of the other compounds were calculated accordingly.

Concentration of reactants in Set 1 and 2 were the same as in the preliminary concentration test with only the acid concentration reduced by half in each set. In Set 3 and 4 all the reactants were in stoichiometric proportion to an acid concentration of 0.009M and 0.0045M respectively. The experimental runs for the mixing characterization consisted of at least 5 random replicates per concentration set.

5.4 RESULTS AND DISCUSSION

5.4.1 Pressure drop

The measured pressure drop of the microreactors as a function of the flow rate Q is shown in Figure 5.6. Both microdevices show the linear relation described by the Hagen-Poiseuille equation (Eq. 2) up to 14.0 mL/min with the LLMR producing pressure drops approximately 5 times greater than the SAR. Above 14.0 mL/min the microreactors show a quadratic trend that is in agreement with the relationship:

$$\Delta P \propto v^2 \tag{5.19}$$

derived from the analysis of the friction loss factor for turbulent flow in tubes. This behavior is an indication of the onset of the transitional flow regime at 20 mL/min for the SAR and 15 mL/min for the LLMR corresponding to *Re* values of 665 and 750 respectively.

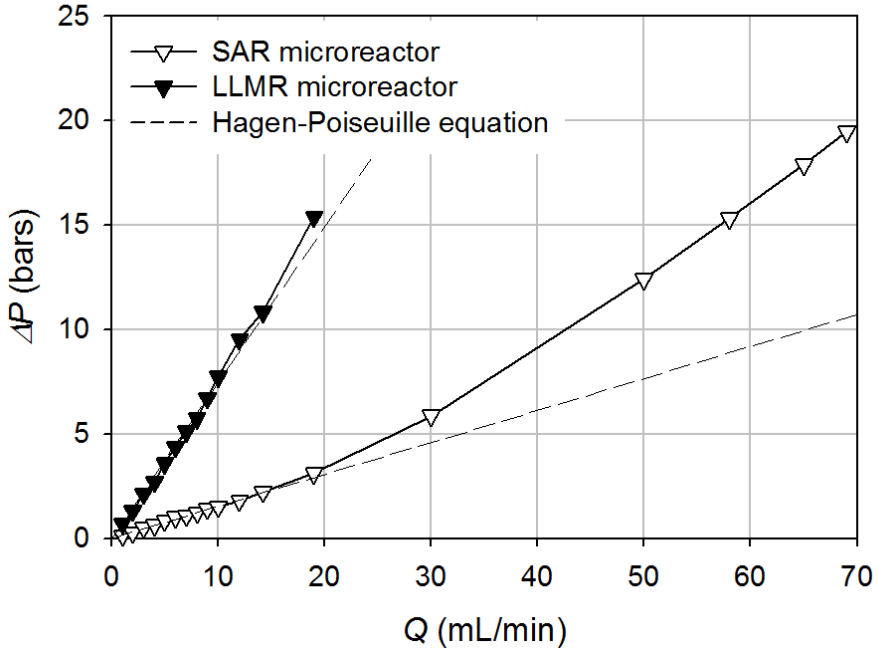

Figure 5.6 Experimental pressure drops of the SAR and LLMR as a function of the volumetric flow rate.

This can be confirmed in Figure 5.7 where the pressure drop data is transformed to a non-dimensional friction factor *f* and plotted as a function of *Re* calculated as described in Section 5.2.1.

The experimental pressure drop of the investigated microreactors is in agreement with the laminar flow theory. The values of *Re* >2100 reached in the SAR (*e.g.* 2105, 2430, 2724 and 2890) fall within the prediction of the classical Blasius correlation for the transitional and turbulent flow regime.

The equivalent diameters d_{eq} of the microreactors obtained from Eq. 5.2 are 0.602 mm for the SAR and 0.411 mm for the LLMR. These values can be used for further estimation of pressure drops at different *Re*. The flow conditions at 0.2, 1.0, 2.0 and 20.0 mL/min that will be further used during the analysis correspond respectively to *Re* values of 6, 35, 70 and 665 for the SAR, and 10, 52, 105 and 1005 for the LLMR.

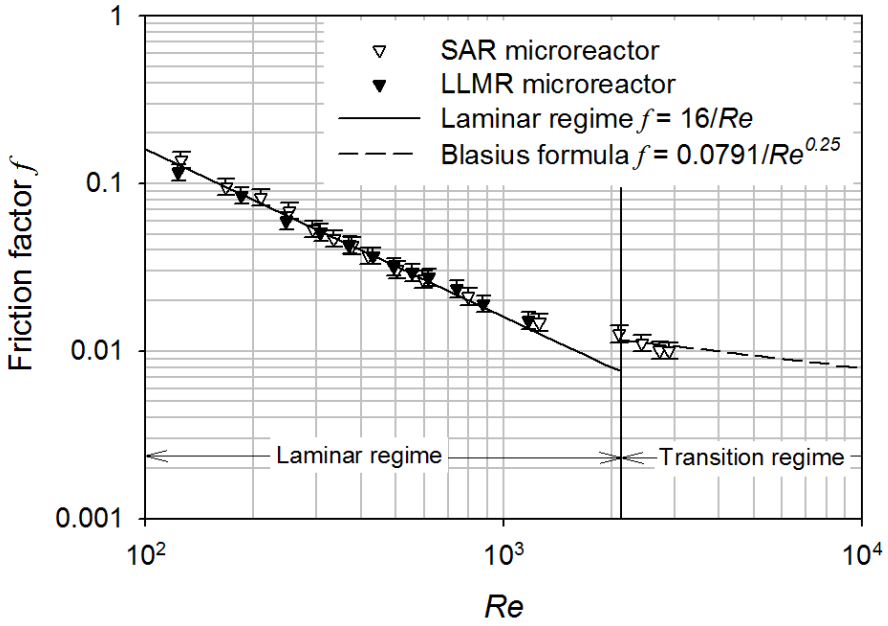

Figure 5.7 Friction factor *f* as a function of *Re* for the SAR and LLMR microreactors.

5.4.2 Residence Time Distribution

5.4.2.1 Flow Distribution in the SAR Microreactor

The distribution manifolds are responsible for the parallelization of flow before the mixing stage in the SAR microreactor. A preliminary characterization was conducted by varying the flow ratio r_Q defined as the ratio of flow rates of Inlet 1 over Inlet 2. Figure 5.8 shows the concentration-time curves recorded for 8 combinations from the 25 flow conditions investigated. The reproducibility of the RTD experiments was verified qualitatively by observation of the shape of the curves and quantitatively by comparing their mean residence time and variance. The signals obtained for $r_Q \geq 0.1$ were highly reproducible whereas for other ratios a distinguishable concentration-time relationship could not be observed.

For $r_Q = 1$ smooth curves were recorded except at 0.1 mL/min (Figure 5.8c) where small peaks are detected. These peaks observed for $r_Q = 1$ when Inlet 1 is set at 0.1 mL/min are more pronounced

as r_Q is decreased (*i.e.* by increasing the flow rate of Inlet 2) until a distinctive concentration-time relationship in the signal disappears (Figure 5.8a, 5.8b, 5.8c) as previously noted.

The uneven peaks in Figure 5.8b are known to indicate specific flows like recirculation, flow in parallel paths, or by-passing (**Levenspiel, 1999**). Since during the experimental procedure the tracer is injected only through Inlet 1 it is concluded that for flow rate ratios different than one the pressure difference between distribution manifolds has a significant influence on the hydrodynamic efficiency of the SAR. When $r_Q > 1$ the influence of the lower velocity stream on the tracer distribution is not reflected on the recorded signal. On the other hand, when $r_Q < 1$ the tracer is transported by the lower pressure stream and the spectrophotometric signal registers a considerable influence of the higher pressure stream on the tracer distribution at the outlet of the microreactor.

For the moment, there is no information available regarding the minimal pressure or range of flow conditions in which the SAR microreactor must operate for optimal hydrodynamic performance. The results indicate that smooth concentration-time curves are obtained when $r_Q \geq 1$. However, the observation of smooth curves at $r_Q \geq 1$ does not necessarily imply that the tracer is evenly distributed in the complete working volume of the microreactor since the mean residence time calculated at these flow conditions are shorter than those expected from theory thus indicating the possibility of by-passing and/or recirculation. The influence of the pressure imbalance between feeding ports on the SAR hydrodynamic behavior is evident. This phenomenon may require further investigation using for instance computational fluid dynamics. The imbalance produced by using different feeding ratios can be further amplified by the distribution manifold geometrical design. In order to isolate this latter effect and for comparison with the LLMR microreactor, the rest of the RTD analysis is based on four flow conditions with $r_Q = 1$.

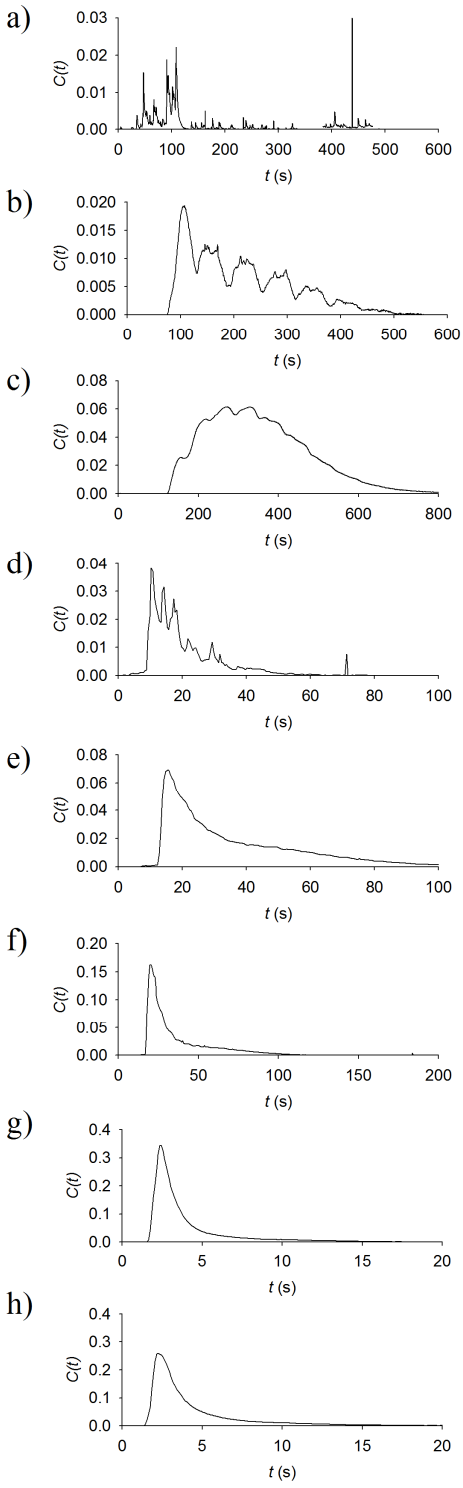

	Flow rate (mL/min)		
	Inlet 1 (injection)	Inlet 2	Ratio (inlet 1 / inlet 2)
a)	0.1	10.0	0.01
b)	0.1	1.0	0.1
c)	0.1	0.1	1
d)	1.0	10.0	0.1
e)	1.0	1.0	1
f)	1.0	0.1	10
g)	10.0	0.1	100
h)	10.0	1.0	10

Figure 5.8 Concentration-time curves for different flow rate ratios in the SAR microreactor.

5.4.2.2 Mean Residence Time Values

Figure 5.9 shows the mean residence time t_m resulting from subtracting the mean time of the input signal from the mean time of the output curves recorded at the end of the outlet port. The time spent in the outlet line is not subtracted since the necessary tube fittings prevent proper manipulation and inhibition of a reaction before this point. The experimental results follow the trend expected from the theoretical mean time calculated by dividing the volume of the microreactor by the total volumetric flow rate. For equal feeding rates the observed mean residence times from 0.2 to 2.0 mL/min are longer than those expected from theory.

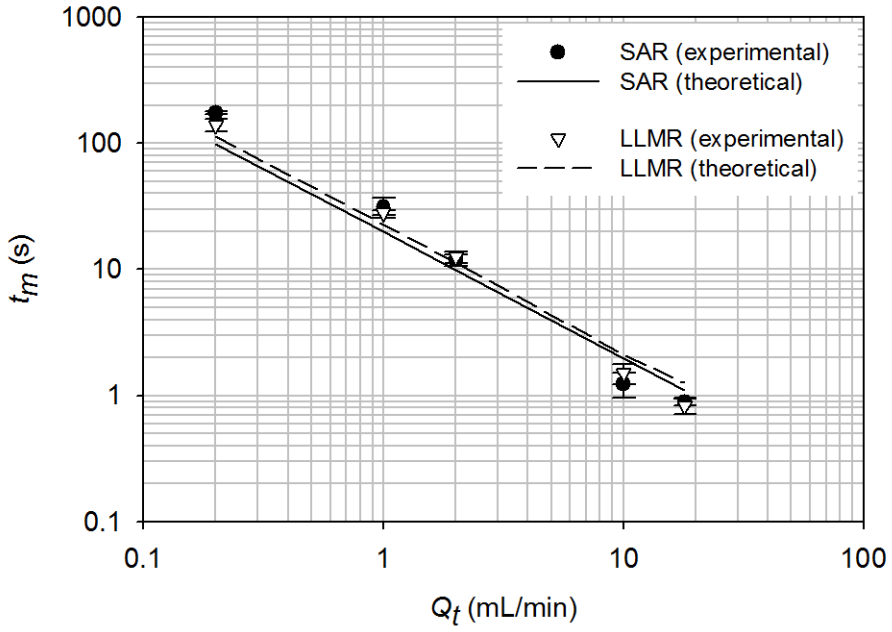

Figure 5.9 Mean residence times of the SAR and LLMR microreactors as a function of the total volumetric flow rate for a feeding ratio equal to one.

According to **Levenspiel (1999)** the probable causes for this effect are that the closed-closed boundary condition assumed in the derivation of the theoretical mean residence time is not fully satisfied, incorrect measurement of active volume or volumetric flow rate, or adsorption of tracer to the reactor walls. Since the latter two options have been verified and discarded as discussed in Section 3, this means that at sufficiently low fluid velocities the tracer can repeatedly cross the boundaries of the system by the effect of axial dispersion thus imposing the open-open boundary conditions. Moreover, the tailing effect produced by the tracer flowing at sufficiently low

velocities near the reactor wall is known to broaden the RTD of flow systems operating in laminar regime (**Nauman and Buffham, 1983**).

The opposite is observed above 2.0 mL/min where the average residence times are shorter than expected for both microdevices. Due to the parallel flow configuration inside these microreaction units, this observation at higher flow velocities suggests by-passing of the tracer through only a number of the microchannels. The observed mean residence times for both microreactors are close in magnitude due to the comparable active volumes and lengths of both microdevices.

5.4.2.3 Influence of Input Signals

The dimensionless input signals are shown in Figure 5.10 at different flow conditions. The 1/8 in. tube produces distributions with a sharp first-appearance time and a distinctive shoulder around the mean. While the inputs obtained from the 1/16 in. tube show the same tailing effect, they exhibit an explicit exponential decay response. The difference is most evident at 0.1 mL/min where the peak and broad shoulder produced by the 1/8 in. tube is in contrast to the curve produced by the 1/16 in. tube. These input signals did not fit the pure convection model used to describe laminar flow with negligible diffusion in empty tubes. The reduced diameter of the inlet tube of the LLMR allows a faster homogenization of the tracer in the radial direction improving the distribution.

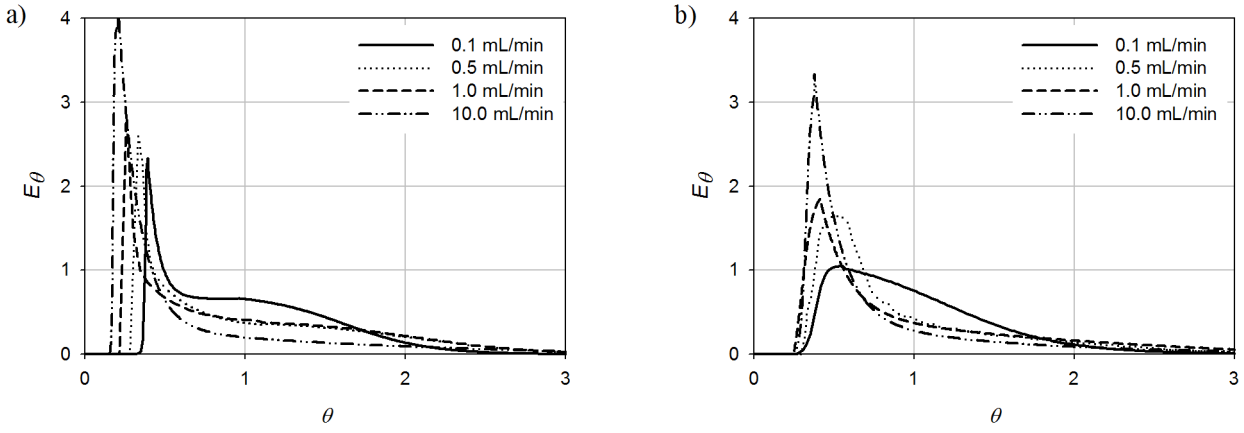

Figure 5.10 Input signals in non-dimensional form recorded for two different inlet tube diameters: a) 1/8 in., b) 1/16 in.

5.4.2.4 Recorded Output Signals

For qualitative comparison with the input signals, the output signals as obtained at the outlet of the microreactors were analyzed prior to deconvolution. The recorded output signals reflect the behavior of the composite flow systems described in Table 5.2. Using the maximum t_m estimated in the preceding section (~170 s) and the maximum equivalent diameter listed in Table 5.2 (2 mm) the dimensionless diffusion term in Eq. 5.15 is 0.19. Thus, radial diffusion at the current flow conditions should not be neglected. In this scenario radial diffusion acts to improve the mixing performance of the microreactors even in laminar flow regime.

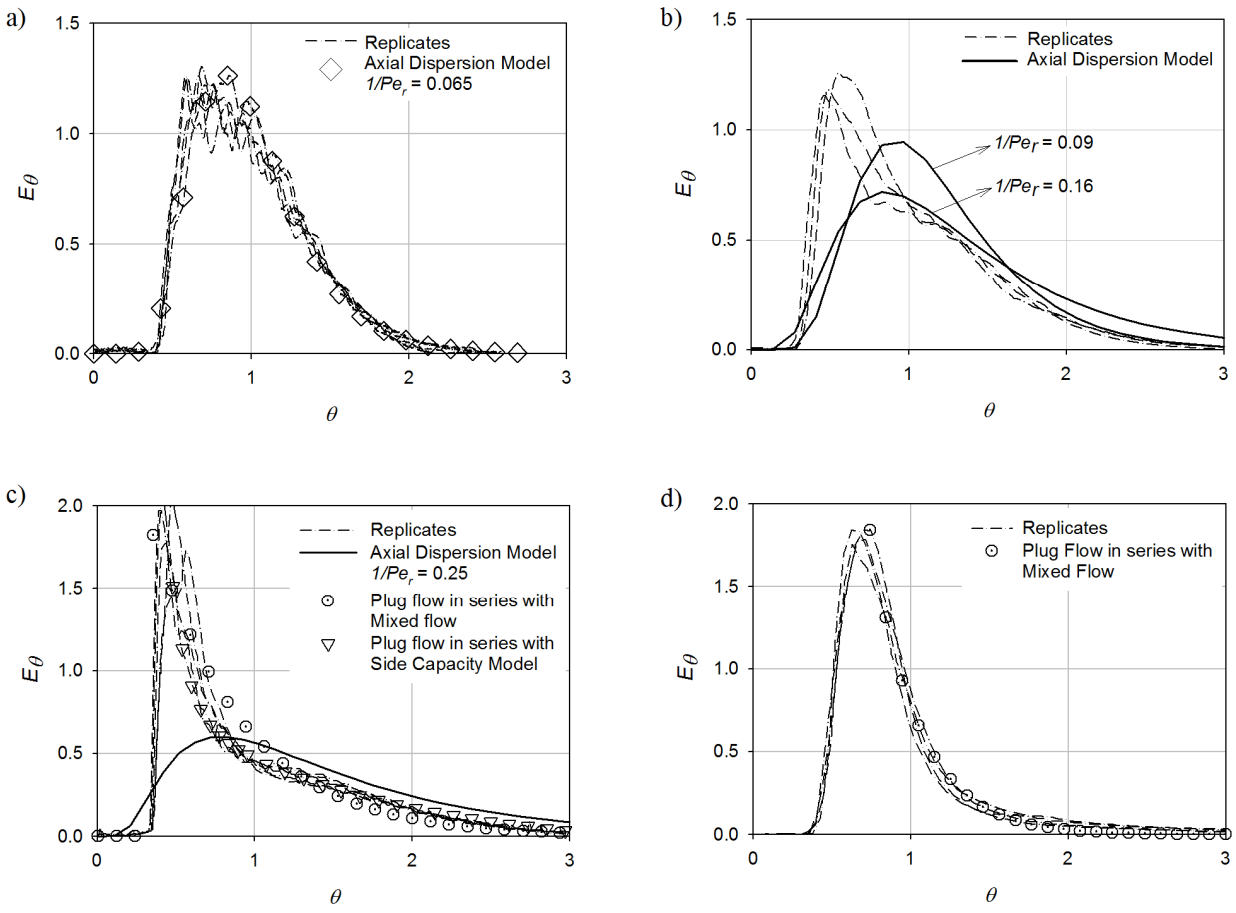

Figure 5.11 Output signals before deconvolution recorded at the outlet of the SAR microreactor for different *Re*: a) 6 (0.2 mL/min), b) 35 (1.0 mL/min), c) 70 (2.0 mL/min) and d) 665 (20.0 mL/min).

The dimensionless exit-age distributions recorded at the outlet of the SAR microreactor (Figure 5.11) show that the axial dispersion model provides an accurate fitting of the output curve at *Re* =6 (0.2 mL/min). Despite the prevailing laminar conditions the flow system based on the SAR microreactor effectively promotes the distribution of tracer in the radial direction. An empty tube with of equivalent *ΔP-V* would have an approximate length of 1158 mm. For this tube and using the *Sc* of water (~1000) the correlation provided by Eq. 5.14 predicts values of $1/Pe_r$ of 0.019, 0.095, 0.191 and 1.90 for the flow rates investigated. At *Re* =6 the vessel dispersion number obtained for the SAR ($1/Pe_r$ ~0.065) is greater than the limit for small deviations from plug flow ($1/Pe_r < 0.01$) and an empty tube with equivalent *ΔP-V* would yield a narrower distribution at this condition ($1/Pe_r$ ~0.019). At higher *Re* values (Figure 5.11b-d) the skewness of the output signal shifts to the left of the mean (θ =1) exhibiting a sharp first-appearance time followed by a tailing effect, thus the flow system comprising the SAR falls beyond the accuracy of the axial dispersion model for open-open boundary conditions.

The distributions in Figure 5.11b-d exhibit an exponential decay response which is better predicted when a compartment flow model is assumed, *e.g.* a combination of a mixed flow reactor preceded by a plug flow reactor. It is further observed that at *Re* =70 (2.0 mL/min) the *side capacity model* (SCM) provides a better fit of the exponential decay. The SCM physically represents a main mixed flow reactor with constant interchange of fluid with a smaller mixed flow unit connected in parallel. Mixed flow reactors in parallel are used to represent by-passing or stagnancy (**Nauman, 2008**). Since using both inlets during the experimental runs reduces the risk of stagnant zones, this type or curves support the notion of by-passing already detected in previous sections. By-passing can be produced by an unbalanced flow distribution. Since only flow rate combinations with r_Q =1 are considered in this section, this imbalance is probably caused by the geometry of the SAR manifolds.

The conclusion from this preliminary analysis of the composite flow system is that from the flow rate range investigated, the most desirable behavior in the SAR microreactor is obtained at *Re* =6 corresponding to a flow rate of 0.2 mL/min (*i.e.* 0.1 mL/min per inlet) where complete mixing in the radial direction is obtained at the longest mean residence time (~170 s) while still achieving a Gaussian distribution. The more Gaussian and narrow a RTD distribution is, the closer the vessel

is to plug flow operation. The higher flow conditions exhibit the behavior of vessels with good mixing (*i.e.* mixed flow reactors) although with an exponential distribution. Exponential distributions produce different levels of conversion and in certain chemical reaction applications are not the optimal responses.

A similar qualitative behavior is observed for the LLMR (Figure 5.12). An empty tube of equivalent *ΔP-V* would have an approximate length of 973 mm. For this tube and using again the *Sc* of water (~1000) the correlation provided by Eq. 5.14 predicts values of $1/Pe_r$ of 0.023, 0.114, 0.227 and 2.27. This equivalent tube of the LLMR would produce a slightly broader distribution than the equivalent tube of the SAR. However, at *Re* =10 (0.2 mL/min) the actual LLMR microreactor exhibits a narrower RTD ($1/Pe_r$ ~ 0.051) than the SAR microreactor ($1/Pe_r$ ~ 0.065) albeit at the expense of greater pressure drop.

Starting at *Re* =52 (1.0 mL/min) the LLMR shows a defined shift towards the mixed flow behavior with the side capacity model providing an accurate fit. Therefore, at higher flow rates (Figure 5.12c-d) the LLMR flow system cannot be compared directly with the $1/Pe_r$ values predicted by the axial dispersion model for an equivalent circular tube. At *Re* =10 the flow system featuring the LLMR exhibits the behavior of complete radial mixing and a narrow distribution of residence times.

The output curves of both microreactors at *Re* >52 are similar in shape (*e.g.* exponential decay) to those of the input curves recorded at the corresponding flow conditions. The distinctive shapes of the tracer input signals at *Re* <10 are changed to Gaussian distributions after flowing through the microreactors. This improved Gaussian response is attributed to efficient flow distribution and radial homogenization in the complete working volume of the microreactors at sufficiently low fluid velocities. The microfluidic structures are capable to recombine the flow to the extent of improving the non-ideal distribution of the tracer input.

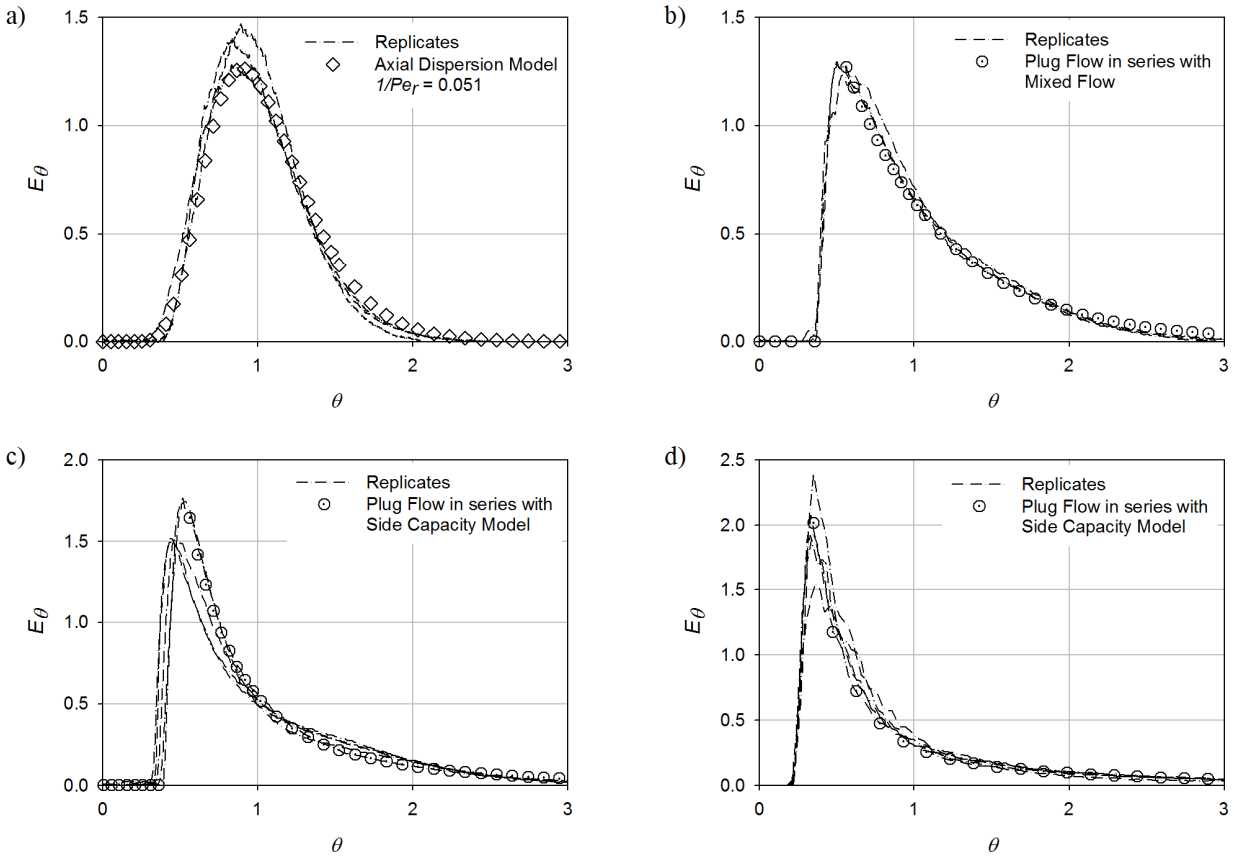

Figure 5.12 Output signals before deconvolution recorded at the outlet of the LLMR microreactor for different *Re*: a) 10 (0.2 mL/min), b) 52 (1.0 mL/min), c) 105 (2.0 mL/min) and d) 1050 (20.0 mL/min).

5.4.2.5 Deconvolution of the response signal in the Fourier domain

Prior to the inverse transformation of the deconvoluted $E(s)$ signals a filtering stage was applied. A low band pass filter with a frequency cut off of 0.7 Hz yielded the best results by significantly reducing the level of noise of the inverse transformed signal. The $E(t)$ functions thus obtained were fitted with the axial dispersion model for open-open boundary conditions to estimate the parameter $1/Pe_r$. To corroborate the suitability of the direct deconvolution in the Fourier domain and verify the accuracy of the axial dispersion model to represent the RTD of the microreactors the reverse procedure was performed. At each flow condition a random replicate of the input signal was convoluted in the time domain with the exact fitting curves obtained by the axial

dispersion model. This convolution routine in the time domain was developed specifically for our application using the programming platform of the Origin 6.0 software where the NLSF procedure is based on the classical Levenberg-Marquardt algorithm. The calculated signal is compared with any random replicate from the output signals recorded experimentally. Such comparison is presented in Figure 5.13 for the SAR and in Figure 5.14 for the LLMR. As it can be seen, the agreement is satisfactory. Thus, the axial dispersion model is capable to sufficiently reproduce the flow behavior of the microreactors investigated. These results and the adequate curve fit demonstrate the suitability of the Fourier domain deconvolution to be applied during the RTD analysis of non-transparent microreactors with large peripheral fluid line volumes.

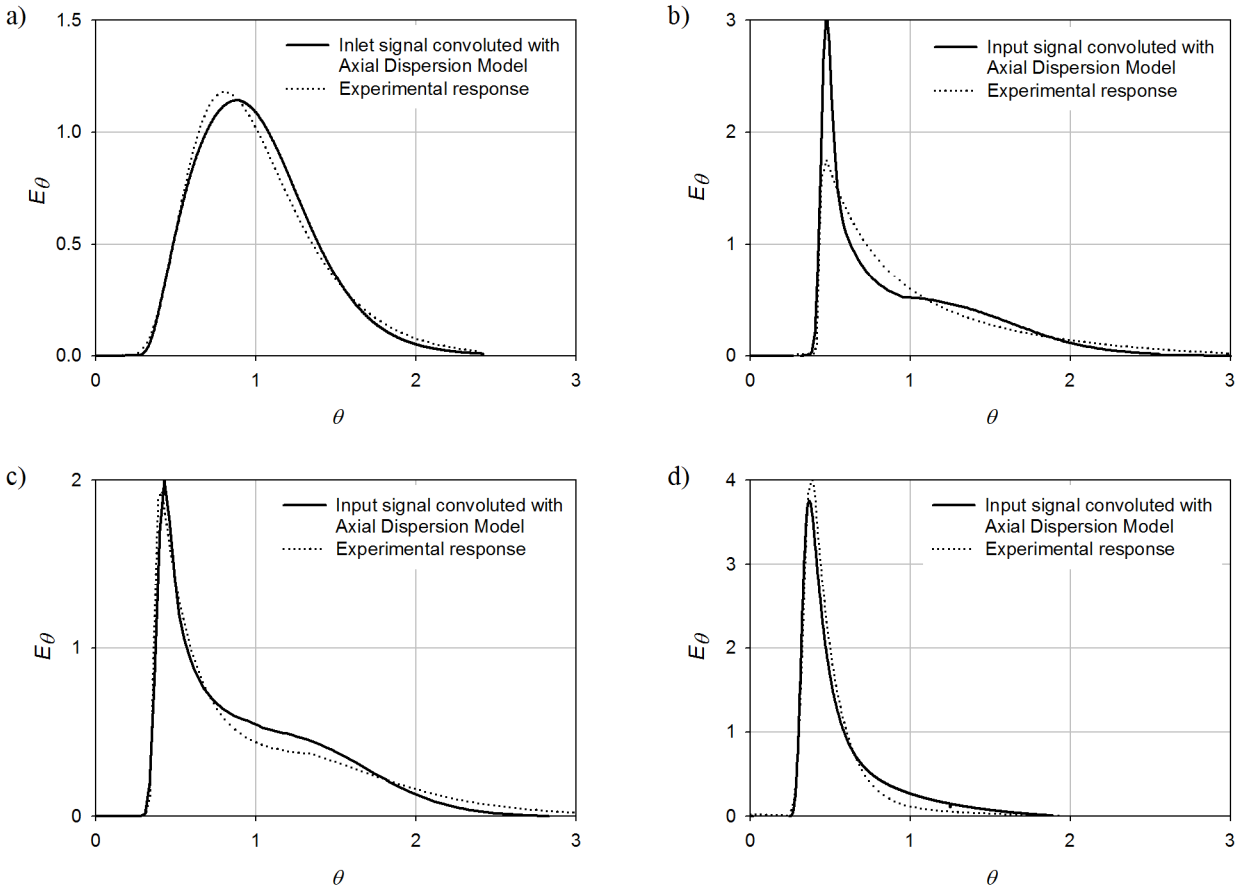

Figure 5.13 Comparison of the original recorded responses at the outlet of the SAR microreactor with the curves obtained by time domain convolution of the input signals with the axial dispersion model for different *Re*: a) 6, b) 35, c) 70, and d) 665.

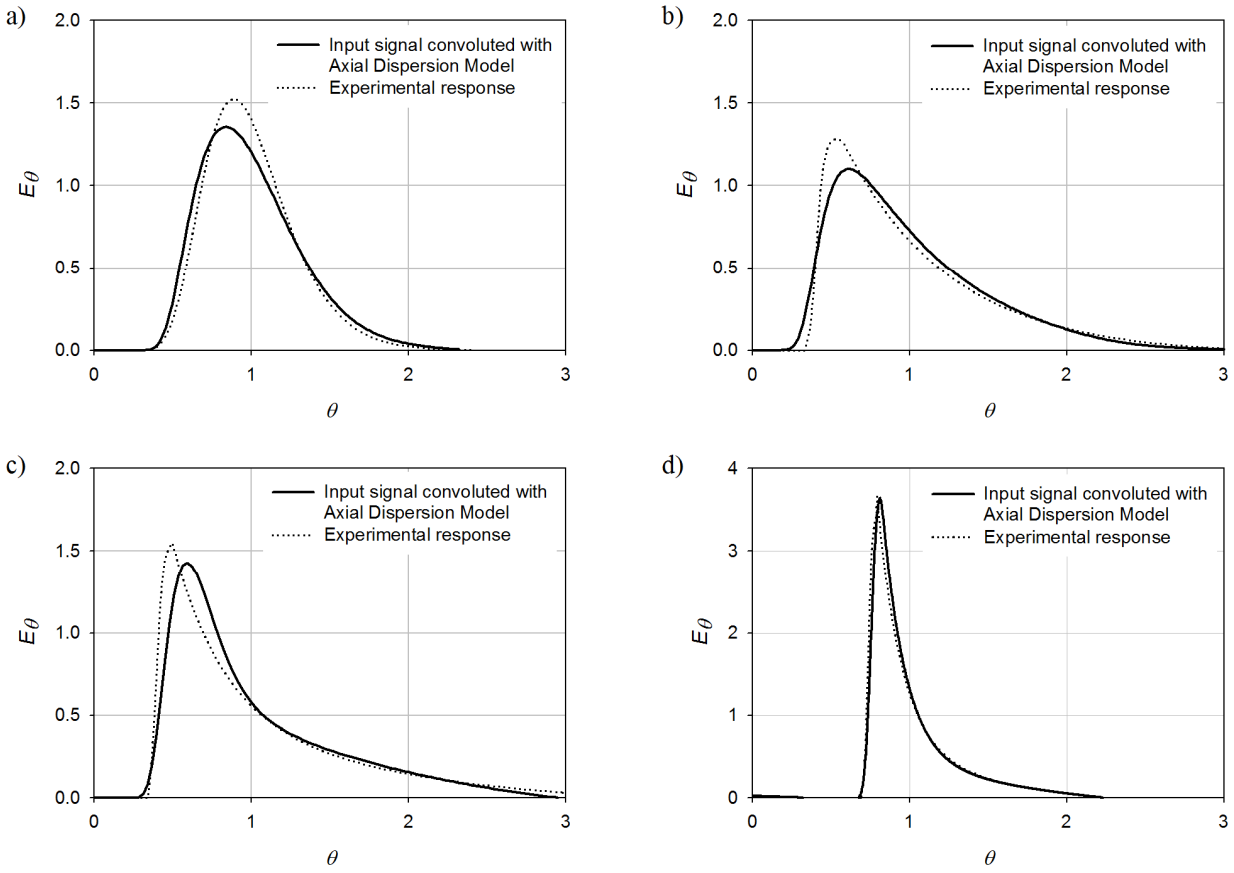

Figure 5.14 Comparison of the original recorded responses at the outlet of the LLMR microreactor with the curves obtained by time domain convolution of the input signals with the axial dispersion model for different *Re*: a) 10, b) 52, c) 105, d) 1005.

The RTD curves produced by the axial dispersion model are shown in Figure 5.15. At 0.2 mL/min the LLMR exhibits a narrower response than the SAR thus having better spatial mixing capabilities in this range (*Re* <10). At 1.0 and 2.0 mL/min (35< *Re* <105) the SAR microreactor significantly improves in comparison to the LLMR and finally at 20.0 mL/min (*Re* >665) both microreactors perform almost equally.

The $1/Pe_r$ values of the SAR exhibit a monotonic decrease as a function of flow rate, thus narrowing the RTD. This observation is in agreement with the monotonic increase from 1.0 to 2.0 mL/min (*Re* =20-40) observed by **Köhler *et al.* (2010)** for a single split-and-recombination structure. This monotonic decrease is in contrast with the correlation in Eq. 5.14 that predicts an

increase of the vessel dispersion number $D/v \cdot l$ in laminar flow conditions when the fluid velocity is also increased.

According to Eq. 5.13, for increasing flow rate and constant length a reduction of the term $D/v \cdot l$ requires the axial dispersion coefficient D to remain constant or at least to decrease its dependence as a function of fluid velocity. The axial dispersion coefficient D accounts for the spreading effects caused by molecular diffusion and elongated velocity profiles in laminar flow. For Bodenstein numbers $Bo = Re \cdot Sc$ greater than 30 the axial dispersion coefficient can be defined as (Levenspiel, 1999):

$$D = \frac{v^2 \cdot d_{eq}^2}{192 \cdot D_{diff}} \tag{5.20}$$

Once the $1/Pe_r$ values are known, the axial dispersion coefficients can be obtained from Figure 5.15.

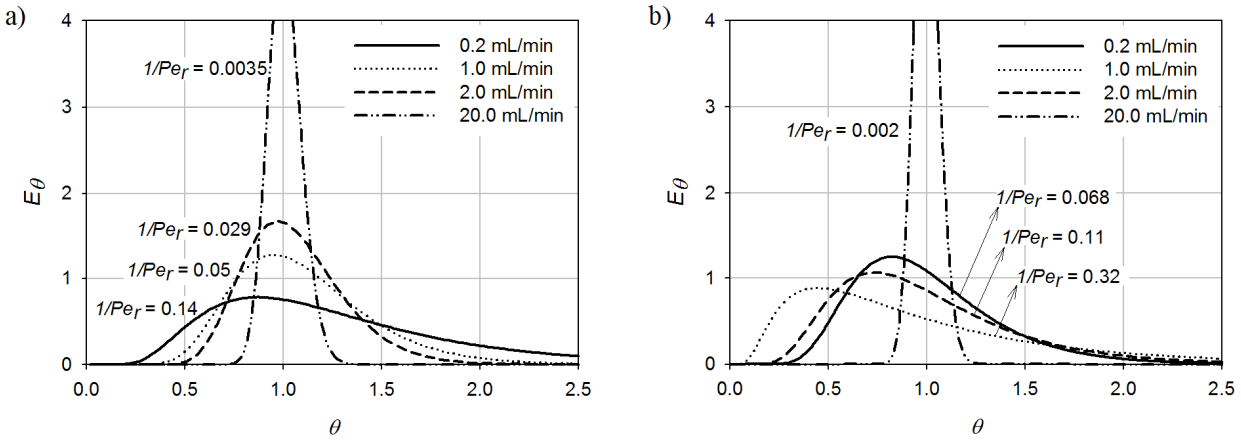

Figure 5.15 Dimensionless RTD for r_Q =1 reproduced by the axial dispersion model using the fitting parameters obtained from the deconvoluted microreactor response signals: a) SAR, b) LLMR.

The dependence of the parameter D as a function of the fluid velocity is shown in Figure 5.16 where the microreactors are compared with circular tubes having equivalent pressure drop and

l/d_{eq} ratio. For the empty tubes the parameter D shows the quadratic dependence expressed in Eq. 5.20, which establishes that in laminar regime an increase in velocity results in an increase of the axial dispersion due to a more pronounced profile elongation.

The reduction of the dependence of D on velocity from the power of 2 to the power of 0.15 reveals the excellent flow homogenization capabilities of the SAR microfluidic network in which axial dispersion effects, otherwise expected by elongated velocity profiles at sufficiently large velocities, are greatly reduced.

This homogenization mechanism can be explained as follows. For r_Q =1 and at sufficiently low fluid velocities a better flow distribution is achieved and the tracer input reaches all the microchannels of the manifold. In principle the microfluidic structure should only broaden the already non-ideal shape of the input distribution. The tracer undergoes a series of split-and-recombination stages at each microchannel and the Gaussian behavior of the combined flow at the exit of the microreactor is the result of the statistical summation of all these consecutive effects. The axial dispersion produced by the inlet tube is minimized in the microreactor resulting in the reduction of D. At higher flow conditions the same mixing capabilities may also be achieved although possibly only through only a reduced number of microchannels.

The $1/Pe_r$ values of the LLMR exhibit a non-monotonic behavior with a shift in direction between 0.2 and 1.0 mL/min corresponding to Re of 10 and 52 respectively. Interestingly this type of behavior was observed also by **Köhler *et al.* (2010)** in an interdigital micromixer exhibiting viscosity-independent shifts in RTD direction at Re <60 (*e.g.* flow rates between 0.05-3 mL/min). Since non-monotonic shifts were also observed on simple structures such as PTFE tubing **Köhler *et al.* (2010)** attribute this behavior not only to complex microfluidic structures but also to spontaneous changes in the transport mechanisms such as the engulfment flow regime (**Kockmann *et al.*, 2006**). For the LLMR the quadratic dependence of D on the fluid velocity was found to decrease to the power of 0.11 in the range of Re >52 (1.0 to 20 mL/min). For Re <52 the value of D followed the quadratic trend of Eq. 5.20. More experiments would be useful to confirm the dependence in this range.

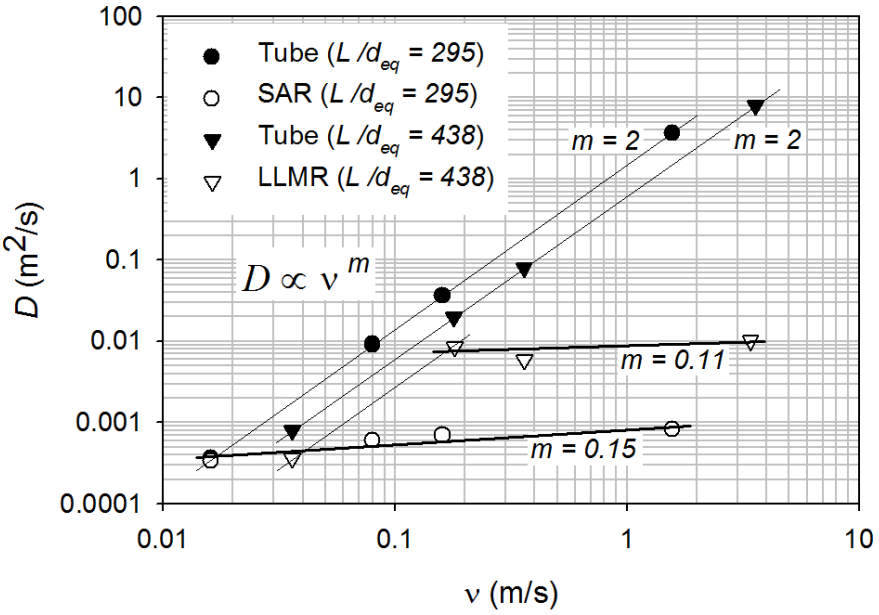

Figure 5.16 Comparison of the axial dispersion coefficient *D* of the microreactors with those of circular tubes with equivalent pressure drop and geometrical ratio l/d_{eq}.

5.4.3 Villermaux/Dushman method

The final *pH* of the solutions after the mixing analysis varied from 8.16 to 9.56 which are in agreement with the values recommended by **Guichardon & Falk (2000)** and **Panić *et al.* (2004)** to avoid both the thermodynamic formation and disassociation of iodine.

The preliminary tests showed that suitable sensitivity is obtained with concentration sets 2-4 (Figure 5.17). The mixing comparison is conducted using only Set 3 and Set 4 since they are in stoichiometric proportion. The results in Figure 5.17 using different concentrations show the trend of a quadratic reduction of mixing performance as a function of flow rate as is usually observed in this type of experiments.

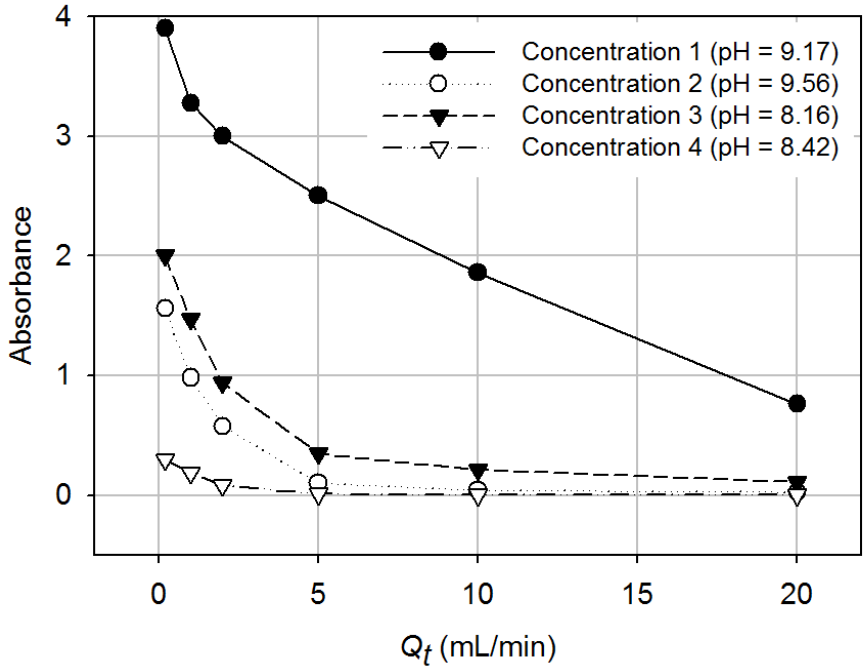

Figure 5.17 Absorbance of triiodide for the SAR microreactor using different concentrations.

The values of the segregation index of the two microreactors and the T-junction are shown in Figure 5.18 as a function of *Da*. In continuous flow reactors a value of *Da* lower than 0.1 will usually give less than 10% conversion and a value greater than 10 will give more than 90%.

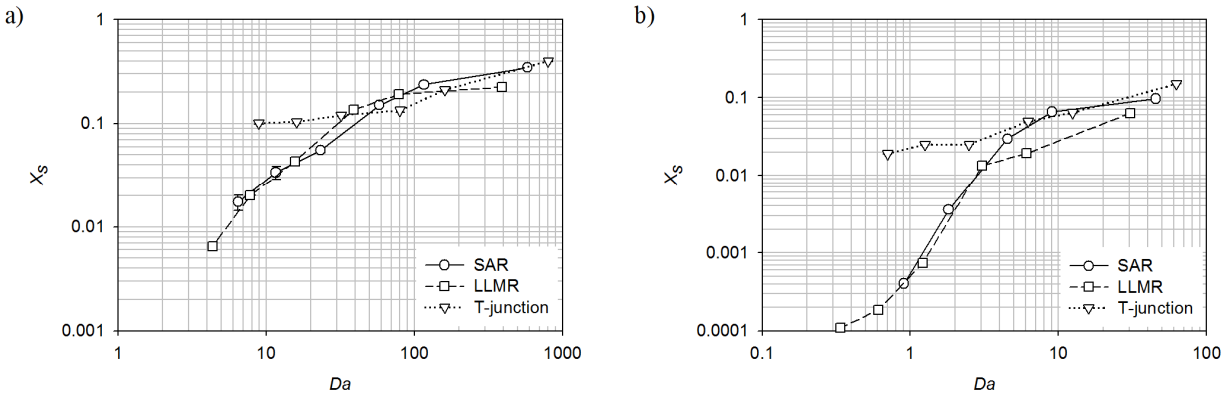

Figure 5.18 Comparison of mixing performance of the SAR, LLMR and T-junction as a function of the mean time: a) 0.009M of acid, t_{cr} = 0.17; b) 0.0045M of acid, t_{cr} = 2.17 s.

For an acid concentration of 0.009M most of the experimental conditions fall in the range of *Da* >10 and it is assumed that the reaction has reached completion and the values of the segregation index are the result of the improved mixing mechanism. Interestingly, the three geometries show similar mixing capabilities at *Da* >30 for 0.009M of acid and *Da* >4 for 0.0045M.

This can be explained by considering the time scale for molecular diffusion at the microscale, which can be estimated as:

$$t_{diff} \propto \frac{R^2}{2 \cdot D_{diff}} \tag{5.21}$$

Thus the T-junction with an internal diameter of 2 mm requires approximately 415 s for achieving complete diffusion in the radial direction whereas the SAR microreactor with typical microchannel widths of 0.5 mm requires approximately 30 seconds and the LLMR with widths of 0.045 mm requires about 1 second. At sufficiently low flow rates the mixing capabilities of the T-junction are comparable to those of the microreactors since the time scale for diffusion in the T-junction is in the same order of magnitude as the mean residence time (~200 s). The improvement of the microreactors is quite evident at shorter residence times where the mixing process is not limited by the diffusion mechanism.

Due to the design of the LLMR, the mixing is achieved by multilamination of the reactants before entering the distribution manifold in the reaction section. Since the mixing mechanism does not depend on the manifold characteristics this allows for an improved mixing performance even at low flow conditions, *i.e.* large values of *Da*. For higher flow rates, the SAR and LLMR mixing trend is fairly identical corresponding to *Da* <20 with 0.009M and *Da* <3 with 0.0045M.
This indicates that even with an unbalanced flow distribution and uneven concentration of reactants in the SAR microreactor, the split-and-recombination sequence in the individual mixing microchannels produces an overall highly efficient mixing mechanism for the entire microreactor as compared to a conventional T-junction and the multilamination mechanism.

One of the most interesting results is observed in Figure 5.19 where a comparison of the mixing performance is made by plotting the segregation index as a function of the energy dissipation of the microreactors (Eq. 5.1). It can be seen that both microreactors are capable to produce comparable levels of mixing. However, the energy required by the SAR microreactor to achieve a specific mixing task is approximately one order of magnitude lower than the energy input required by the LLMR.

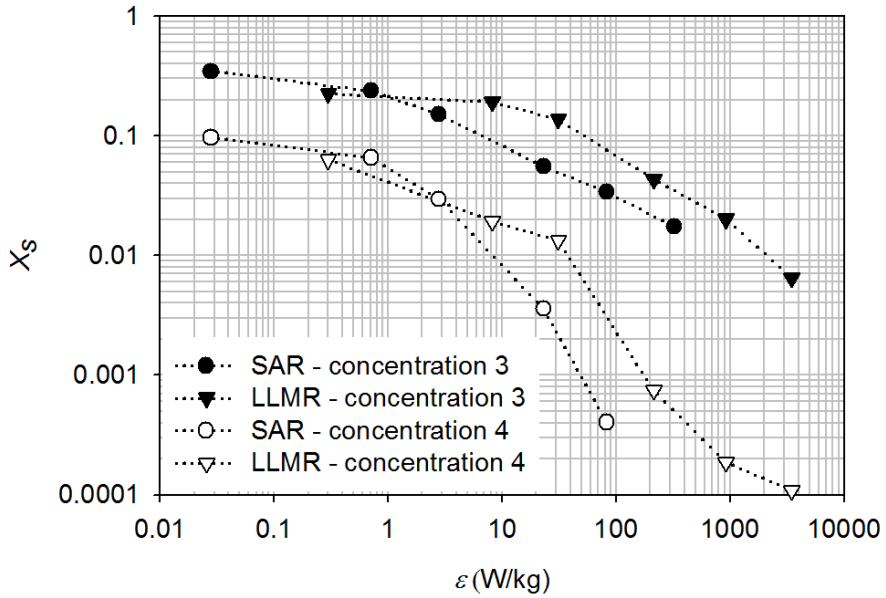

Figure 5.19 Comparison of the segregation indexes of the SAR and LLMR microreactors as a function of the power dissipation at two different concentrations.

5.5 CONCLUDING REMARKS

The hydrodynamic and mixing characteristics of a split-and-recombination and a multilamination microreactor operating in laminar flow regime were investigated by means of RTD analysis and the Villermaux/Dushman method. The one-shot tracer input approach successfully allowed the RTD characterization of non-transparent microreactors with unavoidable large peripheral volumes relative to the microreactors active volumes. The $E(t)$ function recovery procedure by deconvolution in the Fourier domain proved to be a reliable method for signal treatment during

RTD analysis which simplifies the computational time as compared to other methods. Thus, this simple approach can be applied for the characterization of any microreaction unit.

The flow behavior in the microfluidic structures was found to be adequately represented by the axial dispersion model. The use of this model is recommended since the relationship between the model parameters and the geometry of the reactor is well established from a theoretical basis. The decrease of the quadratic dependence of the axial dispersion coefficient on fluid velocity observed for both microreactors is attributed to the efficient tracer homogenization in the radial direction achieved by the micromixing mechanisms investigated.

The hydrodynamic performance of the SAR microreactor is significantly affected by the flow distribution stage in the embedded manifolds. Non-homogeneous flow distribution was found to be caused by hydrodynamic imbalances (*i.e.* different ratios of flow rates) and by imbalances produced by the geometrical design.

From the RTD analysis it was found that the SAR and LLMR operate more efficiently at long mean residence times, *i.e.* $Da > 10$. On the other hand, the iodide-iodate system showed that depending on the acid concentration the SAR and LLMR operate more efficiently at low *Da* since at $Da > 10$ the segregation indexes obtained are comparable to those produced by a T-junction of higher diameter. This reveals the effectiveness of short diffusion lengths in the microreactors where fast mixing by diffusion is achieved even at short residence times. This suggests that flow rates producing values of $Da < 10$ are the optimal operating conditions to take advantage of the fast mixing capabilities of these microreactor models. A slightly better mixing performance can be achieved by the multilamination structure when compared to the SAR especially at low velocity conditions although at the expense of a much larger energy expenditure. The SAR mechanism advantage thus consists in achieving comparable mixing performance at considerably lower pressure drops.

Since flow visualization is restricted in both microreactors further investigation by means of CFD is recommended to clarify the extent of role of the manifold design on the flow distribution in the microchannel network.

5.6 ACKNOWLEDGEMENTS

The authors thank to *Atotech GmbH* (Berlin, Germany) for providing the SAR microreactor. Also, we gratefully acknowledge the financial support from the Natural Science and Engineering Research Council of Canada (NSERC), the National Council of Science and Technology of Mexico (CONACYT) and the oil company TOTAL.

5.7 NOTATION

A	area under the concentration curve, mol-s/m^3
Bo	Bodenstein number, dimensionless
C	concentration, mol/m^3
C_{cr}	characteristic concentration, M^{n-1}
C_{in}	tracer input concentration signal, mol/m^3
C_{out}	tracer output concentration signal, mol/m^3
d_{eq}	equivalent diameter, m
D	axial dispersion coefficient, m^2/s
D_{diff}	molecular diffusion coefficient, m^2/s
Da	Damköhler number, dimensionless
E	exit-age distribution function, dimensionless
f	friction factor, dimensionless
k_{cr}	characteristic reaction constant, M^{1-n}/s
l	length, m
n	reaction order
P	pressure, Pa
Pe_r	reaction Peclet number, dimensionless
Q	volumetric rate of flow, m^3/s
r_Q	ratio of flow rates, dimensionless
Re	Reynolds number, dimensionless

s	frequency, Hz
Sc	Schmidt number, dimensionless
t	time, s
t_{cr}	characteristic reaction time, s
t_{diff}	diffusion time, s
t_m	mean residence time, s
T	temperature, K
v	fluid mean velocity, m/s
V	active volume, m^3
X_s	segregation index
Y	yield of the Dushman reaction, dimensionless
Y_{st}	yield of the Dushman reaction in total segregation, dimensionless

Greek letters

ε	energy dissipation, W/kg
μ	Newtonian viscosity, Pa-s
ρ	density, kg/m^3
θ	dimensionless time, t/t_m

5.8 REFERENCES

Adeosun, J. T., & Lawal, A. (2009). Numerical and experimental studies of mixing characteristics in a T-nuction microchannel using residence-time distribution. *Chemical Engineering Science, 64*, 2422-2432.

Awtrey, A. D., & Connick, R. E. (1951). The absorption spectra of I_2, I_3-, I-, IO_3-, S_4O_6- and S_4O_3-. Heat of the reaction I_3- = I_2 + I-. *Journal of the American Chemical Society, 73*, 1842-1843.

Bavière, R., Ayela, F., Le Person, S., & Favre-Marinet, M. (2004). *An experimental study on water flow in smooth and rough rectangular microchannels.* Paper presented at the Second International Conference on Microchannels and Minichannels, Rochester, N.Y., U.S.A.

Bayer, T., Pysall, D., & Wachsen, O. (2000). *Micro mixing effects in continuous radical polymerization.* Paper presented at the 3rd International Conference on Microreaction Technology IMRET 3, Berlin.

Bird, R. B., Stewart, W. E., & Lightfoot, E. N. (2002). *Transport Phenomena* (2nd ed.): Wiley.

Boskovic, D., & Loebbecke, S. (2007). Modelling of the residence time distribution in micromixers. *Chemical Engineering Journal, 135*(SUPPL. 1), S138-S146.

Bucci, A., Celata, G. P., Cumo, M., Serra, E., & Zummo, G. (2004). *Water single-phase fluid flor and heat transfer in capillary tubes.* Paper presented at the Second Internacional Conference on Microchannels and Minichannels, Rochester, NY, USA.

Cantrel, L., Chaouche, R., & Chopin-Dumas, J. (1997). Diffusion Coefficients of Molecular Iodine in Aqueous Solutions. *Journal of Chemical Engineering Data, 42*, 216-220.

Custer, J., & Natelson, S. (1949). Spectrophotometric determination of microquantities of iodine. *Analytical Chemistry, 21*(8), 1005-1009.

Ehrfeld, W., Gärtner, C., Golbig, K., Hessel, V., Konrad, R., Löwe, H., et al. (1997). *Fabrication of components and systems for chemical and biological microreactors.* Paper presented at the 1st International Conference on Microreaction Technology, Berlin.

Ehrfeld, W., Golbig, K., Hessel, V., Lowe, H., & Richter, T. (1999a). Characterization of Mixing in Micromixers by a Test Reaction: Single Mixing Units and Mixer Arrays. *Industrial & Engineering Chemistry Research, 38*(3), 1075-1082.

Ehrfeld, W., Hessel, V., & Haverkamp, V. (1999b). *Microreactors, Ullmann's Encyclopedia of Industrial Reactors*. Weinheim: Wiley-VCH.

Engler, M., Kockmann, N., Kiefer, T., & Woias, P. (2004). Numerical and experimental investigations on liquid mixing in static micromixers. *Chemical Engineering Journal, 101*(1-3), 315-322.

Fogler, H. S. (1999). *Elements of Chemical Reaction Engineering*. New Jersey, USA: Pretince-Hall.

Fournier, M. C., Falk, L., & Villermaux, J. (1996a). New parallel competing reaction system for assessing micromixing efficiency - experimental approach. *Chemical Engineering Science, 51*(22), 5053-5064.

Fournier, M. C., Falk, L., & Villermaux, J. (1996b). New parallel competing reaction system for assessing micromixing efficiency - determination of micromixing time by a simple mixing model. *Chemical Engineering Science, 51*(23), 5187-5192.

Gamrat, G., Favre-Marinet, M., Le Person, S., Baviere, R., & Ayela, F. (2008). An experimental study and modelling of roughness effects on laminar flow in microchannels. *Journal of Fluid Mechanics, 594*, 399-423.

Günther, M., Schneider, S., Wagner, J., Gorges, R., Henkel, T., Kielpinski, M., et al. (2004). Characterisation of residence time and residence time distribution in chip reactors with modular arrangements by integrated optical detection. *Chemical Engineering Journal, 101*(1-3), 373-378.

Guichardon, P., & Falk, L. (2000a). Characterisation of micromixing efficiency by the iodide-iodate reaction system. Part I: experimental procedure. *Chemical Engineering Science, 55*(19), 4233-4243.

Guichardon, P., & Falk, L. (2000b). Characterisation of micromixing efficiency by the iodide-iodate reaction system. Part II: kinetic study. *Chemical Engineering Science, 55*(19), 4245-4253.

Ham, J.-H., & Platzer, B. (2004). Semi-empirical equations for residence time distributions in disperse systems – Part 1: Continuous phase. *Chemical Engineering Technology, 27*(11), 1172-1178.

Hardt, S., & Schönfeld, F. (2000). Laminar mixing in different interdigital micromixers-part 2: Numerical Simulations. *AIChE Journal, 40*(3), 578-584.

Hardt, S., & Schönfeld, F. (2003). Laminar mixing in different interdigital micromixers: II. Numerical simulations. *AIChE Journal, 49*(3), 578-584.

Haverkamp, V., Ehrfeld, W., Gebauer, K., Hessel, V., Löwe, H., Richter, T., et al. (1999). The potential of micromixers for contacting of disperse liquid phases. *Fresenius Journal of Analytical Chemistry, 364*, 617-624.

Herbo, C., & Sigallia, J. (1957). Principes de l'iodimétrie absortiométrique. *Analytica Chimica Acta, 17*, 199.

Hessel, V., & Löwe, H. (2003). Microchemical engineering: components, plant concepts user acceptance - part 1. *Chemical Engineering Technology, 26*, 13-24.

Hessel, V., Löwe, H., & Schönfeld, F. (2005). Micromixers a review on passive and active mixing principles. *Chemical Engineering Science, 60*, 2479-2501.

Judy, J., Maynes, D., & Webb, B. W. (2002). Characterization of frictional pressure drop fro liquid flows through microchannels. *International Journal of Heat and Mass Transfer, 45*, 3477-3489.

Kockmann, N., Kiefer, T., Engler, M., & Woias, P. (2006). Convective mixing and chemical reactions in microchannels with high flow rates. *Sensors and Actuators, B: Chemical, 117*(2), 495-508.

Köhler, J. M., Schleiff, B., Schneider, S., Boskovic, D., Henkel, T., & Groß, G. A. (2010). Characterization of viscosity dependent residence time distribution in the static micromixer Statmix6. *Chemical Engineering Journal, 160*(3), 845-851.

Kölbl, A., Kraut, M., & Schubert, K. (2008). The iodide iodate method to characterize microstructured mixing devices. *AIChE Journal, 54*(3), 639-645.

Levenspiel, O. (1999). *Chemical Reaction Engineering*. USA: Wiley.

Löb, P., Hardt, S., & Löwe, H. (2000). Steering of a liquid mixing speed in interdigital micromixers-from very fast to deliberately slow mixing. *Chemical Engineering and Technology, 27*(3), 340-345.

Löb, P., Pennemann, H., Hessel, V., & Men, Y. (2006). Impact of fluid path geometry and operating parameters on l/l-dispersion in interdigital micromixers. *Chemical Engineering Science, 61*(9), 2959-2967.

Lohse, S., Kohnen, B. T., Janasek, D., Dittrich, P. S., Franzke, J., & Agar, D. W. (2008). A novel method for determining residence time distribution in intricately structured microreactors. *Lab on a Chip, 8*, 431-438.

Lowe, H., Ehrfeld, W., Hessel, V., Richter, T., & Schiewe, J. (2000). *Micromixing technology.* Paper presented at the 4th International Conference on Microreaction Technology, IMRET 4, Atlanta, USA.

Mann, U. (2009). *Principles of Chemical Reactor Analysis and Design - New Tools for Industrial Chemical Reactor Operations* (2nd. ed.): John Wiley & Sons.

Men, Y., Hessel, V., Löb, P., Löwe, H., Werner, B., & Baier, T. (2007). Determination of the segregation index to sense the mixing quality of pilot- and production-scale microstructured mixers. *Trans. IChemE, Part A, Chemical Engineering Research and Design, 85*(A5), 605-611.

Nauman, E. B. (2008). *Chemical Reactor Design, Optimization and Scaleup* (2nd. ed.). New Jersey, USA: John Wiley & Sons.

Nauman, E. B., & Buffham, B. A. (1983). *Mixing in Continuous Flow Systems*. USA: John Wiley & Sons.

Newson, J. D., & Riddiford, A. C. (1961). Limiting currents for the reduction of the tri-iodide ion at a rotating platinum disk cathode. *Journal of the Electrochemical Society, 108*(7), 695-698.

Palmer, D. A., Ramette, R. W., & Mesmer, R. E. (1984). Triiodide ion formation equilibrium and activity coefficients in aqueous solution. *Journal of Solution Chemistry, 13*(19), 673-683.

Panic, S., Loebbecke, S., Tuercke, T., Antes, J., & Boskovic, D. (2004). Experimental approaches to a better understanding of mixing performance of microfluidic devices. *Chemical Engineering Journal, 101*(1-3), 409-419.

Ruff, I., Friedrich, V. J., & Csillag, K. (1972). Kinetics and Mechanism of the Triiodide-Iodide Exchange Reaction. *The Journal of Physical Chemistry, 76*(2), 162-165.

Schönfeld, F., & Hardt, S. (2004). Simulation of Helical Flows in Microchannels. *AIChE Journal, 50*(4), 771-778.

Schubert, K., Brandner, J., Fichtner, M., Linder, G., Schygulla, U., & Wenka, A. (2001). Microstructure devices for applications in thermal and chemical process engineering. *Microscale Thermophysical Engineering, 5*, 17-39.

Smith, S. W. (1997). *The Scientist and Engineer's Guide to Signal Processing*: California Technical Publishing.

Stroock, A. D., Dertinger, S. K. W., Ajdari, A., Mezic, I., Stone, H. A., & Whitesides, G. M. (2002). Chaotic mixer for microchannels. *Science, 295*(5555), 647-651.

Trachsel, F., Günther, A., Khan, S. A., Thalmann, M., & Jensen, F. (2004). Transport and reaction in microscale segmented gas-liquid flow. *Lab Chip, 4*, 278-286.

Trippa, G., & Jachuck, R. J. J. (2004). *Characterization of mixing efficiency in narrow channels by using the iodide-iodate reaction system.* Paper presented at the Second International Conference on Microchannels and Minichannels.

Weast, R. C. (1986). *Handbook of Chemistry and Physics*. Florida, USA: CRC Press.

Westerterp, K., R., Swaaij, W. P. M. v., & Beenackers, A. C. M. (1984). *Chemical reactor design and operation*. Great Britain: Wiley.

Wong, S. H., Ward, M. C. L., & Wharton, C. W. (2004). Micro T-mixer as a rapid mixing micromixer. *Sensors and Actuators B, 100*, 359-379.

Wörz, O., Jäckel, K. P., Richter, T., & Wolf, A. (2001). Microreactors - A New Efficient Tool for Reactor Development. *Chemical Engineering & Technology, 24*(2), 138-142.

CHAPTER 6

NUMERICAL INVESTIGATION OF THE HYDRODYNAMICS OF A SPLIT-AND-RECOMBINATION AND MULTILAMINATION MICROREACTORS

Lionel S. Méndez-Portillo, Mourad Heniche, Charles Dubois, Philippe A. Tanguy

Department of Chemical Engineering, École Polytechnique de Montréal
P.O. Box 6079, Station Centre-Ville, Montreal, QC.
Canada H3C 3A7

ABSTRACT

The hydrodynamics and residence time distribution (RTD) of two microreactors based on the split-and-recombination (SAR) and multilamination mixing mechanisms respectively were investigated. It was found that the design of the distribution manifolds of the SAR mechanism produces an unbalanced flow distribution. For feeding ratios different than one, by-passing and recirculation occur within the SAR manifold structures whereas for equal flow rates the RTD curves show that the SAR flow behavior can be accurately described by the pure convection model. The manifold used in the multilamination microreactor achieves a homogeneous distribution of flow and its interdigital structure generates an alternated pattern of fluid layers in the mixing section which is maintained for Re <140. After this point the ordered arrangement is broken and two large segregated zones are formed. In the absence of molecular diffusion both microreactors reach limiting values of scale and intensity of segregation that were found to be independent of the energy applied to the system.

6.1 INTRODUCTION

In the rapidly developing field of chemical micro process engineering, microreaction technology is seen as a powerful approach for process intensification. Many applications can be thought of in the chemical industry, and polymer reaction engineering is certainly one field that could exploit the theoretical benefits of microreaction technology. Indeed, polymerization reactions are usually exothermic and highly sensitive to the level of mixing of the reactants and can benefit from the high heat transfer rates and efficient mixing allowed in microreactors. Whereas a low throughput can be anticipated from microreactors due to their characteristic small active volume, high selectivity and yield (**Bayer *et al.*, 2000; Wörz *et al.*, 2001; Yoshida *et al.*, 2005**) can favourably impact the overall performance of a polymerization process in the microscale. This compromise between low throughput and reaction performance makes microreaction technology an attractive alternative for targeted applications such as on-demand production of polymers or fine chemicals.

Selectivity and overall yield of a reaction are related to the degree of mixing and the time spent by the reactants inside the chemical reactor which in turn are governed by diffusion effects and the specific flow patterns of the reaction vessel. Thus, knowledge of the spatial and temporal mixing characteristics of the flow system is necessary in order to predict yield and conversion of chemical reactions.

So far, microprocessing conditions achievable in microfluidic devices have often been exploited without a complete understanding of how their reduced geometries affect the fluid flow patterns and consequently the transport processes. The flow patterns inside a chemical reactor have a direct impact on the amount of time and area of contacting of the reactants which can lead to unexpected concentration gradients and unreacted material. The distinctive flow patterns of a chemical reactor are the result of the relationship between the fluid properties, flow conditions and the geometry of the vessel. Proper knowledge of these contacting patterns is required in order to predict the behavior of a continuous flow reactor. Thus, direct visualization of flow patterns is one of the most appropriate approaches to understand 3D flow phenomena in chemical reactors. However, this technique is not possible in microreactors that are constructed from non-transparent materials. Microfluidic devices are usually composed by several microchannels in parallel and in some cases by different flow sections in serial arrangements. This generates intricate flow paths that lead to difficult interpretation of experimental results and possible flow maldistribution cannot be easily located. Furthermore, the performance of the distribution manifolds embedded in microreactors plays a critical role on the homogeneous distribution of the flow and consequently on the level of concentration of reactants in the parallel microchannel network. Inhomogeneous flow distribution may lead to poor reaction selectivity and degrade the overall yield of the process.

A series of investigations used CFD simulations in order to gain a better insight of the flow patterns of new micromixing mechanisms (**Mengeaud *et al.*, 2002; Stroock *et al.*, 2002a; Stroock *et al.*, 2002b; Hardt & Schönfeld, 2003**); on the optimization of microchannel shapes and distribution manifolds (**Kim *et al.*, 2000; Gobby *et al.*, 2001; Chen & Chen, 2002; Commenge *et al.*, 2002; Tonomura *et al.*, 2004**); on the characterization of mixing efficiency of microdevices (**Aubin *et al.*, 2003; Engler *et al.*, 2004; Wong *et al.*, 2004; Aubin *et al.*, 2005;**

Serra *et al*., 2005; Kockmann *et al*., 2006; Gamrat *et al*., 2008; Lee & Lee, 2008; Yu *et al*., 2008; Cortes-Quiroz *et al.*, 2010); and on the calculation of numerically based residence time distributions (RTD) (**Adeosun & Lawal, 2005; Adeosun & Lawal, 2009; Aubin *et al*., 2009; Cantu-Perez *et al.*, 2010, 2011**). Most of the above studies focused on T-junctions and the staggered-herringbone mixer (SHM). Presently there is a large family of available microreactor models and knowledge about their hydrodynamic performance is a key requirement in order to find suitable applications.

We conducted an experimental characterization of the performance of two microreactors known as potential candidates for industrial applications. One unit was a prototype design using the split-and-recombination (SAR) mixing principle while the other was an already commercialized model using the mixing mechanism of multilamination of flow by means of an interdigital structure. The results indicated the possibility of by-passing and/or recirculation. Since visual inspection is restricted in the microreactors investigated, numerical flow simulations (CFD) can be used as a useful complementary tool for the analysis of the fluid mechanics inside these microfluidic devices.

In the forthcoming, our objective is to provide further insight on the hydrodynamic performance and RTD of the two microreactors by means of CFD, and especially to clarify the extent of the role of the manifold design on the flow distribution in the microchannel network.

6.2 DESCRIPTION OF THE MICROREACTORS

Two microreactors have been considered in this work. A prototype microreactor featuring a split-and-recombination mechanism (further referenced as SAR) was provided by *Atotech GmbH* (Berlin, Germany). Another liquid/liquid microreactor (further referenced as LLMR) was acquired from *IMM GmbH* (Mainz, Germany) under the model designation *LLMR-MIX-SI* and is based on the multilamination of flow by means of an interdigital structure. Both microreactors are equipped with an integrated forced-convection heat exchanger. The maximal pressure rating

provided by the manufacturers is 100 bar for the SAR and 50 bar for the LLMR. The geometric characteristics of the microchannels considered in this investigation are given in Table 6.1.

Table 6.1 Geometrical values of the microchannels used for the simulations

Microreactor	Section	Number of channels	Width (mm)	Height (mm)	Length (mm)	Volume experimental (μL)	Volume 3D model (μL)
SAR	Mixing	5	0.5	0.15	48.1	20	57.2
	Reaction	31	0.3	0.15	23.6	107	106.7
LLMR	Mixing	36	0.045	0.25	0.9	4	3.8
	Reaction	8	0.07	0.9	75	132	132.1

The computer-aided design solid models of the 3D flow path of the microreactors were based on the blueprints provided by the manufacturer in the case of the SAR, and on geometrical values and sketches disclosed in the user assembly manual in the case of the LLMR. The volumes of the 3D models are accurate to ± 1% of the values we previously obtained experimentally except for the mixing section of the SAR microreactor which is almost three times higher than the value obtained experimentally.

6.2.1 Split-and-recombination microreactor

The SAR microreactor consists of a stacked arrangement of 8 plates. In the concept of stacked arrangement of plates, the flow passages are machined into the plate surfaces forming carved or tunnel-like structures. Each cover plate has a distribution manifold machined in the bottom surface that allows the fluids to be divided into five mixing microchannels that use the classical split-and-recombination principle. The mixing section is created by two plates featuring a G-shaped structure (**Antes *et al.*, 2003; Ferstl *et al.*, 2004; Bošković *et al.*, 2007**), which is employed to arrange the splitting elements longitudinally along the flow direction (Figure 6.1a).

The assembly order of the plates is depicted in Figure 6.1b. The Mixing Plate 1 has five columns with five rows of G-shaped structures machined *in the bottom* of its surface while the Mixing Plate 2 has five columns with five rows of *inversed* G-shaped structures machined *in the top* of its

surface but shifted longitudinally a certain distance in relation to those machined in the Mixing Plate 1.

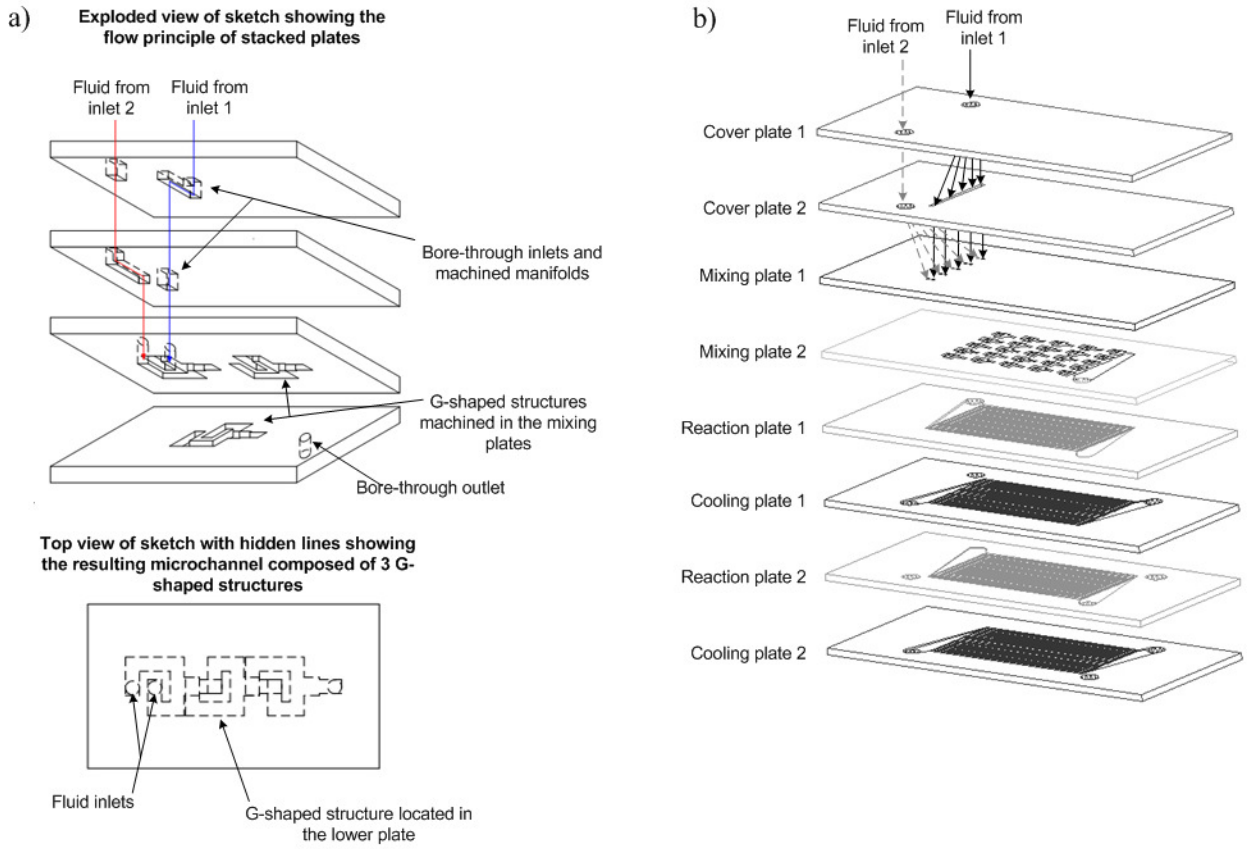

Figure 6.1 Schematic of the SAR microreactor plates: a) stacking order, b) flow principle.

When the two mixing plates are assembled one above the other, each of the outlets of the G-shaped structures in the Mixing Plate 1 coincides exactly with the shifted inlet of the microstructures of the Mixing Plate 2 thus creating a total of five long mixing microchannels composed of 10 G-shaped structures (Figure 6.2). In this way the fluid inside is switching from the upper to the lower plate as the mixing proceeds. The outlets of the mixing cavities converge to a structure that recombines the flow of the five microchannels.

After passing the micromixing section the now mixed fluids flow along two stacked plates that are connected in series. These plates consist of two trapezoidal manifolds at the inlet and outlet of 31 straight parallel microchannels machined on the plate surface. The reaction plates increase the residence time of the microreactor.

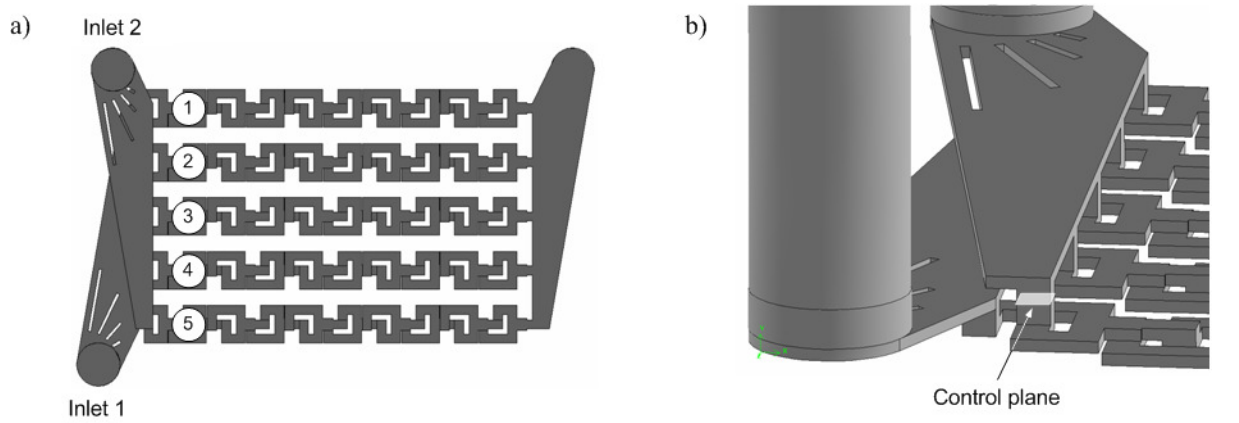

Figure 6.2 Flow path of the mixing section of the SAR microreactor: a) top view of the complete mixing section, b) isometric detail of each manifold attaching to the five G-shaped structures.

The heat exchanger plates are isolated from the flow path of the mixing and reaction plates, therefore they are not included in the geometry. The solid model of the resulting flow path of the SAR microreactor used for the simulations is presented in Figure 6.3.

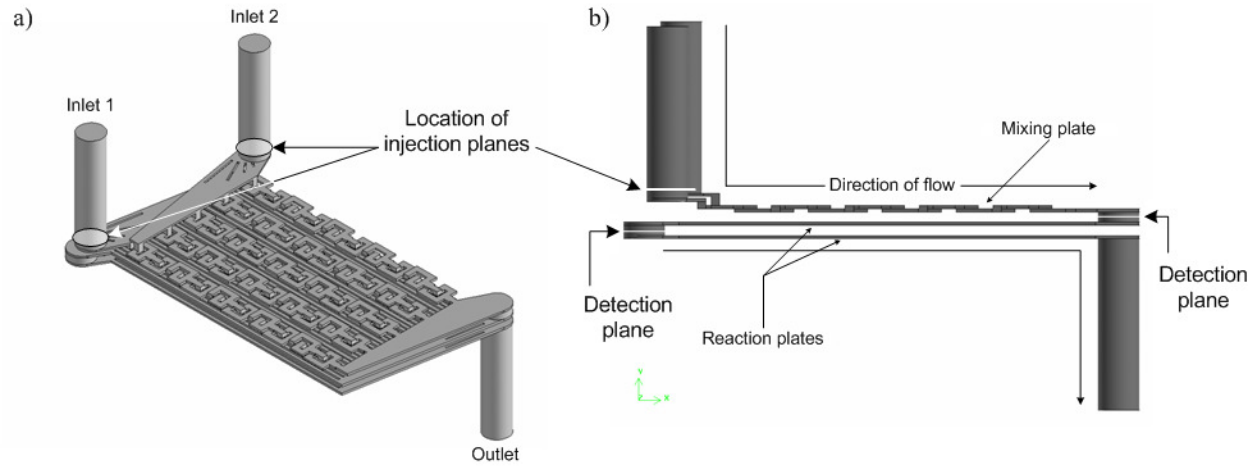

Figure 6.3 Isometric (a) and lateral (b) views of the 3D flow path of the complete mixing and reaction sections featured by the SAR microreactor including inlet and outlet ports.

The distribution and collection manifolds are manufactured with a trapezoidal shape. This type of manifolds have been applied in other parallel channel microdevices (**Ferstl *et al.*, 2004;**

Bošković & Loebbecke, 2008) and proposed as the optimized shape that minimizes space time under the constraint of flow uniformity (**Commenge *et al.*, 2002; Tonomura *et al.*; 2004**).

6.2.2 LLMR-MIX-SI Multilamination Microreactor

The LLMR microreactor (**Wörz *et al.*, 2001; Hessel *et al.*, 2004**) consists of a stack of four machined plates. The first plate is composed of two inlets that feed the reactants into a mixer inlay in which the fluids are contacted in a bi-layer configuration. The multilamination mechanism takes place in the mixer inlay (Figure 6.4). The second plate acts as the reaction section and is machined on both sides. After the mixing stage a distribution manifold separates the flow into eight microchannels with a depth of 900 μm and a high aspect ratio of 15.

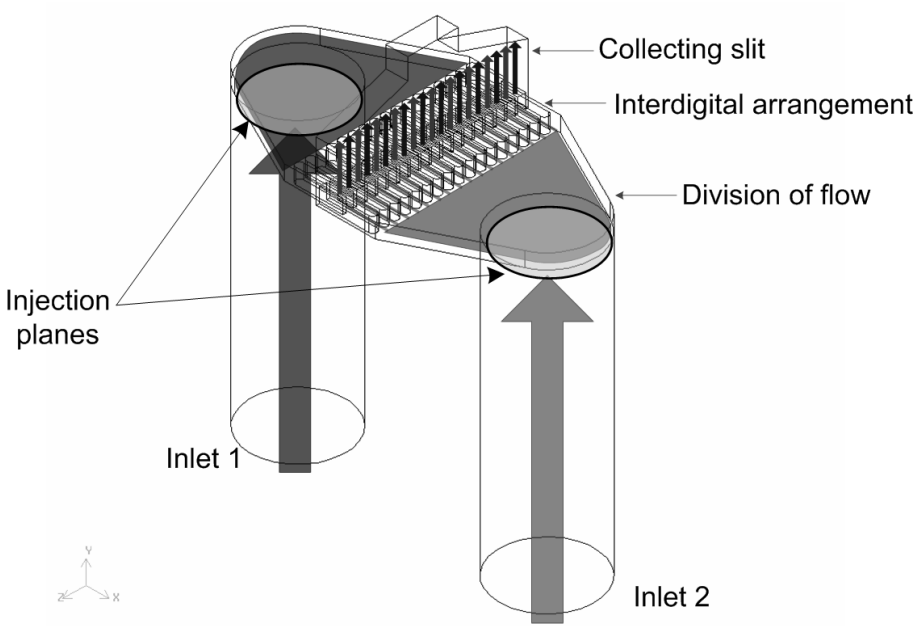

Figure 6.4 Schematic of the interdigital inlay of the LLMR in which multilamination takes place.

A third plate is added with a set of four microchannels for the purpose of cooling on the top side of the reaction plate. The fluids are collected and redirected to the outlet port via the fourth plate. The solid model of flow path of the LLMR is presented in Figure 6.5. For the purpose of schematic representation, the reaction channels of the LLMR in Figure 6.5 have been shortened

to 10 mm. However, during the numerical simulations the original microchannel length of 75 mm was used.

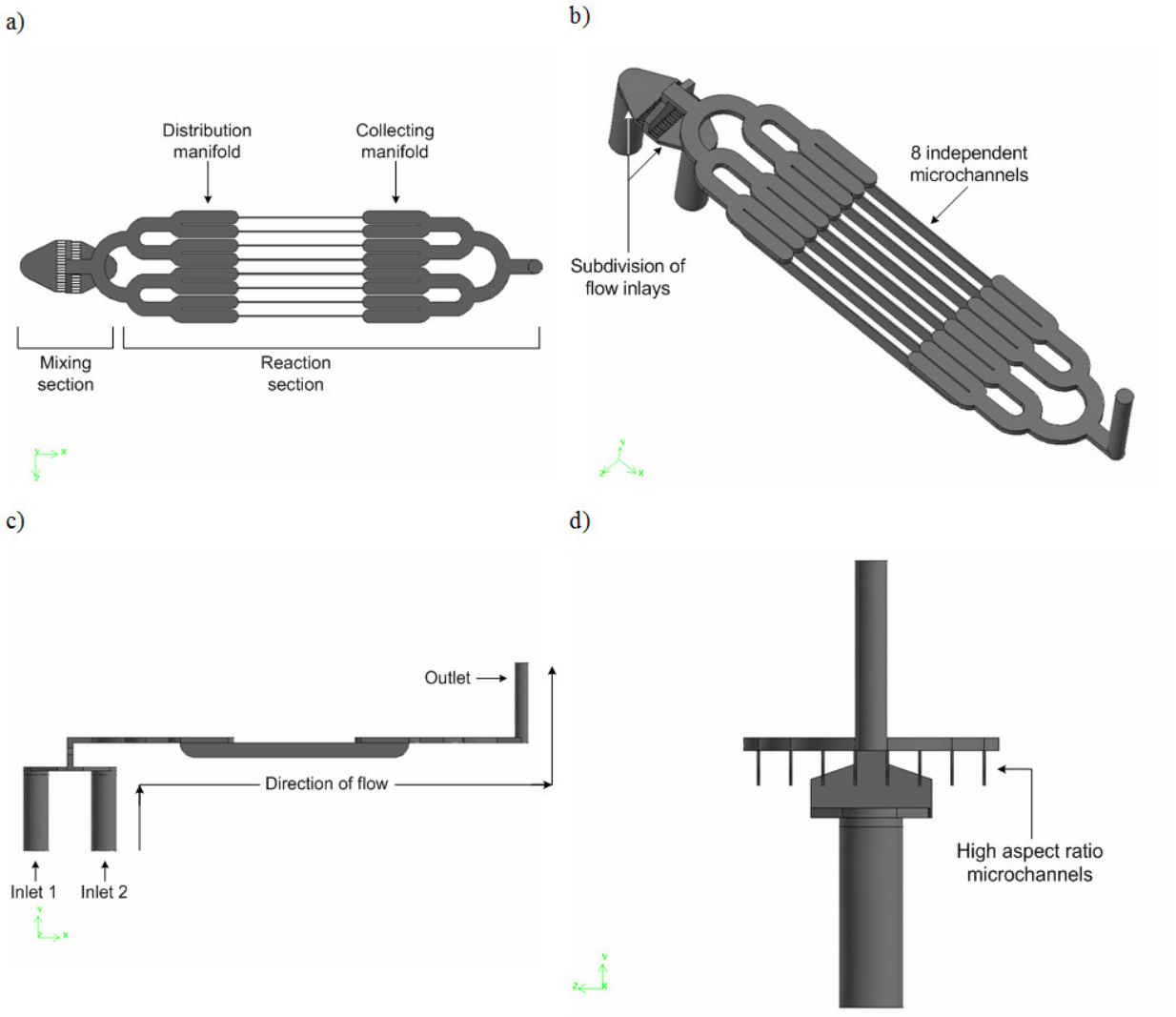

Figure 6.5 Views of the LLMR flow path with inlets and outlet ports: a) top, b) isometric, c) front, and d) lateral.

6.3 NUMERICAL METHODOLOGY

A two-step numerical approach previously referenced as the *decoupled CFD-mixing approach* (**Heniche *et al.*, 2005**) is followed. Such strategy has been applied for the numerical characterization of macroscopic static mixers (**Rauline *et al.*, 1996; Rauline *et al.*, 2000; Heniche *et al.*, 2005**) and microfluidic devices (**Aubin *et al.*, 2003; Aubin *et al.*, 2005; Aubin *et al.*, 2009; Cantu-Perez *et al.*, 2010a-b**). The first step consists of the computation of the flow variables (*e.g.* velocity and pressure) in the flow vessel geometry by means of CFD. The second step consists of analyzing the mixing performance and the residence time distribution (RTD) by means of the particle tracking technique. One limitation of this approach is that the effect of the viscosity ratio between the fluids to be mixed is not taken into account. However, its application is useful for certain mixing systems where the fluids exhibit similar viscosities upon contact, *e.g.* monomers and organic solvents in continuous free-radical polymerization processes.

6.3.1 Scale and Intensity of Segregation

In the context of CFD the mixing performance is usually evaluated by the concepts of *scale and intensity of segregation* proposed by **Danckwerts (1952)** to describe the mixing process of two miscible liquid species. The scale of segregation is a measure of the size of the clumps that result from a break-up mechanism undergone by the two fluid species. The intensity of segregation is a measure of the homogeneity of the two fluids across the boundaries of said clumps. Therefore, the scale and intensity of segregation are respectively related to the dispersive and distributive characteristics of the system.

In a mixture composed of species *A* and *B*, the scale of segregation is estimated by measuring the total concentration of one component in the mixture along a straight line joining two points in the reference plane of interest. The content *J* of species *A* in a line-sample of length *X* is defined by:

$$J = \int_0^X a \; dx \tag{6.1}$$

where a is the concentration of A at a point distance x from one end of the line. If the content J is determined for a large number of such line-samples in different regions of the mixture then the scale of segregation can be determined as:

$$S_s = \frac{\sigma_J^2}{2X\sigma_a^2} \tag{6.2}$$

where σ^2 represents respectively the variances of J and a which are defined by:

$$\sigma_J^2 = \overline{(J - \bar{a}X)^2} \tag{6.3}$$

$$\sigma_a^2 = \overline{(a - \bar{a})^2} \tag{6.4}$$

The intensity of segregation is a statistical parameter defined by **Danckwerts (1952)** as:

$$I_s = \frac{\sigma_a^2}{\bar{a} \cdot \bar{b}} \equiv \frac{\sigma_b^2}{\bar{a} \cdot \bar{b}} \tag{6.5}$$

where σ^2 represents the variance, and a and b represent the concentrations of two different miscible species in terms of their volume fractions. The intensity of segregation I_s characterizes the extent to which the concentration of any of the two species in a delimited clump departs from the mean value of the mixture. As defined in Eq. 6.5 the intensity of segregation has a value of 0 when the concentration is uniform throughout all the clumps, and a value of 1 in a complete segregated state when the concentration in any clump is either only a or b.

Danckwerts (1952) states that during the mixing of two miscible liquids the value of I_s is progressively reduced by the effect of molecular diffusion and not directly affected by the mechanical process of mixing. Thus, in the absence of diffusion the mixture would remain "grainy" or segregated. Relying on the statistical nature of the definition of intensity of segregation the particle tracking method has been exploited for the mixing characterization of microfluidic devices (**Aubin *et al.*, 2003; Aubin *et al.*, 2005; Aubin *et al.*, 2009**) and at least one

example of an stochastic approach (*e.g.* random walk model) has been coupled with this method in order to account for the effect of molecular diffusion (**Cantu-Perez *et al.*, 2010, 2011**).

In this investigation we translate the concepts proposed by Danckwerts to estimate the scale (S_s) and intensity (I_s) of segregation by means of the particle tracking method. The calculation of S_s and I_s is based on the spatial distribution of the tracer particles *positions* detected at specific reference planes perpendicular to the flow direction. The concentration of the particles positions is quantified as a function of predefined spatial regions or grid cells. The cell size, which can be viewed as the clump size in the Danckwerts definition, will dictate the level of resolution for the estimation of I_s. The intensity of segregation estimated by the particle tracking method is the result of mechanistic effects only and disregards the effect of molecular diffusion. However, these mechanistic effects are of great importance in laminar flow systems that promote intensive radial mixing by means of split-and-recombination mechanisms, *e.g.* static mixers, microreactors. Due to the nature of the geometries analyzed in the present investigation the scale and intensity of segregation are evaluated as a function of the flow conditions at a constant downstream position located at the outlet plane of the mixing sections of the microreactors.

The coefficient of variation *COV* is a statistical parameter frequently used to quantify the degree of mixing in continuous flow systems by means of CFD (**Rauline *et al.*, 1996; Rauline *et al.*, 2000; Aubin *et al.*, 2003; Heniche *et al.*, 2005**). Statistically the *COV* is defined as the ratio of the standard deviation of a variate divided by the mean value of its distribution:

$$COV_a = \frac{s_a}{\bar{a}} \tag{6.6}$$

where s_a is the standard deviation of the concentration of species *a* defined as:

$$s_a = \sqrt{\frac{1}{N-1} \cdot \sum_{i=1}^{N} (a_i - \bar{a})^2} \tag{6.7}$$

It is usually stated that the *COV* varies from 0 to 1 with zero indicating a complete mixed stated while 1 represents complete segregation. The *COV* is a measure of relative variability about the

mean and is recommended that this coefficient be used in ratio form and not as a percentage since it can readily exceed unity (**Rosander, 1957**). Values of $COV > 1$ are statistically possible even if volume fractions are used when certain number of grid cells exhibit a concentration that is far greater than the mean. Thus, the use of COV to characterize the degree of segregation between 0 and 1 from Eq. 6.6 should be taken with care. In this study the concept of intensity of segregation was chosen since the values of I_s as defined in Eq. 6.5 consistently vary between 0 and 1.

6.3.2 Residence Time Distribution

Two approaches can be followed for the numerical calculation of residence time distributions (RTD) in continuous flow systems where distribution functions at a given cross section can be reproduced from: 1) the concentration of species obtained by solving the continuity and convection-diffusion equations, 2) the residence time of massless particles injected in the flow field.

Nauman (**2008**) has raised concerns about the capabilities of CFD codes to account for the low fluid velocities near the walls of the system which can pose practical problems during the calculation of numerically based RTD. A strategy of particle restitution has been applied to macroscopic static mixers (**Hobbs & Muzzio, 1997**) and recently to microfluidic devices (**Aubin *et al.*, 2009**) in order to conserve the tracer particles that are lost in the region near the walls. In turn this strategy has been questioned (**Wörner, 2010**) since the reinstated particles do not conserve their flow history and thus the theoretical criteria of infinite mean in the absence of molecular diffusion is not met.

However, according to **Nauman (1977)** the exit-age distribution function in laminar flow systems without diffusion asymptotically approaches a dependence of t^{-3} therefore producing a finite mean. It has been demonstrated (**Nauman, 1991**) that such a distribution has an infinite first moment with an asymptote proportional to t^{-2} when the RTD is weighted by surface area and not by volumetric flow rate. **Nauman (1991)** states that in a laminar flow system, the exit-age distribution function weighted by volumetric flow rate will exhibit a first moment equal to V/Q

even in the absence of molecular diffusion, with V being the total volume of the flow vessel and Q the total volumetric flow rate.

The weighting of the tracked particles by volumetric flow rate is performed by assigning to each particle a fraction of the volumetric flow rate $\Delta Q_i = v_n \cdot \Delta A$, where v_n is the velocity normal to the inlet surface evaluated at the inlet surface and ΔA is the area of the inlet associated to each particle. Each volume fraction is calculated relatively to the radial position $r_i(x,y)$ of each particle over the area A_{in} of the inlet tube as:

$$\Delta Q_i = 2v\left(1-\left(\frac{r_i}{R}\right)^2\right)\left(\frac{A_{in}}{N_t}\right) \tag{6.8}$$

where v is the mean flow velocity, R is the radius of the inlet tube, and N_t is the total number of tracer particles. The exit-age distribution function is then obtained by constructing a histogram of the volume fractions and their corresponding residence times. The ratio $\Delta Q_i/Q$ represents the fraction of particles having a residence time equal to t_i. Due to the discrete nature of the results the bin size at each frequency count must be defined prior to the construction of the histogram. The shape of the histogram is largely dependent on the choice of the bin size. If a large bin size is chosen the spike rate of the distribution cannot be accurately represented. On the contrary, if the bin size is too small the time histogram fluctuates greatly and the underlying rate cannot be discerned. During the RTD analysis of flow vessels the shape of the histogram, *i.e.* the RTD curve, is of critical importance for diagnosing purposes of special flows such as by-passing, recirculation or stagnancy. Thus, the relevance of selecting an appropriate bin size for such applications is evident.

Several methods exist to define the bin size of a histogram depending on the number of available data points. One robust criterion frequently used in statistic analysis is the Freedman-Diaconis estimator (**Freedman & Diaconis, 1981**) which relies on the calculation of the first and third interquartiles and thus is not as susceptible to fluctuations as other estimators relying simply on the variance. More recently, a histogram bin width optimization method was developed by **Shimazaki & Shinomoto (2007)** which is based on the minimization of the *mean integrated*

squared error (MISE) of a preliminary histogram fitted to the underlying rate of the available data. In this method an arbitrary number of bins N_b of size δ is selected and the number of events k_i in each bin is quantified. The mean μ_k and variance σ_k^2 are calculated as follows:

$$\mu_k = \frac{1}{N_b}\sum_{i=1}^{N_b} k_i \tag{6.9}$$

$$\sigma_k^2 = \frac{1}{N_b}\sum_{i=1}^{N_b} (\mu_k - k_i)^2 \tag{6.10}$$

The optimal bin size is the value of δ that minimizes the cost function $C(\delta)$:

$$C(\delta) = \frac{2\mu_k - \sigma_k^2}{\delta^2} \tag{6.11}$$

For the histograms obtained in the present investigation it was found that both estimators yielded similar results with differences in bin size of around 3% and the obtained optimal number of bins varied from 182 to 200.

6.3.3 Numerical Flow Conditions

The 3D modeling of the flow field requires the simultaneous numerical solution of the steady-state incompressible Navier-Stokes momentum (6.12) and continuity (6.13) equations tackled below by means of the finite element method.

$$\rho\left(\frac{\partial \mathbf{v}}{\partial t} + \mathbf{v}\cdot\text{grad}\,\mathbf{v}\right) = -\text{grad}\,p - \text{div}\,\boldsymbol{\tau} \tag{6.12}$$

$$\text{div}\,\mathbf{v} = 0 \tag{6.13}$$

Where ρ is the fluid density, $\mathbf{v}$ is the velocity vector, p is the pressure, and $\boldsymbol{\tau}$ is the stress tensor. The 3D solid models and the corresponding unstructured mesh were generated with GAMBIT

(ANSYS, Inc.) software using block partitions to refine the mesh as required. Due to the complexity of the geometry and the aspect ratios of the microchannels, the final mesh required approximately 3.8 million elements for the SAR microreactor and 6.1 million elements for the LLMR microreactor. The mesh of the LLMR required an increased number of elements due to the length of the 8 high aspect ratio microchannels in the reaction section. In order to overcome this computationally expensive problem, the low order MINI finite element (**Arnold *et al.*, 1984**) implemented in the commercial 3D finite element software (**Coesnon *et al.*, 2008**) POLY3D (Rheosoft, Inc.) was applied, yielding a total of approximately 2.2 million and 3.5 million equations for the SAR and LLMR respectively. This type of finite element is inexpensive with respect to the number of degrees of freedom per element generated, which impact directly on the size of the final linear system. Due to the presence of the convective term in the Navier-Stokes equations, the problem is non-linear. In order to solve the respective system of equations a Newton-Raphson iterative scheme was used.

Convergence problems were encountered in preliminary simulations for the SAR microreactor due to the small volume size of the tetrahedral elements needed. The volume of the elements was calculated by dividing the active volume of the microreactor by the number of elements in the mesh yielding a volume of ~$4.3 \cdot 10^{-14}$ m^3 per element. Since this value is close to the machine epsilon (~10^{-15}), a change of units to millimetres and grams was mandatory to converge the solution of the flow solver. All simulations were run on an IBM-P690 computer cluster consisting of a 64-bit multiprocessing UNIX server with 16 RISC POWER4 processors sharing 64GB of memory. In order to aid the convergence of the fluid problem, the viscosity parameter in the simulations was increased in some conditions. Once convergence was achieved, the viscosity value was reduced about 10% and the procedure was repeated until the initially targeted viscosity was reached. Each simulation required approximately 10 hours of CPU time.

The fluid properties considered for the simulations correspond to the flow of water in steady-state laminar regime. The flow conditions considered for the simulations are summarized in Table 6.2 where the flow ratio r_Q is defined as the ratio of flow rates of Inlet 1 over Inlet 2. The boundary conditions imposed are:

1. no-slip velocity at the wall surfaces;
2. zero radial velocity at the inlets;
3. parabolic velocity profile in the axial direction;
4. free flow condition in the axial direction at the outlet;

It must be mentioned that the surface finish of the interior microchannel walls might have an impact on the hydrodynamic conditions in the microreactors. Such irregularities on the microchannel surfaces can be accounted for as a decrease in the effective hydrodynamic diameter of each individual microchannel. The objective of the present work is to evaluate the global mixing and RTD characteristics of the specific microreactor designs investigated without considering any local instabilities produced by the surface roughness inside individual microchannels. Therefore, for the purpose of simplification we have assumed a smooth surface finish for the interior microchannel walls.

Table 6.2 Flow conditions considered in the simulations

Condition	Q (mL/min)			Flow ratio (r_Q)
	Inlet 1	Inlet 2	Total	
1	0.1	0.1	0.2	1
2	0.1	1.0	1.1	0.1
3	0.1	10.0	10.1	0.01
4	0.5	0.5	1.0	1
5	1.0	1.0	2.0	1
6	10.0	10.0	20.0	1

6.3.4 Particle Tracking Method

The particle tracking technique performed in this study is based on the methodology developed by **Heniche & Tanguy (2006)**. Preliminary runs were performed on the SAR microreactor in order to determine the influence of the number of tracer particles injected. Five cases were investigated using 5 200, 13 000, 31 000, 63 000 and 100 000 tracer particles.

The injection consisted of a circular plane in which the tracer particles were evenly distributed covering only 94% of the radius of the inlet plane (1/8 and 1/16 in. for the SAR and LLMR

respectively). This value of 0.94*R* has been proposed by **Nauman (2008)** as a guideline to avoid the injection of tracer particles in close proximity to the walls of the vessel which would contribute to long tailing effects. Reference planes were defined at each inlet of the microchannels of the splitting manifolds as well as at the outlet plane of the mixing and reaction sections of the microreactors.

The amount of tracer particles lost in each case was around 50-60%. It was found that neither the shape of the histogram nor the magnitudes of the first and second moment of the distributions were affected by the number of tracer particles injected. Thus, the rest of the analysis was performed using 5 200 tracer particles in order to reduce the computation time.

6.4 RESULTS AND DISCUSSION

6.4.1 Pressure Drop

The pressure drop values obtained from the simulations are compared to experimental data and converted to a non-dimensional friction factor *f*. The conversion is made by calculating an equivalent diameter d_{eq} that for a given flow rate would produce the same pressure drop as the microreactors. The numerical results are plotted in Figure 6.6 as a function of the Reynolds number calculated as:

$$Re = \frac{\rho \, v \, d_{eq}}{\mu} \tag{6.14}$$

The numerical results show an excellent agreement with both laminar flow theory and experimental data. The numerical values for d_{eq} are 0.522 mm for the SAR and 0.311 mm for the LLMR which are also in agreement with the respective values of 0.506 and 0.344 mm obtained from experiments. The flow rates of 0.2, 1.0, 2.0 and 20.0 mL/min correspond respectively to *Re* values of 8, 41, 83 and 825 for the SAR, and 14, 68, 136 and 1363 for the LLMR.

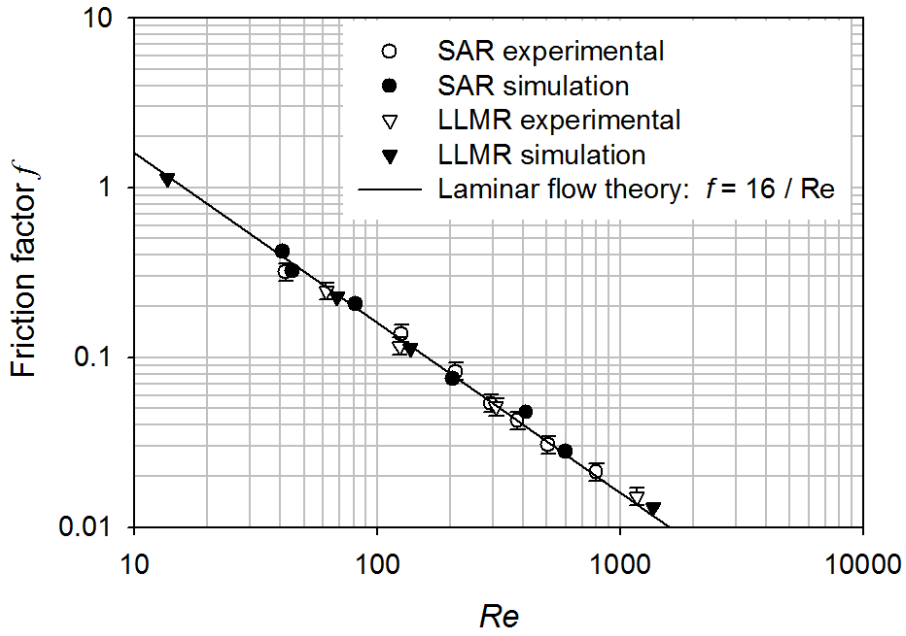

Figure 6.6 Comparison of the friction factor calculated from the numerical and experimental data for the SAR and LLMR microreactors.

6.4.2 Flow Distribution

The flow rate delivered to each microchannel of the SAR has been normalized with the theoretical value expected in the situation of homogeneous distribution, *i.e.* 20% of the volumetric flow rate per inlet being delivered into each microchannel. It was found that for all the hydrodynamic conditions investigated there is an imbalance in the flow distribution in the SAR trapezoidal manifolds. Figure 6.7 shows the pathlines obtained in the manifold of Inlet 1 at different flow conditions when r_Q =1 (*i.e.* conditions 1, 4, 5 and 6). The pathlines have been normalized by the maximal flow velocity at each flow condition. The manifold of Inlet 2 (not shown) exhibits the same trend.

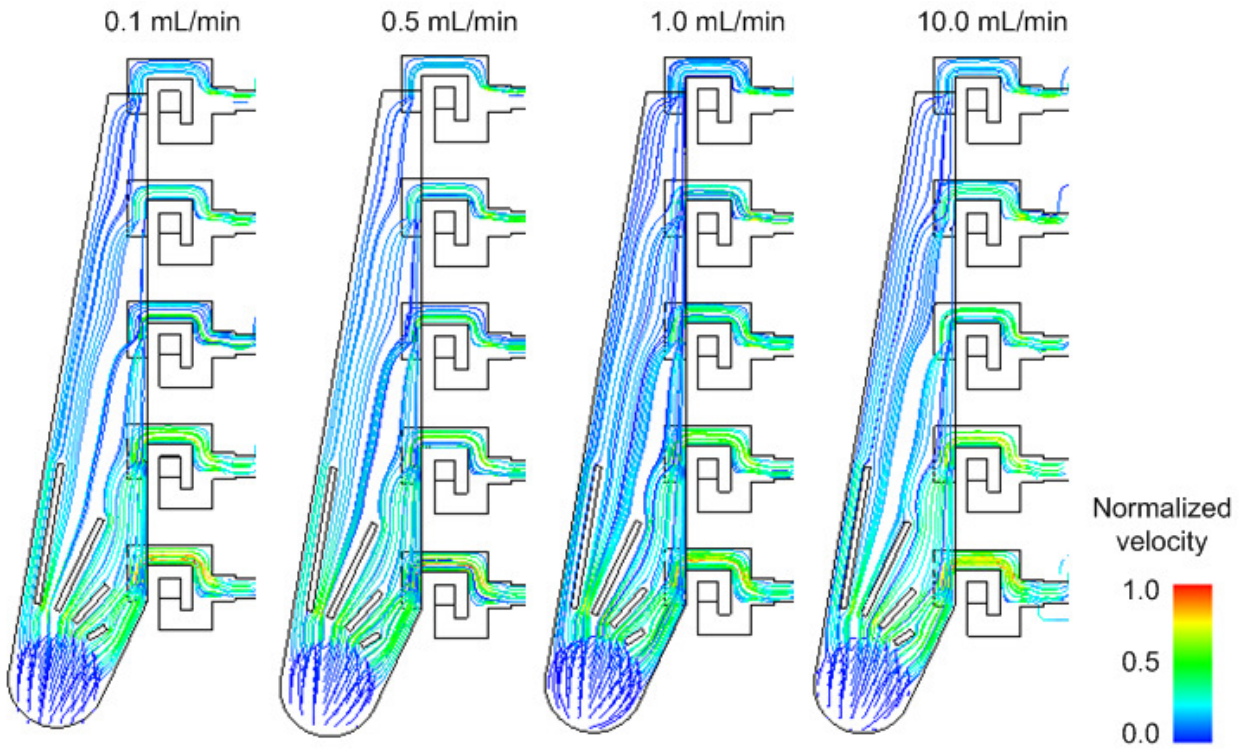

Figure 6.7 Fluid pathlines in the SAR manifold for different flow conditions when r_Q =1.

The flow imbalance (Figure 6.8) exhibits an almost linear asymmetry with respect to the center channel with differences of approximately 5% per adjacent channel. The microchannel closest to its respective inlet receives as much as 10% more fluid than the center channel while the microchannel farthest to the inlet exhibits a 10% deficit. However, a slight reduction in this difference is observed as the flow rate is increased. This suggests that a better flow distribution may be obtained at higher flow rates although at the expense of higher pressure drops.

The flow distribution in the LLMR (not shown) occurs after the mixing section and before entering the reaction passages. Although the distribution of flow does not have a direct impact on the mixing stage of the LLMR it was found that the axially symmetrical manifold design can produce a homogeneous flow distribution in parallel microchannel networks.

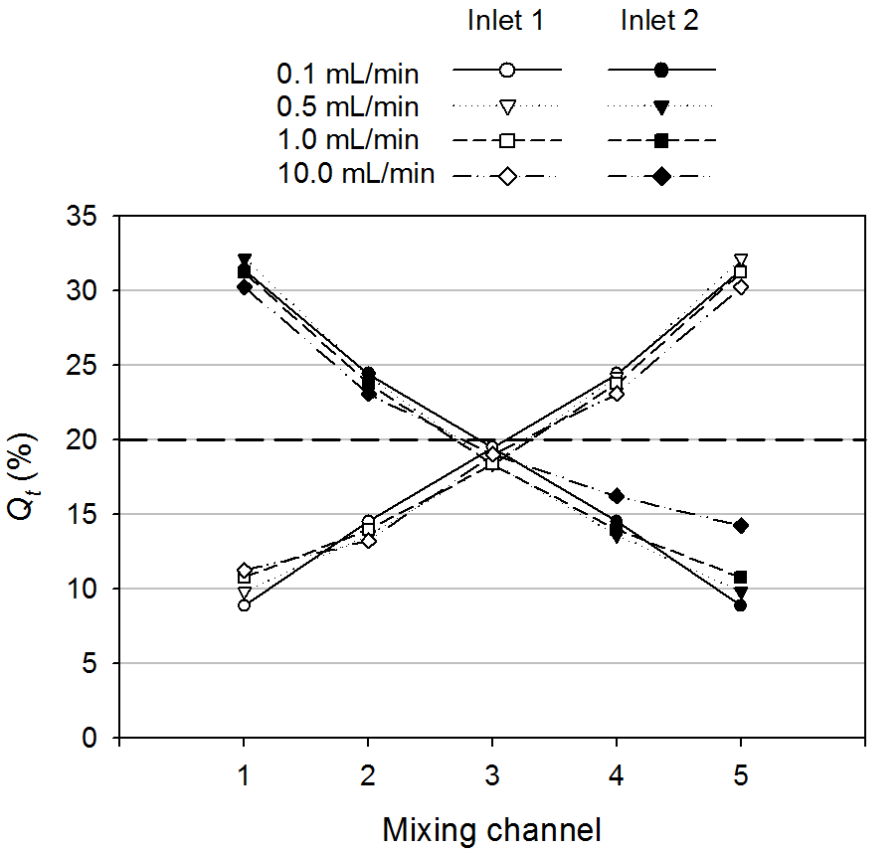

Figure 6.8 Percentage of the total flow rate that is delivered to each mixing microchannel in the SAR microreactor.

The flow imbalance is further verified using the particle tracking method. In an optimal flow distribution situation the total amount of particles detected at the entrance of each mixing microchannel of the SAR should be composed of an equal amount of particles coming from each inlet. For the three flow conditions with r_Q =1 (Figure 6.9) the flow composition in each microchannel is nearly identical and follows the trend shown in Section 6.4.2 where only the central channel achieves a 50/50 composition. There is approximately a 12.5% variation per adjacent channel with the ones closest to the inlets receiving as much as 25% more particles than the center channel.

For the case of different feeding ratios the volumetric flow rate of Inlet 1 was kept constant at 0.1 mL/min while the flow rate of Inlet 2 was increased from 0.1 mL/min to 1.0 and 10.0 mL/min. In this situation the effect of *by-passing* is observed with particles injected through Inlet 1 flowing

only through Channel 4 and 5 when Inlet 2 is at 1.0 mL/min and only through Channel 5 when Inlet 2 is increased to 10.0 mL/min.

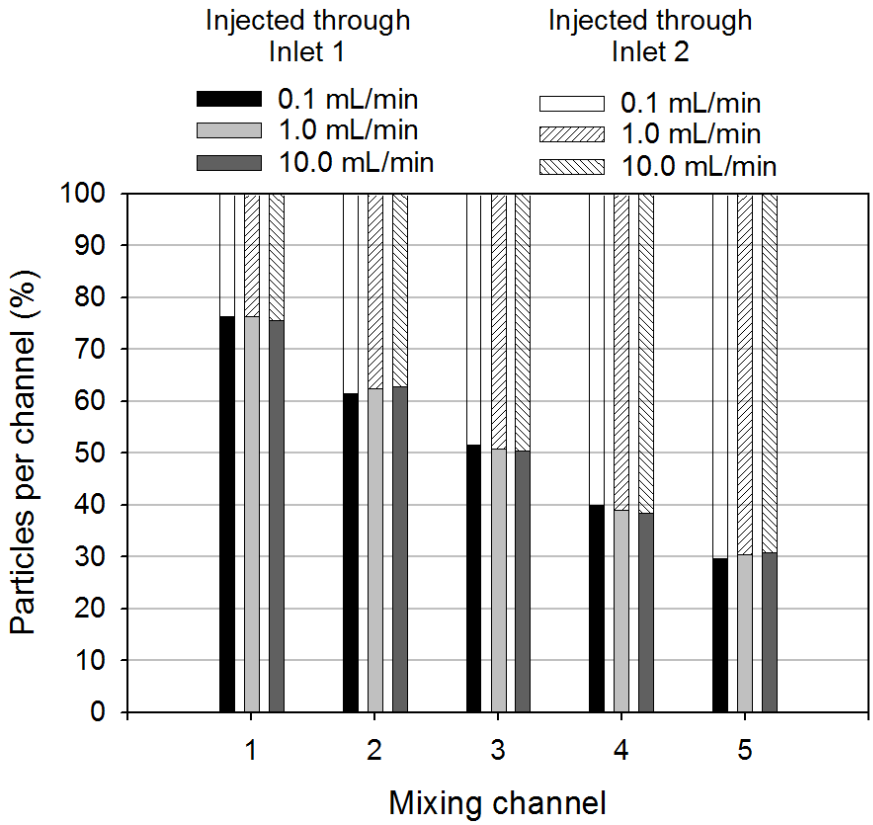

Figure 6.9 Percentage of particles injected through Inlet 1 and Inlet 2 that reach each mixing microchannel for r_Q =1.

The tracer pathlines in Figure 6.10 (in red and blue) confirms a recirculation effect of the fluid delivered through Inlet 2 (blue) and a by-passing effect of the fluid delivered through Inlet 1 (red) when $r_Q \neq 1$. The recirculation of fluid delivered through Inlet 2 around the G-shaped structures is produced by the pressure difference that forces the fluid into the distribution manifold of Inlet 1. Upon colliding with the upcoming stream the fluid from Inlet 1 is by-passed through a reduced number of channels.

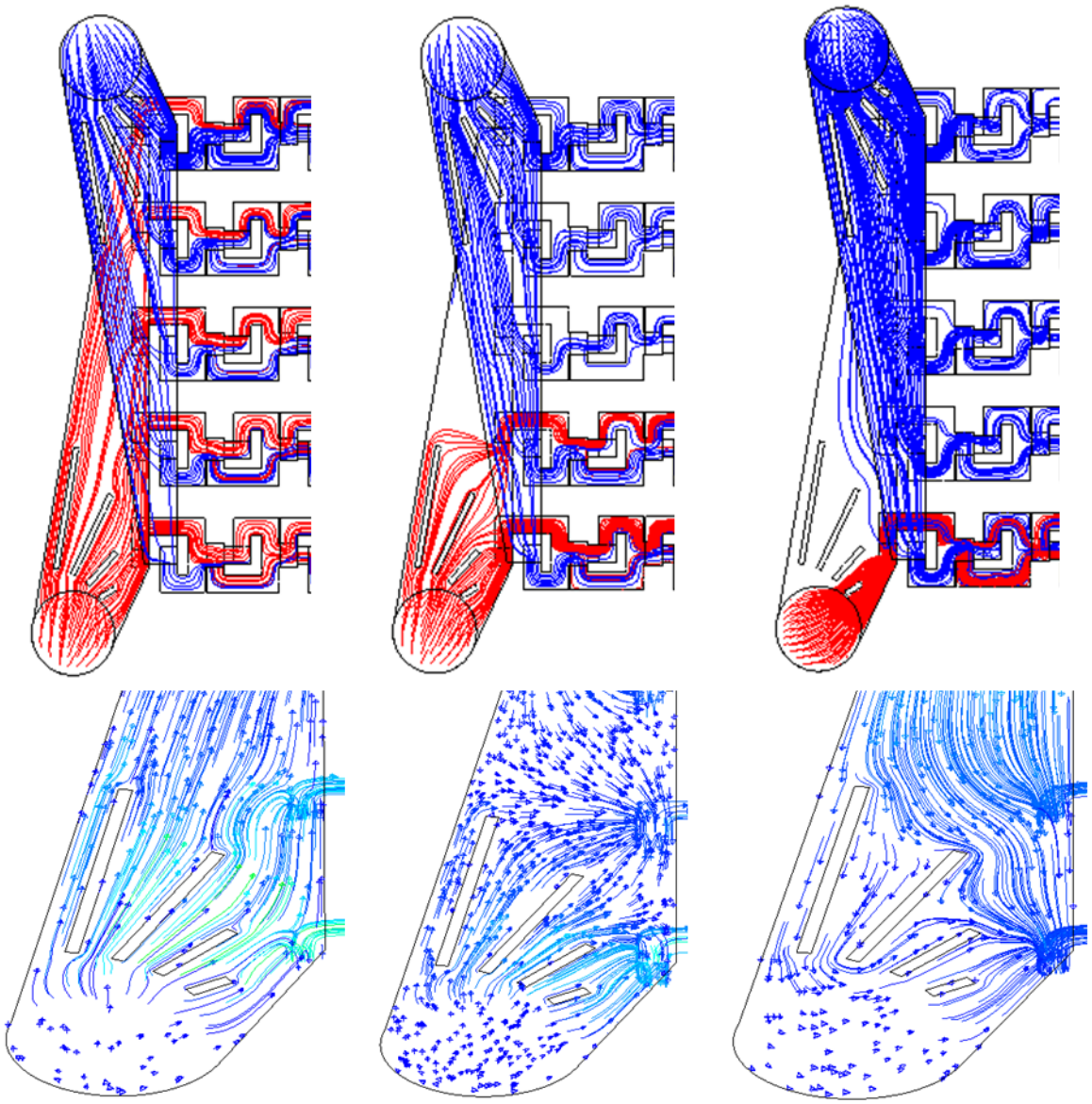

Figure 6.10 Details of the tracer pathlines in the manifolds of Inlet 1 (red) and Inlet 2 (blue) of the SAR microreactor (upper images); and velocity vectors in the manifold of Inlet 1 (lower images) for different flow ratios: a) r_Q=1, b) r_Q=0.1 and c) r_Q=0.01.

At r_Q =0.01, Inlet 1 contributes as much as 85% of the total composition of the microchannel (Figure 6.11). The pressure imbalance has a great impact on the flow distribution capabilities of the trapezoidal manifold structure and renders the SAR microreactor as a less suitable alternative

to be used, for instance, in emulsification processes since in such applications the droplet size and droplet size distribution is frequently controlled by the ratio of flow rates.

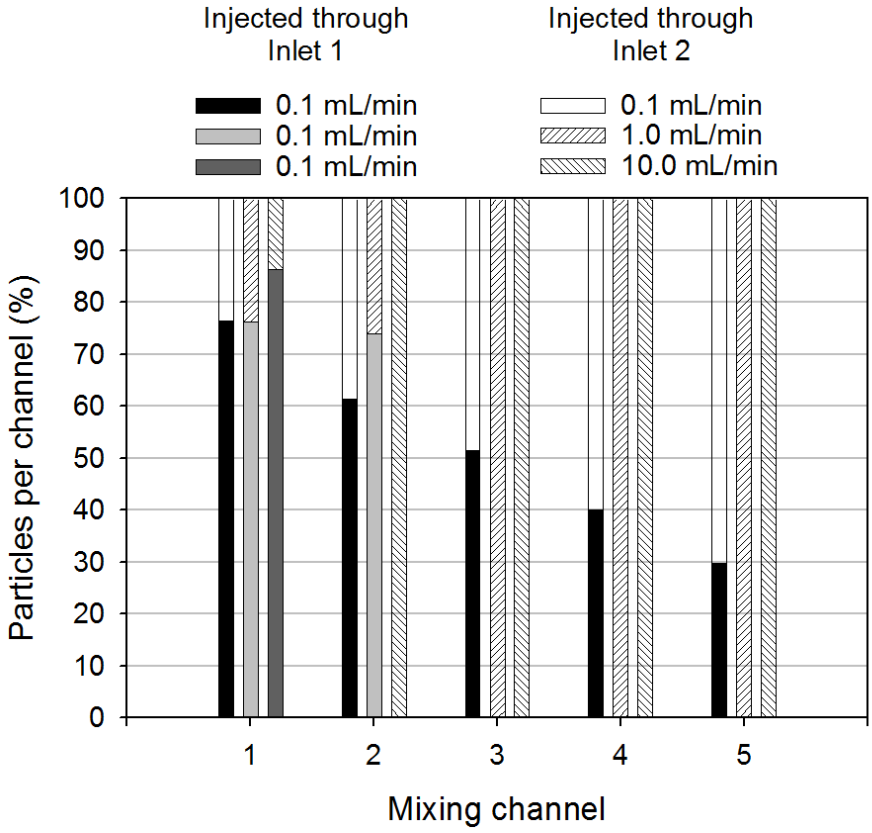

Figure 6.11 Percentage of particles injected through Inlet 1 and Inlet 2 that reach each mixing microchannel for $r_Q \neq 1$.

6.4.3 Mixing Characterization: Scale and Intensity of Segregation

The scale and intensity of segregation were evaluated at the outlet plane of the mixing section for both microreactors. The outlet planes of the mixing sections of the SAR and LLMR microreactors are circular and rectangular respectively. A squared reference plane was used for the SAR while a rectangular grid was used for the LLMR. In order to determine the influence of the grid size during the mixing analysis the scale and intensity of segregation of the SAR microreactor were calculated as a function of the total number of cells in the reference plane for two flow conditions with r_Q =1. The maximum number of cells must not exceed the number of particles reaching the reference plane. The minimum number of tracer particles arrived at the

reference plane was 4935, thus to avoid statistical distortion the maximum number of cells was fixed to 4900 (*i.e.* 70 cells per side of a squared grid). The results in Figure 6.12 show that the magnitude of S_s does not follow a linear trend as a function of the cell number for the two flow conditions investigated. Interestingly the difference between both conditions at each cell number remains constant irrespective of the absolute value of S_s. The values of I_s show a linear increase as a function of the number of cells. This is due to the size of the individual grid cells in comparison to the scale of segregation of the tracer particles. If the cell size is lower than a limiting value of the scale of segregation, then the concentration of tracer particles in each cell will be likely to be either only A or B thus affecting the value of I_s. The limit of S_s is selected as the mean of the values in Figure 6.12. This mean of S_s at the exit of the mixing section of the microreactors was found to be 0.18 mm for the SAR and 0.03 mm for the LLMR.

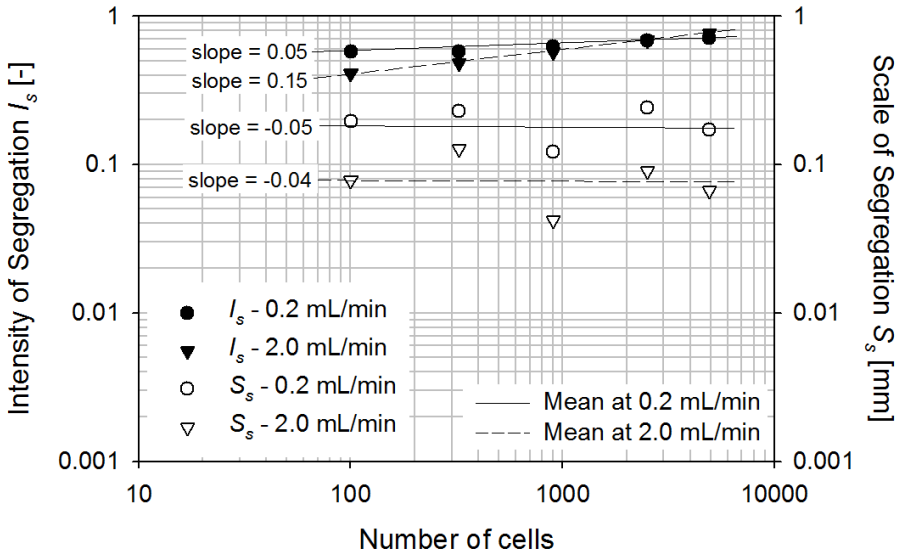

Figure 6.12 Scale and intensity of segregation of the SAR mixing section at two different flow conditions with r_Q =1.

The effect of the cell size on the value of I_s can be better observed in Figure 6.13 where the intensity of segregation of the SAR and LLMR for cell sizes lower and higher than the limit value of S_s are plotted as a function of the energy dissipation defined as:

$$\varepsilon = \frac{\Delta P \cdot v}{\rho \cdot l} \tag{6.15}$$

where v is the flow mean velocity, ρ is the mass density and l is the microreactor or tube length between the pressure detection points. When the cell size is lower than the limit of S_s the intensity of segregation is considerably increased.

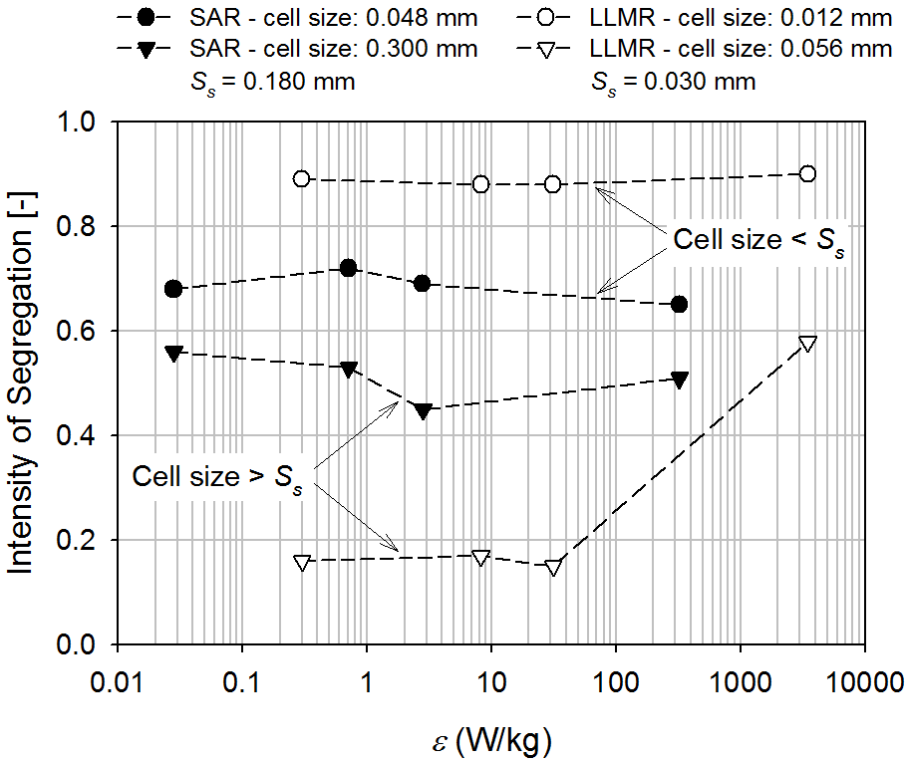

Figure 6.13 Intensity of Segregation as a function of the power dissipation for the mixing section of the SAR and LLMR obtained using two different cell sizes.

Since the values of scale of segregation for the SAR and LLMR microreactors are in the range of ~0.1 mm and ~0.01 mm respectively, then in the presence of molecular diffusion the LLMR will lead to shortest mixing times between fluid layers. One interesting result that deserves attention is that from a fluid mechanics perspective the intensity of segregation achieved by these microreactors is not significantly affected by the amount of energy applied to the system.

For the cases when the cell size is greater than the limiting value of S_s, the SAR mixing section achieves an average I_s value of 0.53. For the LLMR an average I_s value of 0.16 is reached except at 20.0 mL/min where a higher state of segregation (~0.58) is observed.

This behavior is analyzed in Figure 6.14 using Poincaré maps at the exit plane of the mixing section of the LLMR for different *Re*. In the context of CFD, a Poincaré map can be defined as the surface of intersection between the tracer particles and a subspace perpendicular to the fluid flow. It is worth to underline that the interdigital mixing structure of the LLMR produces an alternated pattern of layers of tracer particles. The ordered arrangement of the tracer particles is compressed in the center and stretched at the edges as the flow rate is increased. At *Re* =1363 (20.0 mL/min) the layered and alternate arrangement is broken and while the value of the scale of segregation remains close the mean value, the average value of I_s is increased from 0.16 to 0.58. The tracer particles at *Re* =1363 are segregated in two major pockets along the longest dimension of the exit plane. The alternated arrangement produced by the LLMR geometry can be maintained for *Re* <140.

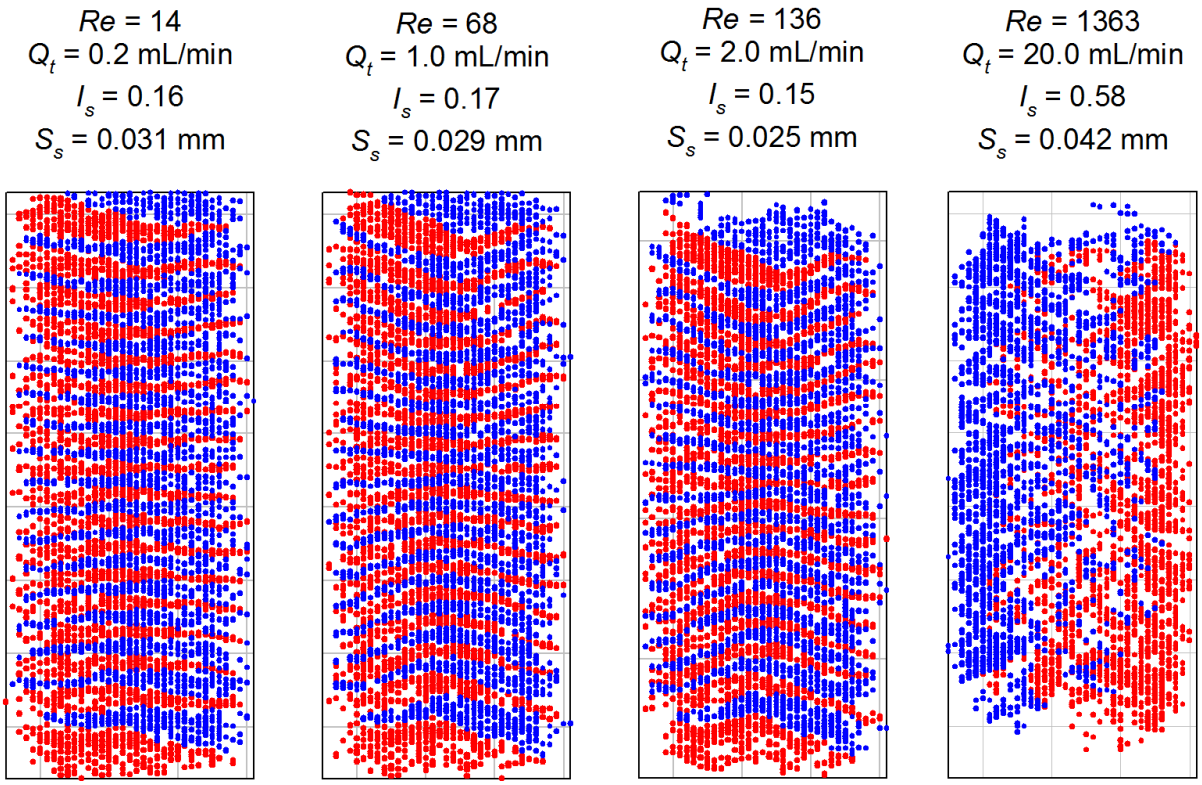

Figure 6.14 Poincaré maps produced by the interdigital structure of the LLMR for different *Re* with r_Q =1.

The effect of r_Q on the values of I_s and S_s as well as on the disposition of the Poincaré maps for the LLMR is shown in Figure 6.15.

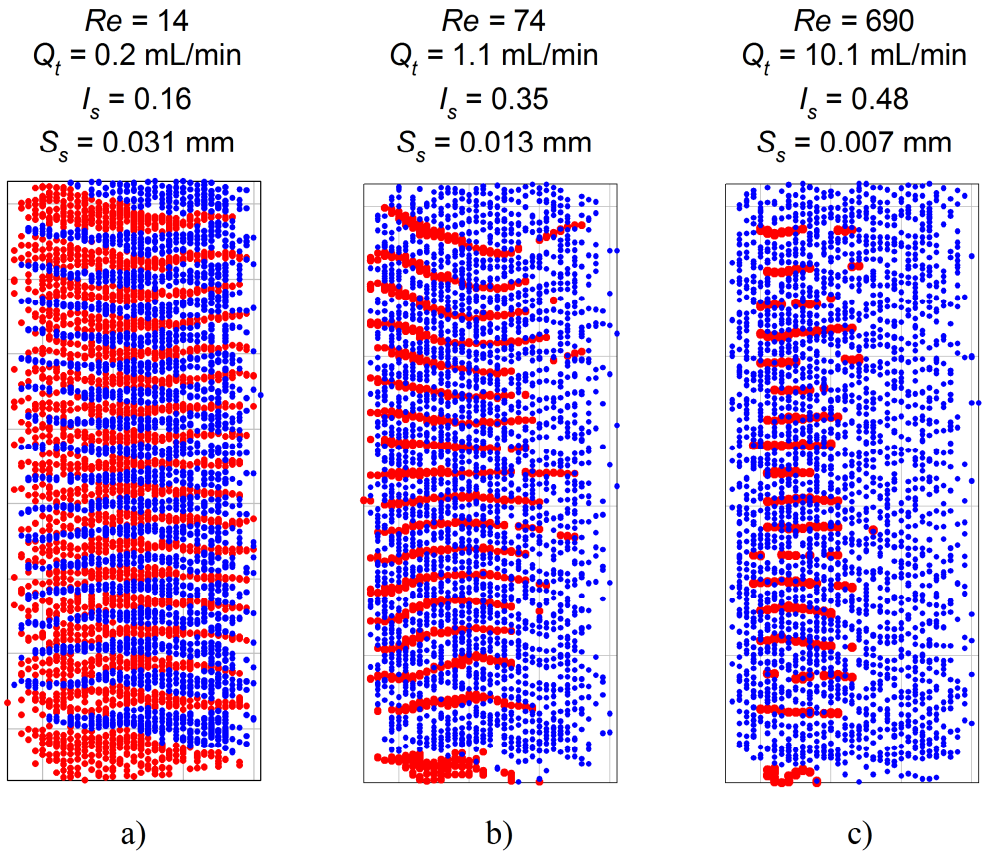

Figure 6.15 Poincaré maps generated by the interdigital structure of the LLMR for different flow ratios: a) r_Q =1, b) r_Q =0.1, and c) r_Q =0.01.

As the flow ratio is decreased, a higher state of segregation is produced and a lower scale of segregation is achieved for the stream injected through Inlet 1, *i.e.* the fluid segments represented by the red particles (the opposite effect is observed for the stream supplied through Inlet 2 represented by the blue particles). Thus, for flow ratios different than one the intercalated arrangement generated by the interdigital structure is distorted and the layer thicknesses are disproportional as compared to the balanced condition when r_Q =1.

The Poincaré maps at the exit of the mixing section of the SAR are shown in Figure 6.16. For r_Q =1 (Figure 6.16a) the average values of S_s and I_s are 0.18 mm and 0.5 respectively. The cases for

$r_Q \neq 1$ (Figure 6.16b) confirm the strong uneven distribution of tracer positions produced by the SAR manifolds. The scale of segregation diminishes for the red tracer particles (*i.e.* increases for the blue particles) as r_Q is increased. It can be seen that the Poincaré maps configuration depends on *Re*. More precisely, at low velocity conditions the particles concentrate in one half section of the circular exit plane. Then, as *Re* increases the particles shift towards the center of the plane until arriving to the opposite half section. It was found that neither the number of tracer particles injected nor the grid size affect this behavior.

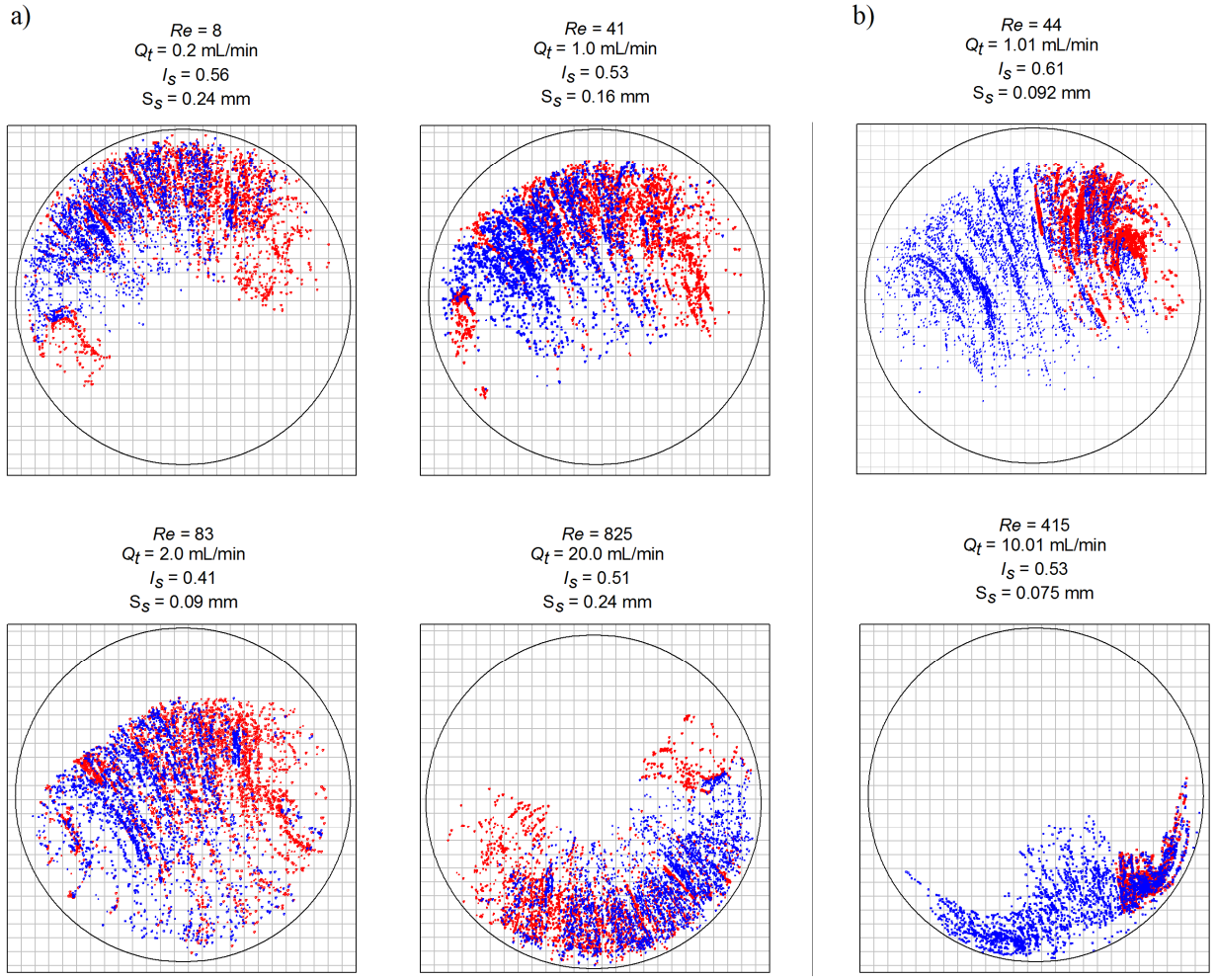

Figure 6.16 Poincaré maps at the exit plane of the SAR mixing section at different *Re*: a) r_Q =1, b) $r_Q \neq 1$.

The control plane of the SAR microreactor is placed in the straight outlet tube as close as possible to the exit of the mixing section following a 90 degree bend thus the location of the tracer

particles might be affected by inertial effects. For the SAR microreactor the corners of the grid outside the circular control plane were not included during the calculations and the analysis of scale and intensity of segregation was conducted only in the zones were tracer particles were detected.

The configuration of the Poincaré maps in Figure 6.16 strongly depends on *Re* and r_Q thus revealing the importance of the operating conditions on the mixing capabilities of the SAR microreactor. In our case we found that the condition at *Re* =83 and r_Q =1 yields the lowest value of scale and intensity of segregation.

6.4.4 Residence Time Distribution

The mean residence times obtained numerically are listed in Table 6.3 along with the theoretical and experimental values previously obtained.

Table 6.3 Mean residence times of the SAR and LLMR microreactors obtained by CFD

	Flow rate (mL/min)	Mean Residence Time t_m (s)				
		Experimental	Theory	CFD	Error (%) CFD-Theory	Error (%) CFD-Experimental
SAR	0.2	79.73 ± 1.18	57.27	57.58	0.6	27.7
	1.0	11.25 ± 0.85	11.45	10.91	4.8	3.1
	2.0	5.84 ± 0.19	5.72	5.51	3.8	5.6
	20.0	0.57 ± 0.01	0.57	0.58	2.8	1.7
LLMR	0.2	38.53 ± 3.45	39.91	36.67	8.1	4.82
	1.0	7.18 ± 0.19	7.98	7.40	7.2	2.9
	2.0	3.79 ± 0.23	3.98	3.75	5.9	1.1
	20.0	0.37 ± 0.02	0.39	0.35	10.1	5.4

The experimental t_m of the SAR at 0.2 mL/min differs considerably from the value obtained by CFD and that expected from theory. This experimental observation is not an anomaly but a confirmed and repeatable result.

This can be explained considering the intrinsic geometry of the SAR microfluidic structure where at sufficiently low fluid velocities the tracer has enough time to spread inside the manifold and

microchannel network by means of molecular diffusion, thus originating this type of delayed tracer responses.

In our previous experimental findings it was found that the classical Axial Dispersion Model (ADM) was capable of describing the microreactor behavior only at Re =6 (0.2 mL/min) and that for Re >35 a compartment flow model using a plug flow in series with the Side Capacity Model provided a better fit. In the experimental scenario the molecular diffusion greatly contributed to the spread of the tracer at Re =6. In this study, the particle tracking method disregards molecular diffusion and thus the ADM was not capable to fit the SAR flow behavior.

The microfluidic structure of the SAR microreactor can be regarded as a series of plug flow reactors with different flow rates connected in parallel. Such flow arrangements are known to produce exponential decay curves rather than Gaussian distributions (**Levenspiel, 1999**). On the other hand, the mixing principle of the LLMR relies on the direct multilamination of flow by the interdigital structure and no recombination of fluid is performed during the mixing stage. Compared to the SAR, the LLMR resembles more closely the characteristics of an open pipe. Figure 6.17 shows the RTD curves of the mixing and reaction sections of both microreactors in dimensionless form.

In the absence of molecular diffusion the pure Convection Model (**Levenspiel, 1999**) accurately describes the RTD of the microreactors under laminar flow regime. The convection model can be defined in dimensionless form as:

$$E_\theta = \begin{cases} 0 & for \quad \theta < 0.5 \\ \dfrac{1}{2\theta^3} & for \quad \theta \geq 0.5 \end{cases} \tag{6.16}$$

Figure 6.17 provides no indication of recirculation or stagnancy when r_Q =1. The reaction section of the LLMR is also well characterized by the pure convection model since the flow configuration comprises a set of parallel microchannels with equal volumetric rates of flow.

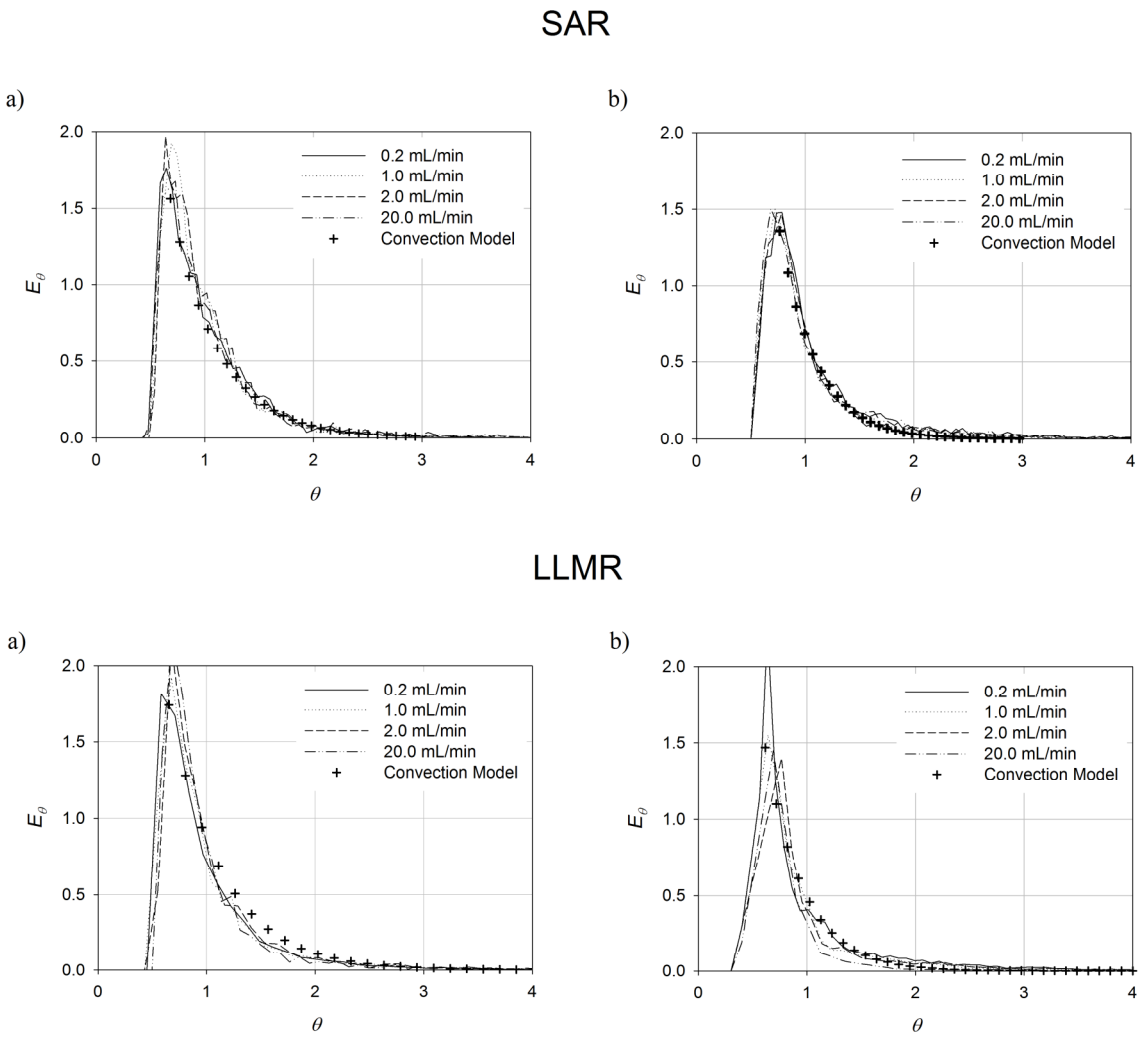

Figure 6.17 RTD functions in dimensionless form obtained numerically for the SAR and LLMR microreactors: a) mixing section, b) reaction section.

6.5 CONCLUSIONS

The pressure drop results of the SAR and LLMR microreactors are in excellent agreement with laminar flow theory and experimental results yielding tube-equivalent diameters of 0.522 mm and 0.311 mm respectively.

It has been shown that with the SAR microreactor principle, the manifolds design produces an unbalanced flow distribution in the microchannel network. This imbalance results in variations of

composition of 12.5% between adjacent microchannels. For the cases when an equal feeding ratio is used only the central microchannel achieves a 50/50 composition.

The visualization of the velocity fields by CFD and the mixing analysis with the particle tracking method confirm the presence of recirculation and by-passing in the SAR microfluidic structure for $r_Q \neq 1$. Thus, the use of feeding ratios other than one further deteriorate any flow imbalance already present due to the geometry of the distribution manifolds. Improved designs are required in order to make SAR microreactors industrially successful. While not directly affecting the mixing mechanism of the microreactor, the symmetrical manifold construction of the LLMR proved to evenly distribute the flow under all the conditions investigated and can be used as a guideline for the design optimization of microreactors requiring distribution of flow in several substreams.

The scale and intensity of segregation concepts originally proposed by Danckwerts allowed for the quantification of mixing efficiency by means of the particle tracking method. It was found that in the absence of molecular diffusion, the intensity and scale of segregation achieved by both microreactors at $r_Q = 1$ are not significantly affected by the amount of energy applied to the system except for the LLMR at $Re = 1363$. In contrast, these same characteristics were considerably affected at $r_Q \neq 1$ proving that unbalanced flow ratios are not the optimal operating conditions for the mixing mechanisms of both microreactors. The RTD obtained by means of CFD were accurately described by the pure convection flow model and the shape of the curves showed that the mixing and reaction sections of both microreactors exhibit the behavior of tubular reactors under laminar flow conditions with no recirculation or stagnancy present for $r_Q = 1$.

6.6 ACKNOWLEDGEMENTS

The authors thank to *Atotech GmbH* (Berlin, Germany) for providing the SAR microreactor. Also, we gratefully acknowledge the financial support from the Natural Science and Engineering Research Council of Canada (NSERC), the National Council of Science and Technology of Mexico (CONACYT) and the oil company TOTAL.

6.7 REFERENCES

Adeosun, J. T., & Lawal, A. (2005). Mass transfer enhancement in microchannel reactors by reorientation of fluid interfaces and stretching. *Sensors and Actuators B: Chemical, 110*(1), 101-111.

Adeosun, J. T., & Lawal, A. (2009). Numerical and experimental studies of mixing characteristics in a T-nuction microchannel using residence-time distribution. *Chemical Engineering Science, 64*, 2422-2432.

Antes, J., Boskovic, D., Krause, H., Loebbecke, S., Lutz, N., Tuercke, T., et al. (2003). Analysis and improvement of strong exothermic nitrations in microreactors. *Chemical Engineering Research and Design, 81*(7), 760-765.

Arnold, D., Brezzi, F., & Fortin, M. (1984). A stable finite element for the stokes equations. *Calcolo, 21*(4), 337-344.

Aubin, J., Fletcher, D. F., Bertrand, J., & Xuereb, C. (2003). Characterization of the Mixing Quality in Micromixers. *Chemical Engineering & Technology, 26*(12), 1262-1270.

Aubin, J., Fletcher, D. F., & Xuereb, C. (2005). Design of micromixers using CFD modelling. *Chemical Engineering Science, 60*(8-9), 2503-2516.

Aubin, J., Prat, L., Xuereb, C., & Gourdon, C. (2009). Effect of microchannel aspect ratio on residence time distributions and the axial dispersion coefficient. *Chemical Engineering and Processing: Process Intensification, 48*(1), 554-559.

Bayer, T., Pysall, D., & Wachsen, O. (2000). Micromixing effect in continuous radical polymerization. *Microreaction Technology: 3rd International Conference on Microreaction Technology, Proceedings of IMRET 3, Springer-Verlag, Berlin*, 165-170.

Boskovic, D., & Loebbecke, S. (2008). Modelling of the residence time distribution in micromixers. *Chemical Engineering Journal, 135*(SUPPL. 1), S138-S146.

Bothe, D., Stemich, C., & Warnecke, H.-J. (2006). Fluid mixing in a T-shaped micro-mixer. *Chemical Engineering Science, 61*(9), 2950-2958.

Cantu-Perez, A., Barrass, S., & Gavriilidis, A. (2010). Residence time distributions in microchannels: Comparison between channels with herringbone structures and a rectangular channel. *Chemical Engineering Journal, 160*(3), 834-844.

Cantu-Perez, A., Bi, S., Barrass, S., Wood, M., & Gavriilidis, A. (2011). Residence time distribution studies in microstructured plate reactors. *Applied Thermal Engineering, 31,* 634-639.

Chen, Y., & Cheng, P. (2002). Heat transfer and pressure drop in fractal tree-like microchannel nets. *International Journal of Heat and Mass Transfer, 45*(13), 2643-2648.

Coesnon, B., Heniche, M., Devals, C., Bertrand, F., & Tanguy, P. A. (2008). A fast and robust fictitious domain method for modelling viscous flows in complex mixers: The example of propellant make-down. *International Journal for Numerical Methods in Fluids, 58*(4), 427-449.

Commenge, J. M., Falk, L., Corriou, J. P., & Matlosz, M. (2002). Optimal Design for Flow Uniformity in Microchannel Reactors. *AIChE Journal, 48*(2), 345-358.

Cortes-Quiroz, C. A., Azarbadegan, A., Zangeneh, M., & Goto, A. (2010). Analysis and multi-criteria design optimization of geometric characteristics of grooved micromixer. *Chemical Engineering Journal, 160*(3), 852-864.

Danckwerts, P. V. (1952). The definition and measurements of some characteristic mixtures. *Applied Scientific Research, A3*, 279.

Engler, M., Kockmann, N., Kiefer, T., & Woias, P. (2004). Numerical and experimental investigations on liquid mixing in static micromixers. *Chemical Engineering Journal, 101*(1-3), 315-322.

Ferstl, W., Loebbecke, S., Antes, J., Krause, H., Haeberl, M., Schmalz, D., et al. (2004). Development of an automated microreaction system with integrated sensorics for process screening and production. *Chemical Engineering Journal, 101*(1-3), 431-438.

Freedman, D., & Diaconis, P. (1981). On the histogram as a density estimator: L_2 Theory. *Probability Theory and Related Fields, 57*(4), 453-476.

Gamrat, G., Favre-Marinet, M., Le Person, S., Baviere, R., & Ayela, F. (2008). An experimental study and modelling of roughness effects on laminar flow in microchannels. *Journal of Fluid Mechanics, 594*, 399-423.

Gobby, D., Angeli, P., & Gavriilidis, A. (2001). Mixing chacteristics of T-type microfluidic mixers. *Journal of Micromechanics and Microengineering, 11*(2), 126-132.

Hardt, S., & Schonfeld, F. (2003). Laminar mixing in different interdigital micromixers: II. Numerical simulations. *AIChE Journal, 49*(3), 578-584.

Heniche, M., & Tanguy, P. A. (2006). A new element-by-element method for trajectory calculations with tetrahedral finite element meshes. *International Journal for Numerical Methods in Engineering, 67*(9), 1290-1317.

Heniche, M., Tanguy, P. A., Reeder, M. F., & Fasano, J. B. (2005). Numerical investigation of blade shape in static mixing. *AIChE Journal, 51*(1), 44-58.

Hessel, V., Hardt, S., & Löwe, H. (2004). *Chemical Micro Process Engineering: Fundamentals, Modelling and Reactions*. Weinheim: Wiley-VCH.

Hobbs, D. M., & Muzzio, F. J. (1997). The Kenics static mixer: a three-dimensional chaotic flow. *Chemical Engineering Journal, 67*(3), 153-166.

Kim, S. J., Kim, D., & Lee, D. Y. (2000). On the local thermal equilibrium in microchannel heat sinks. *International Journal of Heat and Mass Transfer, 43*(10), 1735-1748.

Kockmann, N., Kiefer, T., Engler, M., & Woias, P. (2006). Convective mixing and chemical reactions in microchannels with high flow rates. *Sensors and Actuators, B: Chemical, 117*(2), 495-508.

Lee, S. W., & Lee, S. S. (2008). Rotation effect in split and recombination micromixing. *Sensors and Actuators B: Chemical, 129*(1), 364-371.

Levenspiel, O. (1999). *Chemical Reaction Engineering*. USA: Wiley.

Mengeaud, V., Josserand, J., & Girault, H. H. (2002). Mixing processes in a zigzag microchannel: Finite element simulations and optical study. *Analytical Chemistry, 74*(16), 4279-4286.

Nauman, E. B. (1977). The Residence Time Distribution for Laminar Flow in Helically Coiled Tubes. *Chemical Engineering Science, 32*, 287-293.

Nauman, E. B. (1991). On residence time and trajectory calculations in motionless mixers. *Chemical Engineering Journal, 47*, 141-148.

Nauman, E. B. (2008). Residence Time Theory. *Industrial & Engineering Chemistry Research, 47*, 3752-3766.

Rauline, D., Le Blevec, J. M., Bousquet, J., & Tanguy, P. A. (2000). A comparative assessment of the performance of the Kenics and SMX static mixers. *Chemical Engineering Research and Design, 78*(3), 389-396.

Rauline, D., Tanguy, P. A., Le Blevec, J. M., & Bousquet, J. (1996). Numerical investigation of the performance of several static mixers. *The Canadian Journal of Chemical Engineering, 76*, 527-535.

Rosander, A. C. (1957). *Elementary Principles of Statistics*. Toronto: D. Van Nostrand Co. Inc.

Schönfeld, F., & Hardt, S. (2004). Simulation of Helical Flows in Microchannels. *AIChE Journal, 50*(4), 771-778.

Schwesinger, N., Frank, T., & Wurmus, H. (1996). Modular microfluid system with an integrated micromixer. *Journal of Micromechanics and Microengineering, 6*(1), 99-102.

Serra, C., Sary, N., Schlatter, G., Hadziioannou, G., & Hessel, V. (2005). Numerical simulation of polymerization in interdigital multilamination micromixers. *Lab on a Chip, 5*(9), 966-973.

Shimazaki, H., & Shinomoto, S. (2007). A method for selecting the bin size of a time histogram. *Neural Computation, 19*(6), 1503-1527.

Stroock, A. D., Dertinger, S. K., Whitesides, G. M., & Ajdari, A. (2002a). Patterning flows using grooved surfaces. *Analytical Chemistry, 74*(20), 5306-5312.

Stroock, A. D., Dertinger, S. K. W., Ajdari, A., Mezic, I., Stone, H. A., & Whitesides, G. M. (2002b). Chaotic mixer for microchannels. *Science, 295*(5555), 647-651.

Tonomura, O., Tanaka, S., Noda, M., Kano, M., Hasebe, S., & Hasimoto, I. (2004). CFD-based optimal design of manifold in plate-fin microdevices. *Chemical Engineering Journal, 101*(1-3), 397-402.

Wong, S. H., Ward, M. C. L., & Wharton, C. W. (2004). Micro T-mixer as a rapid mixing micromixer. *Sensors and Actuators B: Chemical, 100*(3), 359-379.

Wörner, M. (2010). Approximate residence time distribution of fully develop laminar flow in a straight rectangular channel. *Chemical Engineering Science, 65*(11), 3499-3507.

Wörz, O., Jäckel, K. P., Richter, T., & Wolf, A. (2001). Microreactors - A New Efficient Tool for Reactor Development. *Chemical Engineering & Technology, 24*(2), 138-142.

Yoshida, J., Nagaki, A., Iwasaki, T., & Suga, S. (2005). Enhancement of Chemical Selectivity by Microreactors. *Chemical Engineering & Technology, 28*(3), 259-266.

Yu, L., Nassar, R., Fang, J., Kuila, D., & Varahramyan, K. (2008). Investigation of a novel microreactor for enhancing mixing and conversion. *Chemical Engineering Communications, 195*(7), 745 - 757.

CHAPTER 7

FREE-RADICAL POLYMERIZATION OF STYRENE USING A SPLIT-AND-RECOMBINATION (SAR) AND MULTILAMINATION MICROREACTOR

Lionel S. Méndez-Portillo, Charles Dubois, Philippe A. Tanguy

Department of Chemical Engineering, École Polytechnique de Montréal
P.O. Box 6079, Station Centre-Ville, Montreal, QC.
Canada H3C 3A7

ABSTRACT

The objective of this investigation was to characterize the heat transfer capabilities of two microreactors, and to demonstrate their potential as chemical reactors for conducting the continuous free-radical polymerization of styrene monomer. The microreactors operate respectively with the split-and-recombination (SAR) and multilamination mixing mechanism; and both units feature an integrated forced-convection heat exchanger. For the highest flow conditions investigated, the SAR and multilamination heat exchangers achieved maximum overall heat transfer coefficients of 3.02 and 2.8 kW/m^2-K respectively reaching efficiencies of ~0.95. Monofunctional, bifunctional, and tetrafunctional peroxide initiators were used for the polymerization runs at two reaction temperatures, *e.g.* 100 and 130 ^{o}C. The monofunctional initiator was able to produce conversions higher than 20% at 100 ^{o}C, the bifunctional initiator achieved the same level of conversion at 130 ^{o}C, and the tetrafunctional initiator produced higher levels of conversion at both temperatures. Low values of polydispersity indexes (*PDI* <1.7) were obtained for all the reaction conditions investigated with the samples obtained in the multilamination microreactor exhibiting an overall lower value than those produced in the SAR configuration.

7.1 INTRODUCTION

Microreaction technology is presently a well established subfield of the chemical microprocess engineering that relies on high surface-to-volume ratios for enhanced heat transfer, and fast mixing by molecular diffusion. Mass and heat transfer intensification have been the main driver for extensive research and characterization of microdevices that presently can be mass produced by state-of-the-art manufacturing techniques. Such manufacturing methods have allowed for the construction and commercialization of tightly assembled metallic microreactors designed for high pressure and temperature conditions. These mechanically robust microdevices along with their

fast mixing and efficient heat transfer (**Brandner *et al.*, 2000; Schubert *et al.*, 2001**) have opened a new envelope of reaction conditions otherwise inaccessible in macroscopic equipment.

Despite the aforementioned advantages of microreaction technology there are still concerns about its potential application for industrial production. These concerns refer to limited yields (**Ehrfeld *et al.*, 2001**) and high energy consumption in processes involving highly viscous and/or non-Newtonian fluids (*e.g.* polymerization reactions). Whereas a low throughput can be anticipated from microreactors due to their characteristic small active volume, improved selectivity and yield (**Bayer *et al.*, 2000; Wörz *et al.*, 2001a; Yoshida *et al.*, 2005**) have been demonstrated for chemical processes conducted in the microscale. This compromise between low throughput and improved reaction performance presents the microreaction technology as an attractive alternative for targeted applications such as on-demand production of polymers or fine chemicals.

Polymerization reactions are usually highly exothermic and are extremely sensitive to the level of mixing of the reactants (**Nauman & Buffham, 1983**). Polymer reaction engineering applications could fully exploit the benefits of microreaction conditions in terms of temperature control and fast mixing. Free-radical polymerization is an important method for the industrial synthesis of polymers as free-radicals are compatible with a wide variety of functional groups which are not compatible with ionic and metal-catalyzed polymerizations (**Yoshida *et al.*, 2005**). Since free-radical polymerization reactions are highly exothermic, the molecular weight and molecular weight distribution largely depend on the heat transfer and temperature control during the reaction. Generally, the heat of reaction in polymerizations increases in proportion to the reactor volume while the heat removal capacity decreases due to the reduction of the surface-to-volume ratio. In the microscale, the heat transfer rate increases due to the large surface-to-volume ratios encountered in microreactors (**Schubert *et al.*, 2001**) and the temperature control becomes more efficient leading to a better control of molecular weight distribution (**Bayer *et al.*, 2000**).

The first investigation to report the advantages of microreaction technology in polymer reaction engineering applications was made by **Bayer *et al.* (2000)**. While the operating conditions and technical data were not disclosed, they reported a reduction of the distribution of molecular weights during the solution polymerization of acrylates such as polymethyl methacrylate

(PMMA) and polyacrylic acid (PAA) thus preventing fouling of the tubular reactor in which the high molecular weight species (~10^5 – 10^6 g/mol) were assumed to cause precipitation inside a static mixer originally used as a premixing stage of the continuous process.

Single channel T-junction microreactors have been used to some extent for such type of reactions (**Nisisako *et al*., 2004; Chang *et al*., 2004a-b)** although only in two occasions in continuous operation **(Iwasaki & Yoshida, 2005; Okubo *et al.*, 2009**). Moreover, the microreactors have been used as premixing stages while the actual polymerization is conducted in coiled tubing reactors. Nevertheless, experimental investigations on the performance of interdigital or split-and-recombination microreactors for conducting free-radical polymerizations have not been reported until now.

Regarding the heat transfer capabilities of microreactors **Wörz *et al.* (2001a)** have discussed the possibility of conducting very fast and exothermic reactions in microreactors in *isothermal operation*. They refer to a temperature increase of 1-2 degrees C as the limit for fulfilling the criterion of isothermal conditions. Indeed the use of microreaction conditions allowed a considerable reduction of undesired temperature gradients from 50 to 1 degree C as compared to a conventional macroscale process (**Wörz *et al.*, 2001a**).

The most significant experimental result on high heat transfer capabilities was made by **Schubert *et al.* (2001)** who reported a heat transfer coefficient of ~25.0 kW/m^2-K for a single-microchannel crossflow heat exchanger with an active volume of 1 cm^3 at a flow rate of 0.7 m^3/hr producing pressure drops of ~6 bars. In the same work a maximal heat transfer coefficient of 54.5 kW/m^2-K was reported for a microcolumn heat exchanger at a flow rate of 0.37 m^3/hr. Microcolumn heat exchangers consist of several stacked metallic foils with parallel microchannels. Although this type of microcolumn heat exchanger exhibited a considerably higher heat transfer coefficient as compared with the 18.2 kW/m^2-K obtained with the microchannel heat exchanger at the same flow rate, the pressure drop reported for the column heat exchanger was approximately 2.5 times higher. Counterflow micro heat exchangers have also exhibited high heat transfer coefficients around 10 kW/m^2-K at flow rates of 3 x 10^{-3} m^3/hr

(**Ehrfeld *et al.*, 1999**). These values are in contrast with the values usually encountered in macroscopic equipment (*e.g.* ~ 1.2 kW/m^2-K) for such counterflow configurations.

Microtubes and micromixers can significantly improve the control of polymerization reactions; the former by allowing a rapid removal of the heat released by the polymerization and the latter by promoting an efficient mixing of the reactants. A microfluidic device combining both advantages would be desirable for the control of a wider range of polymerization reactions. Experimental studies on continuous flow polymerization reactions conducted in microreaction equipment are limited and investigations dealing with polymerizations in commercial microreactors are not available so far. Characterization of polymerization processes conducted in microreactors is required in order to assess the benefits and possible drawbacks of this type of technologies as compared to conventional large-scale polymerization techniques.

In this context our research group has previously conducted the experimental characterization of the performance of two mechanically robust microreactors with potential for industrial applications. One unit was a prototype design using the split-and-recombination (SAR) mixing principle while the other was an already commercialized model using the mixing mechanism of multilamination of flow by means of an interdigital structure.

The objective of the present investigation is to conduct the free-radical polymerization of styrene inside these two previously studied microreactors featuring different mixing mechanisms and equipped with integrated forced-convection heat exchangers. One critical step in the development of this work is the characterization of the heat transfer capabilities of the microdevices.

7.2 DESCRIPTION OF THE MICROREACTORS

Two microreactors were considered in this work. A prototype microreactor featuring a split-and-recombination (SAR) mechanism was provided by *Atotech* (Berlin, Germany). Another microreactor based on the multilamination of flow by means of an interdigital configuration was acquired from *IMM GmbH* (Mainz, Germany) under the model designation *LLMR-MIX-SI*

(**Richter *et al.*, 1998, 2000; Caravieilhes *et al.*, 2001; Ehrfeld *et al.*, 2001; Wörz *et al.*, 2001a-b**).

The SAR microreactor is composed of an arrangement of 8 stacked plates. The flow path of the reactive fluids (Figure 7a) is composed of a mixing section and two reaction plates connected in series. The flow path of the heat transfer fluid (Figure 7b) is composed of two plates connected in parallel and placed beneath each reaction plate. Thus, due to the parallel arrangement of the heat transfer plates and the serial arrangement of the reaction plates, one heat transfer plate will always operate in parallel flow mode while the other will operate in counterflow mode. The plate operating in counterflow mode will depend on the port to which the heat transfer fluid pump is connected. In this work the counterflow denomination is applied to the case when the Reaction Plate 2 is in counterflow mode relative to both cooling plates (*i.e.* the cooling fluid pump is connected to the port located besides the reactive fluids outlet).

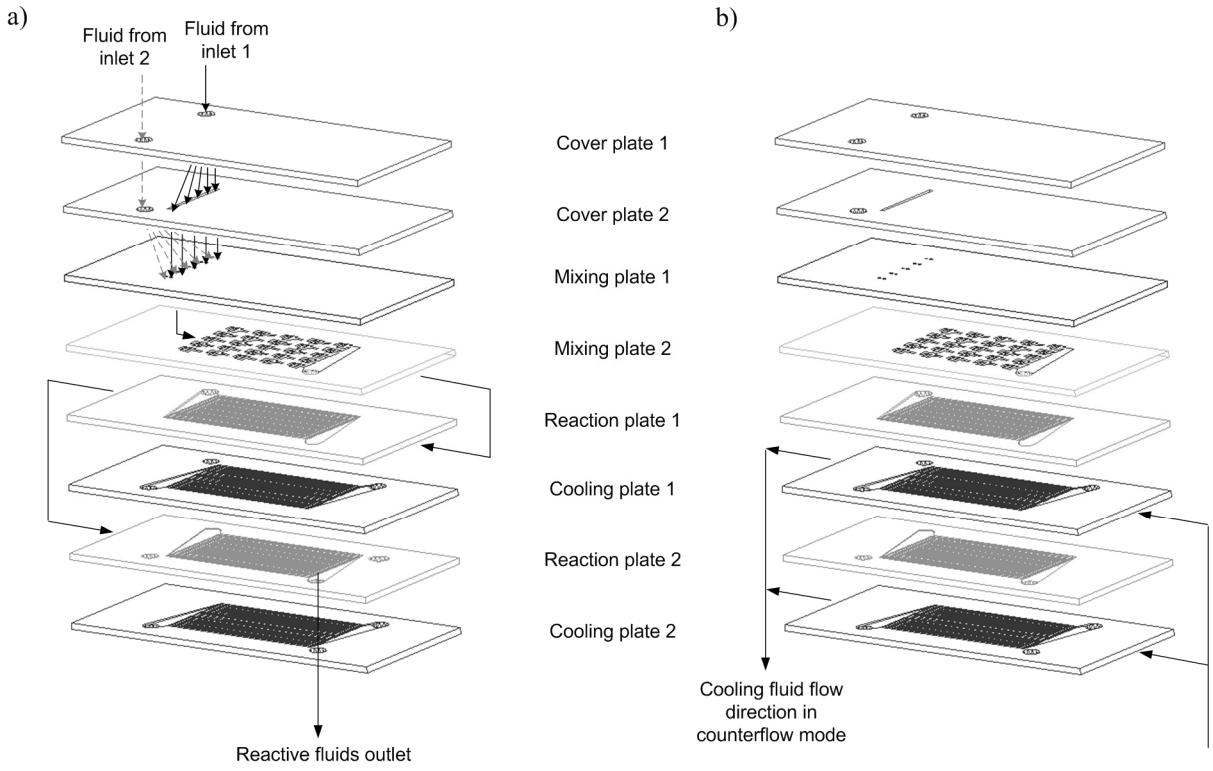

Figure 7.1 Schematic of the SAR microreactor plates depicting the direction of flow: a) reactive fluids, b) heat transfer fluid in counterflow arrangement as applied in this work.

The LLMR possesses two heat transfer passages: one consists of parallel microchannels machined on the other side of the reaction plate that run along the reaction microchannels in an intercalated arrangement; the other consists of parallel microchannels machined in the cover plate of the reaction passages that run along the top surface of each reaction channel. These two passages are independent of each other and can be operated in direct parallel of counterflow configuration.

7.3 METHODS OF CHARACTERIZATION

7.3.1 Overall Heat Transfer Coefficient

Information of the heat transfer performance of the microreactors can be obtained from an overall energy and mass balance made at the boundaries of the system, *i.e.* at the inlet and outlet ports of the reactors. There are two common methods to characterize the thermal capabilities of a heat-exchanger configuration: the *logarithmic mean temperature difference* (LMTD) method, and the *effectiveness-Number of Transfer Units* (*ε-NTU*) method. The LMTD method is useful when the inlet and outlet temperatures are known beforehand and the heat flow, size (*i.e.* surface area), or overall heat transfer coefficient (U_o) of the heat exchanger need to be determined. Due to the logarithmic function involved in the LMTD, calculating the inlet and outlet temperatures for a given heat exchanger using the LMTD method requires an iterative procedure that is avoided by applying the *ε-NTU* method. The *ε-NTU* method is based on the effectiveness of the heat-exchanger for transferring a given amount of heat, and is also useful for the comparison between various types of heat-exchangers. In this work, the LMTD method is used to estimate the overall heat transfer coefficient of the microreactors and the *ε-NTU* method is then applied for the purpose of comparison.

The overall heat transfer coefficient U_o can be obtained from an analogous expression to the Newton's law of cooling defined as:

$$Q = U_o \cdot A_T \cdot \Delta T \tag{7.1}$$

where Q is the overall heat transfer rate, A_T is the available surface for heat transfer, and ΔT is the temperature difference between the hot and cold fluids. In the LMTD method this temperature difference is defined as:

$$\Delta T_{\ln} = \frac{\Delta T_2 - \Delta T_1}{\ln\left(\frac{\Delta T_2}{\Delta T_1}\right)} \tag{7.2}$$

where the temperature differences ΔT_1 and ΔT_2 are the differences between the temperatures of the hot (T_h) and cold (T_c) streams at the inlet (T_i) and outlet (T_o) f the heat exchanger. These temperatures differences are defined according to the flow configuration of the heat exchanger. For the parallel flow exchanger they are defined as:

$$\begin{bmatrix} \Delta T_1 = T_{h,i} - T_{c,i} \\ \Delta T_2 = T_{h,o} - T_{c,o} \end{bmatrix} \tag{7.3}$$

And for the counterflow configuration they are defined as:

$$\begin{bmatrix} \Delta T_1 = T_{h,i} - T_{c,o} \\ \Delta T_2 = T_{h,o} - T_{c,i} \end{bmatrix} \tag{7.4}$$

In the ε-NTU method the effectiveness ε is defined as the ratio of the actual heat transfer rate to the maximum possible heat transfer rate. The actual heat transfer can be computed by either calculating the heat lost by the hot fluid or the heat gained by the cold fluid. The maximum possible heat transfer is obtained if the fluid having the lowest combined thermal heat capacity were to undergo a temperature change equal to the maximum temperature difference present in the heat-exchanger. The energy balance requires this fluid to be the one with the minimum value of heat capacity C_{min}. Therefore, the term C_{min} corresponds to the fluid having the minimum value of the capacity rate $m \cdot C_p$, where m is the mass flow rate, and C_p is the specific heat of the fluid. Thus, the effectiveness of a heat exchanger is defined as:

$$\varepsilon = \frac{C_h (T_{h.i} - T_{h.o})}{C_{min} (T_{h.i} - T_{c.i})} = \frac{C_c (T_{c.i} - T_{c.o})}{C_{min} (T_{h.i} - T_{c.i})} \tag{7.5}$$

The heat exchanger effectiveness is related to the physical characteristics of the equipment and to the flow conditions and properties of the fluid by means of the parameters *NTU* and C_{min}. The number of transfer units (NTU) is a dimensionless parameter that is widely used for heat exchanger analysis and is defined as:

$$NTU = \frac{U \cdot A}{C_{min}} \tag{7.6}$$

Mathematical expressions relating ε as a function of *NTU* and C_{min} have been developed for different heat exchangers flow configurations, *e.g.* parallel flow, counterflow, shell and tube, cross flow (**Incropera & DeWitt, 1985; Holman, 1997; Mills, 1999**).

7.4 EXPERIMENTAL

7.4.1 Set-up

The experimental set-up is depicted in Figure 7.2. Two high permeation liquid chromatography (HPLC) pumps with maximum pumping capacity of 10 mL/min and 0.1 mL/min increments were used to supply the fluids to the microreactors. A calibrated differential pressure transducer (Omega PX81-100DV) was connected to Inlet 1 and the outlet of the microreactors. A gauge pressure transducer (Omega PX61C1-1k-GV) was connected to the Inlet 2 of the microreactors. The uncertainty of the measurement for this type of transducers is 0.25% f.s. (~0.0172 bars). Thermocouples (Omega KMQSS-062G-6) were used to register the temperatures at the inlets and outlets of the microreactor and their corresponding cooling systems. All connections were made using *Swagelok*® stainless steel tubing (i.d. 1.75 mm) and fittings.

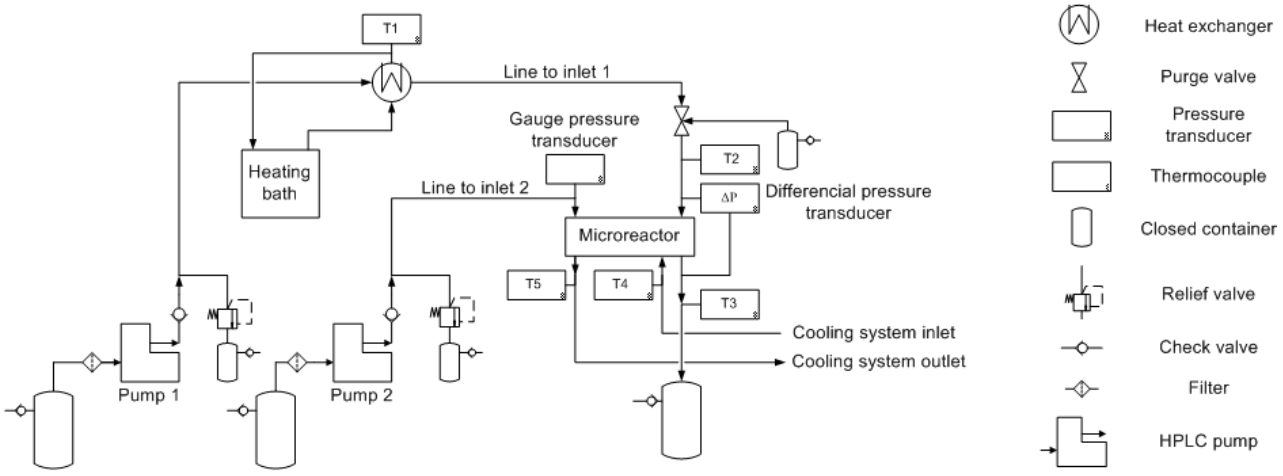

Figure 7.2 Schematic of the experimental set-up used for the heat transfer and polymerization experiments.

7.4.2 Heat Transfer Characterization

For the heat transfer experiments water was used as the hot and cold fluid. The water was preheated in-line up to 95 degrees C before entering the microreactors. Cold water was supplied at 23 degrees C. The values of the density and specific heat of water at these temperatures and at the resulting outlet temperatures in the heat-exchangers were taken from **Holman (1997)**. In order to determine the influence of the particular flow arrangement of the SAR heat exchanger this microreactor was characterized by connecting the Cooling Plate 2 in parallel and counterflow mode in relation to the Reaction Plate 2. The LLMR heat exchanger system is equipped with parallel straight microchannels, thus it was characterized in counterflow mode only since this arrangement operates more efficiently. Two flow rates were investigated for the hot fluid (*e.g.* 4.0 mL/min and 8.0 mL/min) resulting in two values of heat capacity of the hot stream (C_h) for which at least four different flow rates were investigated in the cold side. The cold stream was supplied by a third HPLC pump with a maximum feeding capacity of 10.0 mL/min and the flow rates used resulted in ratios of heat capacities $C_r = C_{cold}/C_{hot}$ equal to 0.25, 0.5, 1 and 1.25. In order to verify the maximum heat transfer coefficient attainable at each C_h condition, the cooling system was also connected to the tap water supply for a flow rate approximately of 430 mL/min which

allowed to reach values of C_r >>1. For the case of the LLMR each cooling plate was analyzed separately. The experimental runs consisted of at least five replicates per flow condition.

7.4.3 Styrene Polymerization

Regular grade styrene (Aldrich Chemical) was washed three times with a two-fold excess of sodium hydroxide solution (1N), rinsed with distilled water, and dried with calcium sulphate (white Drierite) in order to remove the inhibitor (**Boundy & Boyer, 1952**). Three types of chemical initiators were used as received from Arkema Inc.: the monofunctional initiator benzoyl peroxide (Luperox A75); the bifunctional initiator 1,1-bis(tert-butylperoxy)-cyclohexane (Luperox 331M80); and the tetrafunctional initiator polyether poly-tert-butylperoxy carbonate 50% (Luperox JWEB50). Methyl ethyl ketone (MEK) and methanol were used as solvent and non-solvent for polystyrene, respectively, without any further purification.

The continuous free-radical bulk polymerization of styrene monomer was conducted at 100 and 130 degrees C for three different mean residence times in both microreactors achieved by using total flow rates of 0.2, 1.0 and 2.0 mL/min. These conditions were selected following our previous findings of the optimal hydrodynamic and mixing conditions for these microreactors. The inhibited styrene monomer was fed through Pump 1 at 0.1, 0.5 and 1.0 mL/min, and heated in-line to the desired polymerization temperature by a counterflow heat exchanger connected to a heating bath operated with silicon oil. The chemical initiators were dissolved in styrene monomer for a partial concentration of 0.2M and feed through Pump 2 at equal flow rates as Pump 1 and 23 degrees C. Our previous findings indicate that unbalanced flow ratios produce by-passing and recirculation in the SAR microreactor, hence only flow ratios equal to one were investigated.

Conversion was estimated gravimetrically by dissolving the sample in MEK, precipitating the polymer product with methanol, filtered with sintered glass crucibles, and dried to constant weight under vacuum following the ASTM 703-44T procedure for determination of methanol-soluble content of polystyrene (**Boundy & Boyer, 1952**). The molecular weight distribution was determined by gel permeation chromatography in a *Breeze HPLC System* (Waters Co.) using two separation columns models *HR 4.0* and *HR MB-M* (Waters Co.) in series filled with

tetrahydrofuran and heated to 30 degrees C. The system was calibrated with narrow polystyrene standards from Sigma-Aldrich Co.

7.5 RESULTS AND DISCUSSION

The heat transfer coefficients of the SAR microreactor are shown in Figure 7.3 for the case of parallel and counterflow mode. The SAR heat exchanger configuration is capable to achieve higher overall heat transfer coefficients when the Reaction Plate 2 is operated in counterflow mode. The case of C_h =0.14 W/K was also investigated in order to corroborate the U_o trend at lower values of heat capacity. A maximum value of 3.04 kW/m^2-K was reached in the SAR microreactor using a cold flow rate of 400 mL/min in counterflow mode.

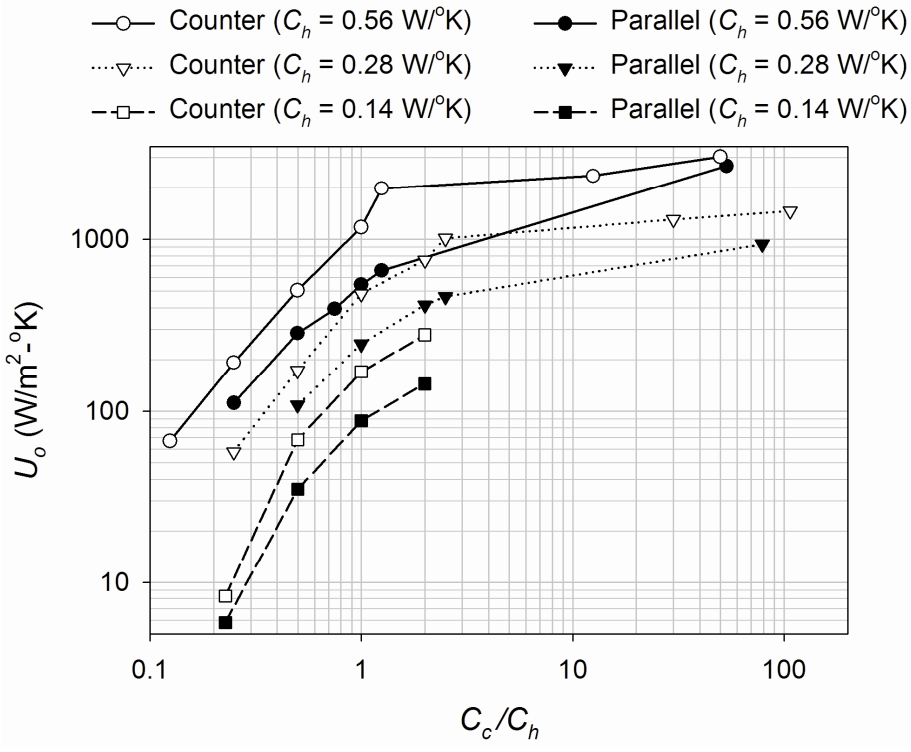

Figure 7.3 Overall heat transfer coefficient as a function of heat capacity for the SAR microreactor.

The efficiency of the SAR heat exchanger are shown in Figure 7.4 as a function of the heat capacity ratio C_r. The counterflow mode of the SAR heat exchanger showed to be more efficient for all the flow conditions investigated and capable to achieve η values higher than 0.95 at heat capacity ratios lower than 30. Hence, the SAR heat transfer configuration operates more efficiently when the Reaction Plate 1 works in parallel flow mode and the Reaction Plate 2 operates in counterflow.

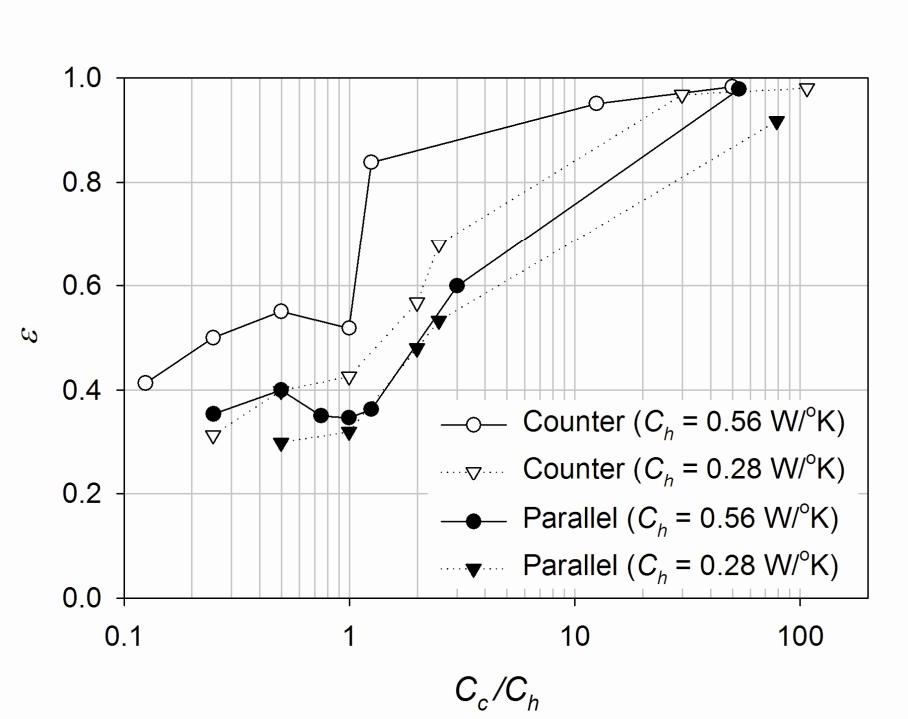

Figure 7.4 Heat transfer efficiency ε as a function of heat capacity for the SAR microreactor.

This is due to the Reaction Plate 1 having only one adjacent surface exposed to the Cooling Plate 1 whereas both sides of Reaction Plate 2 are in direct contact with one cooling plate. The total heat transfer surface estimated for the SAR microreactor is 7.5 x 10^{-4} m^2 yielding a surface-to-volume ratio of 7010 m^{-1}. For C_r <1 the efficiency has a non-monotonic behavior for the higher heat capacity investigated (*i.e.* 0.56 W/K) irrespective of the flow configuration. This behavior can be caused by the loss of heat from the heat exchanger to the surroundings at the outer casing and at the end sections of the heat exchanger (**Hausen, 1983**). Since the microreactors were isolated by casings of ceramic material, thus the heat loss at the end ports of the heat exchanger is likely to be the main cause of this effect. Higher fluid velocities in the hot stream of the heat

exchanger results in increased thermal emission to the surroundings and a decreased heat absorption of the colder fluid. This will affect the temperature differences of the fluids, and the behavior of the exit temperatures is known to vary exponentially as a function of the inlet temperatures when $C_r \neq 1$ (**Hausen, 1983**).

The heat transfer coefficients for the top and bottom cooling plates of the LLMR are shown in Figure 7.5. The maximum overall heat transfer coefficient estimated for the LLMR was 2.8 kW/m^2-K at m_c =420 mL/min. For C_r <1 the difference between both passages are less than 10.5%.

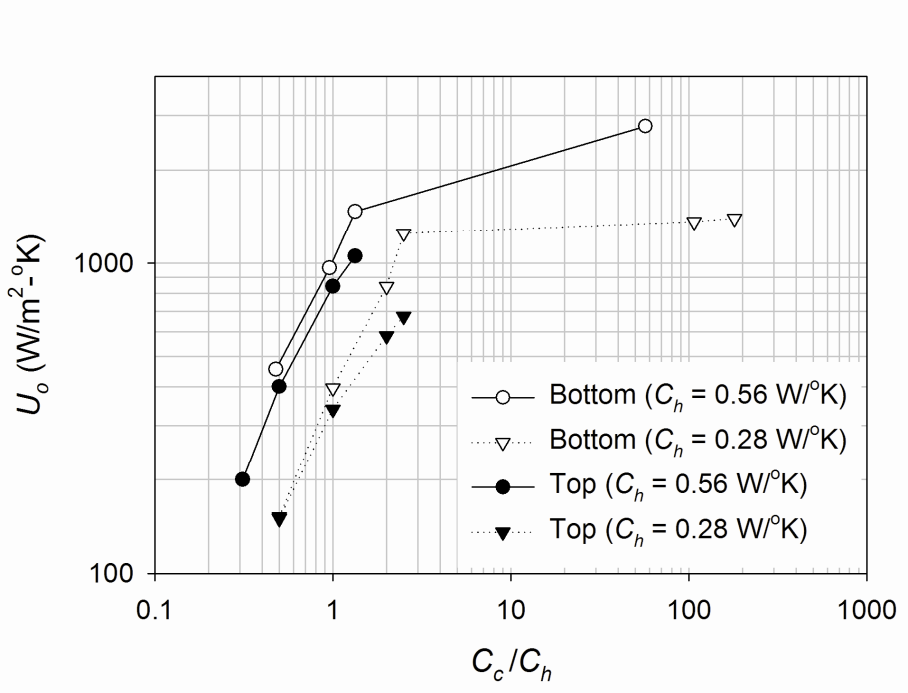

Figure 7.5 Overall heat transfer coefficient as a function of heat capacity for both cooling passages of the LLMR microreactor operating in counterflow mode.

Figure 7.6 shows the effectiveness of the LLMR microreactor heat transfer plates. Both plates reach efficiencies above 0.7 at C_r =2. In this case the lower plate operates at 97% of efficiency. Also, the same non-monotonic behavior of the SAR for C_r <1 at C_h =0.58 W/K is observed for the LLMR as well, which confirms that this effect is independent of the fluidic structure or flow mechanism. The surface-to-volume ratios estimated for the top and bottom plates are 1 110 m^{-1} and 26 670 m^{-1} respectively.

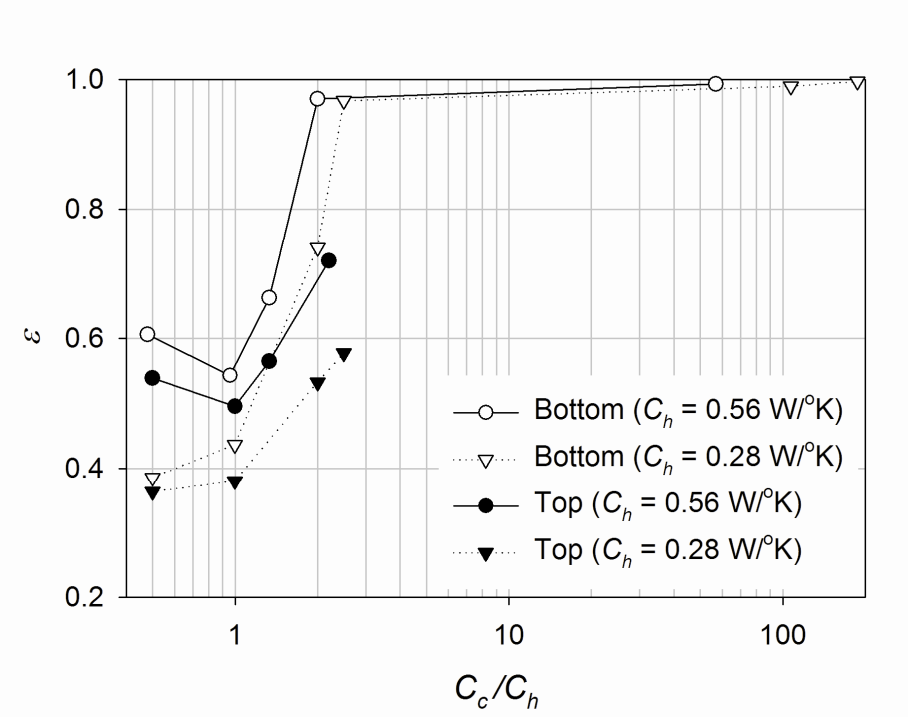

Figure 7.6 Heat transfer efficiency ε as a function of heat capacity for both cooling passages of the LLMR microreactor operating in counterflow mode.

At the balanced condition of C_r =1, the top and bottom plates of the LLMR operate at efficiencies of 0.50 and 0.55 respectively while the SAR reaches a value of 0.51 for the counterflow mode and 0.34 for parallel flow. For the purpose of comparison with values reported in the literature, it is worth to mention that the overall heat transfer coefficients of 54.5 kW/m^2-K for microcolumns and 18.2 kW/m^2-K for microchannels reported by **Schubert *et al.* (2001)** were obtained using water mass flow rates in the range of 370 kg/hr which corresponds to 6 167 mL/min, *i.e.* 1000 times higher than the flow rate range investigated in this study.

7.5.1 Continuous Styrene Polymerization

The effect of the type of initiator and polymerization temperature on the polymerization rate was studied first. Figure 7.7 shows the level of conversion (X) of polystyrene as a function of the mean residence time using the monofunctional initiator L-A75. Conversions higher than 20% were achieved at 130 degrees C. For the purpose of comparison the kinetic model for bulk

styrene polymerization through bifunctional initiators proposed by **Villalobos *et al.* (1991)** was used. In order to simulate the behavior of monofunctional initiators using this model, a high value of the secondary decomposition rate constant was used. The model predicts a linear functionality of the polymerization rate for low ranges of conversions. The results obtained are in agreement with the model predictions. However, the lower values at higher mean residence times can be attributed to the fact that monofunctional peroxide initiators have the most effective decomposition rate at lower temperatures (*e.g.* ~90 degrees C). Polymerization temperatures above this value are not recommended for monofunctional initiators since at such high levels of initial polymerization rate the system runs out of initiator and conversions <85% can be expected. However, these conditions can result beneficial for cases where only a prepolymerization stage (*e.g.* X ~0.3) is intended.

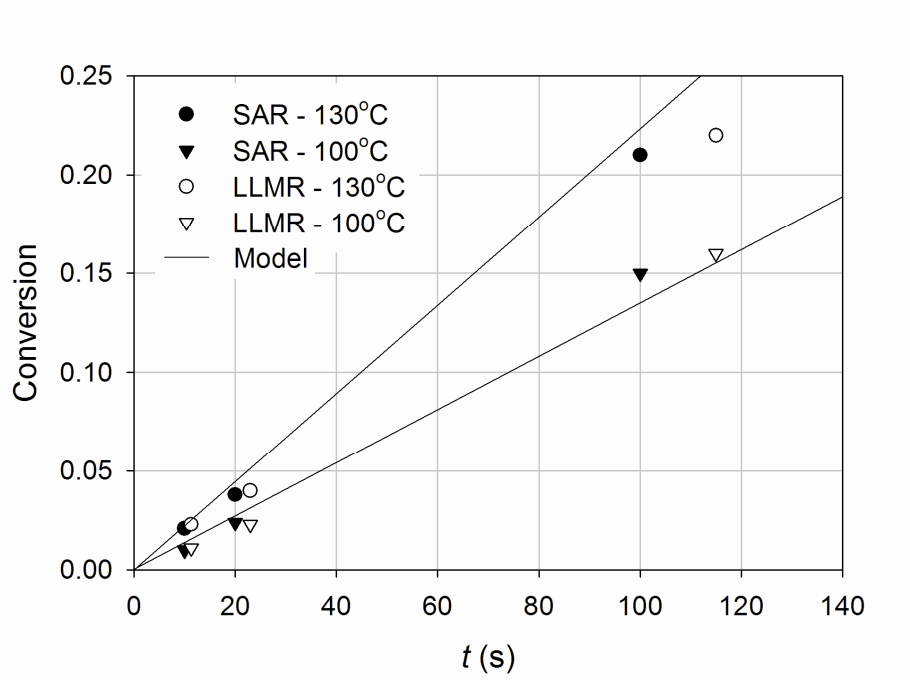

Figure 7.7 Effect of polymerization temperature on monomer conversion in both microreactors using the monofunctional initiator Luperox A75.

The effect of temperature on monomer conversion for the polymerization with the bifunctional initiator is shown in Figure 7.8. The use of the bifunctional initiator at 130 degrees C allowed conversions above 25% for both microreactors, while at 100 degrees C conversions lower than 5% were obtained. This is due to the fact that the bifunctional initiator L-331M80 is known to be

more efficient at temperatures above 100 degrees C (**Choi & Lei, 1987; Villalobos *et al.*, 1991**). The results also agree with the model prediction for bifunctional initiators.

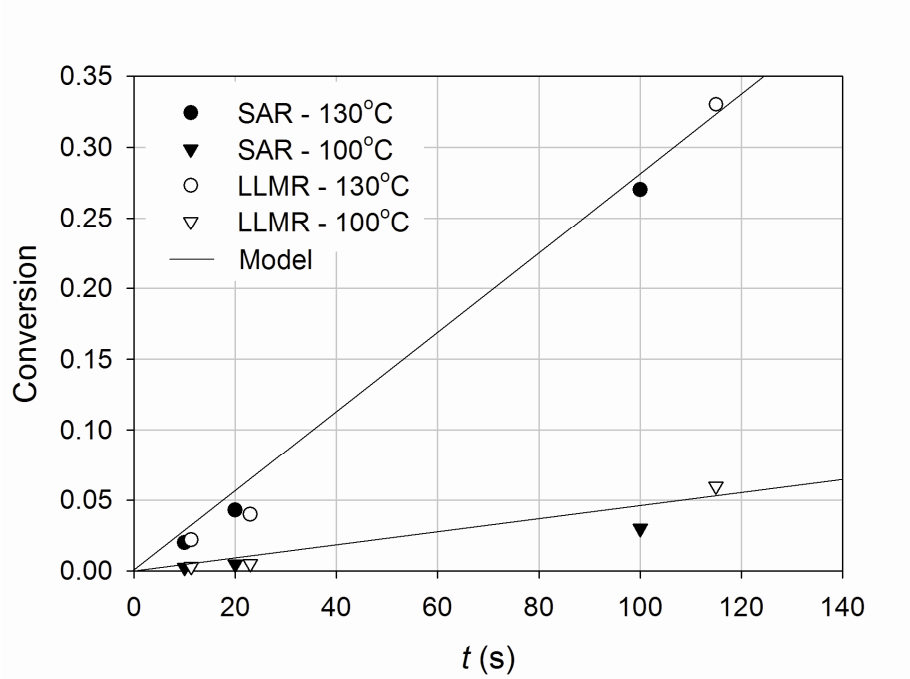

Figure 7.8 Effect of polymerization temperature on monomer conversion in both microreactors using the bifunctional initiator Luperox 331M80.

The tetrafunctional initiator L-JWEB50 allowed to reach conversions of approximately 20% and 35% at 100 and 130 degrees C respectively (Figure 7.9). The **Villalobos *et al.* (1991)** model was not used to predict the behavior of the tetrafunctional initiator since it does not take into account the decomposition mechanism of a tetrafunctional initiator. Due to its initial reaction rate, this tetrafunctional initiator can be used for processes requiring a prepolymerization stage of approximately 30% of conversion which can be achieved at mean residence times of ~120 s. One possible drawback of this type of tetrafunctional initiator is that the initiation sites of the radical groups could produce a branched polymer product (**Fityani-Trimm *et al.*, 2003**). Indeed, a degree of branching has been reported for polystyrene samples produced by tetrafunctional initiators in contrast to linear polystyrenes obtained by monofunctional initiation (**Scorah *et al.*, 2005; Scorah *et al.*, 2007**). The analysis performed in these studies were conducted using samples in which conversion was brought to completion (*i.e.* X >0.99). However, **Fityani-Trimm *et al.* (2003)** reported results of molecular weights as a function of elution volumes for polystyrene samples at different levels of conversion produced by the tetrafunctional initiator L-

JWEB50. Such results exhibited greater scatter at the higher end of the elution volume range. Such scatters were attributed to non-size exclusion effects such as absorption of highly branched polymer onto the separation column (**Wintermantel *et al.*, 1993**).

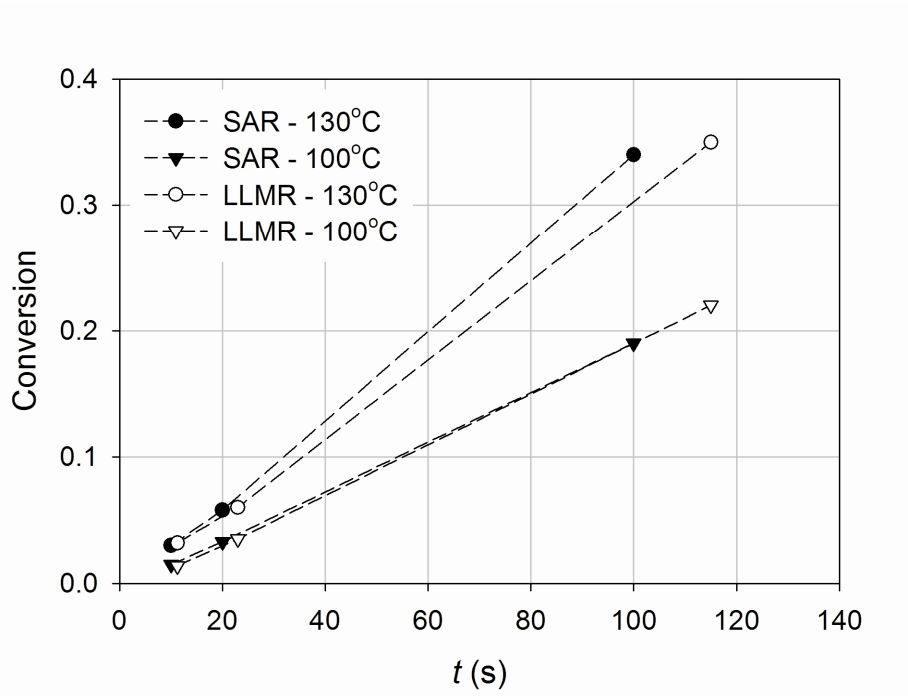

Figure 7.9 Effect of polymerization temperature on monomer conversion in both microreactors using the tetrafunctional initiator Luperox JWEB50.

The polymer weight average molecular weights M_w obtained using the mono-, bi- and tetrafunctional initiators are listed in Table 7.1 along with their respective polydispersity index. In general, the high temperature condition produces molecular weights around 40 000 g/mol except with the tetrafunctional initiator where M_w ~100 000 g/mol are obtained. The polymerization condition at 100 degrees C while obtaining higher order molecular weights also produces lower levels of conversion. Except for the monofunctional initiator at 130 degrees C, the values of *PDI* obtained are close to the limiting value of 1.5 which would be obtained for a free-radical polymerization with termination by combination in an ideal batch or plug flow reactor. These values are expected at the lowest conversions and an increase to *PDI* >1.6 is observed for the highest conversions achieved, *i.e.* X ~0.35.

Table 7.1 Molecular weights and polydispersity indexes of polystyrene samples produced in the SAR and LLMR microreactors using three types of chemical initiators

Initiator	Temperature (°C)	SAR			LLMR		
		X	M_w x 10^{-3} (g/mol)	PDI	*X*	M_w x 10^{-3} (g/mol)	PDI
Monofunctional L-A75	130	0.02	25	1.52	0.023	23	1.51
		0.038	26	1.51	0.04	25	1.55
		0.21	39	1.54	0.24	45	1.56
	100	0.01	49	1.53	0.01	45	1.51
		0.024	50	1.54	0.023	48	1.51
		0.15	55	1.54	0.16	52	1.53
Bifunctional L-331M80	130	0.02	35	1.57	0.022	36	1.55
		0.043	38	1.59	0.04	37	1.55
		0.27	48	1.64	0.33	52	1.62
	100	0.0025	70	1.56	0.0031	73	1.54
		0.0048	72	1.56	0.0052	75	1.55
		0.03	73	1.58	0.06	85	1.56
Tetrafunctional L-JWEB50	130	0.03	38	1.55	0.032	72	1.52
		0.058	43	1.57	0.06	80	1.53
		0.34	100	1.65	0.35	140	1.62
	100	0.015	37	1.57	0.014	74	1.54
		0.033	44	1.56	0.035	82	1.55
		0.19	102	1.54	0.22	145	1.52

It must be mentioned that the estimation of molecular weights by GPC analysis was made using linear polystyrene standards during the calibration procedure. Thus, caution must be taken when interpreting the molecular weight results especially of the polymer samples obtained by the tetrafunctional initiator which will surely produce a branched polymer.

7.6 CONCLUSIONS

The heat transfer capabilities of two commercial microreactors were investigated along with their reaction performance as a function of conversion, molecular weight and type of initiator during the continuous free-radical bulk polymerization of styrene. Overall heat transfer coefficients of 3.04 and 2.8 kW/m^2-K were obtained for the SAR and LLMR respectively at flow rates of ~420 mL/min. The SAR heat exchanger proved to be more efficient when its second reaction plate operates in counterflow mode. The difference between the surface-to-volume ratio of the bottom

and top heat transfer plates of the LLMR is about 24 times. However, both plates exhibited similar performance implying that its heat transfer capabilities easily exceed the thermal requirements imposed by the flow conditions investigated (e.g. ΔT ~70 degrees C). Hence, this microreactor is suitable for more challenging heat transfer tasks.

It was demonstrated that the microreactors used in this investigation are capable to achieve at least 30% of conversion in continuous flow with the appropriate combination of reaction temperature, flow rate, initiator type and concentration. Although low weight average molecular weights are obtained, low polydispersity indexes are also achieved. This effect can be fully exploited for the production of materials where these characteristics are of great importance such as paints, coatings and films. Also, polymerization in microreactors can be applied as the initiation protocols of processes requiring a prepolymerization stage. For the levels of conversion achieved, both microreactors produced polydispersity indexes close to the theoretical limiting value of 1.5. Overall, the LLMR microreactor produced lower *PDI* values as compared to the SAR mechanism. This agrees with our previous findings that at equal flow conditions, the LLMR exhibits a slightly better mixing performance.

7.7 ACKNOWLEDGEMENTS

The authors thank to *Atotech GmbH* (Berlin, Germany) for providing the SAR microreactor; and *Aldrich Chemicals* for providing samples of the chemical initiators. Also, we gratefully acknowledge the financial support from the Natural Science and Engineering Research Council of Canada (NSERC), the National Council of Science and Technology of Mexico (CONACYT) and the oil company TOTAL.

7.8 NOTATION

A_T	Heat transfer area, m^2
C_c	Cold fluid heat capacity, W/K
C_h	Hot fluid heat capacity, W/K
C_p	Specific heat, J/kg-K
C_r	Heat capacity ratio, dimensionless
ε	Heat transfer efficiency, dimensionless
m	Mass flow rate, kg/s
M_w	Weight average molecular weight, g/mol
T_c	Temperature of the cold fluid, K
T_h	Temperature of the hot fluid, K
T_i	Temperature at the inlet, K
T_o	Temperature at the outlet, K
ΔT_{ln}	Logarithmic mean temperature difference, dimensionless
U_o	Overall heat transfer coefficient, W/m^2-K
X	Conversion, dimensionless

7.9 REFERENCES

Bayer, T., Pysall, D., & Wachsen, O. (2000). *Micromixing effect in continuous radical polymerization.* Paper presented at the Microreaction Technology: 3rd International Conference on Microreaction Technology, Proceedings of IMRET 3.

Boundy, R. H., & Boyer, R. F. (1952). *Styrene: Its Polymers, Copolymers and Derivatives*. New York: Reinhold Publishing Corporation.

Brandner, J., Fichtner, M., & Schubert, K. (2000). *Electrically heated microstructure heat exchangers and reactors.* Paper presented at the Microreaction Technology: 3rd International Conference on Microreaction Technology, Proceeding of IMRET 3, Berlin.

Caravieilhes, S., de Bellefon, C., & Tanchoux, N. (2001). Dynamic methods and new reactors for liquid phase molecular catalysis. *Catalysis Today, 66*(2-4), 145-155.

Chang, Z., Liu, G., Fang, F., Tian, Y., & Zhang, Z. (2004b). Gamma-ray-initiated dispersion polymerization of PMA in microreactor. *Chemical Engineering Journal, 101*, 195-199.

Chang, Z., Liu, G., Tian, Y., & Zhang, Z. (2004a). Preparation of micron-size monodisperse poly(vinyl acetate) microspheres with gamma-rays-initiated dispersion polymerization in microreactor. *Materials Letters, 58*, 522-524.

Choi, K. Y., & Lei, G. D. (1987). Modeling of Free-Radical Polymerization of Styrene by Bifunctional Initiators. *AIChE Journal, 33*(12), 2067-2076.

Ehrfeld, W., Hessel, V., Löwe, H. (2001). *Microreactors: New Technology for Modern Chemistry* (1st ed.). Weinheim: Wiley-VCH.

Ehrfeld, W., Hessel, V., & Haverkamp, V. (1999). *Microreactors, Ullmann's Encyclopedia of Industrial Reactors*. Weinheim: Wiley-VCH.

Fityani-Trimm, S., Dhib, R., & Penlidis, A. (2003). Free Radical Polymerization of Styrene with a New Tetrafunctional Peroxide Initiator. *Macromolecular Chemistry and Physics, 204*(3), 436-442.

Hardt, S., & Schonfeld, F. (2003). Laminar mixing in different interdigital micromixers: II. Numerical simulations. *AIChE Journal, 49*(3), 578-584.

Hausen, H. (1983). *Heat transfer in counterflow, parallel flow and cross flow.* (2nd. ed.). New York: McGraw-Hill.

Holman, J. P. (1997). *Heat Transfer* (8th ed.): McGraw-Hill.

Incropera, F., & DeWitt, D. (1985). *Introduction to Heat Transfer*. New York: John Wiley & Sons, Inc.

Iwasaki, T., & Yoshida, J.-i. (2005). Free Radical Polymerization in Microreactors. Significant Improvement in Molecular Weight Distribution Control. *Macromolecules, 38*(4), 1159-1163.

Mills, A. F. (1999). *Heat Transfer* (2nd. ed.). New Jersey: Pretince-Hall, Inc.

Nagasawa, H., Aoki, N., & Mae, K. (2005). Design of a New Micromixer for Instant Mixing Based on the Collision of Micro Segments. *Chemical Engineering & Technology, 28*(3), 324-330.

Nisisako, T., Torii, T., & Higuchi, T. (2004). Novel microreactors for functional polymer beads. *Chemical Engineering Journal, 101*, 23-29.

Okubo, Y., Maki, T., Nakanishi, F., Hayashi, T., & Mae, K. (2009). Precise control of polymer particle properties using droplets in the microchannel. *Chemical Engineering Science, doi: 10.1016/j.ces.2009.06.004*.

Richter, T., Ehrfeld, W., Gebauer, K., Golbig, K., Hessel, V., Lowe, H., et al. (1998). *Metallic microreactors: components and integrated systems.* Paper presented at the Process miniaturization: 2nd International Conference on Microreaction Technology, IMRET 2, New Orleans, USA.

Richter, T., Ehrfeld, W., Hessel, V., Lowe, H., Storz, M., & Wolf, A. (2000). *A flexible multi component microreaction system for liquid phase reactions.* Paper presented at the 3rd International Conference on Microreaction Technology, Proceeding of IMRET 3, Berlin.

Schönfeld, F., & Hardt, S. (2004). Simulation of Helical Flows in Microchannels. *AIChE Journal, 50*(4), 771-778.

Schubert, K., Brandner, J., Fichtner, M., Linder, G., Schygulla, U., & Wenka, A. (2001). Microstructure devices for applications in thermal and chemical process engineering. *Microscale Thermophysical Engineering, 5*, 17-39.

Scorah, M. J., Dhib, R., & Penlidis, A. (2005). Use of a Novel Tetrafunctional Initiator in the Free Radical Homo- and Copolymerization of Styrene, Methyl Methacylate and alfa-Methyl Styrene. *Journal of Macromolecular Science, Part A: Pure and Applied Chemistry, 42*(4), 403 - 426.

Scorah, M. J., Tzoganakis, C., Dhib, R., & Penlidis, A. (2007). Characterization by dilute solution and rheological methods of polystyrene and poly(methyl methacrylate) produced with a tetrafunctional peroxide initiator. *Journal of Applied Polymer Science, 103*(2), 1340-1355.

Stroock, A. D., Dertinger, S. K. W., Ajdari, A., Mezic, I., Stone, H. A., & Whitesides, G. M. (2002). Chaotic mixer for microchannels. *Science, 295*(5555), 647-651.

Villalobos, M. A., Hamielec, A. E., & Wood, P. E. (1991). Kinetic Model for Short-Cycle Bulk Styrene Polymerization through Bifunctional Initiators. *Journal of Applied Polymer Science, 42*, 629-641.

Wintermantel, M., Antonietti, M., & Schmidt, M. (1993). Structure determination of polymers by size-exclusion chromatography equipped with multiangle light scattering and viscosity detectors. *Journal of Applied Polymer Science: Applied Polymer Symposium, 52*, 91-103.

Wörz, O., Jäckel, K. P., Richter, T., & Wolf, A. (2001a). Microreactors - A New Efficient Tool for Reactor Development. *Chemical Engineering & Technology, 24*(2), 138-142.

Wörz, O., Jäckel, K. P., Richter, T., & Wolf, A. (2001b). Microreactors, a new efficient tool for optimum reactor design. *Chemical Engineering Science, 56*, 1029-1033.

Yoshida, J., Nagaki, A., Iwasaki, T., & Suga, S. (2005). Enhancement of Chemical Selectivity by Microreactors. *Chemical Engineering & Technology, 28*(3), 259-266.

CHAPTER 8

GENERAL DISCUSSION AND CONCLUSIONS

The general objective of this project was to develop a better understanding of the hydrodynamic and mixing characteristics of the split-and-recombination and multilamination microreactors designs in order to test the feasibility of microreaction technology to be used for continuous polymer production. Two microreaction units with integrated forced-convection heat exchangers were selected. One prototype unit featured the split-and-recombination (SAR) mixing principle, while the other was a commercial microreactor operating under the mixing principle of multilamination of flow by means of an interdigital structure. The work was divided in three main parts: the first step consisted in the hydrodynamic and mixing characterization of the microreactors; the second stage focused on the numerical investigation of the flow distribution and mixing capabilities of the mixing mechanism of the microreactors; and finally the last step focused on the heat transfer characterization and the application of the microreactors for the continuous free-radical polymerization of styrene monomer. The conclusions of each of these three parts are summarized in the following sections.

8.1 HYDRODYNAMIC AND MIXING CHARACTERIZATION

One of the most important parameters to analyze during the evaluation of the hydrodynamic and mixing performance of continuous flow tubular reactors is the pressure drop produced by the fluid flow. Hence, the pressure drops produced by a Newtonian fluid in laminar regime was the first information extracted from the microreactors. The SAR and multilamination microreactors produced pressure drops equivalent to that of circular tubes with diameters of 0.602 mm and 0.411 mm respectively. The microreactor featuring the SAR mechanism produced pressure drops approximately five times lower than the multilamination unit. This was due to the flow-splitting mechanism used by the SAR geometry in which the mixing and reaction stages are conducted in 5 and 31 parallel microchannels respectively. However, the residence time distribution (RTD)

characterization showed that effects of recirculation and by-passing were exhibited at certain flow conditions when the feeding ratio was different than one, thus the SAR microreactor low pressure drop was achieved at the cost of an uneven flow distribution.

The microreactors investigated featured fluid lines and connection ports that cannot be avoided in practice. This presented inherent experimental difficulties during the RTD analysis such as restricted flow visualization, constrained measurement at precise inlet and outlet planes, and influence of the volumes of peripheral fluid lines in the input signals. Instead of adapting the injection/detection set-up to the specific microfluidic devices used in our study, we proposed to follow a more general approach that could be applied to any microfluidic device. Thus, the classical pulse-input injection technique was performed upstream following the necessary precautions to recover the true exit-age distribution function of the microreactors by deconvolution in the Fourier domain. The convolution of these recovered functions with any input signal independently measured, resulted in highly reproducible convoluted responses that accurately fitted the responses obtained experimentally. Hence, we have successfully demonstrated that the classical pulse-input technique in junction with a proper deconvolution routine in the Fourier domain is a suitable approach that can be applied for the RTD characterization of any microfluidic device.

The axial dispersion characteristics of the microreactors were compared to those that would be obtained in circular tubes with equivalent pressure drops and volumes. The decrease of the quadratic dependence of the axial dispersion coefficient on fluid velocity observed for both microreactors is attributed to the efficient tracer homogenization in the radial direction achieved by the micromixing mechanisms investigated.

The RTD analysis showed that the microreactors are capable to achieve the same levels of tracer homogenization in the radial direction at shorter axial lengths than those required by an open tube. Thus, when compared to laminar flows in open tubes the micromixing mechanisms investigated were capable to achieve the same degree of mixing at shorter residence times.

An important finding during the comparison of the mixing performance was that although both microreactors could reach the same level of mixing, the SAR unit required considerable less energy input; *e.g.* approximately one order of magnitude lower than the multilamination microreactor. The SAR mechanism advantage thus consists in achieving comparable mixing performance at considerably lower pressure drops.

The RTD analysis showed that the SAR and multilamination microreactors operate more efficiently at long mean residence times, *i.e. Da* >10. On the other hand, the iodide-iodate system showed that depending on the acid concentration the SAR and LLMR operate more efficiently at low *Da* since at *Da* >10 the segregation indexes obtained are comparable to those produced by a T-junction of higher diameter. This reveals the effectiveness of short diffusion lengths in the microreactors where fast mixing by diffusion was achieved even at short residence times. Thus, flow rates producing values of *Da* <10 are the optimal operating conditions to take advantage of the fast mixing capabilities of these microreactor models.

8.2 Numerical Investigation of the Mixing Performance and Residence Time Distribution Characteristics

The use of CFD simulations allowed to accurately determine the internal flow characteristics of the microfluidic structures otherwise inaccessible by means of direct visualization. It was found that with the SAR microreactor principle, the manifolds design produces an unbalanced flow distribution in the microchannel network when the flow ratio of the inlets is equal to one. This imbalance results in variations of composition of 12.5% between adjacent microchannels and only the central microchannel achieves a 50/50 composition. The visualization of the velocity fields by CFD and the mixing analysis with the particle tracking method confirm the presence of recirculation and by-passing in the SAR microfluidic structure for flow ratios different than one. Thus, the use of these flow conditions further deteriorates any flow imbalance already present due to the geometry of the distribution manifolds. This is a noteworthy conclusion since through the adjustment of the volume rate of flow the concentration of reactants and the mean residence time under reaction conditions can be modified. Such adjustments can provide a measure of

control within short time frames due to the small active volumes of microreaction equipment. However, the detrimental effect of the manifold in the flow distribution at feeding ratios other than one prevents the use of this strategy as a mechanism of dynamic control during the course of a chemical reaction.

While not directly affecting the mixing process in the microreactor, the symmetrical manifold design of the LLMR used in the heat transfer section proved to evenly distribute the flow under all the flow ratios and conditions investigated. This operating principle can be used as a guideline for the design optimization of microreactors requiring distribution of flow in several substreams.

The scale and intensity of segregation concepts originally proposed by Danckwerts allowed for the quantification of mixing efficiency by means of the particle tracking method as a function of the flow conditions in the mixing section of the microreactors. It was found that from a purely mechanistic perspective, *i.e.* in the absence of molecular diffusion, the scale and intensity of segregation achieved by both microreactors at flow ratios equal to one was not significantly affected by the amount of energy applied to the system. Also, the scale of segregation achieved was independent of the flow conditions and mainly affected by the geometrical parameters of the microchannel structures. Thus, fluid layers with approximately the same thickness are produced. When molecular diffusion is considered in such scenarios a comparable scale of segregation would translate to mixing times in the same order of magnitude for all the flow conditions investigated with the lowest flow conditions producing the same level of radial mixing and higher conversions, *i.e.* longest residence times. In contrast, the same characteristics of scale and intensity of segregation were considerably affected at flow ratios other than 1 proving that unbalanced flow ratios are not optimal for the SAR and multilamination mixing mechanisms. The RTD obtained by means of CFD were accurately described by the pure convection flow model and the shape of the curves showed that the mixing and reaction sections of both microreactors exhibit the behavior of tubular reactors under laminar flow conditions with no recirculation or stagnancy present for flow ratios equal to one, therefore confirming this ratio as the optimal operation condition for mixing of Newtonian fluids using the specific microreactor models investigated.

8.3 CONTINUOUS FREE-RADICAL POLYMERIZATION OF STYRENE IN THE SAR AND MULTILAMINATION MICROREACTORS

The heat transfer characterization of the integrated forced-convection heat exchangers was the first step followed in the last stage of the project. Due to the stacked plates arrangement used by the SAR microreactor, the heat transfer mechanism can be regarded as a mixture of the parallel and counterflow mode. Both of its reaction plates are connected in series with the respective inlet and outlet ports, whilst the two corresponding heat transfer plates are connected in parallel to their respective inlet and outlet ports. Thus irrespectively of how the heat transfer fluid feeding system is connected, one reaction plate operates in parallel mode while the other operates in counterflow. The LLMR heat exchanger operates by means of two sets of straight passages covering the length of the microreactor; one consisting of channels running atop the reaction microchannels, while the other consists of intercalated channels of high aspect ratio placed in between the reaction passages. Thus, pure parallel or counterflow arrangement was possible with the LLMR heat exchanger.

Overall heat transfer coefficients of 3.04 and 2.8 kW/m2-K were obtained for the SAR and LLMR respectively at flow rates of ~420 mL/min. The SAR heat exchanger proved to be more efficient when its second heat transfer plate operates in counterflow mode, i.e. when the heat transfer fluid pump is connected at the same end where the mixed fluids or products outlet is located. When a balanced thermal condition was used, i.e. equal thermal capacities on both sides of the heat exchanger, the microreactors heat exchangers exhibited efficiencies of approximately 0.5. This suggests that both systems could operate at higher thermal capacities and with greater thermal loads.

One of the most important contributions of this project was to demonstrate that the microreactors used in this investigation are capable to achieve at least 30% of conversion in continuous flow with the appropriate combination of reaction temperature, flow rate, initiator type and concentration. For the levels of conversion achieved, both microreactors produced polydispersity indexes close to the theoretical limiting value of 1.5. Overall, the LLMR microreactor produced lower PDI values as compared to the SAR mechanism. This agrees with our previous

experimental and numerical results about the mixing capabilities of these microreactors from which was concluded that when operating at equal conditions, the LLMR exhibits a slightly better mixing performance. Although low weight average molecular weights were obtained at these conversions, low polydispersity indexes were also achieved. These properties obtained at microreaction conditions can be fully exploited for the production of materials where such characteristics are of great importance, e.g. paints, coatings and films. Also, the microreactors exhibited the capabilities to be applied as the initiation protocols of larger processes requiring a prepolymerization stage.

8.4 SUMMARY

Under the scope of the general objective of the project and based on the results obtained, we conclude that using an appropriate combination of operating parameters the microreactors investigated are indeed capable to achieve the targeted conversion of 30% which is critical in the HIPS system. However, due to the hydrodynamic characteristics at low fluid velocities (*i.e.* long mean residence times) it would be challenging to carry out a polymerization to completion. It is recommended that the microreactors to be better exploited in a prepolymerization stage. This is especially evident if one considers that for high conversions longer residence times would be required. Longer residence times equal to lower fluid velocities, and lower fluid velocities are not the optimal flow conditions where conventional T-junctions can reach the same level of mixing performance. Since it was shown that the microreactors were more mixing efficient at shorter mean residence times. Also, the split-and-recombination mechanism exhibited an efficient mixing performance when compared to the multilamination mechanism, however the flow distribution stage is of critical consideration. It was found that variation of the flow ratio can provide a measure of dynamic control in microfluidic structures for controlling reactions rates and heat transfer control, however it was shown that these flow conditions are not the optimal operating parameters for the specific microreactors designs investigated.

CHAPTER 9

RECOMMENDATIONS FOR FUTURE RESEARCH

During the development of the specific objectives of this project a number of new opportunities for future research were identified. These opportunities are related to the improvement of certain aspects of the available methodologies for conducting the experimental and numerical hydrodynamic characterization of microfluidic devices, as well as to expand on the available data in order to establish sound correlations between flow conditions produced in commercial microreactors and their mixing and RTD performance.

9.1 HYDRODYNAMIC AND MIXING CHARACTERIZATION

- Determination of the effect of varying viscosity and non-Newtonian behavior on the mixing performance of these microfluidic structures.

- Expanding and incrementing the work on the mixing and RTD characteristics of the microreactors for a larger *Da* number range, at least one order of magnitude in each direction. This would include the flow rate ranges already investigated in order to confirm trends and to establish experimental correlations as a function of the microreactors geometrical parameters.

- Since enough evidence has been published about the suitability of the *Empirical Flow Model* to reproduce the tracer distribution behavior in microreactors, the relationship of the empirical model parameters with both the geometry of the reactor and the parameters of the physical process must be explored. The investigation should establish at least meaningful correlations between the parameters of the classical Axial Dispersion Model and the statistical coefficients used by the empirical model for laminar flow in tubes.

9.2 Numerical Investigation of the Mixing Performance and Residence Time Distribution Characteristics

- The use of the particle tracking technique for the determination of RTD presents an opportunity to isolate the effects of splitting-and-recombination of flow mixing principles from the effects of molecular diffusion in the laminar flow regime. Also, the particle tracking technique can simplify and speed up the analysis during geometry optimization routines. However, there are factors inherent to the numerical approach and statistical manipulation of data that contributes to discrepancies between numerical results and laminar flow theory, *e.g.* differences in mean residence times, improper tail truncation, and divergence of variance properties. Such discrepancies can overshadow the presence of undesired flow behaviors such as recirculation, by-passing and stagnancy.

- Conceptualization of new flow distribution geometries and optimization of existing designs. Trapezoidal manifolds are claimed to be an optimized geometry for the balanced distribution of main flows into several substreams, yet experimental evidence and numerical results suggests inhomogeneous distribution. Less complicated 3D structures must be proposed featuring preferably symmetrical manifold designs along the flow axis.

9.3 Continuous Free-Radical Polymerization of Styrene in the SAR and Multilamination Microreactors

- Determination of the shear rate inside of the microreactors as a function of the microchannel geometry and flow conditions, and its effects on the stability characteristics, particle size and particle size distribution of emulsification and seed latexes processes.

- Characterization of polystyrene properties at full conversions brought about other means after a prepolymerization stage up to 30% of conversion in the microreactors.

- To determine the effect of the level of conversion on the process viscosity in the microreaction polymerization system.

- Investigate the effect of the mixing conditions achieved by these microreactors on the morphology and properties of high-impact polystyrene which are known to be influenced by the mixing state of reactants before and during its phase inversion that typically occurs below the 30% of conversion limit.

- Further investigation of the heat transfer efficiency behavior as a function of the flow thermal capacity of the microreactor. The flow ratio between the cold and hot fluid streams can provide a level of dynamic temperature control at the microscale. Low flow rates are common in microfluidic equipment, and the impact of a varying flow ratio in the microreactors must be further investigated in order to determine the reactor performance in terms of temperature control and effectiveness.

REFERENCES

Adeosun, J. T., & Lawal, A. (2005). Mass transfer enhancement in microchannel reactors by reorientation of fluid interfaces and stretching. *Sensors and Actuators B: Chemical, 110*(1), 101-111.

Adeosun, J. T., & Lawal, A. (2009). Numerical and experimental studies of mixing characteristics in a T-nuction microchannel using residence-time distribution. *Chemical Engineering Science, 64*, 2422-2432.

Amador, C., Wenn, D., Shaw, J., Gavriilidis, A., & Angeli, P. (2008). Design of a mesh microreactor for even flow distribution and narrow residence time distribution. *Chemical Engineering Journal, 135*(Supplement 1), S259-S269.

Ananthakrishnan, V., Gill, W. N., & Barduhn, A. J. (1965). Laminar Dispersion in Capillaries. *AIChE Journal, 11*(6), 1063-1072.

Antes, J., Boskovic, D., Krause, H., Loebbecke, S., Lutz, N., Tuercke, T., et al. (2003). Analysis and Improvement of Strong Exothermic Nitrations in Microreactors. *Chemical Engineering Research and Design, 81*(7), 760-765.

Arnold, D., Brezzi, F., & Fortin, M. (1984). A stable finite element for the stokes equations. *Calcolo, 21*(4), 337-344.

Arnold, J., Dasbach, U., Ehrfeld, W., Hesch, K., & Löwe, H. (1995). Combination of excimer laser micromachining and replication processes suited for large scale production (Laser-LIGA). *Applied Surface Science, 86*, 251.

Aubin, J., Fletcher, D. F., Bertrand, J., & Xuereb, C. (2003). Characterization of the Mixing Quality in Micromixers. *Chemical Engineering & Technology, 26*(12), 1262-1270.

Aubin, J., Fletcher, D. F., & Xuereb, C. (2005). Design of micromixers using CFD modelling. *Chemical Engineering Science, 60*(8-9), 2503-2516.

Aubin, J., Prat, L., Xuereb, C., & Gourdon, C. (2009). Effect of microchannel aspect ratio on residence time distributions and the axial dispersion coefficient. *Chemical Engineering and Processing: Process Intensification, 48*(1), 554-559.

Awtrey, A. D., & Connick, R. E. (1951). The absorption spectra of I_2, I_3-, I-, IO_3-, S_4O_6- and S_4O_3-. Heat of the reaction I_3- = I_2 + I-. *Journal of the American Chemical Society, 73*, 1842-1843.

Baillagou, P. E., & Soong, D. S. (1985). *Polymer Engineering & Science, 25*, 212.

Bavière, R., Ayela, F., Le Person, S., & Favre-Marinet, M. (2004). *An experimental study on water flow in smooth and rough rectangular microchannels.* Paper presented at the

Second International Conference on Microchannels and Minichannels, Rochester, N.Y., U.S.A.

Bayer, T., Heinichen, H., & Natelberg, T. (2000b). *Emulsification of silicon oil in water - comparison between a micromixer and a conventional stirred tank.* Paper presented at the 4th International Conference on Microreaction Technology - IMRET 4, Atlanta, Georgia, USA.

Bayer, T., Jenck, J., & Matlosz, M. (2005). IMPULSE - A New Approach to Process Design. *Chemical Engineering & Technology, 28*(4), 431-438.

Bayer, T., Pysall, D., & Wachsen, O. (2000). Micromixing effect in continuous radical polymerization. *Microreaction Technology: 3rd International Conference on Microreaction Technology, Proceedings of IMRET 3, Springer-Verlag, Berlin*, 165-170.

Bayer, T., Pysall, D., & Wachsen, O. (2000a). *Micro mixing effects in continuous radical polymerization.* Paper presented at the 3rd International Conference on Microreaction Technology IMRET 3, Berlin.

Bird, R. B., Stewart, W. E., & Lightfoot, E. N. (2002). *Transport Phenomena* (2nd ed.): Wiley.

Boskovic, D., & Loebbecke, S. (2008). Modelling of the residence time distribution in micromixers. *Chemical Engineering Journal, 135*(SUPPL. 1), S138-S146.

Bothe, D., Stemich, C., & Warnecke, H.-J. (2006). Fluid mixing in a T-shaped micro-mixer. *Chemical Engineering Science, 61*(9), 2950-2958.

Boundy, R. H., & Boyer, R. F. (1952). *Styrene: Its Polymers, Copolymers and Derivatives*. New York: Reinhold Publishing Corporation.

Brandner, J., Fichtner, M., & Schubert, K. (2000). *Electrically heated microstructure heat exchangers and reactors.* Paper presented at the Microreaction Technology: 3rd International Conference on Microreaction Technology, Proceeding of IMRET 3, Berlin.

Bucci, A., Celata, G. P., Cumo, M., Serra, E., & Zummo, G. (2004). *Water single-phase fluid flor and heat transfer in capillary tubes.* Paper presented at the Second Internacional Conference on Microchannels and Minichannels, Rochester, NY, USA.

Cabral, P. A., Melo, P. A., E. C. Biscaia, J., Lima, E. L., & Pinto, J. C. (2003). Free-radical solution polymerization of styrene in a tubular reactor - effects of recycling. *Polymer Engineering & Science, 43*(6), 1163-1179.

Cantrel, L., Chaouche, R., & Chopin-Dumas, J. (1997). Diffusion Coefficients of Molecular Iodine in Aqueous Solutions. *Journal of Chemical Engineering Data, 42*, 216-220.

Cantu-Perez, A., Barrass, S., & Gavriilidis, A. (2010). Residence time distributions in microchannels: Comparison between channels with herringbone structures and a rectangular channel. *Chemical Engineering Journal, 160*(3), 834-844.

Cantu-Perez, A., Bi, S., Barrass, S., Wood, M., & Gavriilidis, A. (2011). Residence time distribution studies in microstructured plate reactors. *Applied Thermal Engineering, 31*, 634-639.

Caravieilhes, S., de Bellefon, C., & Tanchoux, N. (2001). Dynamic methods and new reactors for liquid phase molecular catalysis. *Catalysis Today, 66*(2-4), 145-155.

Chang, Z., Liu, G., Fang, F., Tian, Y., & Zhang, Z. (2004b). Gamma-ray-initiated dispersion polymerization of PMA in microreactor. *Chemical Engineering Journal, 101*, 195-199.

Chang, Z., Liu, G., Tian, Y., & Zhang, Z. (2004a). Preparation of micron-size monodisperse poly(vinyl acetate) microspheres with gamma-rays-initiated dispersion polymerization in microreactor. *Materials Letters, 58*, 522-524.

Chen, C. C. (1994). A continuous bulk polymerization process for crystal polystyrene. *Polymer-plastics Technology and Engineering, 33*(1), 55-81.

Chen, Y., & Cheng, P. (2002). Heat transfer and pressure drop in fractal tree-like microchannel nets. *International Journal of Heat and Mass Transfer, 45*(13), 2643-2648.

Choi, K. Y., & Lei, G. D. (1987). Modeling of Free-Radical Polymerization of Styrene by Bifunctional Initiators. *AIChE Journal, 33*(12), 2067-2076.

Citron-Cordero, R., Mostello, R. A., & Biesenberger, J. A. (1968). *Canadian Journal of Chemical Engineering, 46*, 434.

Coesnon, B., Heniche, M., Devals, C., Bertrand, F., & Tanguy, P. A. (2008). A fast and robust fictitious domain method for modelling viscous flows in complex mixers: The example of propellant make-down. *International Journal for Numerical Methods in Fluids, 58*(4), 427-449.

Commenge, J. M., Falk, L., Corriou, J. P., & Matlosz, M. (2002). Optimal Design for Flow Uniformity in Microchannel Reactors. *AIChE Journal, 48*(2), 345-358.

Cortes-Quiroz, C. A., Azarbadegan, A., Zangeneh, M., & Goto, A. (2010). Analysis and multi-criteria design optimization of geometric characteristics of grooved micromixer. *Chemical Engineering Journal, 160*(3), 852-864.

Custer, J., & Natelson, S. (1949). Spectrophotometric determination of microquantities of iodine. *Analytical Chemistry, 21*(8), 1005-1009.

Danckwerts, P. V. (1952). The Definition and Measurement of Some Characteristics of Mixtures. *Applied Scientific Research, 3*(Section A), 279-296.

Danckwerts, P. V. (1953). Continuous Flow Systems: Distribution of Residence Times. *Chemical Engineering Science, 2*(1), 1-13.

Ehrfeld, W., Hessel, V., Löwe, H. (2001). *Microreactors: New Technology for Modern Chemistry* (1st ed.). Weinheim: Wiley-VCH.

Ehrfeld, W., Gärtner, C., Golbig, K., Hessel, V., Konrad, R., Löwe, H., et al. (1997). *Fabrication of components and systems for chemical and biological microreactors.* Paper presented at the 1st International Conference on Microreaction Technology, Berlin.

Ehrfeld, W., Golbig, K., Hessel, V., Lowe, H., & Richter, T. (1999). Characterization of Mixing in Micromixers by a Test Reaction: Single Mixing Units and Mixer Arrays. *Industrial & Engineering Chemistry Research, 38*(3), 1075-1082.

Ehrfeld, W., Golbig, K., Hessel, V., Lowe, H., & Richter, T. (1999a). Characterization of Mixing in Micromixers by a Test Reaction: Single Mixing Units and Mixer Arrays. *Industrial & Engineering Chemistry Research, 38*(3), 1075-1082.

Ehrfeld, W., Hessel, V., & Haverkamp, V. (1999). *Microreactors, Ullmann's Encyclopedia of Industrial Reactors*. Weinheim: Wiley-VCH.

Ehrfeld, W., Hessel, V., & Haverkamp, V. (1999b). *Microreactors, Ullmann's Encyclopedia of Industrial Reactors*. Weinheim: Wiley-VCH.

Ehrfeld, W., & Lehr, H. (1995). Deep X-ray lithography for the production of three dimensional microstructures from metals, polymers and ceramics. *Radiation Physics and Chemistry, 45*(3), 349-365.

Ehrfeld, W., Lehr, H., Michel, F., & Wolf, A. (1996). *Micro electro discharge machining as a technology in micromachining.* Paper presented at the SPIE Symposium on Micromachining and Microfabrication, Austin, TX, USA.

Engler, M., Kockmann, N., Kiefer, T., & Woias, P. (2004). Numerical and experimental investigations on liquid mixing in static micromixers. *Chemical Engineering Journal, 101*(1-3), 315-322.

Falk, L., & Commenge, J. M. (2010). Performance comparison of micromixers. *Chemical Engineering Science, 65*(1), 405-411.

Fan, Z., Zhou, X., Luo, L., & Yuan, W. (2010). Evaluation of the performance of a constructal mixer with the iodide-iodate reaction system. *Chemical Engineering and Processing: Process Intensification, 49*(6), 628-632.

Ferstl, W., Loebbecke, S., Antes, J., Krause, H., Haeberl, M., Schmalz, D., et al. (2004). Development of an automated microreaction system with integrated sensorics for process screening and production. *Chemical Engineering Journal, 101*(1-3), 431-438.

Fityani-Trimm, S., Dhib, R., & Penlidis, A. (2003). Free Radical Polymerization of Styrene with a New Tetrafunctional Peroxide Initiator. *Macromolecular Chemistry and Physics, 204*(3), 436-442.

Fogler, H. S. (1999). Elements of Chemical Reaction Engineering (3rd. ed.). New Jersey: Pretince-Hall.

Fournier, M. C., Falk, L., & Villermaux, J. (1996a). New parallel competing reaction system for assessing micromixing efficiency - experimental approach. *Chemical Engineering Science, 51*(22), 5053-5064.

Fournier, M. C., Falk, L., & Villermaux, J. (1996b). New parallel competing reaction system for assessing micromixing efficiency - determination of micromixing time by a simple mixing model. *Chemical Engineering Science, 51*(23), 5187-5192.

Freedman, D., & Diaconis, P. (1981). On the histogram as a density estimator: L_2 Theory. *Probability Theory and Related Fields, 57*(4), 453-476.

Gamrat, G., Favre-Marinet, M., Le Person, S., Baviere, R., & Ayela, F. (2008). An experimental study and modelling of roughness effects on laminar flow in microchannels. *Journal of Fluid Mechanics, 594*, 399-423.

Gobby, D., Angeli, P., & Gavriilidis, A. (2001). Mixing chacteristics of T-type microfluidic mixers. *Journal of Micromechanics and Microengineering, 11*(2), 126-132.

Günther, A., Khan, S. A., Thalmann, M., Trachsel, F., & Jensen, K. F. (2004). Transport and reaction in microscale segmented gas-liquid flow. *Lab on a Chip, 4*(4), 278-286.

Günther, M., Schneider, S., Wagner, J., Gorges, R., Henkel, T., Kielpinski, M., et al. (2004). Characterisation of residence time and residence time distribution in chip reactors with modular arrangements by integrated optical detection. *Chemical Engineering Journal, 101*(1-3), 373-378.

Guichardon, P., & Falk, L. (2000a). Characterisation of micromixing efficiency by the iodide-iodate reaction system. Part I: experimental procedure. *Chemical Engineering Science, 55*(19), 4233-4243.

Guichardon, P., Falk, L., & Villermaux, J. (2000b). Characterisation of micromixing efficiency by the iodide-iodate reaction system. Part II: kinetic study. *Chemical Engineering Science, 55*(19), 4245-4253.

Ham, J.-H., & Platzer, B. (2004). Semi-empirical equations for residence time distributions in disperse systems – Part 1: Continuous phase. *Chemical Engineering Technology, 27*(11), 1172-1178.

Hamer, J. W., & Ray, W. H. (1986). *Chemical Engineering Science, 41*, 3095.

Hardt, S., & Schönfeld, F. (2000). Laminar mixing in different interdigital micromixers-part 2: Numerical Simulations. *AIChE Journal, 40*(3), 578-584.

Hardt, S., & Schönfeld, F. (2003). Laminar mixing in different interdigital micromixers: II. Numerical simulations. *AIChE Journal, 49*(3), 578-584.

Hausen, H. (1983). *Heat transfer in counterflow, parallel flow and cross flow.* (2nd. ed.). New York: McGraw-Hill.

Haverkamp, V., Ehrfeld, W., Gebauer, K., Hessel, V., Löwe, H., Richter, T., et al. (1999). The potential of micromixers for contacting of disperse liquid phases. *Fresenius Journal of Analytical Chemistry, 364*, 617-624.

Heniche, M., & Tanguy, P. A. (2006). A new element-by-element method for trajectory calculations with tetrahedral finite element meshes. *International Journal for Numerical Methods in Engineering, 67*(9), 1290-1317.

Heniche, M., Tanguy, P. A., Reeder, M. F., & Fasano, J. B. (2005). Numerical investigation of blade shape in static mixing. *AIChE Journal, 51*(1), 44-58.

Herbo, C., & Sigallia, J. (1957). Principes de l'iodimétrie absortiométrique. *Analytica Chimica Acta, 17*, 199.

Hessel, V., Ehrfeld, W., Freimuth, H., Löwe, H., Richter, T., Stadel, M., Weber, L., Wolf, A. (1997). *Fabrication and interconnection of ceramic microreaction systems for high temperature applications.* Paper presented at the International Conference on Microreaction Technology, IMRET 1, Berlin.

Hessel, V., Hardt, S., & Löwe, H. (2004). *Chemical Micro Process Engineering: Fundamentals, Modelling and Reactions*. Weinheim: Wiley-VCH.

Hessel, V., & Löwe, H. (2003). Microchemical engineering: components, plant concepts user acceptance - part 1. *Chemical Engineering Technology, 26*, 13-24.

Hessel, V., Löwe, H., & Schönfeld, F. (2005). Micromixers a review on passive and active mixing principles. *Chemical Engineering Science, 60*, 2479-2501.

Hobbs, D. M., & Muzzio, F. J. (1997). The Kenics static mixer: a three-dimensional chaotic flow. *Chemical Engineering Journal, 67*(3), 153-166.

Holman, J. P. (1997). *Heat Transfer* (8th ed.): McGraw-Hill.

Incropera, F., & DeWitt, D. (1985). *Introduction to Heat Transfer*. New York: John Wiley & Sons, Inc.

Iwasaki, T., & Yoshida, J.-i. (2005). Free Radical Polymerization in Microreactors. Significant Improvement in Molecular Weight Distribution Control. *Macromolecules, 38*(4), 1159-1163.

James, J. B., Terry, S. C., & Barth, P. W. (1993). Silicon micromechanical devices. *Scientific American, 14*, 248.

Judy, J., Maynes, D., & Webb, B. W. (2002). Characterization of frictional pressure drop fro liquid flows through microchannels. *International Journal of Heat and Mass Transfer, 45*, 3477-3489.

Kim, S. J., Kim, D., & Lee, D. Y. (2000). On the local thermal equilibrium in microchannel heat sinks. *International Journal of Heat and Mass Transfer, 43*(10), 1735-1748.

Kirner, T., Albert, J., Günther, M., Mayer, G., Reinhäckel, K., & Köhler, J. M. (2004). Static micromixers for modular chip reactor arrangements in two-step reactions and photochemical activated processes. *Chemical Engineering Journal, 101*(1-3), 65-74.

Knight, J. B., Vishwanath, A., Brody, J. P., Austin, R. H. (1998). Hydrodynamic focusing on a silicon ship: mixing nanoliters in microseconds. *Physical Review Letters, 80*(17), 3863.

Kockmann, N., Kiefer, T., Engler, M., & Woias, P. (2006). Convective mixing and chemical reactions in microchannels with high flow rates. *Sensors and Actuators, B: Chemical, 117*(2), 495-508.

Köhler, J. M., Schleiff, B., Schneider, S., Boskovic, D., Henkel, T., & Groß, G. A. (2010). Characterization of viscosity dependent residence time distribution in the static micromixer Statmix6. *Chemical Engineering Journal, 160*(3), 845-851.

Kölbl, A., Kraut, M., & Schubert, K. (2008a). The iodide iodate method to characterize microstructured mixing devices. *AIChE Journal, 54*(3), 639-645.

Kölbl, A., Kraut, M., & Schubert, K. (2010). On the scalability of microstructured mixing devices. *Chemical Engineering Journal, 160*(3), 865-872.

Kölbl, A., & Schmidt-Lehr, S. (2008b). The iodide iodate reaction method: The choice of the acid. *Chemical Engineering Science, 65*(5), 1897-1901.

Kussul, E. M., Rachkovskij, D. A., Baidyk, T. N., & Talayev, T. S. (1996). Micromechanical engineering: a basis for the low-cost manufacturing of mechanical microdevices using microequipment. *Journal of Micromechanical Microengineering, 6*, 410-425.

Lee, J., & Kwon, S. (2009). Mixing efficiency of a multilamination micromixer with consecutive recirculation zones. *Chemical Engineering Science, 64*, 1223-1231.

Lee, S. W., & Lee, S. S. (2008). Rotation effect in split and recombination micromixing. *Sensors and Actuators B: Chemical, 129*(1), 364-371.

Levenspiel, O. (1999). *Chemical Reaction Engineering* (3rd. ed.). USA: John Wiley & Sons.

Löb, P., Hardt, S., & Löwe, H. (2000). Steering of a liquid mixing speed in interdigital micromixers-from very fast to deliberately slow mixing. *Chemical Engineering and Technology, 27*(3), 340-345.

Löb, P., Klaus, S. D., Hessel, V., Hardt, S., Hofmann, C., Löwe, H., et al. (2004). Steering of Liquid Mixing Speed in Interdigital Micro Mixers - From Very Fast to Deliberately Slow Mixing. *Chemical Engineering & Technology, 27*(3), 340-345.

Löb, P., Pennemann, H., & Hessel, V. (2004). g/l-dispersion in interdigital micromixers with different mixing chamber geometries. *Chemical Engineering Journal, 101*, 75-85.

Löb, P., Pennemann, H., Hessel, V., & Men, Y. (2006). Impact of fluid path geometry and operating parameters on l/l-dispersion in interdigital micromixers. *Chemical Engineering Science, 61*(9), 2959-2967.

Lohse, S., Kohnen, B. T., Janasek, D., Dittrich, P. S., Franzke, J., & Agar, D. W. (2008). A novel method for determining residence time distribution in intricately structured microreactors. *Lab on a Chip, 8*, 431-438.

Lowe, H., Ehrfeld, W., Hessel, V., Richter, T., & Schiewe, J. (2000). *Micromixing technology.* Paper presented at the 4th International Conference on Microreaction Technology, IMRET 4, Atlanta, USA.

Lynn, S., & Huff, J. E. (1971). Polymerization in a tubular reactor. *AIChE Journal, 17*, 475-481.

Mann, U. (2009). *Principles of Chemical Reactor Analysis and Design - New Tools for Industrial Chemical Reactor Operations* (2nd. ed.): John Wiley & Sons.

Men, Y., Hessel, V., Löb, P., Löwe, H., Werner, B., & Baier, T. (2007). Determination of the segregation index to sense the mixing quality of pilot- and production-scale microstructured mixers. *Trans. IChemE, Part A, Chemical Engineering Research and Design, 85*(A5), 605-611.

Mengeaud, V., Josserand, J., & Girault, H. H. (2002). Mixing processes in a zigzag microchannel: Finite element simulations and optical study. *Analytical Chemistry, 74*(16), 4279-4286.

Merrill, L. S., & Hamrin, C. E. (1970). Conversion and temperature profiles for complex reactions in laminar and plug flow. *AIChE Journal, 16*(2), 194-198.

Meyer, T., David, R., Renken, A., & Villermaux, J. (1988). Micromixing in a static mixer and an empty tube by a chemical method. *Chemical Engineering Science, 43*(8), 1955-1960.

Meyer, T., & Renken, A. (1990). Characterization in a tubular polymerization reactor by a new chemical method. *Chemical Engineering Science, 45*(8), 2793-2800.

Mills, A. F. (1999). *Heat Transfer* (2nd. ed.). New Jersey: Pretince-Hall, Inc.

Nagasawa, H., Aoki, N., & Mae, K. (2005). Design of a New Micromixer for Instant Mixing Based on the Collision of Micro Segments. *Chemical Engineering & Technology, 28*(3), 324-330.

Nauman, E. B. (1977). The Residence Time Distribution for Laminar Flow in Helically Coiled Tubes. *Chemical Engineering Science, 32*, 287-293.

Nauman, E. B. (1991). On residence time and trajectory calculations in motionless mixers. *Chemical Engineering Journal, 47*, 141-148.

Nauman, E. B. (2008a). *Chemical Reactor Design, Optimization and Scaleup* (2nd ed.). New Jersey: John Wiley & Sons, Inc.

Nauman, E. B. (2008b). Residence Time Theory. *Industrial & Engineering Chemistry Research, 47*, 3752-3766.

Nauman, E. B., & Buffham, B. A. (1983). *Mixing in continuous flow systems*.

Newson, J. D., & Riddiford, A. C. (1961). Limiting currents for the reduction of the tri-iodide ion at a rotating platinum disk cathode. *Journal of the Electrochemical Society, 108*(7), 695-698.

Nguyen, K. T., Streiff, F., Flaschel, E., & Renken, A. (1990). Motionless mixers for the design of multitubular polymerization reactors. *Chemical Engineering & Technology, 13*(3), 214-220.

Nisisako, T., Torii, T., & Higuchi, T. (2004). Novel microreactors for functional polymer beads. *Chemical Engineering Journal, 101*, 23-29.

Okubo, Y., Maki, T., Nakanishi, F., Hayashi, T., & Mae, K. (2009). Precise control of polymer particle properties using droplets in the microchannel. *Chemical Engineering Science, doi: 10.1016/j.ces.2009.06.004*.

Palmer, D. A., Ramette, R. W., & Mesmer, R. E. (1984). Triiodide ion formation equilibrium and activity coefficients in aqueous solution. *Journal of Solution Chemistry, 13*(19), 673-683.

Panic, S., Loebbecke, S., Tuercke, T., Antes, J., & Boskovic, D. (2004). Experimental approaches to a better understanding of mixing performance of microfluidic devices. *Chemical Engineering Journal, 101*(1-3), 409-419.

Park, J. M., & Kwon, T. H. (2008). Numerical Characterization of Three-Dimensional Serpentine Micromixers. *AIChE Journal, 54*(8), 1999-2008.

Paul, E. L., Atiemo-Obeng, V. A., & Kresta, S. M. (2004). Handbook of Industrial Mixing - Science and Practice: John Wiley & Sons.

Pennemann, H., Hardt, S., Hessel, V., Löb, P., & Weise, F. (2005). Micromixer Based Liquid/Liquid Dispersion. *Chemical Engineering & Technology, 28*(4), 501-508.

Rauline, D., Le Blevec, J. M., Bousquet, J., & Tanguy, P. A. (2000). A comparative assessment of the performance of the Kenics and SMX static mixers. *Chemical Engineering Research and Design, 78*(3), 389-396.

Rauline, D., Tanguy, P. A., Le Blevec, J. M., & Bousquet, J. (1996). Numerical investigation of the performance of several static mixers. *The Canadian Journal of Chemical Engineering, 76*, 527-535.

Rauline, D., Tanguy, P. A., Le Blevec, J.-M., & Bousquet, J. (1998). Numerical Investigation of the Performance of Several Static Mixers. *The Canadian Journal of Chemical Engineering, 76*, 527-535.

Richter, T., Ehrfeld, W., Gebauer, K., Golbig, K., Hessel, V., Lowe, H., et al. (1998). *Metallic microreactors: components and integrated systems.* Paper presented at the Process miniaturization: 2nd International Conference on Microreaction Technology, IMRET 2, New Orleans, USA.

Richter, T., Ehrfeld, W., Hessel, V., Lowe, H., Storz, M., & Wolf, A. (2000). *A flexible multi component microreaction system for liquid phase reactions.* Paper presented at the 3rd International Conference on Microreaction Technology, Proceeding of IMRET 3, Berlin.

Richter, T., Ehrfeld, W., Wolf, A., Gruber, H. P., & Worz, O. (1997). *Fabrication of microreactor components by electro discharge machining.* Paper presented at the Microreaction Technology: 1st International Conference on Microreaction Technology, Berlin.

Rosander, A. C. (1957). *Elementary Principles of Statistics*. Toronto: D. Van Nostrand Co. Inc.

Ruff, I., Friedrich, V. J., & Csillag, K. (1972). Kinetics and Mechanism of the Triiodide-Iodide Exchange Reaction. *The Journal of Physical Chemistry, 76*(2), 162-165.

Schönfeld, F., & Hardt, S. (2004). Simulation of Helical Flows in Microchannels. *AIChE Journal, 50*(4), 771-778.

Schubert, K., Brandner, J., Fichtner, M., Linder, G., Schygulla, U., & Wenka, A. (2001). Microstructure devices for applications in thermal and chemical process engineering. *Microscale Thermophysical Engineering, 5*, 17-39.

Schwesinger, N., Frank, T., & Wurmus, H. (1996). Modular microfluid system with an integrated micromixer. *Journal of Micromechanics and Microengineering, 6*(1), 99-102.

Scorah, M. J., Dhib, R., & Penlidis, A. (2005). Use of a Novel Tetrafunctional Initiator in the Free Radical Homo- and Copolymerization of Styrene, Methyl Methacylate and alfa-Methyl Styrene. *Journal of Macromolecular Science, Part A: Pure and Applied Chemistry, 42*(4), 403 - 426.

Scorah, M. J., Tzoganakis, C., Dhib, R., & Penlidis, A. (2007). Characterization by dilute solution and rheological methods of polystyrene and poly(methyl methacrylate) produced with a tetrafunctional peroxide initiator. *Journal of Applied Polymer Science, 103*(2), 1340-1355.

Serra, C., Sary, N., Schlatter, G., Hadziioannou, G., & Hessel, V. (2005). Numerical simulation of polymerization in interdigital multilamination micromixers. *Lab on a Chip, 5*(9), 966-973.

Shimazaki, H., & Shinomoto, S. (2007). A method for selecting the bin size of a time histogram. *Neural Computation, 19*(6), 1503-1527.

Smith, S. W. (1997). *The Scientist and Engineer's Guide to Signal Processing*: California Technical Publishing.

Stroock, A. D., Dertinger, S. K., Whitesides, G. M., & Ajdari, A. (2002a). Patterning flows using grooved surfaces. *Analytical Chemistry, 74*(20), 5306-5312.

Stroock, A. D., Dertinger, S. K. W., Ajdari, A., Mezic, I., Stone, H. A., & Whitesides, G. M. (2002b). Chaotic mixer for microchannels. *Science, 295*(5555), 647-651.

Tauscher, W. A. (1996). Static mixing and reaction technology. *Chemical and Petroleum Engineering, 32*(3), 224-237.

Thakur, R. K., Vial, C., Nigam, K. D. P., Nauman, E. B., & Djelveh, G. (2003). Static mixers in the process industries - a review. *Chemical Engineering Research and Design, 81*(7), 787-826.

Tien, N. K., Flaschel, E., & Renken, A. (1985). Bulk polymerization of styrene in a static mixer. *Chemical Engineering Communications, 36*(1), 251-267.

Tonomura, O., Tanaka, S., Noda, M., Kano, M., Hasebe, S., & Hasimoto, I. (2004). CFD-based optimal design of manifold in plate-fin microdevices. *Chemical Engineering Journal, 101*(1-3), 397-402.

Trachsel, F., Günther, A., Khan, S., & Jensen, K. F. (2005). Measurement of residence time distribution in microfluidic systems. *Chemical Engineering Science, 60*(21), 5729-5737.

Trippa, G., & Jachuck, R. J. J. (2004). *Characterization of mixing efficiency in narrow channels by using the iodide-iodate reaction system.* Paper presented at the Second International Conference on Microchannels and Minichannels.

Vikhansky, A. (2008). Effect of diffusion on residence time distribution in chaotic channel flow. *Chemical Engineering Science, 63*(7), 1866-1870.

Vikhansky, A. (2011). Numerical analysis of residence time distribution in microchannels. *Chemical Engineering Research and Design, 89*(3), 347-351.

Villalobos, M. A., Hamielec, A. E., & Wood, P. E. (1991). Kinetic Model for Short-Cycle Bulk Styrene Polymerization through Bifunctional Initiators. *Journal of Applied Polymer Science, 42*, 629-641.

Wallis, J. P. A., Ritter, R. A., & Andre, H. (1975a). Continuous production of polystyrene in a tubular reactor: Part 1. *AIChE Journal, 21*(4), 686-691.

Wallis, J. P. A., Ritter, R. A., & Andre, H. (1975b). Continuous production of polystyrene in a tubular reactor: Part II. *AIChE Journal, 21*(4), 691.

Weast, R. C. (1986). *Handbook of Chemistry and Physics*. Florida, USA: CRC Press.

Westerterp, K., R., Swaaij, W. P. M. v., & Beenackers, A. C. M. (1984). *Chemical reactor design and operation*. Great Britain: Wiley.

Wintermantel, M., Antonietti, M., & Schmidt, M. (1993). Structure determination of polymers by size-exclusion chromatography equipped with multiangle light scattering and viscosity detectors. *Journal of Applied Polymer Science: Applied Polymer Symposium, 52*, 91-103.

Wolf, A., Ehrfeld, W., Lehr, H., Michel, F., Richter, T., Gruber, H., et al. (1997). Mikroreaktorfertigung mittels Funkenerosion. *F & M, Feinwerktechnik, Mikrotechnik, Messtechnik, 6*, 436-439.

Wong, S. H., Ward, M. C. L., & Wharton, C. W. (2004). Micro T-mixer as a rapid mixing micromixer. *Sensors and Actuators B: Chemical, 100*(3), 359-379.

Wörner, M. (2010). Approximate residence time distribution of fully develop laminar flow in a straight rectangular channel. *Chemical Engineering Science, 65*(11), 3499-3507.

Wörz, O., Jäckel, K. P., Richter, T., & Wolf, A. (2001a). Microreactors - A New Efficient Tool for Reactor Development. *Chemical Engineering & Technology, 24*(2), 138-142.

Wörz, O., Jäckel, K. P., Richter, T., & Wolf, A. (2001b). Microreactors, a new efficient tool for optimum reactor design. *Chemical Engineering Science, 56*, 1029-1033.

Wu, T., Mei, Y., Cabral, J. o. T., Xu, C., & Beers, K. L. (2004). A New Synthetic Method for Controlled Polymerization Using a Microfluidic System. *Journal of the American Chemical Society, 126*(32), 9880-9881.

Yoshida, J.-i., Nagaki, A., Iwasaki, T., & Suga, S. (2005). Enhancement of Chemical Selectivity by Microreactors. *Chemical Engineering & Technology, 28*(3), 259-266.

Yu, L., Nassar, R., Fang, J., Kuila, D., & Varahramyan, K. (2008). Investigation of a novel microreactor for enhancing mixing and conversion. *Chemical Engineering Communications, 195*(7), 745 - 757.

Zissi, S., Bertsch, A., Jézéquel, J., Corbel, S., Lougnot, D., & André, J. (1996). Stereolithography and microtechniques. *Microsystem Technologies, 2*(2), 97-102.